APPARATUS AND TEST METHODS FOR MEASURING THE IMPACT OF GOLF BALLS ON TURF AND THEIR APPLICATION IN THE FIELD

Stephen John Haake

Submitted for the Degree
of
Doctor of Philosophy

THE UNIVERSITY OF ASTON IN BIRMINGHAM

1989

THE UNIVERSITY OF ASTON IN BIRMINGHAM

Apparatus and test methods for measuring the impact of golf balls on turf and their application in the field

Stephen J. Haake

Submitted for the Degree of Doctor of Philosophy

1989

An apparatus was developed to project spinning golf balls directly onto golf greens. This employed a modified baseball/practice machine with two counter-rotating pneumatic wheels. The speed of the wheels could be varied independently allowing backspin to be given to the ball. The ball was projected into a darkened enclosure where the impact was recorded using a still camera and a stroboscope. The resulting photographs contained images of the ball along its path before and after impact.

The apparatus was tested on eighteen golf courses, resulting in 721 photographs of impacts. Statistical analysis was carried out on the results of the photographs. Two types of green emerged from this analysis. On the first, the ball tended to rebound with topspin, while on the second, the ball retained backspin after impact if the initial backspin was greater than about 350rads^{-1}.

Statistical techniques were used to analyse the relationships between the tests. These showed the effects of the characteristics of the green on the ball/turf impact. It was found that it was easier to retain backspin on the rebounding ball on a green that was freely drained and had a low amount of *Poa annua* (annual meadow grass) in its sward.

Visco-elastic models were used to simulate the impact of the ball with the turf. Impacts were simulated by considering the ball to be rigid and the turf to be a two layered system consisting of springs and dampers. The model showed good agreement with experiment, but was unable to predict the exact effect of backspin on the rebounding ball. It was speculated that this was due to the dependence of the coefficient of friction on the impact velocity.

Key words: golf ball, impact, turf, playing quality, visco-elastic model.

This thesis is dedicated to my family and friends and especially to my late father.

Acknowledgements

I would like to thank Dr Alastair Cochran for his help and guidance throughout this project. I would also like to thank all at the Sports Turf Research Institute, especially Mike Canaway, who gave constructive criticism and helpful advice. Thanks also go to Gwill Jones who gave many useful ideas in the construction of the apparatus. Special thanks to Tim Colclough who helped with the transportation of the apparatus between golf courses. Without backing from the Royal and Ancient Golf Club of St Andrews this project could not have been carried out. Many thanks also go to the Acushnet Company for their generous financial contribution towards equipment expenditure.

LIST OF CONTENTS

LIST OF FIGURES

CHAPTER 1

CHAPTER 2

CHAPTER 3

CHAPTER 4

CHAPTER 5

LIST OF TABLES

CHAPTER 2

CHAPTER 3

CHAPTER 4

APPENDIX B

APPENDIX D

APPENDIX E

APPENDIX H

Chapter 1 - Introduction

1.1 Background

This project has been carried out at the Sports Turf Research Institute in conjunction with the Interdisciplinary Higher Degrees Scheme at the University of Aston in Birmingham.

The Sports Turf Research Institute is an independent, non-profit making organisation whose objectives are to carry out research and to provide advice and education in the sphere of sports turf. The Institute was founded in 1929 on the St. Ives estate in Bingley, West Yorkshire, under the auspices of the British Golf Union's Joint Advisory Council (now the council of National Golf Unions). The Institute is divided into two main areas: firstly, the Institute offers an advisory service to users of sports turf, e.g. private clubs, industrial sports associations, schools in both the independent and public sectors, and local education Authorities; secondly, specific research contracts are carried out for various clients such as the Sports Council. Indeed, this work was carried out in conjunction with a larger study financed by the Royal and Ancient Golf Club of St Andrews.

1.2 Aims and objectives

Manufacturers of golf balls have carried out many tests to study the behaviour of the ball on impacting with the golf club face. There has also been much work done on the aerodynamics of the ball (for example Bearman and Harvey 1976). There is little information, however, on what is a fundamental part of the game of golf - the impact of the ball with the turf on the green. Buchanan (1984) speculated on why so little research had been done in this area and on what research should be done. It is thought that with a better understanding of the process of impact it may be possible to define a given turf using a few easily measurable quantities and hence to predict how a golf green will play. These tests could then be used to aid the maintenance and construction of golf greens.

With these ideas in mind, the aims of the project were as follows:-

1. To design and develop an apparatus to project golf balls with variable speed, spin and angle on to golf greens and to record the impact of the balls with the turf.
2. To identify measurable characteristics of the turf and to relate the results of the ball impacts to these quantities.
3. To formulate a mathematical model to describe the impact of a golf ball with turf, with the ability to take into account the range of velocities, angles and spins seen in play.

4. From the results of the project, to suggest simple tests that could be performed by greenkeepers to indicate correct maintenance regimes for achieving desirable playing characteristics.

1.3 The impact of golf balls with golf greens

In order to achieve results which will be relevant to the game of golf, it is necessary to design and develop a system which will simulate the impact of golf balls on turf, using the velocities, angles and spins seen in play. It is possible to estimate these three variables if the trajectory of the ball is known. There have been many studies carried out on the flight of the golf ball through the air, mostly through private research for golf ball and golf club manufacturers. Detailed analysis of the lift and drag forces experienced by the golf ball have been published (Davies 1949; Bearman and Harvey 1976) and Cochran and Stobbs (1968) published information on the flight of the golf ball gained from tests carried out for the Golf Society of Great Britain. Figure 1.1 shows typical trajectories of golf balls hit using a driver, a 5-iron and a 9-iron. These were calculated using a computer model which utilised information on the lift and drag of Titleist golf balls gained from wind tunnel tests (details of the model are given in Appendix A). The range of values in the wind tunnel tests covered that of the driver but not necessarily those of the 5- and 9-iron. The most accurate trajectory, therefore, will be that of the driver. The velocities, angles and spins of the ball as it lands are also shown.

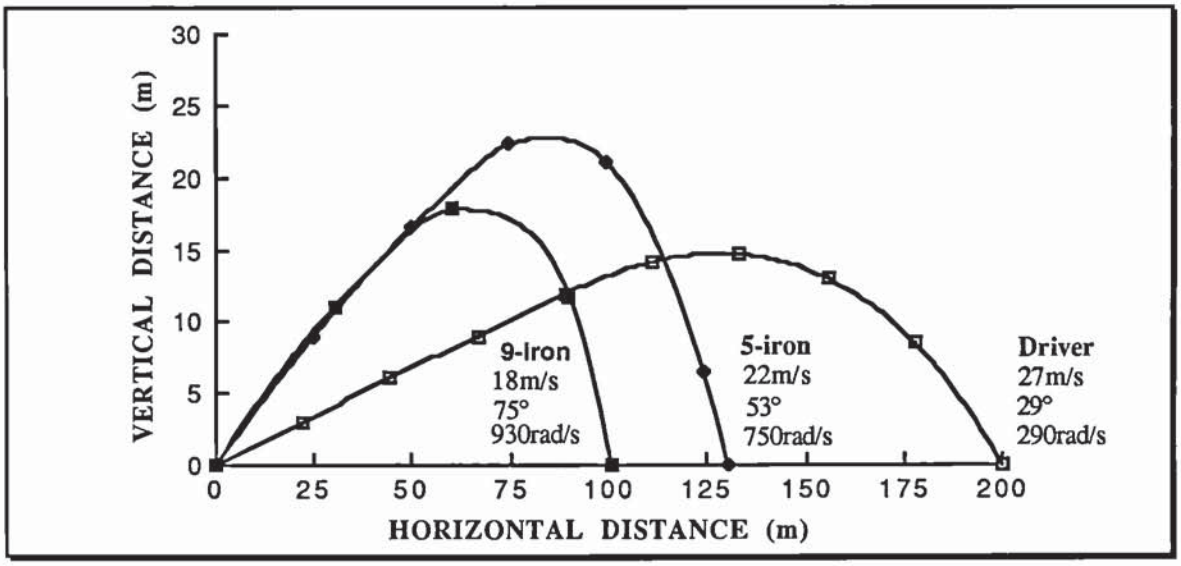

FIGURE 1.1. Computed trajectories of a golf ball hit with a 9-iron, a 5-iron and a driver. The velocities, angles and spins of the incoming balls are shown. (Note that the vertical scale is exaggerated.)

A typical golf ball hit with a 9-iron lands at an approximate velocity of $18ms^{-1}$ at 75° to the horizontal and with a spin of about 930 $rads^{-1}$. A shot played with a driver hits the turf at approximately 29° to the horizontal with a velocity of $27ms^{-1}$ and a spin of $290rads^{-1}$. A

5-iron lies somewhere in this range. This information provides a range of speeds, spins and angles to be taken into account in the development of the apparatus for studying the impact of golf balls with greens.

1.4 Literature review

The purpose of this literature review is to assess the published work on impacts and playing quality and to determine the literature that is of relevance to this project. For convenience, the literature review is split into three categories:-

1. the mechanics of impacts
2. test methods and experimental data on ball impacts, and
3. the playing quality of turf.

These categories are reviewed in the following sections.

(i) The mechanics of impact

Due to a dearth of published work on the mechanics of ball impacts with turf, it has been necessary to review work which deals with impacts in general and to relate this to the impact of golf balls with the turf. A project which studies the impact of one object with another has its roots in mechanics and this is the source of many of the papers.

One of the earliest pieces of work on the impact of elastic spheres was carried out by Hertz (1881) from which the Hertz theory of contact was formulated. This considered the static compression of two isotropic elastic bodies whose surfaces, assumed to be perfectly smooth, were approximated as two paraboloids in the vicinity of the contact point. Mathematical analysis showed that the force experienced by the bodies was,

$$F = k \propto \frac{3}{2} \qquad \text{eqn. 1.1}$$

where k is a constant related to the elastic properties of the bodies and $\propto$ is the relative compression of the bodies. Rayleigh (1906) showed mathematically that Hertz's theory of collisions had wider applications than previously supposed.

Maw *et al.* (1976) developed a mathematical solution for the oblique impact of an elastic sphere on a half space. The Hertzian theory of impact was used for the normal components of force and velocity and it was assumed that the contact area consisted of sticking and slipping regions; the coefficient of friction was taken as a constant in the slipping regions. Maw *et al.* produced a set of equations with two non-dimensional inputs, one related to the angle of incidence and the other to the radius of gyration of the ball. In a later paper Maw *et al.* (1981) described a series of experiments to evaluate their theories. A disc shaped puck, which was a symmetrical slice cut from a sphere, was propelled by a heavy pendulum toward a clamped block of similar material from which it subsequently rebounded. The puck "floated" on an air table; this consisted of a level

table with a regular series of air jets pointing upwards onto which the puck was placed. This provided virtually frictionless conditions. Stroboscopic photography was employed to record the motion of the puck before and after impact. The apparatus used by Maw *et al.* could not achieve the high velocities required for a correct evaluation of their equations. They assumed, therefore, that large local velocities at the point of impact indicated large incoming velocities, that is, a slow puck with a lot of spin impacting at an angle almost normal to the surface was the same as a puck impacting with no spin at a fairly large angle to the surface. In both cases, the velocity of the periphery of the puck relative to the surface at the beginning of impact was the same. Hence, backspin was used to simulate high impact velocities. It is not clear whether the spin after impact was taken into account when analysing the motion of the marks on the puck in the photographs. Spin is extremely important in golf ball impacts since every golf shot imparts backspin to the ball. The equations developed by Maw *et al.*, therefore, may need modification in order to apply in the case golf ball impacts.

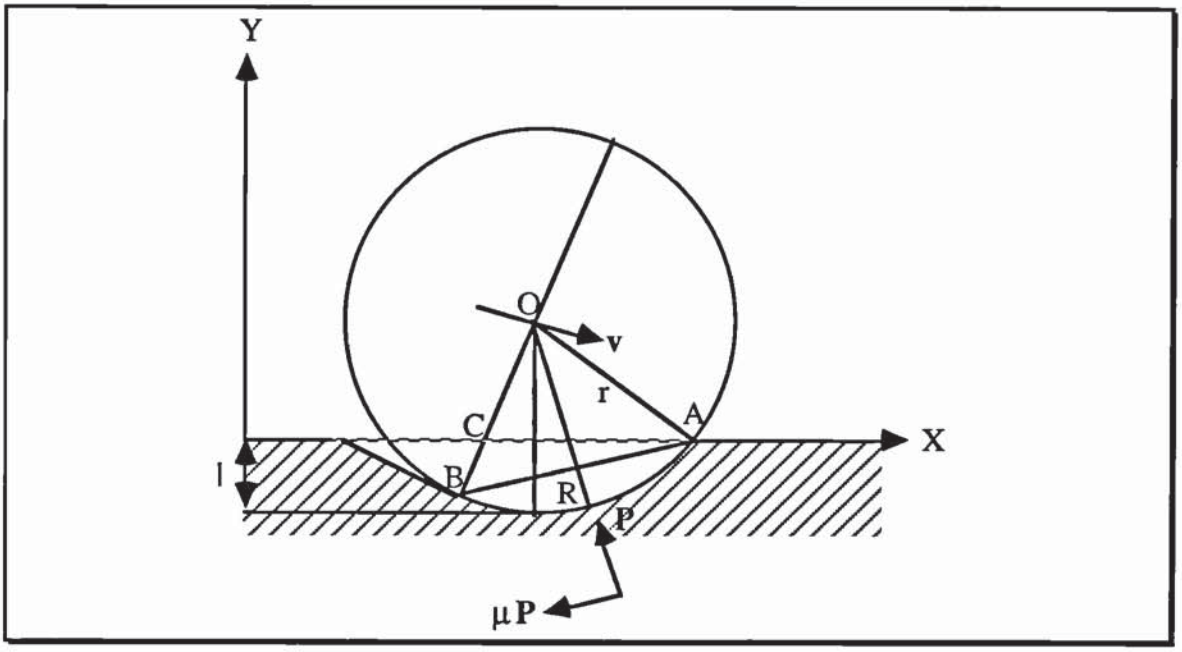

FIGURE 1.2. A section through a solid sphere impacting on a rigid-plastic half space showing the forces used in a model of impact developed by Hutchings *et al.*

Hutchings *et al.* (1976) tried to predict the variation of crater volume with impact angle for a rigid sphere impinging obliquely against an ideal rigid-plastic half space (Figure 1.2) using an iterative numerical procedure to solve the equation of motion of the sphere. It was assumed that the principal force exerted on the sphere by the target could be derived from a normal indentation pressure that was uniformly distributed over the contact area and was independent of both the incoming velocity and the penetration of the sphere. To simplify computation the contact area was assumed to be proportional to the area with AB as diameter and along the line RO. The area of contact was evaluated in terms of the

radius of the sphere, its depth l below the surface and its direction of motion relative to the horizontal.

When Hutchings *et al* (1981) analysed data from the impact of hardened steel spheres of 9.5mm diameter on ductile mild steel targets, they found a large discrepancy with their model. Rickerby *et al.* (1980) also analysed this data and found that the discrepancy mostly disappeared when a better description of the contact area between the sphere and the target was incorporated into the impact model. This allowed for the detachment of the ball from the surface of the pitchmark as the impact progressed.

It was realised, however, that the model had limitations and that it was not valid at low velocities where the elastic strains become comparable with the plastic strains. The model also did not not take into account the build up of material ahead of the sphere and, as a consequence, tended to underestimate the angle of rebound.

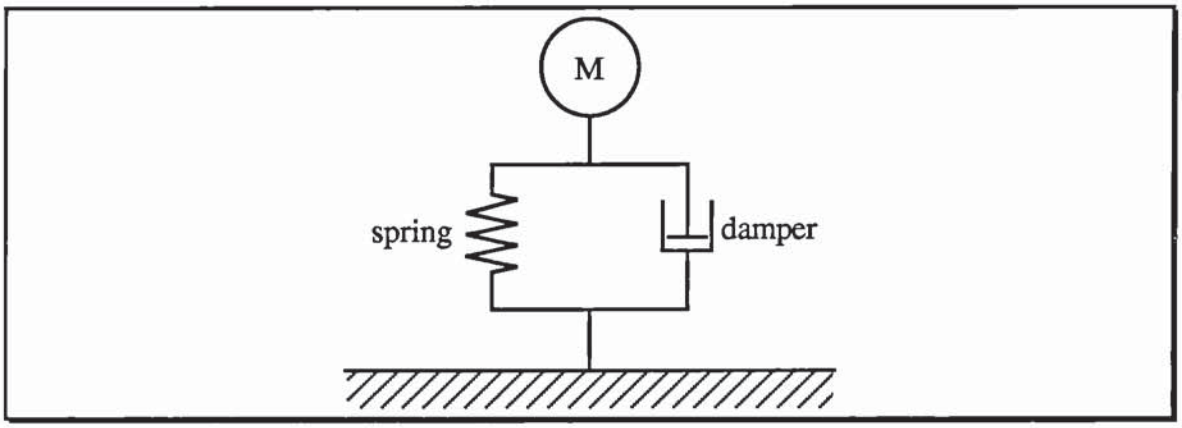

FIGURE 1.3. A simulation of a golf ball impacting with a rigid surface using the Kelvin-Voigt model. The impact is simplified as a mass attached to a spring and a damping component in parallel.

Daish (1972) used classical mechanics to study the mechanics of a ball bouncing on a rigid surface. He assumed that the ball and the ground were not deformed, that there were two individual cases of pure slip and pure sticking and that the coefficients of friction and restitution determined the process of impact. Daish found that the model did not agree with high speed films of cricket balls impacting obliquely on a hard cricket wicket. It was noticed that the ball created a saucer-like depression when it hit the surface and that the ball rebounded from the front inclined face of the depression. This resulted in the forward velocity of the ball being lower than theory predicted with the result that the ball appeared to bounce higher than was expected.

Cochran (1974a) used the Hertz theory of contact to try to model the normal impact of a golf ball on a club face. Despite the fact that the model was based on static deformation, it agreed quite well with data on the contact times of golf balls impacting with golf clubs.

The model, however, predicted a coefficient of restitution of unity and was therefore in disagreement with observation. This predicted that the coefficient of restitution decreased from about 0.8 at slow speeds to 0.7 at speeds of $45ms^{-1}$ and over. A form of damping was required and Cochran used viscoelastic models to solve this problem. Viscoelastic models simulate the forces experienced by the ball in terms of perfectly elastic components and inelastic damping components (Figure 1.3). In the elastic component the force is proportional to the extension (or compression) while in the damping component the stress is proportional to the rate of extension. In the Kelvin-Voigt model shown in Figure 1.3 the coefficient of restitution was found to be independent of the velocity and is therefore inapplicable in the case of golf ball impacts. Replacing the linear spring with a Hertzian spring produced the correct direction of variation of the coefficient of restitution but not the correct magnitudes.

Cochran (1974b) studied oblique impacts of golf balls using simple collision theory and introduced a new concept, the *coefficient of restitution of spin.* This varied from -1 to +1 and was used to take into account the modification of backspin to topspin on impact with the ground. Mathematical analysis suggested that the coefficient of restitution of spin depended on the surface roughness. These models, however, have yet to be verified experimentally.

(ii) Experiments on ball impacts

With the growth in popularity of the game of golf in the earlier part of this century, scientists became interested in the unusual properties of the golf ball. Subsequently, there have been an abundance of publications looking at the aerodynamics of golf balls and spheres (Davies 1949; Cochran and Stobbs 1968; Daish 1972; Bearman and Harvey 1976; Mehta 1985).

The spin of a golf ball was first measured by Tait (1896). He fastened one end of a long light tape to the ball and, after removing all twist, fixed the other end to the ground. The ball was then driven into a clay block attached to a ballistic pendulum and the number of twists of the tape counted. It was found to be twisted from one to two turns after a drive, indicating a spin of 60 to 120 revolutions per second.

Briggs (1945) was amongst the first to study the impact of golf balls. He compared different methods of measuring the coefficient of restitution of golf balls on golf clubs and also studied the spin gained by the balls on impact with metal targets. A method used, developed by Quayle (1924), employed spark photography; a spark gap was placed about one metre from the point of impact while a photographic plate was placed behind the impact zone such that the spark made a shadow of the ball hitting the target on the plate. This was, in effect, an early form of stroboscope photography. Briggs found that

the coefficient of restitution varied with the velocity of the impact. This was explained by Tabor (1955) who found that hysteresis losses in rubber spheres were independent of the magnitude of the deformation but were dependent on the speed of deformation.

Tatara (1983) tried to verify some parts of the Hertz theory by filming the impacts of Japanese-type tennis balls with each other and with the ground. A high speed camera running at 5000 frames per second was used to record the impacts. Tatara found that the results could not be attributed to the Hertz theory alone and suggested that another process was also taking place. It may be interesting to note that Tatara noticed distinct oscillations of the ball after impact.

Putnam *et al.* (1984) looked at the impact of tennis balls with differently strung tennis rackets. Experienced players were first filmed using a high speed camera running at 210 frames per second to find the most suitable velocity of impact. An air gun was used to project the tennis balls and stroboscope photography was used to record the impacts. It was found that alterations to the string configuration did not affect the amount of spin imparted to the ball.

Thorpe and Canaway (1986a) also used photometric methods to measure the pace and bounce of tennis balls on different court surfaces. A pneumatic ball projector was used to project the balls with zero spin while a mechanical ball projector with two counter-rotating drums and a vertical constriction at the mouth produced impacts with spin. The spin was given to the ball when it hit the constriction on leaving the ball projector. This was not particularly precise, however, and gave no continuous variation of the spin. A cine camera running at a speed of 64 frames per second recorded the impacts. The relationships between the variables were studied using correlation and multiple regression techniques. Thus, significant formulae emerged that equated the variables but did not explain the reasons for the links between them. It was found that an unmeasured process was occurring during impact which could not be explained within the scope of the project.

The most comprehensive study of the game of golf was undertaken by the Golf Society of Great Britain and was documented by Cochran and Stobbs (1968). However, most of the work concentrated on the impact of the ball with the club, the techniques of the golfer's swing and the flight of the ball through the air.

(iii) Playing quality of turf

Although rules exist to define the characteristics of golf balls and golf clubs, there are few recommendations on how the golf green should play. Holmes and Bell (1987) defined the playing quality of turf as "the suitability of a turf for a given sport as measured by electronic and mechanical tests or as perceived by players." It is therefore necessary to

find objective tests which relate to the perceptions of players and greenkeepers. Some of those presently used are described below.

Hardness. The "hardness" of the turf has a wide definition but is widely acknowledged to be important. In the past it has been called the "stiffness" of the surface (Bell *et al.* 1985) which is defined as the ratio of the applied force to the amount of deflection of the surface. Many of the techniques for the measurement of stiffness have used similar designs. Stanitski *et al.* (1974) made impact energy absorption tests on three artificial surfaces and on natural grass by measuring the rebound height of a 7.26kg, 138mm diameter sphere dropped from a height of 1.83m. Bowers and Martin (1974) used a similar approach, inserting an accelerometer into the core of a 7.26kg indoor shot and using electronic methods to measure the stopping time, total duration of impact, peak deceleration and average deceleration. The "Stuttgart Artificial Athlete" (DIN 18035 Part 6 1978) was used to measure the deformation of a surface and the peak force caused by the impact of a falling weight of mass 50kg. It was modified and used to study the deformation properties of natural and synthetic turf football surfaces (Winterbottom 1985). A 5.5kg bowling ball containing an accelerometer was used for the "Impact Severity Test" (Sports Council 1984a) from which a curve was obtained showing the deceleration of the ball against time. This was used to calculate the "Severity Index" by integrating the acceleration raised to the power of 2.5 across the contact time of the first impact. This test has been used to examine the potential of a surface to cause injury. Thomas and Guérin (1981) developed a "Sports Simulator" to measure the maximum deflection of a turf after impact with a falling weight and the time taken for the surface to return to close to its original state.

The "Clegg Impact Soil Tester" was originally developed to test the suitability of road base courses (Clegg 1976, 1978; Granelli 1983). The apparatus measures the peak deceleration of a compaction hammer as it hits the surface when dropped from a fixed height; the deceleration increases as the surface becomes stiffer. It has recently been used to examine the stiffness of natural sports surfaces and Lush (1985) used the Impact Tester to investigate the relationship between impact hardness and the rebound resilience of cricket balls. Holmes and Bell (1986a) used the Tester to produce a contour map of surface hardness of a level bowling green showing the soil compaction at the edge of the green caused by player traffic.

Rebound resilience. An alternative measure of hardness is the "ball rebound resilience" test. When a ball is dropped on a surface, the rebound resilience is expressed as the ratio of the rebound height to the original drop height expressed as a percentage. Langvad (1968) dropped footballs from a height of 7m and found that soil type had the greatest effect on ball rebound resilience. Stewart and Adams (1968) dropped cricket

balls from a height of 4.88m onto cricket wickets and found that on a relatively fast pitch the ball bounced stump high or greater and that on a relatively slow pitch the ball bounced less than half the height of the stumps. Subsequently, Stewart and Adams produced a scale relating the ball bounce to the pace of cricket pitches (Stewart and Adams 1970).

Thorpe and Canaway (1986b) released tennis balls from 2.54m (the height specified by the International Tennis Federation for the testing of the acceptability of tennis balls for competition). Colclough and Canaway (1988) dropped golf balls onto fine turf from 5m in order to investigate the relationship between its playing quality and nutrition. A video camera placed on the ground 10m from the drop apparatus was used to record the rebound value.

It is possible that different measures of hardness are related and Holmes and Bell (1987) correlated the Clegg Impact Hardness using different hammer weights with the Severity Index and the Stuttgart Artificial Athlete. It was found that different loadings gave different correlations. This may be due to the different layers which occur in a profile through natural turf. A small mass may only penetrate the grass layer while a much heavier weight may interact with the sub-soil.

Rolling resistance. The roll of the ball across the surface is an important factor in many sports. The "rolling resistance" can be thought of as a force acting at the point of contact between the ball and the surface in a direction opposite to that of the motion of the ball. In golf it is often referred to as the "speed" of the green.

The rolling resistance has usually been measured by rolling a ball down a ramp and recording the distance rolled across the surface to be tested. Langvad (1968) released footballs from a vertical height of 1m down a ramp of 26.6°. This test was also used by Dury and Dury (1983) with footballs, cricket balls and hockey balls.

Work carried out for the United States Golf Association has studied the speed of golf greens. This was measured using a device called a "Stimpmeter" first developed by Stimpson (1974) and is a grooved ramp down which a ball is rolled such that the ball travels with a constant initial speed across the green. Radko (1977, 1978) used the Stimpmeter to recommend green speeds for regular and tournament play and subsequently, work has looked at the influence of management factors on the speed of the green (Thomas 1978; Hoos and Faust 1979; Engel *et al.* 1981; Throssel and Duich, 1981).

Surface friction. Friction between the ball and the surface plays a large part in determining the residual spin of a golf ball after impact. When Daish (1972) studied spin,

bounce and surface friction of golf and cricket balls using high speed film he discovered that the ball could slide during impact with the surface and that the duration of sliding was partly dependent on the surface friction. He also discovered that, as a cricket ball bounces, it forms a saucer-like depression in the surface and thus rebounds from the forward inclined face of the depression causing it to bounce higher than expected. Cochran and Stobbs (1968) described how different amounts of spin given to a golf ball when it is hit, along with various properties of the green, can control the behaviour of the ball after impact with the green.

Thorpe and Canaway (1986a) attempted to relate the data from tennis ball impacts to the coefficient of friction of the surfaces concerned. This was measured by attaching a tennis ball to each apex of a weighted triangular sled and measuring the force required to pull the sled at a constant speed. It was found that the coefficient of friction alone could not explain the effects seen in the ball impacts. Holmes and Bell (1987) used a similar sliding friction apparatus to study the friction characteristics for cricket.

Surface evenness. The evenness of the golf green is important to golfers, who have to use their judgement to predict the contours of the green, but can have no prior knowledge of the small scale undulations of the turf. Holmes and Bell (1986a) studied the undulations on bowling greens using an automatic surveyor's level and the Sports Council (1984a, b) proposed standards for synthetic turf for general sports use using a 3m straight edge. Holmes and Bell (1987) measured the evenness of football pitches using a profile gauge. This consisted of ten rods spaced 200mm apart held in a wooden frame such that, when the frame was placed on the ground, the rods were free to move vertically when displaced by the bumps and hollows of the turf. Colclough and Canaway (1988) used a similar frame 0.5m long with the rods 50mm apart for the measurement of the evenness of fine turf on golf greens.

Ground cover and botanical analysis. The amount of grass cover has been shown to be important in the game of golf (Hoos and Faust 1979; Throssel and Duich 1981) and has been measured in a number of ways (Woolhouse 1976). Laycock and Canaway (1980) described an optical point quadrat frame for the estimation of ground cover and grass species. This has been used frequently in subsequent years (Canaway 1981, 1983; Shildrick *et al.* 1983). A "Reflectance Ratio Meter" was developed by Haggar *et al.* (1983) and was used by Haggar and Isaac (1985) to monitor grass establishment. The apparatus detected the presence of green vegetation against a brown background and although it could measure the percentage ground cover, it could not distinguish between the grass species.

1.5 Summary

The aims of the project were stated early in this chapter and the relevant literature subsequently reviewed. Although the impact of the golf ball on turf has not been studied specifically, there has been work carried out on the impacts of other sports balls. These have used a variety of projection and recording techniques and will be considered in the next chapter when the development of the apparatus for studying golf ball impacts is described. The range of the velocities, angles and spins required in the impact study were determined by estimating the trajectories of golf balls onto the green.

Most work on the mechanics of impact has involved rigid solids. This will be considered further in Chapter 5 when the formulation of a model of impact is discussed. The many tests for playing quality described in this chapter are used as a guide later in Chapter 2 in the choice of suitable tests for measuring the characteristics of the green.

Chapter 2 - Apparatus and test methods

2.1 Introduction

The aim of this chapter is to use the information gained from the literature review as a guide in the development of the apparatus to project and record the impacts of golf balls on turf. It was found in Chapter 1 that, although experiments have been carried out on the impact of elastic spheres on rigid surfaces, the impact of the ball on the green has essentially been ignored. It was first necessary, therefore, to design and develop an apparatus to project golf balls with the desired speeds, spins and angles similar to those found in play (section 1.2). During the development of the ball projection device, a method of recording the impacts was devised. The two sets of apparatus were therefore developed in parallel since modifications in one affected the design of the other.

The United States Golf Association (USGA) was consulted to find its views on the methods that could be used, as were the Acushnet Company and Dunlop/Slazenger Limited. There were frequent discussions with the supervisors for the project and from these, a set of guide-lines for the development of the apparatus emerged. There was a necessity for the apparatus to be light in weight as it was to be used on golf greens. This would limit the damage to the turf and ease the transportation of the apparatus to and from the greens. Each impact caused a pitchmark rendering that particular point on the turf unsuitable for further impacts. The apparatus, therefore, needed to be manoeuvrable after every impact. It was unlikely that a mains power supply would be available near to a green and it was envisaged that the equipment would be powered by a portable generator. As golf would continue to be played on the greens during testing, the interference to play needed to be kept to a minimum. Finally, the initial budget was to be £3,000 paid over three years. This was subsequently increased with an equipment grant of $12,000 from the Acushnet Company.

For convenience, the design of the equipment was separated into three sections; (1) the launching of the golf ball at the green with variable speed, spin and angle; (2) the recording of the motion of the ball before and after impact and (3) the selection and, if necessary, the development of the apparatus to measure the playing characteristics of the green. These are dealt with in the following sections.

2.2 Projecting the golf ball

(i) Choice of apparatus

Commercially available ball projectors are of two types: mechanical and pneumatic. In research both types have been used. Putnam *et al.* (1983) used a pneumatic projector to project tennis balls at tennis rackets and Thorpe and Canaway (1986a) used both types

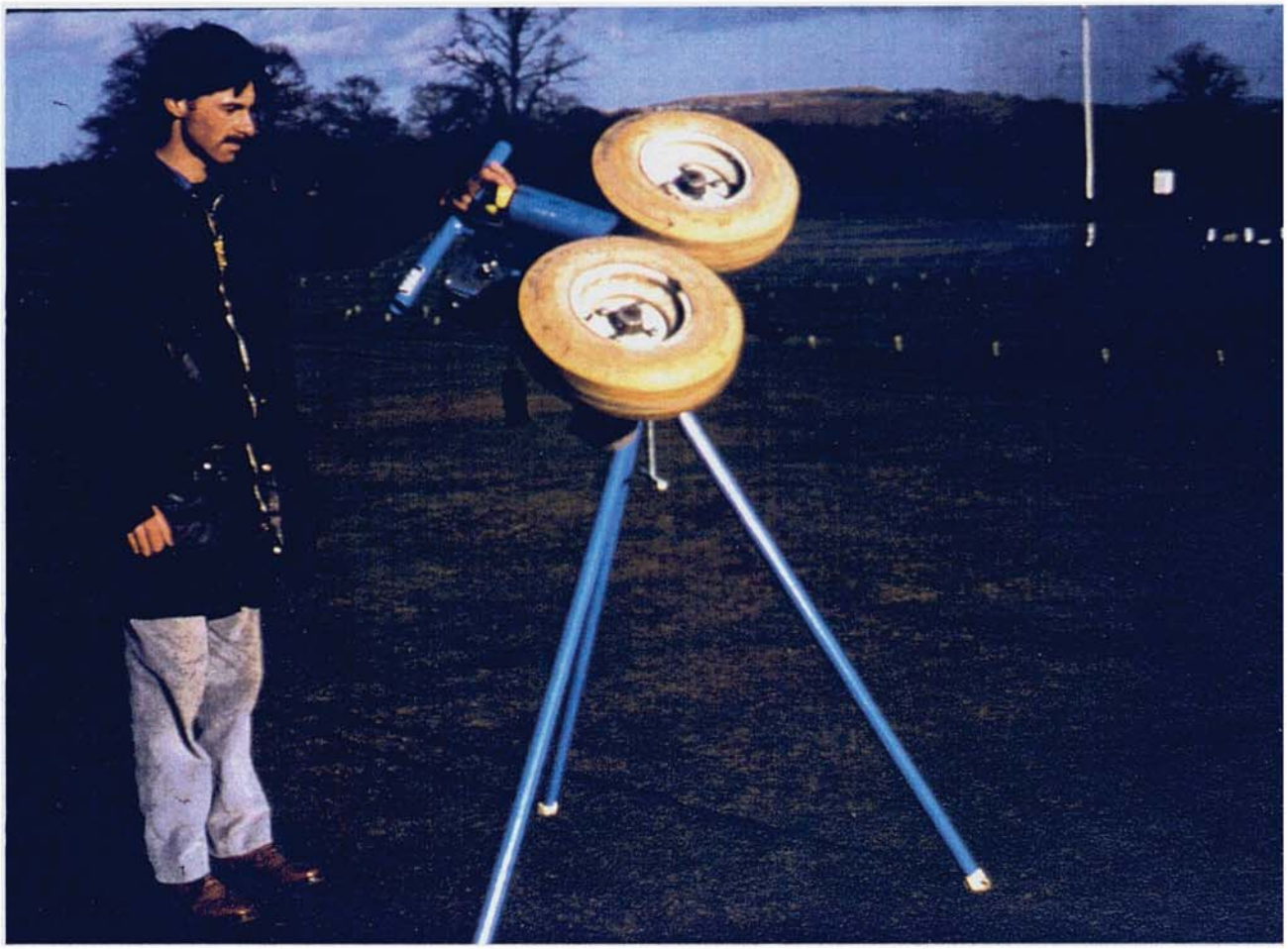

FIGURE 2.1. The original baseball practice machine that was marketed in this country for cricket and tennis. The ball rolls down the chute where it enters the gap between two counter rotating wheels with pneumatic tyres and is subsequently projected out the other side.

of machine in the analysis of ball impacts. Of the two types, the mechanical projector is more suited to golf work because of the importance of spin. Pneumatic projectors have limited scope for controlled variation in spin and were therefore rejected at an early stage. Consequently, a mechanical ball projector was obtained. The "Jugs" bowling machine was franchised in the UK by En-tout-cas Ltd. of Leicester and was marketed as a cricket and tennis practice machine. It was originally designed in the United States as a baseball practice machine and is shown in Figure 2.1. It has two identical 410mm diameter wheels with pneumatic tyres mounted on two 90V d.c. motors and with their axes parallel. The wheels rotate in opposite directions (Figure 2.2). When a ball rolls down the chute it enters the gap between the wheels. It is then gripped and fired out of the other side. The speeds of the two motors can be altered independently in order to impart spin to the balls. A ball attains the approximate average peripheral speed of the wheels, while the spin is determined by the difference in the wheel speeds using,

$$\text{spin} \approx \frac{\text{peripheral velocity of ball}}{\text{diameter of ball}}$$

If the peripheral speeds of the two wheels are $40ms^{-1}$ and $30ms^{-1}$ then a tennis ball of radius 64mm would attain the following;

$$\text{spin} \approx \frac{40 - 30}{0.128} = 79rads^{-1} \text{ and, velocity} \approx \frac{40 + 30}{2} = 35ms^{-1}.$$

As originally supplied, the bowling machine was mounted on a ball joint connected to three legs and could be tilted to almost 45 degrees in any direction about a horizontal plane originating at the ball joint. The scale on the machine purported to fire baseball size balls at up to 100 miles per hour ($44.4ms^{-1}$). The spin attainable by the balls is dependent on the velocity at which the balls are projected. This is limited by the upper and lower velocities of the wheels.

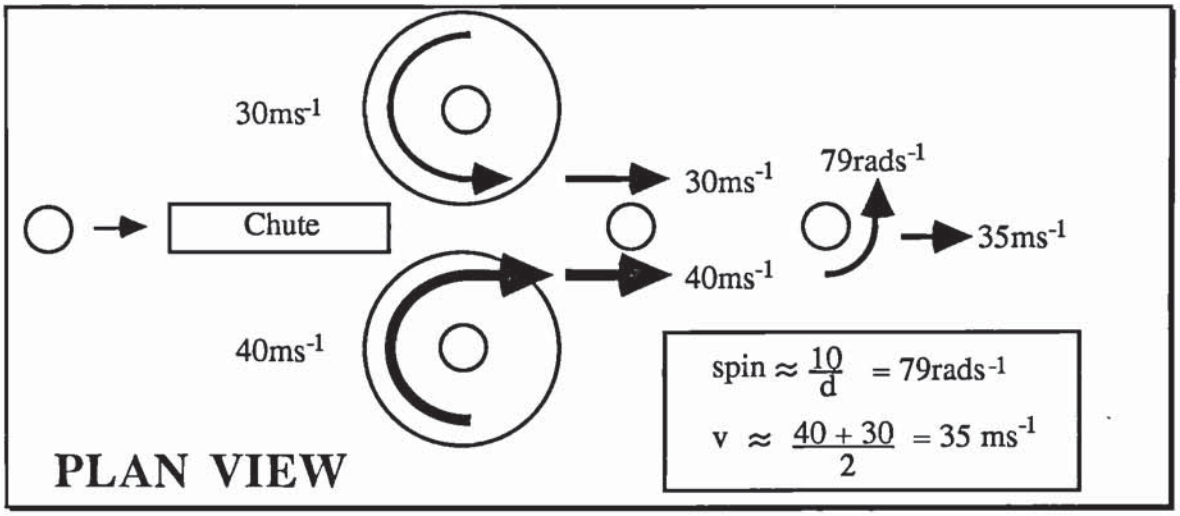

FIGURE 2.2. A schematic diagram showing a method of projecting tennis balls. A ball rolls down the chute and enters the gap where it is gripped by the wheels and projected out the other side. The peripheral velocities of the wheels determine the velocity and spin of the projected ball.

As the velocity of projection approaches these limits, the possible differences in wheel speeds are reduced. This reduces the choice of spin.

It was considered, at this stage, that the "Jugs" bowling machine could have been modified to fire golf balls or used as a model from which to construct a totally new projection device. In conjunction with other projects at the Sports Turf Research Institute, the latter option could have incorporated an adjustable machine to fire footballs, tennis balls and cricket balls as well as golf balls. At this stage, however, the bowling machine was known to work and it was decided to keep to this design as far as was possible.

(ii) Achieving the correct velocity

The new ball firing device was required to project golf balls directly at the ground with speeds up to $30ms^{-1}$, spins up to $930rads^{-1}$ and angles up to 75° (section 1.3). Initial studies using the machine to fire golf balls found that it could not give the balls these speeds and spins and could not fire at the desired angles. When a golf ball entered the gap, it was not gripped firmly by each of the wheels. The ball then moved along the periphery of one of the wheels resulting in a velocity or angle that was not expected. The gap of 37mm seemed to be too large. The manufacturers of the bowling machine, when contacted, recommended that the gap be two thirds of the diameter of the ball to be fired. For golf balls this was 28.4mm; a reduction of 8.6mm. The options considered in the modification of the bowling machine are summarised in Figure 2.3.

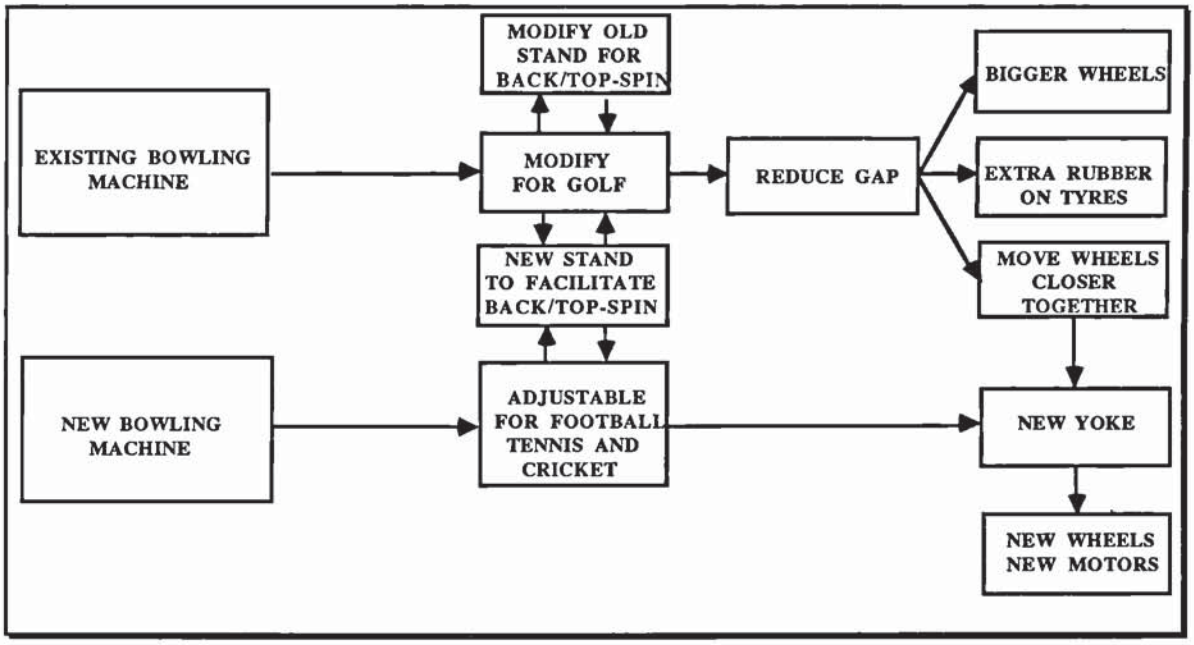

FIGURE 2.3. The options that were considered during the development of the bowling machine.

To decrease the size of the gap between the wheels the first solution involved machining larger wheels and adhering a thickness of rubber to the outside of these. However, there were no firms in the UK that either sold or could manufacture alloy wheel hubs of the correct diameter. It was thought that wheels made out of mild steel (the only type available) would be too heavy and would introduce additional complications such as the need for stronger supports and more powerful motors.

An alternative was to adhere a 100mm wide 4.5mm thick strip of rubber onto the periphery of the existing wheels. This reduced the gap between the wheels to 28mm. When firing golf balls at low velocities, the wheels performed well, but on the first run at a high velocity the rubber became detached proving this solution to be unviable.

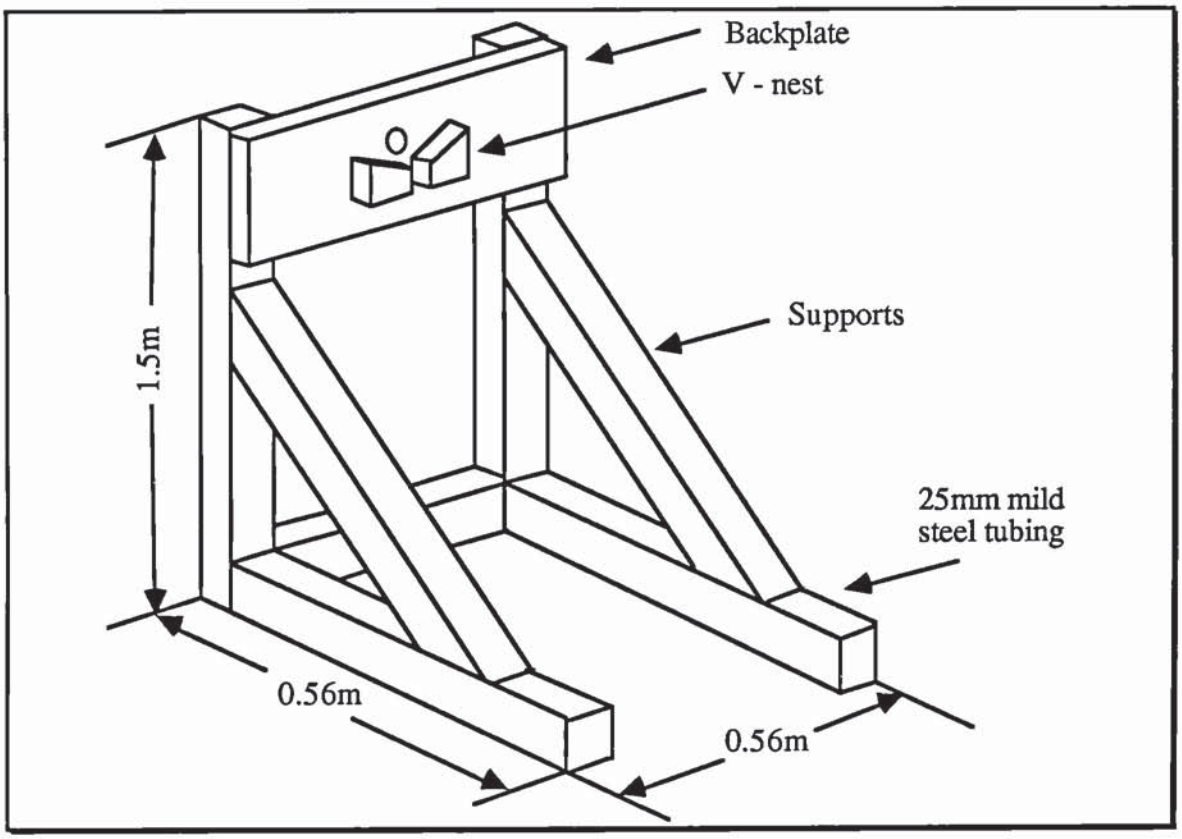

FIGURE 2.4. A schematic diagram (not to scale) showing the design of the stand to hold the ball projection device in a vertical plane thus enabling the projection of the ball with backspin.

A third solution to this problem was to design a new yoke to hold the existing wheels closer together. When the bowling machine was inspected to see how this was to be done, it was found that the motors could be unbolted and new holes for the bolts drilled such that the axes of the motors were approximately 8mm closer together. This proved to be a successful solution.

(iii) Achieving the correct spin

The bowling machine was required to fire golf balls with backspin. This involved supporting the wheels in a vertical plane. Initially, it was thought that the original tripod stand could have been tilted until the wheels were vertical and the motors then supported from underneath in some manner. However, it would not have been easy to move the apparatus between impacts since the centre of gravity was so high. It was therefore decided to design and make a new support for the yoke, motors and wheels and this is shown in Figure 2.4 and Figure 2.5. The stand had a large backplate onto which the bowling machine yoke was bolted and had a V-nest for extra support to the bowling machine body. The struts were made of 25mm mild steel hollow tubing and there were angled supports attached to the horizontal cross members for strength and stability. With the axes of the wheels in a horizontal plane the wheels were able to project the golf balls with topspin or backspin. With the lower wheel rotating faster than the upper wheel the balls emerged with backspin in the same way as the original machine.

It was becoming increasingly difficult to manoeuvre the ball projection device when supported on this stand. A wheel could have been attached to each of the corners of the bottom of the stand but it was thought that, when the projector was in use, the vibrations would have made it move. Instead, two wheels from a golf green top-dressing machine were attached to the bottom of the stand while a handle was attached to the opposite side (Figure 2.5). The side of the stand touching the ground prevented the apparatus from moving during use. This arrangement enabled the ball projector to be moved after each impact and enabled transportation between greens while ensuring that the stand did not damage greens where the projector was used.

Preliminary tests were carried out on the ball projector using a video camera and a stroboscope in a darkened room. A 10W stroboscope loaned by the University of Leeds and a Sony video camera were placed at the point from which the golf balls emerged from the bowling machine. With a stroboscope frequency of 250Hz about 10 images could be recorded on one frame of video tape. Using a ruler placed in the field of view of the camera it was possible to estimate the distances between images directly from the television screen and hence to calculate the speeds. It was found that the ball projector could project golf balls with velocities up to $35ms^{-1}$ and with spins up to about $700rads^{-1}$. The bowling machine dials were marked out in mph and a setting of 30mph on each wheel projected the ball at about 45mph ($20ms^{-1}$). This zero error was found to be consistent throughout the speed range.

The direction at which the golf balls were fired was measured using a clinometer. This employed a small spirit level which was able to rotate within a circular scale, graduated

FIGURE 2.5. The bowling machine after it had been modified to fire golf balls. The two topdressing machine wheels and the handles enabled transportation between greens and between impacts.

every half of a degree. The clinometer was set at the desired angle and placed on the chute on the ball projection device. The angle of the yoke supporting the pneumatic wheels and motors was then altered until the air bubble in the spirit level indicated that the set angle had been reached. Golf balls could be fired at angles up to seventy degrees to the horizontal. At higher angles, the projection of the ball was restricted by the angled struts on the ball projection device stand.

The development of the ball projection device and its stand occurred in parallel with the development of the process for the recording of the impacts. At this stage of the project it was envisaged that the exact values of the spin, speed and angle of the ball after projection would be calculated at the recording stage and were not required from an exact calibration of the projection device.

2.3 Recording the impacts

(i) Introduction

The use of infra-red light beams as timing gates was considered as a method of measuring the velocities and angles of the ball before and after impact. A set of timing gates already in use at the Institute was set up to try and measure the velocity of the ball as it left the bowling machine. As the ball cut the first light-beam a timer was started and then stopped by the passage of the ball through the second beam. However, this was not deemed suitable since an additional method was required to record the spin of the ball. Other methods such as using radar or sonar devices to record the motion of the ball were not considered since the potential cost was high and the analysis required to measure the spin of a rotating object was very complicated.

During the literature review it was found that photometric methods were used most often for recording impacts of spheres with surfaces. Putnam and Baker (1984) used stroboscope photography to study the impact of tennis balls with differently strung tennis rackets as did Maw *et al.* (1981) when they studied the impact of disc shaped pucks with surfaces of a similar material. Tatara (1981) used high speed cine film running at 5000 frames per second (fps) to study the impact of tennis balls with the ground while Thorpe and Canaway (1986) used ordinary cine film running at 64 fps to record the impacts of tennis balls with different playing surfaces. These methods were evaluated and it was found that the use of cine film was not suitable for this project. Using high speed film would have been far too expensive since each film would have cost about £20. It was envisaged that about 500 impacts were required and since there could only be one impact per film, the budget would have been used up very quickly. A normal cine camera running at 64fps would not have been fast enough to record balls impacting at speeds

over $10ms^{-1}$. Even at this slow speed the golf ball images would have been more than 150mm apart and the camera would have had to be at such a distance to see multiple images that the spin would have been unmeasurable. The method of stroboscope photography was ultimately chosen since it appeared to be the cheapest and easiest method of evaluating the impacts of golf balls on turf. It was envisaged that a Polaroid type of instant film would be used which would provide instant records of the impacts. This was the method employed by the USGA and the Acushnet Company in the analysis of the flight of a golf ball after impacting with golf club face.

Preliminary tests on the bowling machine used stroboscope photography employing a Sony video camera and a 10W stroboscope as a light source. However, this source was very weak compared to the amount of background light that is present out of doors and a more powerful stroboscope was needed. A new stroboscope, a Drelloscope 1017N, was subsequently tested and purchased. It was able to run at up to 600 flashes per second, with a flash duration of less than 10μs and with a maximum power output of 200J at 50Hz. It had an illumination area of approximately $7m^2$ at a distance of 2m. The power unit was driven by a pulse generator which provided 10V spiked pulses at the desired frequency.

Initially, this stroboscope was used in conjunction with a Nikon FE 35mm still camera to look at impacts on small pieces of artificial turf. The ball was fired indoors in complete darkness and the camera shutter opened using the "B" setting, while the stroboscope was switched on manually at the appropriate time. The camera shutter was then released after the impact. The film was thus exposed with images of the ball at equal points in time along its incoming and outgoing path. Although the images obtained were ideal for the purposes of analysis, it was not a very refined system since it required the co-ordination of two people to ensure that the delivery of the ball and the opening of the shutter occurred at the same time. An automatic method of activating the stroboscope and camera as the ball entered the field of view was needed and the use of electronic "triggers" was researched.

(ii) Activating the camera and stroboscope

An electronic trigger was designed and built using standard components, the circuit diagram for which is shown in Figure 2.6. A high powered infra-red emitter was located on one side of the chute with a detector placed on the opposite side (infra-red light was used to minimise the effect of sunlight on the detector). The 500kΩ potentiometer connected to pin 2 of the operational amplifier was used to set the voltage level representing the background light close to the voltage level of the detector. When a ball passed in front of the detector, its voltage dropped below that of the background radiation

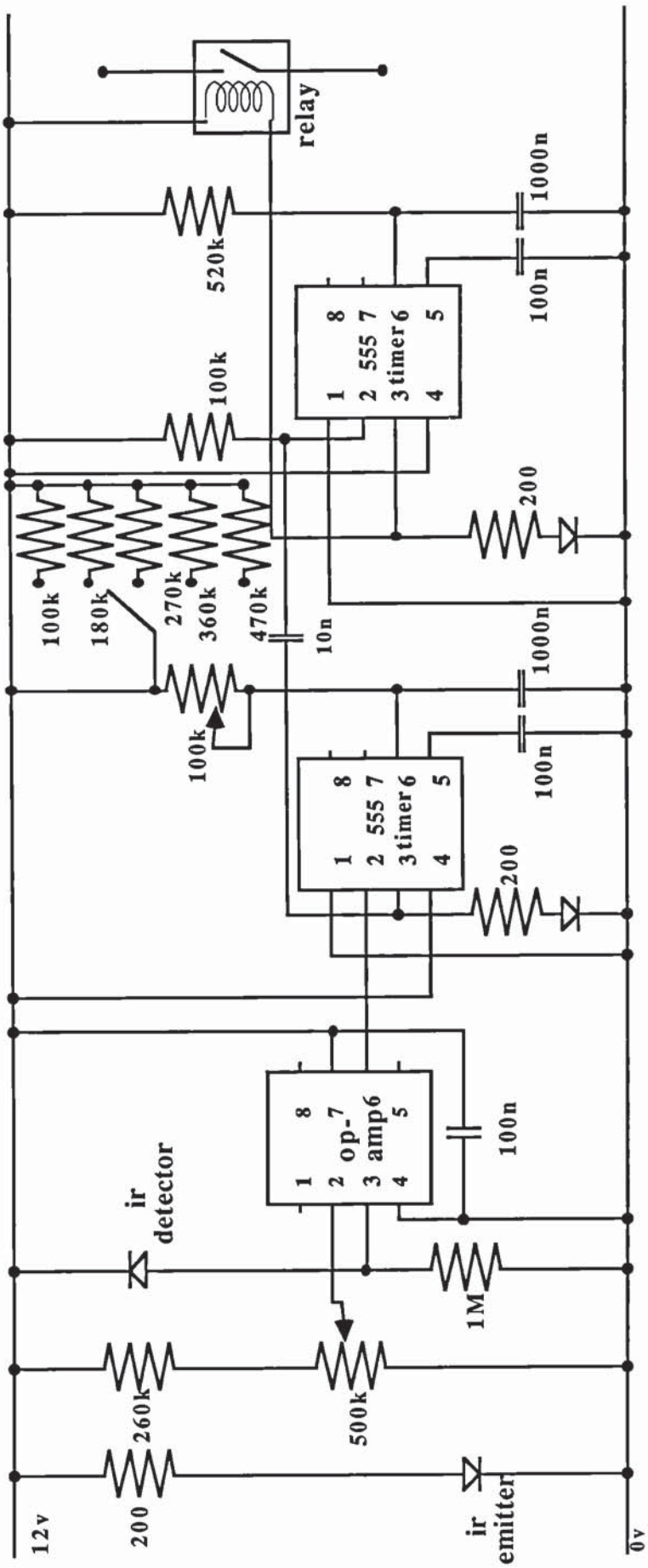

FIGURE 2.6. A circuit diagram of the trigger that was developed to activate the camera and stroboscope as the ball entered the field of view of the camera.

and a pulse was output from the amplifier. This output was then passed to the input of the first 555-timer which subsequently output a square pulse, the length of which was determined by the RC value across pin 6. The falling edge of the output pulse from the first 555-timer caused the second 555-timer to output a pulse half a second long. The final pulse was used to drive a solenoid (replaced by a relay in Figure 2.6) which activated the shutter release of the camera. It was possible to alter the time delay before the output pulse by changing the RC value across pin 6 of the first 555-timer. This was done using a switch to increase the resistance from 100 kΩ up to 470kΩ in 90kΩ intervals. The resistance could be altered continuously throughout this range using a 100kΩ potentiometer connected in series to these resistors. It was necessary to have a variable time delay since the travel time of the ball to the point of impact was different at different velocities and angles. A diode was placed in the 12V line so that incorrect battery connections would not damage the components. The circuit was encased in an diecast aluminium box measuring 14mm x 100mm x 75mm and the 12V power supply, inputs and outputs were connected to 4mm insulated terminals using 4mm banana plugs. Red LED's were connected across the output of the two 555-timers and were attached to the lid of the box. The first indicated the passage of the ball through the light beam while the second indicated the triggering of the camera after a set time delay.

It was found that it was difficult to predict the length of time required for the solenoid to push against the shutter release spring of the camera and hence to set the time delay on the trigger. Camera systems were evaluated and a direct method of using the trigger to activate the camera was found. Consequently a Bronica ETRS camera was purchased which could be activated remotely by electronic means: closing a switch across the relay input on its motor-wind caused the camera shutter to open. The solenoid on the trigger was therefore replaced by a relay switch. The triggering of the camera occurred almost instantaneously with the output of the trigger and the time delay could be set with much more confidence.

The stroboscope was switched on manually at this stage, so as an added refinement the trigger was used to activate the pulse generator which drove the stroboscope power unit shown in Figure 2.7. When used on the "gate" mode, the pulse generator only produced pulses when the gate input voltage was above 1V. This pulse was provided by the second 555 timer in the trigger and was the same pulse as that which closed the trigger relay. The electronic trigger was therefore used to activate both the camera and stroboscope as the ball entered the camera's field of view.

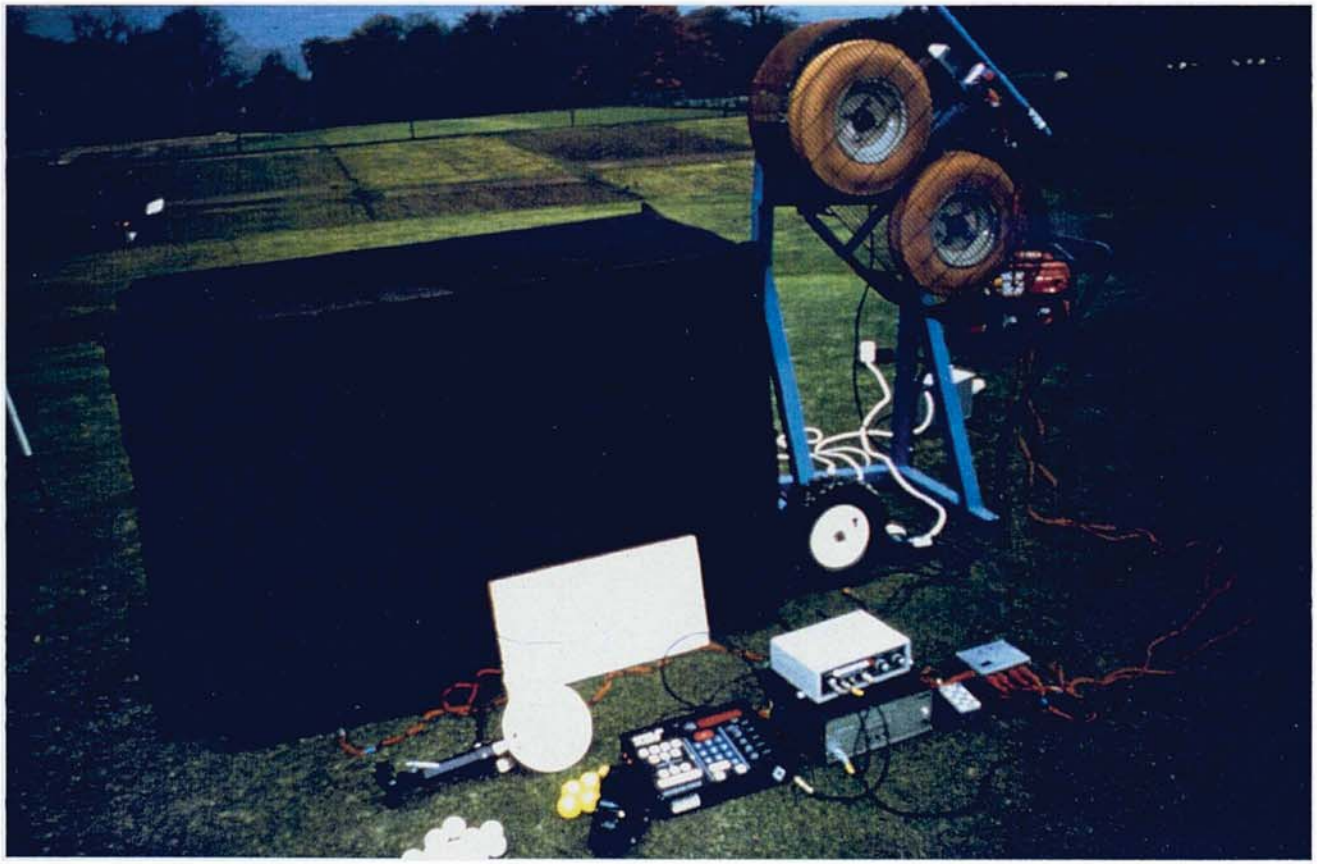

FIGURE 2.7. The complete set of apparatus used to photograph the impact of a golf ball on a green.

(iii) Exposing the film

The Bronica camera had the advantage of interchangeable backs which held different types of film. It was thus possible to set up the system using Polaroid instant film to check that the golf balls were landing in the centre of the camera view and that the camera and stroboscope were being triggered at the appropriate time. It was then possible to change the film back to one containing 220 rollfilm for permanent records and enlargements of impacts.

A distance scale was required in the picture in order to calculate the velocity of the ball through the picture frame. Having a scale in the field of view while the impact was taking place either obscured the view of the impact or reflected too much light from the stroboscope. However, the camera had the facility for multiple exposures and it was possible to pre-expose each frame with an image of a scale placed in the plane of the impact of the ball. This plane was determined by the line of pitchmarks that were visible after setting up the system. The polaroid instant film was used for finding the correct exposures for the scale and for the impact so that one image did not obscure the other.

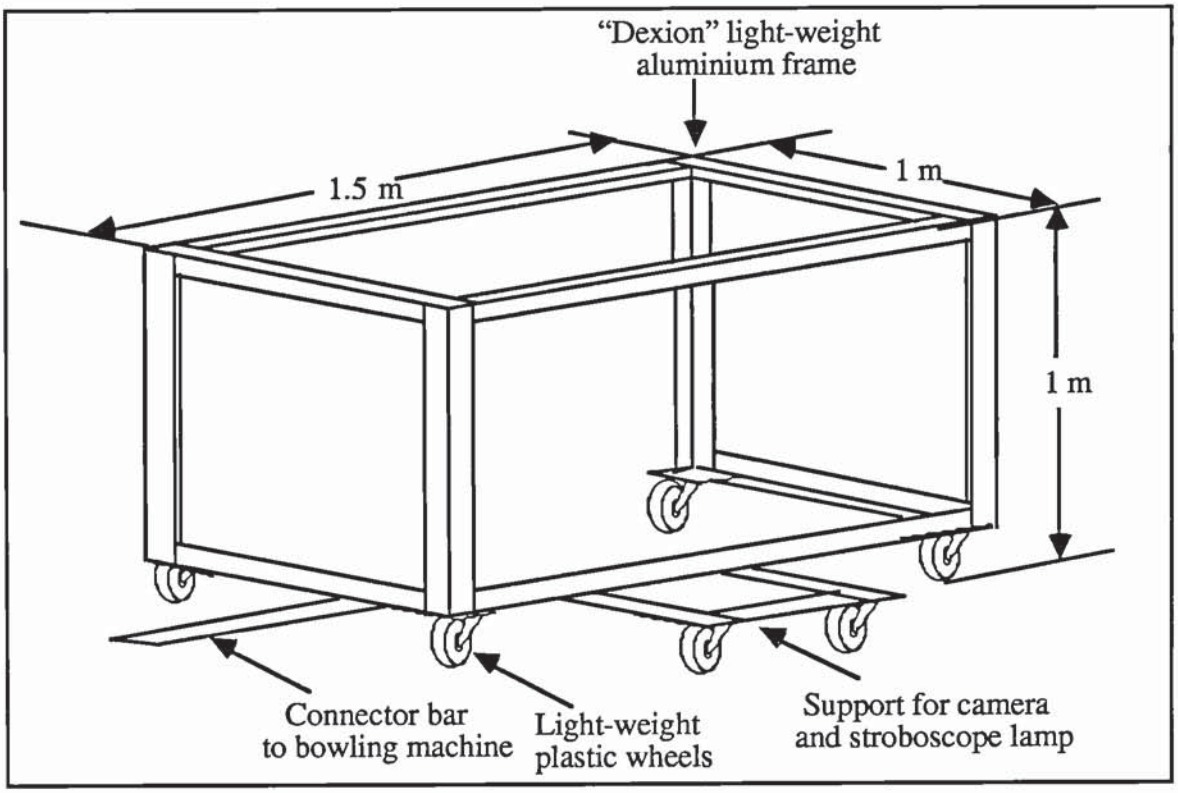

FIGURE 2.8. A schematic diagram to show the construction of the frame of the tent designed to block out the background light from the camera. The frame is usually covered with thick black cloth which has a hole in the end nearest the bowling machine through which to fire the golf balls.

It was necessary to block out the background light during the photograph of the impact because the camera shutter was open for a relatively long duration (one thirtieth of a second) and the intensity of background light was so much greater than that provided by the stroboscope. A small tent frame was constructed from light weight "Dexion" metal measuring 1.5m long by 1m high by 1m wide and having a plastic 100mm diameter wheel on each corner. The camera and stroboscope were attached to a horizontal support which also had two wheels. This ensured that the stroboscope and camera remained in the same place relative to the tent frame whenever the latter was moved. The frame was covered with thick black cloth with a hole in one end through which the ball could be fired. This is shown schematically in Figure 2.9. One side of the cloth could be lifted up in order to move the camera and stroboscope nearer or further away from the bowling machine according to the angle at which the ball was being fired or to alter the camera settings. The bowling machine was attached by a single length of Dexion metal to the frame at the end through which the ball was fired so that when the bowling machine was moved after an impact, the tent, camera and stroboscope lamp moved with it. The bowling machine was pulled backwards since it was difficult to push it along with the tent and keep them both aligned. Restricting the connection between the ball projector and the tent to a single length of metal reduced the vibrations that were passed from the projector stand to the tent frame.

Since the apparatus was to be used on golf greens far away from any power source, a portable power supply was needed. A Robin 1.5kW generator was purchased which provided enough power for the bowling machine (700W) and the stroboscope (200W). The generator was also chosen because it was light enough to be lifted by one person and was relatively unobtrusive, therefore not distracting golfers.

(iv) Summary

The complete set of apparatus is shown in Figure 2.7 and to summarise, a typical golf ball impact is carried out as follows,

1. A golf ball rolls down the chute of the ball projector and cuts the infra-red light beam.
2. The ball enters the gap where it is gripped by the wheels and projected, with the required spin, speed and angle, through the hole in the tent wall towards the ground.
3. As the ball enters the field of view of the camera, the trigger, set to the required time delay, opens the camera shutter and activates the pulse generator which drives the stroboscope.
4. The ball rebounds, the camera shutter closes after one thirtieth of a second and the film automatically winds on.

5. The ball projector, tent, camera and stroboscope lamp are all moved about 100mm ready for the next impact.

After each impact, the depth of the pitchmark created was measured using a USGA green hardness tester (Figure 2.15). This consisted of a brass sphere the size of a golf ball threaded onto a shaft 120mm long. A freely rotating wheel was threaded onto this shaft. The sphere was placed below a metal shoulder on the level ground with the shaft vertical. The wheel was then rotated upwards until it became restricted by the shoulder. This provided a reference distance between the bottom of the sphere and the wheel. When placed in a pitchmark below the shoulder, the wheel was rotated upwards along the thread until it again became restricted. The distance between the bottom of the sphere and the wheel was now larger, the extra distance indicating the depth of the pitchmark. The number of revolutions were counted since each revolution indicated an upward movement of one twentieth of an inch. This gave an estimate of the depth of the pitchmark.

2.4 Application in the field

An example of a photograph of a golf ball impact is shown in Figure 2.10. The ball is entering from the right at 23.6ms^{-1} at an angle of 50° to the horizontal and with about 125rads^{-1} backspin. It can be seen that the ball slows down after impact (to 3.8ms^{-1}) and rebounds at an angle much larger than the angle of incidence (72°). The spin of the ball has been modified to topspin.

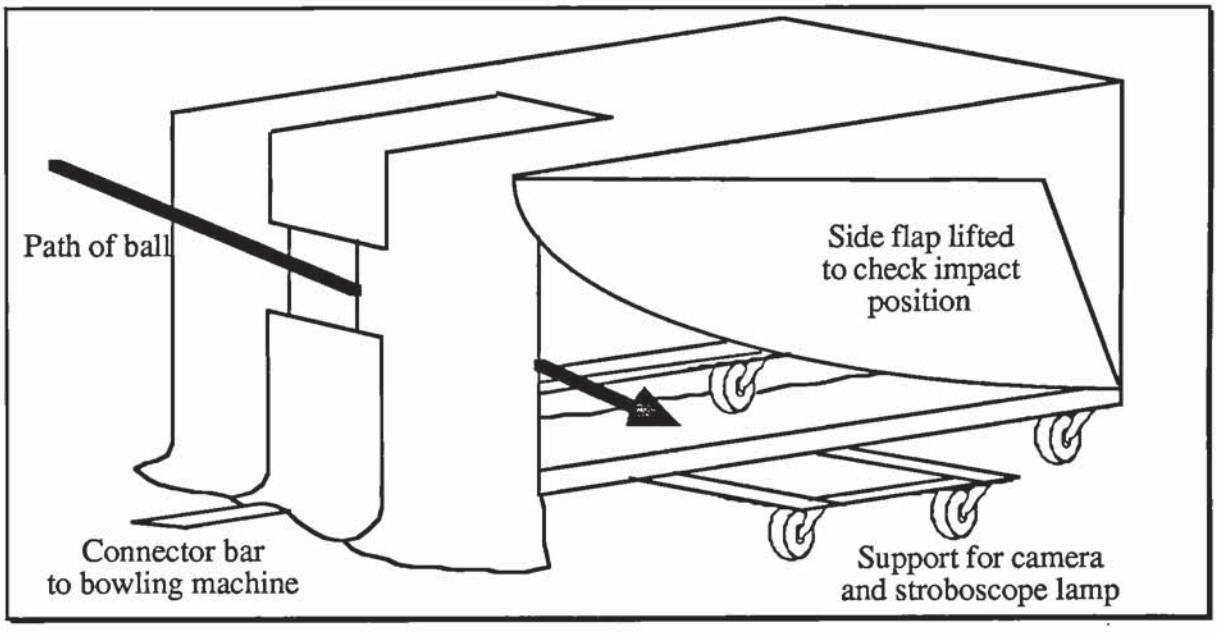

FIGURE 2.9. A schematic diagram showing the enclosure used to reduce background light during the photograph of a ball/turf impact.

Although the apparatus and method used to create this photograph is relatively simple in principle, its use in a field situation is relatively difficult. One of the lessons learnt during

this project was to be prepared for any eventuality and above all to be patient. By the end of the project an accessory kit had been assembled which contained screwdrivers, screws, Allen keys, soldering iron and all manner of electronic spares.

Problems in the field usually related to the electronic trigger required to activate the camera and stroboscope. One necessity was to label clearly all wires connected to the trigger. This was soon discovered when the battery was connected the wrong way round resulting in the loss of the 555 timers, op-amp, emitter and detector. Consequently, a diode was placed on the 12V input line of the trigger and spare detectors, emitters and chips were included in the accessory kit.

One of the practical considerations, when on the green, was to plan the orientation of the apparatus with respect to the path of the sun. If the sun shone onto the detector, it caused false activation of the trigger. If it shone into the tent then the stroboscope photographs became washed out because of too much light. Other practicalities to be taken into account were the size and shape of the green and the position of the flag since play was to continue throughout testing. Surprisingly perhaps, golfers were not restricted by the apparatus as it was usually placed at the back of the green with the flag placed near the front. The greatest problem, in fact, was having the time to answer the questions asked by passing golfers who were understandably bemused by this odd behaviour on a golf green.

When on field work, it was found to be advantageous to have an assistant to aid with the transportation of the apparatus to and from the green on which the tests were carried out. Another advantage was that the assistant could answer the constant barrage of questions!

During the study of the impacts it was found that it was essential to have a fixed procedure so that the camera, stroboscope and projection device were all set correctly. First of all, the bowling machine was set at the correct velocity and using the clinometer, at the angle required. The tent frame was then attached to the ball projection device with the single length of Dexion and the tent cover erected upon it. The tent material had a slit in the side nearest the projection device (see Figure 2.9). Two rectangular pieces of material were attached along this slit using Velcro so that a square hole was created in the side of the tent. The ball was then fired through this hole. The camera and stroboscope could then be screwed onto the support attached to the tent frame and positioned so that the impact point was viewed.

The camera was first loaded with Polaroid film and several test impacts were carried out so that the system could be checked. The main task, at this stage, was in determining the correct time delay for the camera and stroboscope to allow for the passage of the ball from

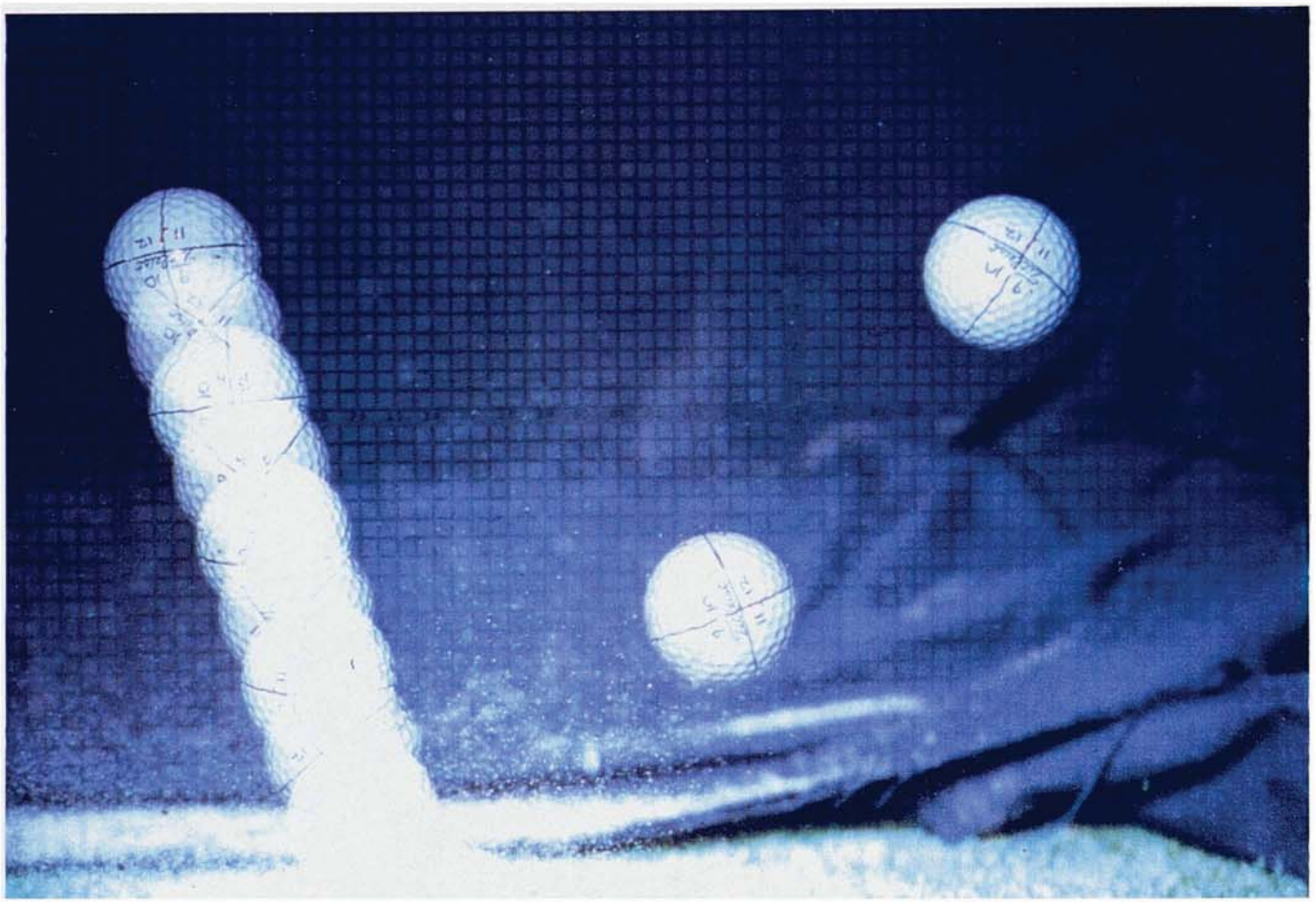

FIGURE 2.10 A stroboscope photograph of a typical impact of a golf ball with natural turf (the ball enters from the right).

the infra-red light beam to the point of impact. Once this was found, the camera was loaded with 220 roll film and a series of tests carried out. Once the angle of incidence and the velocity of the impact was fixed, the settings of the timer and stroboscope could also remain fixed. The complete apparatus could then be moved so that the next impact did not land in a previous pitchmark. It was possible to increase the backspin of the impacting ball without the need to vary the position of the camera and stroboscope and without having to alter the time delay of the trigger. This was achieved by decreasing the velocity of the top wheel on the projection device and increasing the velocity of the bottom wheel by the same amount. Thus, the velocity and angle were kept fixed while the spin was increased.

Before any impacts were studied, the roll of film was marked by taking a photograph of a piece of card on which were details of the golf course, the date and the tests to be carried out. This ensured that the films could be identified after they had been developed. Series of tests were marked by photographing a piece of card on which test information was written.

As discussed earlier, each photograph of an impact was composed of an image of a grid placed in the plane of the impact and the stroboscopic photograph of the impact itself (Figure 2.10). The grid was used as a frame of reference during the analysis and is discussed in the next section. It was exposed using natural light and the camera settings required to obtain the correct exposure was determined using Polaroid film. The camera settings required for the grid and for the impact were very different (f11 at 1/500th, say, against f22 at 1/30th).

With these practical considerations in mind, the photograph of an impact would have taken place as follows. First, the grid was exposed onto the photograph and the camera settings changed in preparation for an impact. The side flap of the tent was fixed in place and the golf ball projected at the turf. The side flap of the tent was lifted up and the position of the impact checked to determine whether it had occurred in the field of view of the camera. Notes were then taken of the picture number, the frequency of the stroboscope, the pitchmark size and any other general observations.

The system was checked when the velocity or angle of impact was changed using the Polaroid film. Regular checks were essential since it was very easy to forget to change camera settings and *anyone* can forget to remove the lens cap!

2.5 Analysis of the photographs

(i) Introduction

The films containing the photographs of the impacts were developed at the STRI using standard techniques. Methods of analysis were then required to remove the information from the pictures. Initially, each picture was printed onto photographic paper and the analysis carried out directly on the print. However, this was a long and expensive process and a quicker and cheaper option was to project the images onto a white sheet. The negatives were then analysed directly. A projector with the correct film holder was not available so an ordinary photographic enlarger was used with a fan mounted on its cooling fins to prevent overheating.

This section describes the methods used to analyse the photographs of the impacts and gives some indication of the errors involved. A photograph of a typical impact is shown in Figure 2.10. The grid provides a reference from which to measure distances to enable the calculation of the velocities. Exposing the grid in the same plane as the impact reduced the effect of distortion of the images due to spherical abberations in the camera lens. However, the grid was not always clear over the whole of the photograph and two methods of analysing the pictures were employed. These methods, along with a method of calculating the three dimensional spin of the ball from two dimensional photographs are described in the following sections.

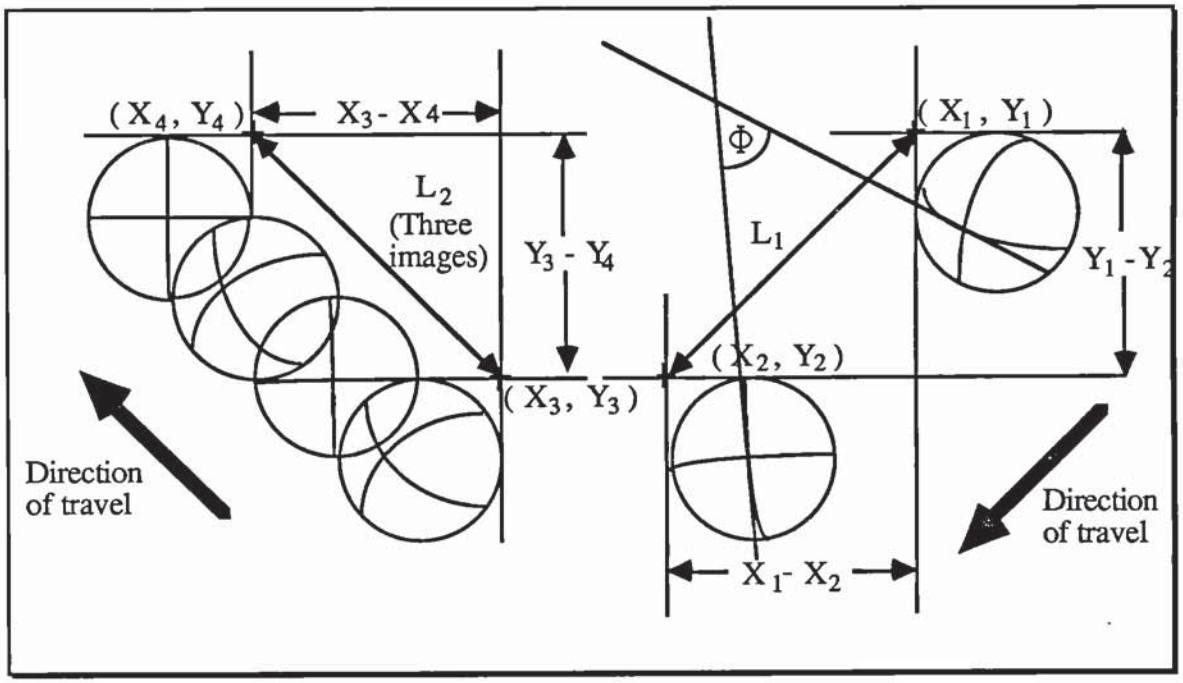

FIGURE 2.11. A method of calculating the velocities and angles before and after impact using a grid exposed onto the photograph.

(ii) A method using co-ordinates representing the position of the ball

Using this method the co-ordinates of points on the ball were read from the scale on the photograph and the distances travelled in the duration between images calculated. Consider an image of the ball on the photograph surrounded by a square with sides equal to the diameter of the ball and whose middle point lies on the centre of the circle. The upper left hand corner of the square was chosen to represent the position of the incoming ball's images. The upper right hand corner was chosen to represent the position of the outgoing ball's images. These correspond to the points (X_1, Y_1), (X_2, Y_2), (X_3, Y_3) and (X_4, Y_4) in Figure 2.11.

Since the grid was placed directly on the ground, the co-ordinates were read with respect to the direction of the average slope of the turf at the point of impact. If the frequency of the stroboscope was F, then the velocities before and after impact are,

$$V_i = F \sqrt{((X_1 - X_2)^2 + (Y_1 - Y_2)^2)} \qquad \text{eqn. 2.1}$$

$$V_f = \frac{F}{M} \sqrt{((X_3 - X_4)^2 + (Y_3 - Y_4)^2)} \qquad \text{eqn. 2.2}$$

The subscripts "i" and "f" denote the incoming and outgoing ball respectively and "M" is the number of images used in the calculation. The direction of the motion of the ball, to the horizontal, can be calculated using the following equations,

$$\Theta_i = \text{TAN}^{-1} \frac{(Y_1 - Y_2)}{(X_1 - X_2)} \qquad \text{eqn. 2.3}$$

and

$$\Theta_f = \text{TAN}^{-1} \frac{(Y_3 - Y_4)}{(X_3 - X_4)} \qquad \text{eqn. 2.4}$$

where the subscripts "i" and "f" again denote the incident and rebounding ball. Usually, there were only two images before impact. After impact, however, the ball was moving much slower resulting in many images of the ball.

The orthogonal circles seen on the golf balls in Figure 2.10 and shown schematically in Figure 2.11 enabled the calculation of the spin before and after impact to be made. The numbers written at the points where the circles crossed were used to ascertain the direction of rotation. The spin was calculated by measuring the angle through which the lines on the ball rotated using a ruler and a protractor. An example would be, for instance, angle Φ in Figure 2.11. Lines on the ball were chosen that were relatively straight and as many images as possible were used. It was possible to mistake the direction of rotation of the outgoing ball; for instance a rotation of 45° in an anticlockwise direction could be mistaken as 315° in a clockwise direction. This could indicate either a small topspin or a large backspin. Knowing the settings of the bowling machine when

the ball was fired resolved this uncertainty. For example, if the ball had been travelling initially with zero spin in the example just given, it would have been unlikely for the ball to rebound with backspin. If a ball rotated through Φ radians in N images, then,

$$\omega = \pm \frac{\Phi \times F}{N} \qquad \text{eqn. 2.5}$$

where the "+" sign denotes topspin and the "-" sign backspin.

Appendix B contains the calculations required to estimate the errors in the use of this method for calculating the velocity and angle before and after impact. It was found that an error of 1mm in placing each of the co-ordinates X_1 to X_4 and Y_1 to Y_4 accumulated to an error of 1.4mm in the calculation of the distances L_1 and L_2 in Figure 2.11. In general, the distance across which L_1 and L_2 were measured was about 70mm and hence the percentage error in these values was approximately 2%.

The error in the co-ordinates produces an error in the calculation of the angle to the horizontal of the ball's motion. If the distance between two images was about 70mm and the ball was travelling at 45° to the horizontal, then an error of 1mm in each of the co-ordinates gave a range in the angle of 43.4° to 46.6° for the angle. This was represented as an error of ±1.6°

The error in the measurement of the angle through which the ball rotated was estimated by repeatedly measuring the angle and finding the standard deviation of the mean. The rotation of a ball was measured repeatedly using images in which the lines on the ball were distinctly curved (as in Figure 2.11). It was found that the standard deviations of these measurements became larger than about 5% if the line was further than half a radius from the centre of the ball. Thus, only lines which were within a half a radius of the centre of the ball were used. Taking the measurement over a number of images helped to reduce the inaccuracy of using slightly curved lines to measure the rotation of the ball.

(iii) Systematic errors using the co-ordinate method

Systematic errors could have occurred when aligning the grid along the true plane of impact. As described earlier, several preliminary impacts were made in order to check that the correct exposure on the camera was being used and that the time delay was correct. The grid was aligned to the line of pitchmarks created. Systematic errors could have occurred at this point since the grid may have been placed at an angle to the plane through which the ball passed or in a parallel plane either nearer or further away than the true plane of impact. In Appendix B it is shown that if lateral displacement is less than one and a half times the radius of the ball or if angular displacement is less than 10°, then the errors incurred are not significant. It was found that these criteria were easily met in practice.

(iii) Analysis of the photographs using the distances between images

If the grid was not exposed correctly onto the photograph then it was difficult to use it as a co-ordinate system for the calculations in the previous section since the 1mm intervals were not visible. Usually, however, the grid was clear enough to see the main lines and as an alternative scale, the distance between two vertical lines and along a horizontal line was measured (denoted by "l" in Figure 2.12). If there were more than two images before or after impact then the distance across as many images as possible were taken and the calculation for the velocity divided by the number of images. The angles of the incoming and outgoing ball were measured with respect to the reference line using a protractor. The spin was measured using the method described in the previous section.

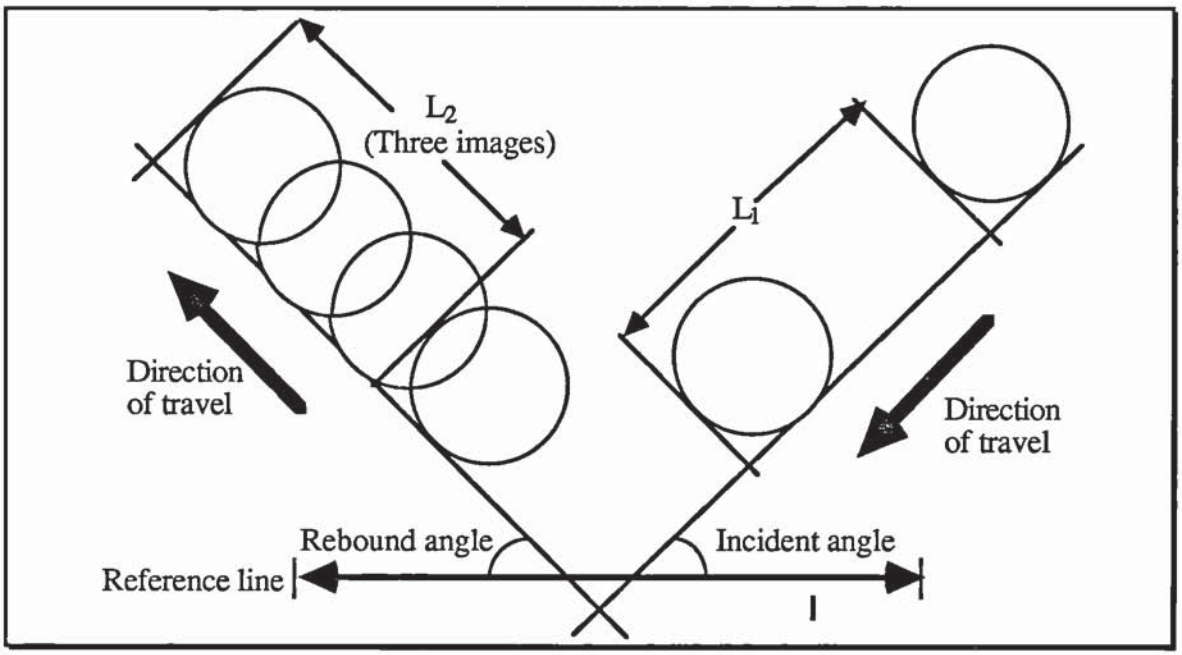

FIGURE 2.12. A method of calculating the velocities of the ball before and after impact. The distances are measured directly from the photograph and converted to "real" distances using the reference line. This gives a scale if the distance "l" in the photograph is known.

The errors were estimated by repeating the same measurement on the same photograph a number of times and calculating the standard deviation of the mean. The angles before and after impact were found to have a standard deviation of less than ±™° while the distances used in the velocity calculation had an error of about ±1.5mm. Thus, a conservative estimate of the errors in measuring the angles of incidence and rebound and the distances between images was ±1° and ±2mm respectively. Since the distance between images for the incoming ball was about 70mm, the error in the distance measurement was about 3%. The errors occurring in the measurement of the angle of rotation of the ball were the same as in the previous section. This method could not take into account the distortions in the lens or the effects of spherical aberrations and was therefore to be used when the co-ordinate method was not suitable.

(iv) A comparison of the two methods for analysing the photographs

Table 2.1 shows the distances between images before and after impact (L_1 and L_2) and the angles of incidence and rebound (Θ_1 and Θ_2) for five photographs calculated using the two different analysis techniques. The titles "coord" and "ruled" refer to the co-ordinate method and the method using a ruler to measure the distance between images. It was found that, in all but one case, the results did not vary significantly between the methods when the errors described in the previous sections were taken into account. This indicated that the distortions due to spherical aberrations in the camera lens were minimal. It was decided, therefore, that the method using a ruler and protractor to measure directly from the photograph was the most suitable since it involved the least number of stages in the analysis. The number of stages in the co-ordinate method could have been reduced by the use of a digitiser to enter the co-ordinates representing the ball directly into a computer.

No.	L_1 (mm)		L_2 (mm)		Θ_1 (°)		Θ_2 (°)	
	coord	ruled	coord	ruled	coord	ruled	coord	ruled
1	81	83	32	32	45	46	39	38
2	75	76	37	37	45	45	36	39
3	80	81	30	30	46	46	44	42
4	83	85	33	32	45	45	38	36
5	83	80	33	34	44	45	38	37

TABLE 2.1. A comparison of the two methods of photograph analysis for five photographs. The distances L_1 and L_2 and the angles Θ_1 and Θ_2 refer to the distances and angles before and after impact respectively.

(v) A method of calculating three-dimensional spin using two dimensional photographs

During the analysis of the pictures using the methods described above, it was considered that estimates of the side spin would help to explain odd results that occurred. The method described in Appendix C was developed to calculate the three dimensional spin of the ball using the co-ordinates of points on images from the two dimensional photographs. It consists of three stages, the first modifies the two dimensional co-ordinates from the photographs to points in three-dimensional space using a method called relief displacement. This is required since points nearer the camera than the plane containing the co-ordinate system are displaced outwards from the centre of the photograph. The second stage calculates the spin axis of the ball using vector analysis and three dimensional geometry. The third stage calculates the magnitude of the spin. It is then possible to calculate the spin in three dimensions.

It was found that the method worked well but that errors accumulated quite quickly due to the subtraction of co-ordinates that were very close together. This occurred because the errors in taking co-ordinates from the photographs were quite large compared to the size of the image of the ball. The method of calculating the three dimensional spin from two dimensional photographs, therefore, would work well if the images of the ball were larger. This could be achieved by having a longer focal length lens or a bigger sports ball and would possibly be more suitable for tennis, cricket or football.

2.6 The physical characteristics of golf greens

At this stage, it is necessary leave the acquisition and analysis of the stroboscope photographs in order to consider the apparatus for determining the characteristics of the greens on which the stroboscope testing was to be done. The relationships between the results of the impacts and the characteristics of the greens will show the effect of maintenance and construction on the ball/turf impacts. This will be carried out in Chapter 4 where the photographs of impacts will be related to the tests described in this section. Existing tests that were simple to use were chosen to measure the green characteristics. Eleven types of measurement were used and these are outlined below.

(i) Ball rebound resilience

Ball rebound resilience is expressed as,

$$\text{ball rebound resilience} = \frac{\text{Bounce height}}{\text{Release height}} \times 100 \qquad \text{eqn. 2.6}$$

This test has been used predominantly for the assessment of football pitches and tennis courts (Holmes and Bell, 1986). Heights of drop were chosen that were relevant to the sport; for instance, footballs were dropped from a height of 3m. Colclough & Canaway (1988) dropped golf balls from a height of 5m. This was a compromise between the heights that golf balls fall from in play and the size of an apparatus that was manageable. Figure 2.13 shows the ball bounce apparatus. Pulling a cord connected to a carrier containing 12 balls on top of the 5m pole caused a ball to be dropped. The rebounding ball was filmed using a video camera against the backdrop of a scale marked out in centimetres. The camera was placed approximately 5m from the scale and a telephoto lens used. This was necessary to reduce parallax errors. The video recording was then analysed frame by frame. If air resistance is neglected, then the ball rebound resilience is related to another commonly used measure of rebound - the coefficient of restitution, e, where:

$$e = \frac{\text{velocity of separation}}{\text{velocity of approach}} \qquad \text{eqn. 2.7}$$

and hence,

$$\text{Ball rebound resilience} = e^2$$

Originally, the coefficient of restitution was considered to be a constant. It has been found, however, that the coefficient of restitution of a golf ball on a hard surface decreases with velocity and increases with temperature (Briggs, 1949).

(ii) Clegg impact soil tester

The Clegg impact soil tester (Clegg 1976, Lush 1985) shown in Figure 2.14 has been used in the past for the measurement of the firmness of road bases and for the assessment of cricket pitches. An indenter is dropped down a guide tube onto the surface to be tested. An accelerometer located in the hammer measures the peak deceleration as it hits the surface and the result is displayed in multiples of $10g$, where g is the acceleration due to gravity. A 0.5kg cylindrical indentor is used most commonly and is dropped from a height of 300mm. A 1kg indenter dropped from a height of 300mm has the same momentum as a golf ball travelling at about $50ms^{-1}$. This is greater than the velocity attained by a golf ball hit with a driver. Three 1kg indenters were developed to try to gain an insight into the maximum forces experienced by a golf ball on impact with the green. The three indenters developed were, a 1.0kg cylindrical indenter, a 1.0kg cylindrical indenter with an end shaped like a golf ball and a 1.0kg hammer with a Titleist golf ball adhered to its end. These are shown in Figure 2.14. An assumption that would be useful in later models is that the ball does not deform. The golf ball shaped indenter and the indenter with a golf ball adhered to its end were designed to study the effects of the elastic properties of the ball on the impact with the ground. It was ensured that the lowest point of each indenter was dropped from 300mm so that direct comparisons between the deceleration values obtained could be made.

(iii) Penetrometer

A penetrometer, designed for the USGA, was used as a measure of the "hardness" of the greens and is shown in Figure 2.15. It has a 51mm long probe with a diameter of 8mm reducing to 4.8mm at the tip. The shaft onto which this probe is threaded moves vertically through the penetrometer body but is restricted by a spring. When the probe is pushed into the ground, the shaft is forced in the opposite direction. The apparatus reaches equilibrium when the bottom of the penetrometer body touches the surface. Part of the probe penetrates into the ground while part has been forced vertically into the penetrometer body. An amount equivalent to that penetrating the ground protrudes out the

FIGURE 2.13. An apparatus used to drop golf balls from 5m. Pulling a cord connected to the ball carrier on the top of the pole opened a mouth through which a golf ball dropped. The rebounding ball was filmed using a video camera against the backsdrop of the scale.

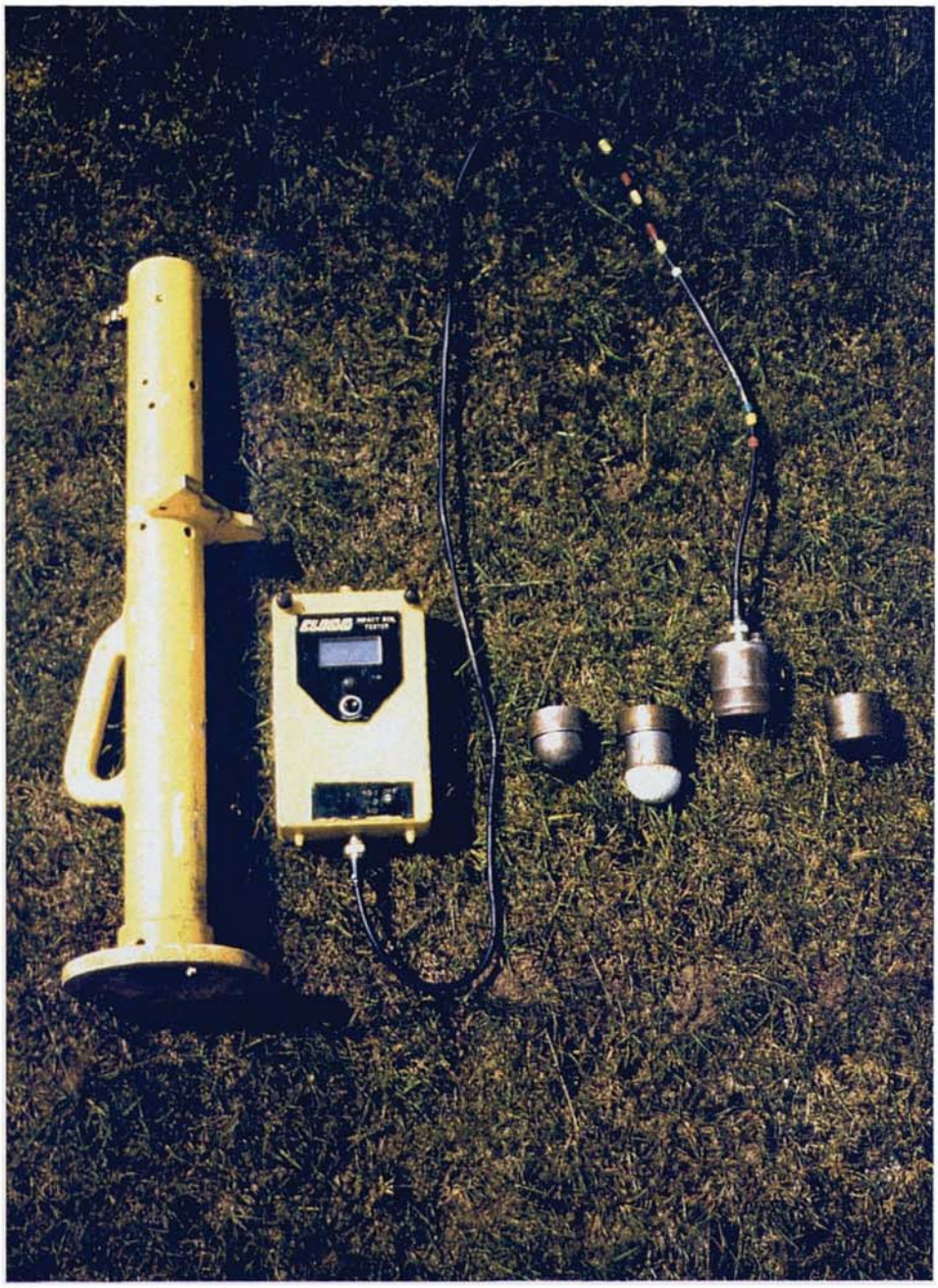

FIGURE 2.14 The Clegg Impact Hardness Tester used as a measure of hardness. The original 0.5kg indenter is shown attached. The three other indenters, when screwed onto the main shaft, weigh 1.0kg.

FIGURE 2.15. The Stimpmeter, above, and below, from left to right, the USGA penetrometer, the USGA green hardness tester and the 180mm soil corer.

top of the penetrometer body. Here, the shaft is graduated in one sixteenths of an inch. It is thus possible to measure the amount of the probe penetrating the ground. The speed and duration of the measurement affects a reading. If the penetrometer is continually pressed on the ground then the probe slowly penetrates the soil. This is due to the sustained downwards force due to the spring. There are two handles at right angles to the penetrometer body. One handle can be rotated half a turn into the body so that the shaft is fixed in position. This ensures that the shaft does not move once the probe has penetrated to its maximum extent and the penetrometer body touches the surface. The larger the penetration of the tip the smaller the amount of the shaft that protrudes out the top of the penetrometer body and the higher the reading. Thus, a "soft" surface is indicated by a large penetration and a high reading.

(iv) Green speed

A device called a Stimpmeter has been used to measure the "speed" of golf greens (Stimpson 1974, Radko 1977, 1978). The Stimpmeter, shown in Figure 2.15, is a V-shaped ramp down which a golf ball is rolled. The ball is placed behind a notch at the top of the ramp which is then tilted forward. When the angle of the ramp reaches about 22° the downwards force of gravity pulls the ball over the notch. The ball rolls down the ramp and across the turf with an initial speed of $1.9ms^{-1}$ as measured using timing gates. This is slightly lower than simple theory might suggest due to the groove that the ball rolls down and the frictional forces experienced by the ball.

The distance that the ball travels across the green is taken as a measure of its speed. The normal procedure is that the most level part of the green is selected and two balls are rolled along the same path but in opposite directions. This procedure is intended to eliminate the effects of any minor slope.

(v) Soil moisture content; Organic matter content; soil composition

Soil properties were determined by laboratory analysis of soil cores taken using a soil sampler 180mm long and with a diameter of 19mm (Figure 2.15). Ten cores were taken from each green and were wrapped in plastic bags to conserve their moisture. In the laboratory they were weighed, dried at 105°C for 24 hours and reweighed to determine their moisture content. An accepted representation of the soil moisture content is the percentage ratio of the dried weight to the original weight (Piper 1950).

Soil organic matter content was determined by loss on ignition. The dried cores were ignited at 400°C for 8 hours and then reweighed. The resultant loss in weight on ignition of the organic matter was expressed as the percentage of the weight before ignition. This is the standard method used at the Sports Turf Research Institute and is described by Baker (1985).

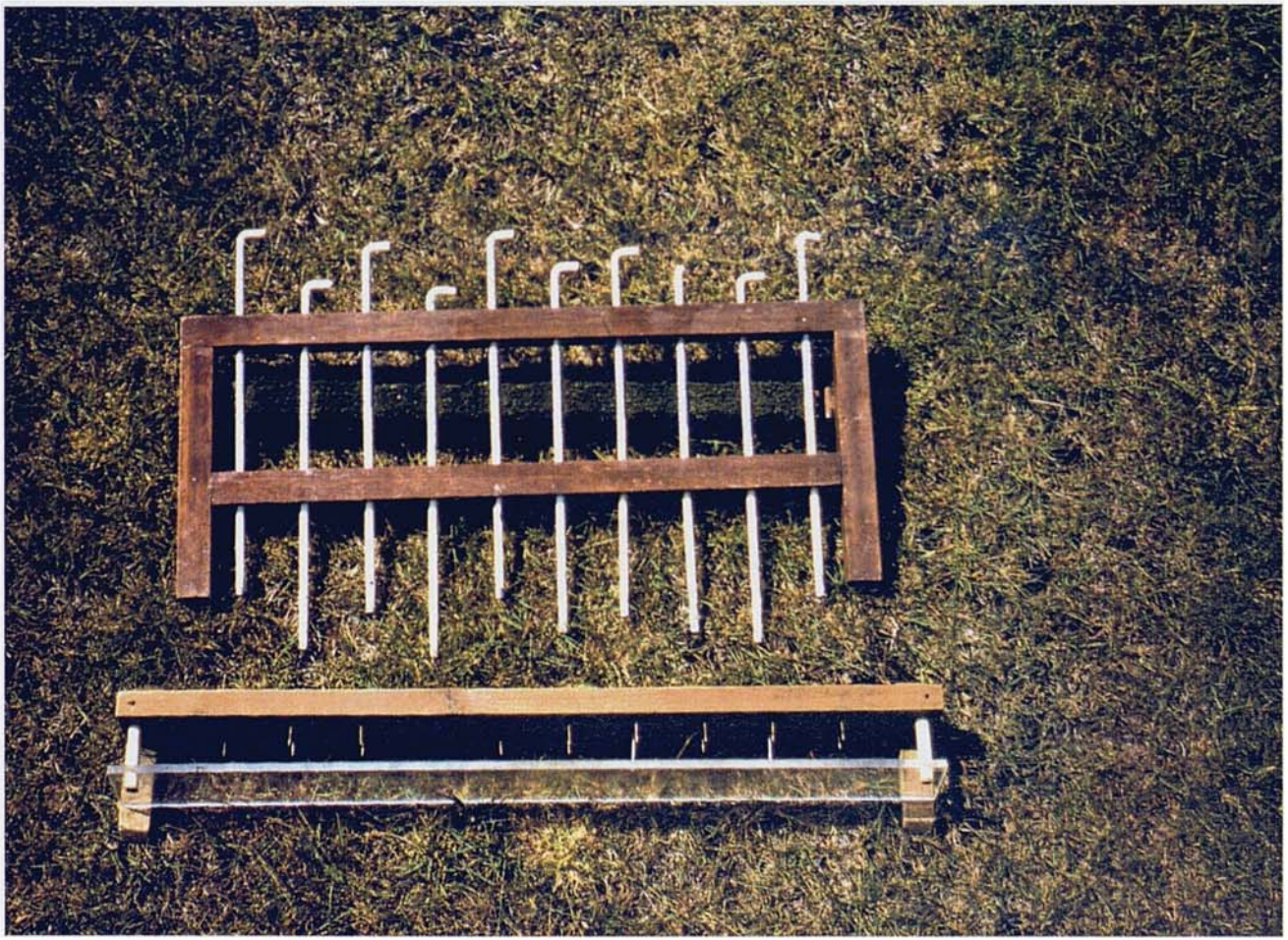

FIGURE 2.16. The levels apparatus (above) was used as a measure of the evenness of the greens. The optical point quadrat frame (below) was used to evaluate the species composition of the greens.

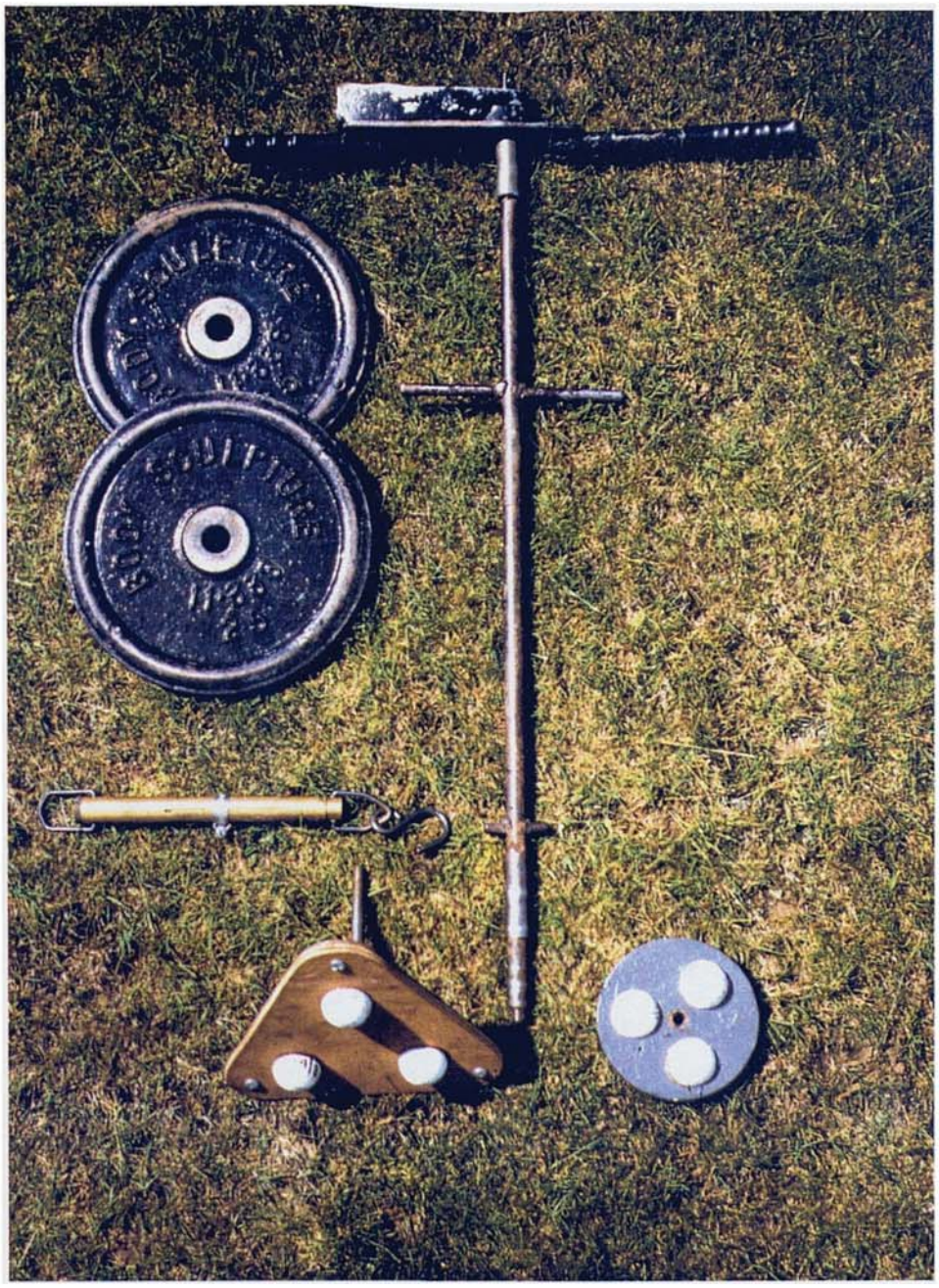

FIGURE 2.17. The friction sled (lower left) and the traction disc (lower right) used as a measure of playing quality.

A particle size analysis of the soil from each green was carried out in order to determine the soil type. The sand fractions were determined by sieving the dried soils through successively finer sieves and the silt and clay fractions were determined by sedimentation (Piper 1950).

(vi) Surface evenness/roughness

In terms of putting, one of the most important features of the green is the surface evenness. This was measured using a profile gauge and consists of ten 6 mm diameter rods spaced 50mm apart in a wooden frame (Figure 2.16). The rods are free to move vertically so that when the frame is placed on the playing surface the rods are displaced by bumps and hollows. Each rod is graduated so that its displacement can be measured to an accuracy of ± 1mm. The roughness of an area was expressed as the mean of ten sample standard deviations of 10 x 10 readings (Holmes and Bell, 1987). The smaller the value of the mean the more even the green.

(vii) Ground cover and species composition

This was studied with an optical point quadrat frame (Laycock and Canaway, 1980). It consists of a horizontal softwood frame 600mm long, on which are mounted two rows of five pins, one row being 20mm above the other and the pins being 100mm apart within rows (Figure 2.16). The apparatus was placed on the turf and sightings were taken down the tips of the pairs of pins on to the vegetation. When the tips were in line, whatever was below was recorded as a species of grass, dead plant material or bare ground.

(viii) Sliding friction

The sliding friction of the surface was measured using a device similar to that used by Thorpe and Canaway (1986). Three half golf balls were adhered 115mm centre to centre to the three corners of a triangular sled (Figure 2.17). This was placed on the ground with the golf balls contacting the ground and with a 10kg weight on the sled, the total weight of the apparatus being 11.2kg. The whole apparatus was towed across the ground at a constant speed using a Newton meter. The speed was determined by the operator and was required to be just enough to overcome the inertial forces resisting the initial movement of the sled. This was estimated to be between 0.5 and 1ms^{-1}. The force required to pull the apparatus divided by the weight of the apparatus gives an estimate of the coefficient of friction at this speed.

(ix) Ball/surface traction

The traction of the green was measured using an apparatus similar to that described by Canaway (1975). Although this test was used to study the player/surface interaction for running sports, it was thought that it might provide a good measure of the shear strength of the green. Three golf balls were adhered to the bottom of a 12mm thick mild steel disc

in place of the usual sports shoe studs (Figure 2.17). This was then screwed onto a 1m long shaft which passed through the centre of two 10kg weights. The apparatus was dropped from a height of 150mm and a torque wrench used to measure the torque required to twist the disc through the turf.

2.7 Summary

The literature review was used as a source of information from which to develop a method of projecting and recording the impacts of golf balls on turf. The projection device subsequently designed employed two counter-rotating pneumatic wheels to project the golf ball. These could be varied independently to produce spin. Stroboscope photography was used to record the impacts. The camera and stroboscope were activated by an electronic trigger which was initially activated when the golf ball passed through an infra-red beam. The photographs were shielded from direct sunlight by a dark canvas enclosure into which the golf balls were projected. This enclosure was attached directly to the ball projection device so that the whole set of apparatus could be moved together after each impact. It was found that the apparatus worked well in the field although a routine had to be developed to ensure the optimum use of the equipment.

Many of the playing quality tests found in the literature review were used or modified to measure the characteristics of golf greens. The following chapter describes the results of the stroboscope photographs found using the apparatus described here.

Chapter 3 - Impacts of golf balls on turf

3.1 Introduction

This chapter describes primarily the results and analysis of the photographs of ball/turf impacts produced with the apparatus described in the previous chapter . Photographs of golf ball impacts were taken on greens around the country. Sixteen sets of data resulted which contained 721 useful photographs of impacts. Statistical analysis was carried out on the impact data and explanations are offered for the results that were found. The tests were carried out for two reasons, (1) to evaluate the apparatus and test methods and (2) to find the important factors in ball turf/impacts. The evaluation of the apparatus is discussed later in Chapter 6 while the ball turf impacts are considered in the later sections of this chapter. Prior to the analysis of the ball/turf impacts, the effect of the construction of the ball on the impacts with the green is considered. Preliminary golf ball impacts studied using a high speed cine-camera are also described.

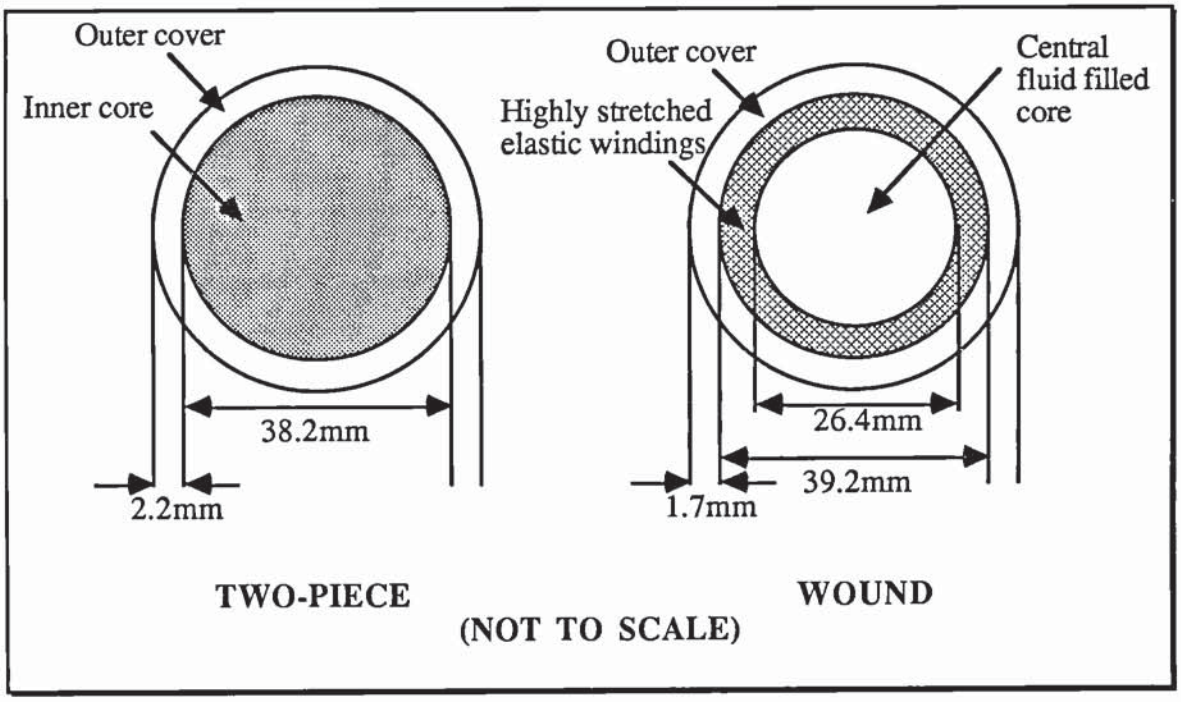

FIGURE 3.1. A diagram showing the construction of a wound and a two-piece golf ball. Both types of ball are covered in a hard plastic cover made from surlyn. The two-piece ball contains solid rubber while the wound ball contains a central fluid filled sac surrounded by tightly stretched elastic windings.

3.2 Tests to compare two constructions of golf ball

(i) The tests

Using the methods described in Chapter 2, two different types of golf ball were projected at a single golf green to determine the influence, if any, of the construction

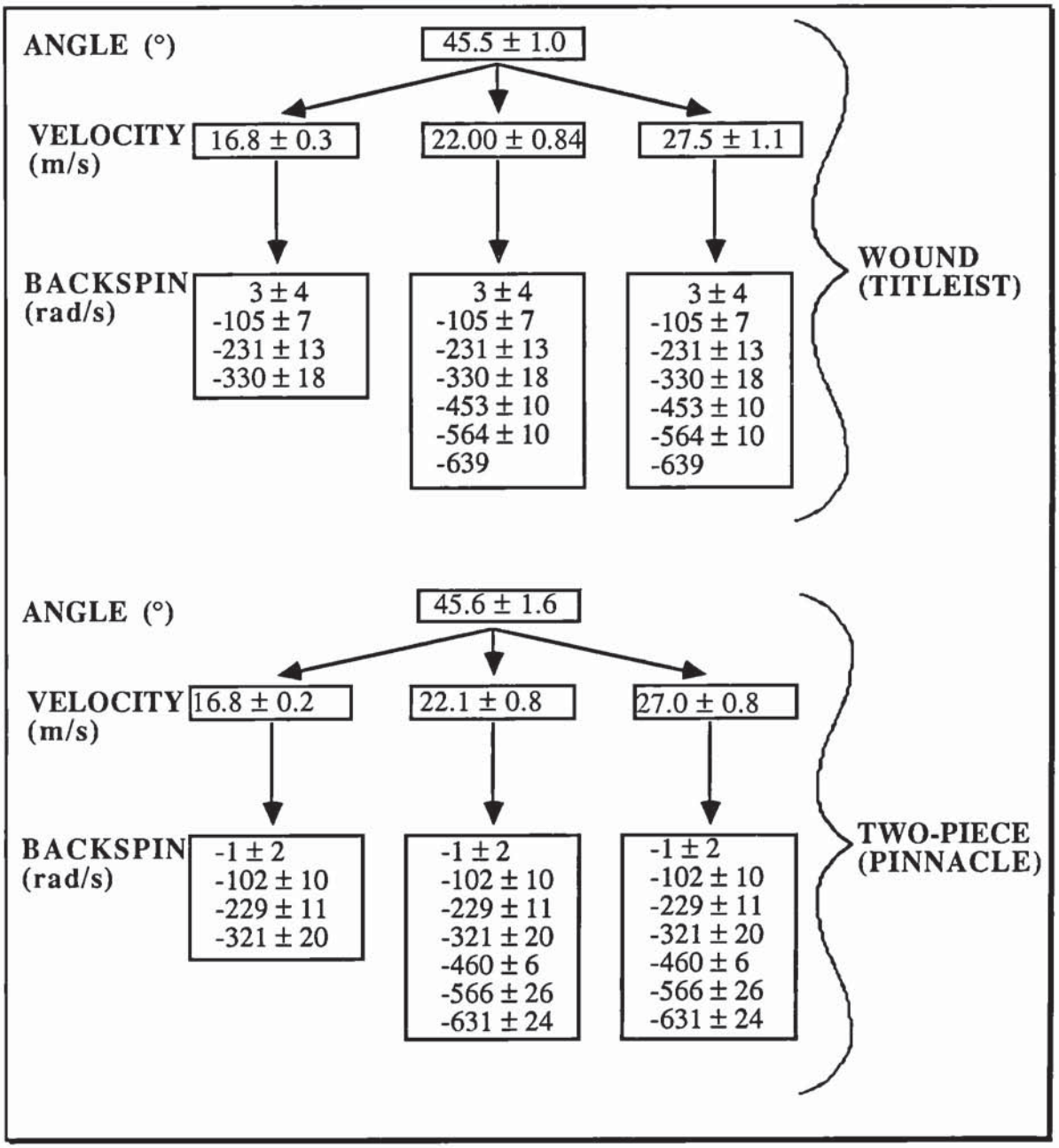

FIGURE 3.2. The means and standard deviations of the velocities, angles and spins used in projecting the Pinnacle and Titleist golf balls in tests to find the influence of ball construction on the impact with the turf.

of the ball on the impact. It might be expected that the construction of the ball would play a large part in this impact. On hard surfaces such as a golf club face, different constructions of ball bounce differently. It is not known, however, if the construction of the ball has the same effect on ball/turf impacts. If the construction has an important role in the impact then it must be incorporated into the model discussed in Chapter 5. If it is less important then it will simplify the modelling process dramatically.

Two types of golf ball were used in the tests described here; the Titleist 384 90 Tour wound ball and the Pinnacle 384 two-piece ball. These are shown schematically in Figure 3.1. Both types of ball conform to the standards laid down by the Royal and Ancient Golf Club of Saint Andrews, weighing a minimum of 45.93g and having a maximum diameter of 42.67mm. The two-piece golf ball has a solid rubber core covered by a shell of surlyn plastic. The wound ball also has this hard outer cover but has an inner core containing a fluid-filled sac surrounded by highly stretched elastic windings. The inner core contains fluid to ensure that the ball is above the minimum weight required.

Thirty one impacts were recorded with the wound ball while thirty two impacts were recorded using the two-piece ball. Information on the impacts was extracted from the photographs using the methods described in section 2.5 and are given in Appendix D. Figure 3.2 shows a comparison of the average initial velocities, angles and spins for the two types of ball. The golf balls were projected at the green at approximately 45° to the horizontal with speeds of about 16.8, 22.0 and 27.5ms^{-1}. The values shown are the averages for the set of data. For instance, the velocity of 22.0±0.8ms^{-1} for the wound ball is the average of 11 impacts at this velocity (Appendix E).

The spin was varied at each in discrete steps at each velocity - it should be noted here that backspin is chosen to be negative and topspin positive. It was possible to attain higher spins at higher velocities since the range of possible wheel speeds on the ball firing device was greater. A comparison of the initial velocities and spins shows that the spins speeds and velocities are essentially the same for each ball. It was concluded therefore that the results of the tests could be used to determine the effect of the construction of the ball on the ball/turf impact.

(ii) Results of the tests

The main body of results of the impacts are shown in Appendix D. Table 3.1, however, shows the results from four typical impacts at the highest velocity studied, two using the wound ball and two using the two-piece ball.

The first two impacts in the table have zero spin while the second two impacts have a backspin of about 640rads^{-1} (backspin is negative). In both cases the wound ball rebounded at a higher angle than the two-piece ball. The spin and the velocity of the ball after impact showed no particular relationship, however. With both types of ball, an increase in the backspin caused an increase in the rebound angle and a decrease in the velocity of rebound. The topspin of the ball also decreased after impact. At this stage, it is the effect of the construction of the ball on the impact that is being

considered. Analysis of the effects of a change in velocity, angle and spin shall be considered in the next section.

It is difficult to determine whether the variations in the impacts above are due to the construction of the ball, inconsistencies in the green or variations in the incident velocity, angle and spin. Regressions were therefore carried out on the results for the two different balls to determine the relationships between the rebound velocity, angle and spin and the incident velocity and spin.

	VELOCITY (ms^{-1})		ANGLE (°)		SPIN ($rads^{-1}$)		DEPTH
	initial	final	initial	final	initial	final	(mm)
2P	27.7	9.1	44	44	0	380.5	3.6
W	27.2	8.3	47	53	0	299.4	4.3
2P	28.1	4.8	48	74	-641.2	178.7	5.3
W	30.5	5.3	48	76	-638.9	175.7	6.6

TABLE 3.1. A table to show the results of typical impacts using two types of golf ball. The letters at the beginning of each row refer to two-piece (2P) or wound (W) golf balls.

Stepwise regressions were used to calculate the relationships between the incident velocity and spin and the velocity, angle and spin after impact. This method calculates the best-fit relationship between the data for one dependent variable with two or more independent variables. Each independent variable is tested individually and then introduced into the equation in order of significance. Once the variable is entered into the equation, it is tested again and removed if it is not significant (see Snedecor and Cochran, 1974 for a fuller description of this method). The regressions are written in the form,

$$y = a + (b_1 \pm \sigma_1)\, x_1 + (b_2 \pm \sigma_2)x_2 + (b_3 \pm \sigma_3)x_3 + \ldots\ldots(b_n \pm \sigma_n)x_n$$

where the b's are the coefficients for each independent variable, the σ's are the corresponding standard errors and n is the number of variables. A correlation coefficient (r) and a level of significance (p) are also given with the regression equation. These show how well the relationship describes the data and the probability that this relationship occurred by chance.

The regression equations found for the impacts with the two balls are shown in equations 3.1 (a), (b), and (c). In these equations V is the initial velocity, ω is the initial spin, Θ is the angle of incidence to the horizontal and the subscripts "i" and "f" denote the initial and final values of the variables respectively. The regressions found were,

(a) For the final velocity,

Two-piece ball: $V_f = 2.79 + (0.20 \pm 0.03)V_i + (0.0045 \pm 0.0006)\omega_i$ $r = 0.86$

Wound ball: $V_f = 2.12 + (0.23 \pm 0.03)V_i + (0.0041 \pm 0.0006)\omega_i$ $r = 0.87$

(b) For the final angle,

Two-piece ball: $\theta_f = 28.42 + (0.9 \pm 0.3)V_i - (0.035 \pm 0.004)\omega_i$ $r = 0.82$

Wound ball: $\theta_f = 30.60 + (0.8 \pm 0.2)V_i - (0.035 \pm 0.006)\omega_i$ $r = 0.90$

(c) For the final spin,

Two-piece ball: $\omega_f = 100.1 + (9.3 \pm 1.8)V_i + (0.26 \pm 0.03)\omega_i$ $r = 0.83$

Wound ball: $\omega_f = 162.7 + (5.7 \pm 1.2)V_i + (0.19 \pm 0.03)\omega_i$ $r = 0.81$

eqn. 3.1

The equations were all significant at the 0.01% confidence level. This means that, using this data, there is a probability of 1 in 10,000 that the relationship occurred by chance.

Consider, for instance, a wound and a two-piece ball impacting at $22ms^{-1}$ and with zero spin. The equations above predict within one standard error that the two-piece ball would rebound between 6.5 and $7.9ms^{-1}$, at an angle between 41.6 and 54.8° and with a spin between 265 and $344rads^{-1}$. The wound ball is predicted to rebound between 6.5 and $7.8ms^{-1}$, at an angle between 43.8 and 52.6° and with a spin between 262 and $315rads^{-1}$. The ranges for the two balls are very similar and it is difficult to say whether the construction of the ball effects the impacts or not. It is therefore necessary to test the coefficients of velocity and spin to find if they are significantly different within their standard errors. If the coefficients are different this would indicate that the construction of the ball has an effect on the impact. The coefficients were tested as follows. If the standard errors of two coefficients b_1 and b_2 were σ_1 and σ_2 respectively, then the variable d can be calculated using the formula,

$$d = \frac{b_1 - b_2}{\sqrt{(\sigma_1^2 + \sigma_2^2)}} \qquad \text{eqn. 3.2}$$

The magnitude of d determines the level of significance of the difference between the two coefficients b_1 and b_2. This can be found using Table 3.2. The coefficients in equations 3.1 (a) and (b) were not found to be significantly different. Since there appeared to be more variation in the coefficients in equation 3.1 (c), the tests to determine the significance of their differences are shown below. For the coefficient of the initial velocity,

$$d = \frac{9.3 - 5.7}{\sqrt{(1.8^2 + 1.2^2)}} = \frac{3.6}{\sqrt{4.68}} = 1.664$$

and, for the coefficient of the initial spin,

$$d = \frac{0.26 - 0.19}{\sqrt{(0.03^2 + 0.03^2)}} = \frac{0.07}{\sqrt{0.018}} = 1.650$$

Comparing these values to those in Table 3.2 it can be seen that the coefficients are different at the 10% level of confidence. The accepted level of confidence used is 5% and therefore these coefficients are not considered to be significantly different.

p	0.10	0.05	0.02	0.01	0.002	0.001
d	1.645	1.690	2.326	2.576	3.090	3.291

TABLE 3.2. A table containing the values of *d* (the unit standard deviation) required for a level of significance p (Bailey, 1959).

There were therefore no significant differences between the coefficients of the regressions for the wound and two-piece balls at the velocities and spins studied. Thus, at the velocities, angles and spins tested, the ball's construction did not affect the impact of the ball with the green. This suggests that the ball can be considered as a rigid solid during impact and will simplify greatly the models of impact formulated in Chapter 5.

3.3 Studies of golf ball impacts using high speed film

(i) Introduction

The use of a high speed camera was tested during the evaluation of methods for recording the ball/turf impact. Test films were subsequently developed and these were found to be quite useful in revealing the dynamic processes involved in an impact. The high speed films could give estimates of the contact time, the depth of penetration of the ball into the ground, and the deformation of the ball. These factors are potentially useful in the development of a model of impact.

The Fastax WF17 high speed camera used in these tests employed a rotating prism mechanism and was able to take pictures at rates up to 8000fps. At this speed, 30m of 16mm film was exposed in 0.7 seconds. The camera was activated by a remote switch and the speed of the film through the camera was altered by varying the voltage applied to the camera motor. Two 1kW video lamps were used to provide additional illumination during the impact. Pegs were placed in the ground in the field of view of the camera to provide a distance scale with which to make measurements. The camera was placed about 5m from the point of impact and a long focal length lens used to minimise the effects of parallax. A disc marked out in segments attached to a motor rotating at 25 revolutions per second was placed behind the impact zone. This provided a time base for the camera and was required to facilitate calculations of velocity and spin.

The ball projection device described in Chapter 2 was used to project golf balls at turf near to a convenient power supply as it was not possible to produce the power required with a portable generator. An analysing projector was used to view the resultant films frame by frame. The rotation of the disc between frames indicated the time lapsed per frame and, by marking the positions and orientations of the ball on successive frames, the velocities, angles and spins were calculated.

(ii) Results

Four impacts with the turf were studied using the high speed camera running at between 1201 and 3260fps (Table 3.3). The impacts studied were carried out on different areas of turf and on different days and were carried out to evaluate the method of high speed photography. The analysis shown here, therefore, is quite general since it is difficult to draw specific conclusions from four different impacts.

Columns 1 to 6 in Table 3.3 show the velocities, angles and spins before and after impact. The next column shows the depth of the pitchmark measured just after the impact. In column 8 it can be seen that the balls were in contact with the ground between 6.1 and 9.2msecs. This is 12 to 18 times longer than the impact of a golf ball with a golf club. Using the change in momentum in the horizontal and vertical directions and the time of contact, the approximate force and its direction were calculated.

Velocity		Angle		Spin		D	T	Film	Average		Force	Rad
ms^{-1}		°		$rads^{-1}$		mm	msecs	speed	F	τ	angle	(eff)
i	f	i	f	i	f			fps	N	Nm	°	mm
24.5	6.1	51	67	-562	274	12	9.2	1201	144	.757	63	5.3
15.0	3.7	52	62	-341	152	8	6.2	1617	125	.633	64	5.1
22.0	7.7	39	70	0	322	7	6.1	3260	192	.440	56	2.3
21.2	7.4	38	42	0	300	7	6.5	3087	150	.385	58	2.6

TABLE 3.3. A table showing the information on four impacts studied using high speed film. Negative spin indicates backspin.

The total average force, the average torque and the angle to the horizontal at which the force acts are shown in columns 10, 11 and 12 in Table 3.3. Since the average force and the average torque are linked (by $\tau = Fr$) it is possible to calculate the effective radius at which the torque is applied (column 13). Figure 3.3 shows the application of the average force during a typical impact. It can be seen that the average force acts off-centre. The resultant torque modifies the initial spin of the ball. Table 3.3 shows that the effective radius varies from 2.3 to 5.3mm (about one tenth to one fifth of the ball's radius) and is larger in the case when the initial backspin is high. As expected,

the forces experienced by the ball are a combination of that due to the spin of the ball and the interaction of the ball's translational motion with the surface.

The magnitude of the vertical force experienced by the golf ball was about 130N, equivalent to a maximum deceleration of about 2800ms^{-2}. The nature of the impact can be considered further if the impact is compared to the motion of a mass on a spring. The maximum deceleration would vary with mass^{-TM} (analysis based on simple harmonic motion). As will be seen in Chapter 4, the maximum deceleration found using the 0.5kg Clegg indenter averaged over all the greens visited was about 57*g* or 563ms^{-2}. The ratio of the mass of the golf ball to the Clegg indenter is 1 to 10.9; the maximum decelerations would therefore be expected to vary in the ratio 3.3 to 1. It can be seen that the decelerations are in fact in the ratio of about 5 to 1. This difference is not surprising since the analogy of the single spring was not expected to be correct; the ball would not lose energy during the impact. The motion must have a viscous component since the coefficient of restitution is not unity. The use of springs and damper components to model the ball turf impact is discussed later in Chapter 5.

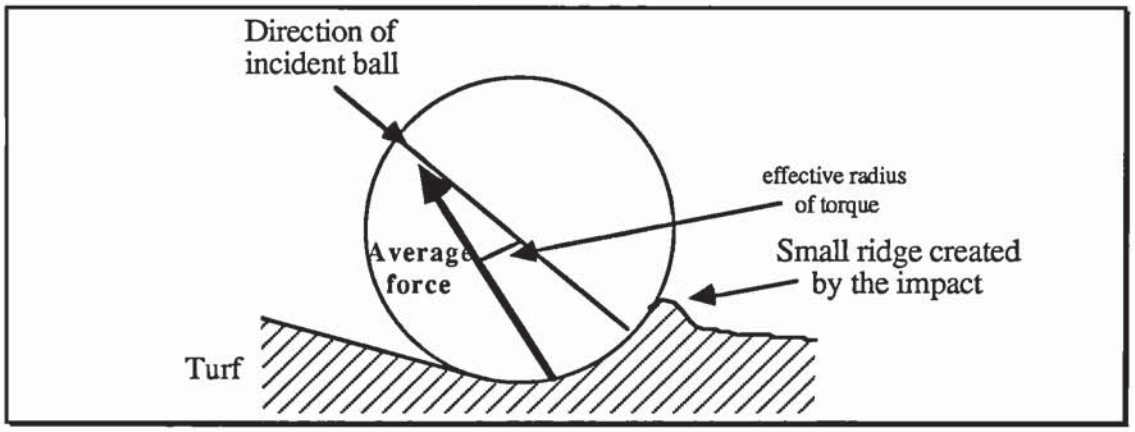

FIGURE 3.3. A diagram to show the direction of the average force in the impact of a golf ball on a golf green as deduced from high speed films of impacts.

An interesting feature seen on the high speed films was that the initial backspin of the ball was modified almost instantaneously to topspin at the beginning of the impact. Furthermore, it appeared that the ball rolled off the surface. It is possible to calculate the spin required for the ball to roll off the surface using,

$$\omega = \frac{V}{r} \qquad \text{eqn. 3.3}$$

where V is the translational velocity and r is the radius of the ball. The first impact shown in Table 3.3 had a rebound velocity of 6.1ms^{-1} and with a radius of 0.0213m, the equivalent spin required for rolling was about 286rads^{-1}. This is not too far from the actual spin of the ball as it left the surface. If the same calculation is performed on the other three impacts it is found that the rolling spins are almost the same as the

VELOCITY(ms^{-1})		ANGLE (degrees)		SPIN ($rads^{-1}$)		Depth
i	f	i	f	i	f	(mm)
17.5	6.4	44	40	0	277.0	3.8
17.8	5.8	45	41	0	245.7	3.1
17.7	6.9	45	38	0	339.5	2.5
17.5	6.3	45	40	-98.3		2.5
17.1	6.0	45	36	-102.7	259.1	2.3
17.4	6.3	46	39	-89.3	268.0	2.0
17.7	6.5	45	40	-218.9	245.7	2.5
17.7	6.4	45	37	-205.5	259.1	1.8
17.7	5.0	45	50	-326.1	234.5	2.3
17.6	5.2	45	47	-328.4	234.5	2.0
22.0	8.1	44	39	0		3.1
22.3	6.8	45	46	-107.2	290.4	3.1
21.8	7.2	45	44	-116.1	254.6	3.3
21.7	6.6	43	47	-107.2	292.6	4.3
22.5	6.5	43	49	-216.7	308.2	
22.1	7.3	44	40	-232.3	277.0	4.3
22.2	6.8	44	46	-214.4	296.3	1.8
22.6	5.9	43	52	-328.4	247.5	4.1
22.0	5.9	44	48	-326.1	249.4	4.3
22.6	7.5	44	43	-457.9	107.2	3.1
21.7	7.6	43	40	-428.9	134.0	2.5
22.7	7.6	43	43	-437.8	147.4	2.5
22.8	7.5	43	44	-536.1	-37.4	2.3
22.5	8.0	44	38	-567.4	-69.2	3.3
27.0	9.1	43	39	0	402.3	3.3
27.5	8.8	45	39	0	402.3	1.2
26.7	7.9	43	45	-99.4	325.4	3.1
28.5	8.3	44	44	-106.2	329.9	4.1
27.1	7.4	45	50	-221.5	305.1	3.8
27.5	5.7	44	63	-212.4	230.5	7.4
26.4	7.1	45	48	-203.7	311.9	5.1
27.5	7.3	44	48	-198.8	316.4	4.1
26.7	6.6	45	51	-348.0	262.1	4.8
28.4	7.1	45	52	-339.0	297.7	4.6
27.7	7.3	44	54	-452.0	230.5	5.1
27.8	7.8	44	44	-565.0	103.9	6.4
28.0	5.7	44	61	-551.4	212.4	6.4
28.2	5.5	44	63	-560.5	212.4	
27.0	8.5	45	48	-90.4	346.9	3.1
28.4	8.0	44	43	-488.2	219.2	4.1
26.9	6.6	45	51			
26.9	6.2	45	54	-664.5	-78.5	
27.5	8.2	44	42	-678.0	-88.1	4.1
25.9	5.9	44	50	-650.9	-59.3	4.6
25.5	6.0	44	54	-650.9	-35.2	

TABLE 3.4. A table containing the results of the impact tests at Ganton golf club. The subscripts "i" and "f" are assigned to the variables before and after impact respectively, the depth is the depth of the pitchmark created by the impact and blank spaces indicate that the variable was not measured.

actual spins of the ball after impact. This suggests that, in these impacts, there was no slip between the surface of the ball and the turf at the end of impact.

In most of the impacts the ball appeared to penetrate up to almost half its diameter into the turf but subsequent measurements found the pitchmarks to be at the most 12mm in depth. This indicated that, if the ball did not compress significantly during impact, then the ground must have partially recovered after the impact had taken place. This may be an important consideration in the modelling of the impacts in Chapter 5.

3.4 Results from the stroboscope photographs of golf ball impacts

(i) The velocities, angles and spins used in the impacts

This section shows the results and analysis of the results from the photographs of ball/turf impacts. The methods described in Chapter 2 were used to project Titleist 384 golf balls at a single green on 16 golf courses. This resulted in 721 photographs of impacts; 450 from 11 greens on which the angle of incidence was fixed at 45° to the horizontal and 271 on 5 greens where the angle of incidence was varied. The photographs of impacts were analysed using the methods described in section 2.5.

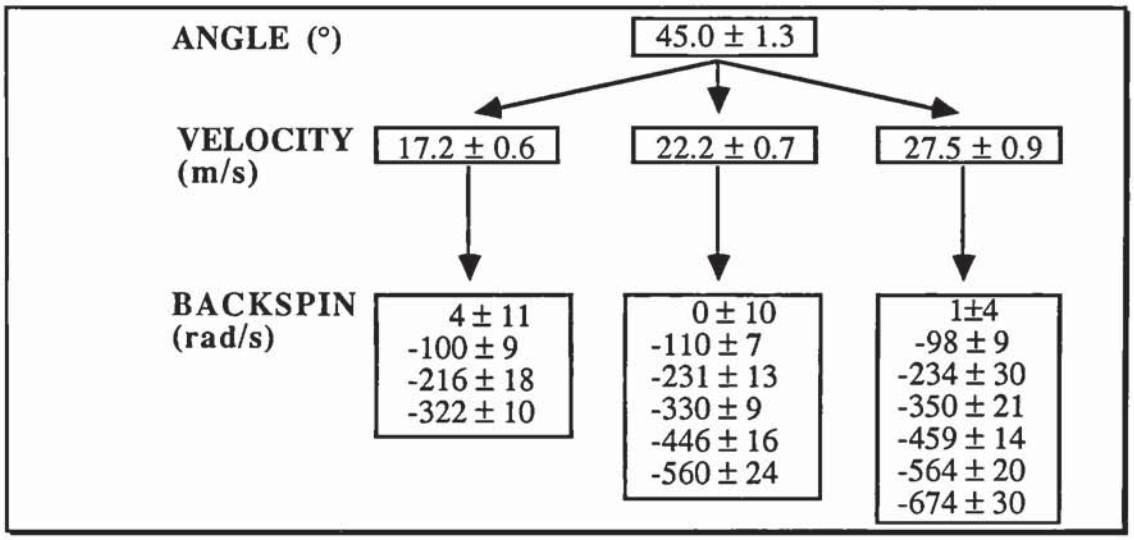

FIGURE 3.4. The velocities and spins and their respective standard deviations used in the golf ball impacts projected at 45° to the horizontal. Negative spin indicates backspin.

The initial and final velocities, angles and spins of all the impacts are shown in Appendix E since there are too many to show here. As an example, the data on the impacts from the green studied at Ganton golf club are shown in Table 3.4. The letters "i" and "f" indicate the initial and final values of the velocity, angle and spin. The depth refers to the depth of the pitchmark created by the impact and blank spaces in the table indicate that the measurement of the variable was not possible.

COURSE	ANGLE	VELOCITY	SPIN
	(°)	(ms^{-1})	($rads^{-1}$)
Belfry	35.1 ± 1.2	16.8 ± 0.4	2 ± 2, -117, -218 ± 3, -378 ± 5
		22.1 ± 0.5	0, -119 ± 5, -246 ± 6, -318 ± 12, 443 ± 7, 590 ± 26
		27.6 ± 0.9	2 ± 3, 119 ± 4, 232 ± 8, 376 ± 13, 478 ± 17, 543 ± 22, 676 ± 22
	44.4 ± 0.9	17.3 ± 0.5	0, -328 ± 6
		22.81 ± 0.4	-2 ± 2, -585
		27.4 ± 0.5	-5, -639
Crewe	36.9 ± 1.3	16.9 ± 1.1	0, -303 ± 18
		22.3 ± 0.2	0, -334 ± 3, -567 ± 33
		27.9 ± 0.7	-7 ± 2
	45.8 ± 1.1	18.0 ± 0.8	0 ± 0, -343 ± 7
		23.1 ± 0.4	6 ± 4, -363 ± 9, -568 ± 1
		27.9 ± 0.3	4 ± 4, -356 ± 4, -648 ± 16
	54.8 ± 1.3	17.4 ± 0.8	0 ± 0, -323 ± 5
		22.7 ± 0.3	6 ± 2, -345, -574 ± 7
		27.4 ± 0.3	-3 ± 3, -384 ± 3, -641 ± 19
Hill Valley	35.0 ± 0.5	17.3 ± 0.3	0 ± 0, 321 ± 7
		22.0 ± 0.3	4 ± 3, -327 ± 3, -545 ± 3
		26.3 ±0.6	35.3 ± 20, -335, -631
	45.9 ± 1.6	17.5 ± 0.2	-1 ± 1, -344
		22.7 ± 0.4	0, -344, -548
		27.1 ± 0.1	-344
Newcastle	45.8 ± 1.3	18.1 ± 0.8	0 ± 0, -341 ± 15
		23.6 ± 0.5	0 ± 0, -530
		29.1 ± 0.8	0 ± 0, -347
	54.2 ± 0.6	18.0 ± 0.7	5 ± 3, -108 ± 7, -227 ± 4, -320 ± 6
		22.5 ± 0.5	5 ± 3, -111 ± 7, -222 ± 14, 330 ± 2, -459 ± 5, -572 ± 4
		27.5 ± 0.4	0 ± 7, -95 ± 4, -238 ± 2, -352
Sutton Park	39.2 ± 0.7	17.2 ± 0.2	5 ± 0, -153 ± 3, -218 ± 6, -317 ± 11
		21.6 ± 0.4	5, -110 ± 4, -230 ± 7, -337, -444 ± 22, -551 ± 3
		27.1 ± 0.3	0 ± 6, -85 ± 2, -239 ± 3, -368 ± 2, -476 ± 8, -573 ± 15, -660 ± 10
	50.2 ± 0.5	16.4 ± 0.5	14 ± 12, -306 ± 21
		22.0 ± 0.2	-2 ± 7, -550± 4
		26.8 ± 0.6	0 ± 5, -543 ± 7

TABLE 3.5. A table containing the velocities, angles and spins of balls projected at the turf on five greens. The errors assigned to the values are the standard deviations.

The velocities and spins for the impacts at 45° are shown in Figure 3.4. Three velocities were studied, approximately 17, 22 and 27ms^{-1}. At zero spin, both wheels on the projection device were set at the same velocity. As stated in section 2.4, the speed of the bottom wheel was then decreased by 2.2ms^{-1} and the top wheel increased by the same amount. In this manner the spin of the ball was gradually increased while keeping the velocity of projection fixed.

The errors shown in Figure 3.4 are the standard deviations of the means. The velocities, angles and spins used on the 5 greens where the angle was varied are shown in Table 3.5. Angles of incidence of 35 and 45° were used at two greens, 45 and 55° were used at one green, 40 and 50° were used at one green and 35, 45 and 55° were used at one green. The angles of impact used on the green at Sutton Park were meant to be 45 and 55° but were 5° lower due to an error in the positioning of the apparatus. Velocities of approximately 17, 22 and 27ms^{-1} were studied at all these angles and the spin was varied in the same way as before. On some greens, however, spins in the mid-range were omitted so that a greater variety of angles could be studied in the time available.

It can be seen in Figure 3.4 and Table 3.5 that the spins attained by the golf balls reached limits at each velocity studied. This was because the lower wheel reached its minimum velocity. Increasing the velocity of the top wheel to increase the spin would also have increased the velocity of the ball.

The spins and angles used encompass those of balls arriving at greens hit with a driver and a 5-iron. These shots therefore, may be considered when analysing the results of the impacts.

(ii) Results: the influence of the initial velocity, angle and spin on the velocity, angle and spin of the ball after impact

If the results in Table 3.4 are considered, relationships between the variables can be observed. For instance, if the velocity of impact is increased then, in general, the velocity of rebound is also increased. However, superimposed on top of this relationship is the effect of the backspin on the impact (in Table 3.4 the angle of impact is kept fixed). However, due to irregularities in the green (and perhaps in the ball) some impacts do not fit exactly a given relationship. Therefore, the most suitable method of expressing the effects of velocity, angle and spin on the impact is in multiple regression form. These are used to determine the "best-fit" relationship. Regressions were used in section 3.2 to determine the effect of the construction of the ball on the impact.

Velocity after impact									
Course	Int	C_V	dC_V	C_Θ	dC_Θ	C_ω	dC_ω	r	p
Austerfield	2.30	0.18	0.03	FIXED ANGLE		.0028	.0005	.73	0.0001
Belfry	11.64	0.21	0.07	-0.23	0.08			.55	0.0001
Bingley	2.47	0.24	0.03	FIXED ANGLE		.003	.001	.86	0.0001
Crewe	11.98	0.10	0.02	-0.16	0.01	.0034	.0003	.94	0.0001
Formby	3.21	0.18	0.01	FIXED ANGLE		.0036	.0006	.91	0.0001
Ganton	4.00	0.14	0.04	FIXED ANGLE		.0017	.0007	.55	0.0001
Hallowes	2.45	0.25	0.04	FIXED ANGLE		.004	.001	.88	0.0001
Hill Valley	18.74			-0.27	0.03	.0016	.0004	.87	0.0001
Keighley	6.52			FIXED ANGLE		.0048	.0008	.71	0.0001
Lindrick	4.51	0.10	0.05	FIXED ANGLE		.0029	.0006	.66	0.0001
M. Allerton	5.29			FIXED ANGLE		.0040	.0008	.64	0.0001
Moor Hall	5.35	0.06	0.02	FIXED ANGLE		.0052	.0005	.84	0.0001
Moortown									
Newcastle	13.48	0.04	0.01	-0.16	0.01	.0043	.0003	.95	0.0001
Sandmoor	3.72	0.16	0.02	FIXED ANGLE		.0038	.0005	.83	0.0001
Sutton Park	12.77	0.10	0.03	-0.19	0.02	.0027	.0006	.79	0.0001

TABLE 3.6. The regression coefficients for the equations relating the velocity of the rebounding ball with the initial velocity and spin. Blank spaces indicate that the variable was not significant in the regression.

The regressions in this section relate one dependent variable with three independent variables (the incident velocity, angle and spin). The coefficients of the regressions for the velocity, angle and spin after impact for each green are shown in Tables 3.6, 3.7 and 3.8. The names of the columns indicate the following:-

Int - the intercept of the equation,

C_V, dC_V - the coefficient and respective standard error of the velocity component,

C_Θ, dC_Θ - the coefficient and respective standard error of the angle component,

C_ω, dC_ω - the coefficient and respective standard error of the spin component,

r - the correlation coefficient,

p - the significance level of the regression.

A blank space in the table indicates that the variable was not significant in the regression for that green.

For example, the regressions found for Crewe were,

$$V_f = 11.98 + 0.10V_i - 0.16\Theta_i + 0.0034\omega_i \qquad \text{eqn. 3.4}$$

$$\Theta_f = -30.3 + 0.98V_i + 1.21\Theta i - 0.027\omega_i \qquad \text{eqn. 3.5}$$

and

$$\omega_f = 584.8 + 2.9V_i - 7.7\Theta i + 0.2\omega_i \qquad \text{eqn. 3.6}$$

The standard errors for each coefficient, correlation coefficients and levels of significance can be also be found in Tables 3.6, 3.7 and 3.8. The meaning of the regressions above become clearer if a specific example is considered. A ball impacting on the green at Crewe at a velocity of 22ms^{-1} at an angle of 45° to the

Angle after impact									
Course	Int	C_V	dC_V	C_Θ	dC_Θ	C_ω	dC_ω	r	p
Austerfield	25.6	1.1	0.2	FIXED ANGLE		-0.023	0.004	.79	0.0001
Belfry	-24.3			1.71	0.24	-0.008	0.004	.73	0.0001
Bingley	29.0	0.6	0.2	FIXED ANGLE		-0.032	0.006	.75	0.0001
Crewe	-30.3	1.0	0.2	1.21	0.10	-0.027	0.003	.93	0.0001
Formby	36.3	0.3	0.1	FIXED ANGLE		-0.028	0.004	.81	0.0001
Ganton	27.2	0.8	0.3	FIXED ANGLE				.33	0.0001
Hallowes									
Hill Valley	-60.1	1.7	0.3	1.74	0.22			.86	0.0001
Keighley	11.5	1.7	0.3	FIXED ANGLE		-0.053	0.008	.86	0.0001
Lindrick	22.6	1.1	0.6	FIXED ANGLE		-0.019	0.007	.66	0.0001
M. Allerton	-14.6	3.1	0.6	FIXED ANGLE		-0.047	0.014	.85	0.0001
Moor Hall	14.1	1.5	0.3	FIXED ANGLE		-0.043	0.005	.86	0.0001
Moortown	17.4	1.7	0.3	FIXED ANGLE		-0.016	0.006	.68	0.0001
Newcastle	-49.9	1.3	0.2	1.40	0.18	-0.036	0.004	.91	0.0001
Sandmoor	36.3	6.6	0.2	FIXED ANGLE		-0.026	0.004	.80	0.0001
Sutton Park	-53.0	1.4	0.2	1.64	0.19	-0.021	0.005	.84	0.0001

TABLE 3.7. The regression coefficients for the equations relating the angle of the rebound to the initial velocity and spin. Blank spaces indicate that the variable was not significant in the regression.

Spin after impact									
Course	Int	C_V	dC_V	C_Θ	dC_Θ	C_ω	dC_ω	r	p
Austerfield	159.3	5.3	1.4	FIXED ANGLE		0.15	0.03	.63	0.0001
Belfry	672.3	5.5	1.6	-12.0	1.8	0.31	0.06	.91	0.0001
Bingley	100.3	11	1.0	FIXED ANGLE		0.21	0.04	.89	0.0001
Crewe	584.8	2.9	0.9	-7.7	0.5	0.20	0.02	.96	0.0001
Formby	147.8	7.4	0.8	FIXED ANGLE		0.35	0.03	.90	0.0001
Ganton	185.6	8.7	2.7	FIXED ANGLE		0.59	0.05	.88	0.0001
Hallowes	90.3	9.7	1.6	FIXED ANGLE				.80	0.0001
Hill Valley	824.6			-12.0	2.2	0.25	0.07	.89	0.0001
Keighley	250.5			FIXED ANGLE		0.29	0.04	.76	0.0001
Lindrick	267.3			FIXED ANGLE		0.16	0.03	.68	0.0001
M. Allerton	217.5			FIXED ANGLE		0.18	0.03	.80	0.0001
Moor Hall	279.1			FIXED ANGLE		0.22	0.02	.85	0.0001
Moortown									
Newcastle	745.3			-9.5	1.1	0.20	0.02	.90	0.0001
Sandmoor	198.7	4.4	0.9	FIXED ANGLE		0.19	0.03	.79	0.0001
Sutton Park	658.7	5.6	0.9	-11.0	0.9	0.29	0.03	.94	0.0001

TABLE 3.8. The regression coefficients for the equations relating the spin after impact with the initial velocity and spin. Negative spin indicates backspin and blank spaces indicate that the variable was not significant in the regression.

horizontal and with zero spin is predicted to rebound with a velocity between 6.4 and 7.6ms^{-1}, at an angle between 39 and 52° and with a spin between 272 and 332rads^{-1}. It should be remembered that backspin is negative spin. These predictions are within one standard error.

In general, the form of the regressions in equations 3.4, 3.5 and 3.6 were found for all the greens studied. The general meaning of these regressions are outlined below. An increase in the incident velocity caused the ball to,

(1) rebound faster

(2) rebound at a steeper angle and

(3) rebound with more topspin.

An increase in the angle of incidence caused the ball to,

(1) rebound slower

(2) rebound at a steeper angle and

(3) rebound with less topspin.

An increase in the backspin of the incident ball caused the ball to,

(1) rebound slower

(2) rebound at a steeper angle and

(3) rebound with less topspin.

If the initial backspin is high enough then backspin would be expected to be retained after impact. It would be very useful to know if impacts in which the ball retains backspin behave in the same way as impacts in which the ball rebounds with topspin. The effect of backspin on the impact is discussed more fully in the following section.

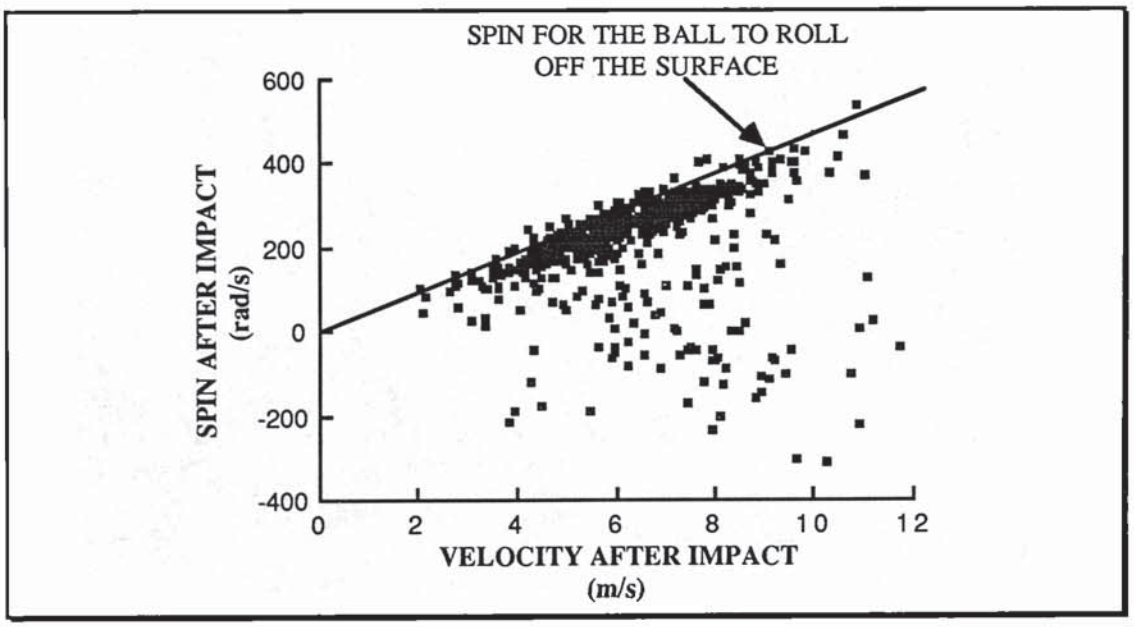

FIGURE 3.6. A graph showing the relationship between the spin after impact and the velocity after impact for all 721 impacts studied. The impacts nearest the line are more likely have rolled off the surface.

(iii) The effect of slip

The analysis of the high speed films in section 3.3 showed that the balls tended to roll off the surface after impact. The relationship between the spin and the velocity after impact for all the impacts recorded using stroboscope photography is shown in Figure 3.6. The line shows the theoretical spin required by a ball for it to roll off the surface, calculated using equation 3.3. For example, a golf ball of radius 21.3mm rolling along the surface at a speed of $5ms^{-1}$ would have a topspin of $234.7rads^{-1}$.

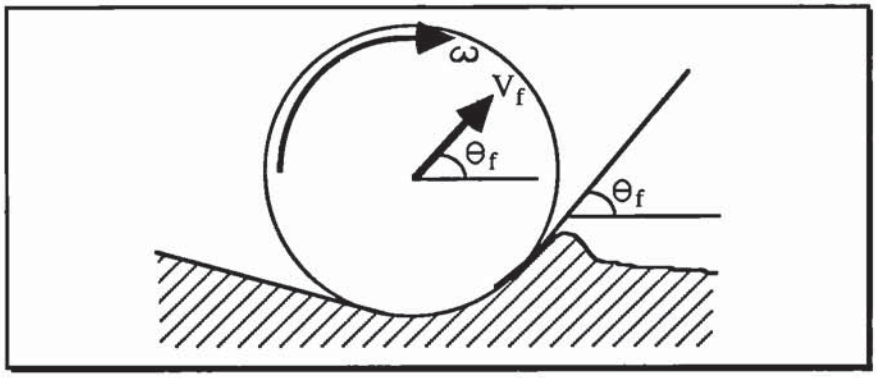

FIGURE 3.7. A schematic representation of a golf ball rolling up the front inclined face of the pitchmark with a topspin related to its absolute velocity.

It can be seen in Figure 3.6 that many of the impacts studied lie close to the line indicating rolling spin. It should be stressed that the velocities used to create this diagram are the absolute velocities and not simply their horizontal components. The closer the impacts lie to the line the more likely it is that the ball rolled off the surface at the end of the impact. The surface along which the ball rolled at the end of the impact must have been at an angle to the horizontal since the ball left the surface at an angle. It is likely, therefore, that the balls rolled up the forward inclined plane of the pitchmark shown schematically in Figure 3.7.

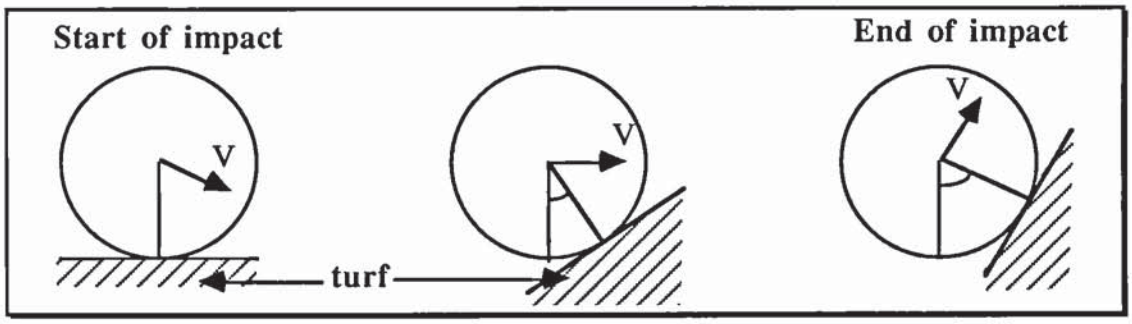

FIGURE 3.8. A diagram representing the modification of the pitchmark during impact. The final direction of the turf determines the direction of the ball after impact.

It can be seen in Figure 3.6 that the main band of points lies parallel to the line for rolling spin and about $50rads^{-1}$ away from it. Thus, many of the balls rebounded from the turf with a topspin just less than that required for rolling. One of the

possible explanations is that most of these impacts *did* roll off the surface and that the topspins were slightly less than the rolling spins because of the modification of the shape of the pitchmark during impact. For instance, consider Figure 3.8. At the beginning of the impact, the plane in contact with the ball is horizontal. As the ball penetrates further the plane alters in angle until it reaches the final angle at which the ball leaves. From the ball's point of view it appears that the ground has rotated around its outer surface.

Thus, if the angle of the ground was altered by 45° and the time of contact was about 9msecs (as found in section 3.3) then the equivalent apparent topspin of the ball was about,

$$\omega = \frac{45°}{9\text{x}10^{-3}\text{s}} = 5000°\text{s}^{-1} \approx 90\text{rads}^{-1}.$$

which is the same order of magnitude as the difference between the band of impacts and the line for impacts to have rolled off the surface in Figure 3.6.

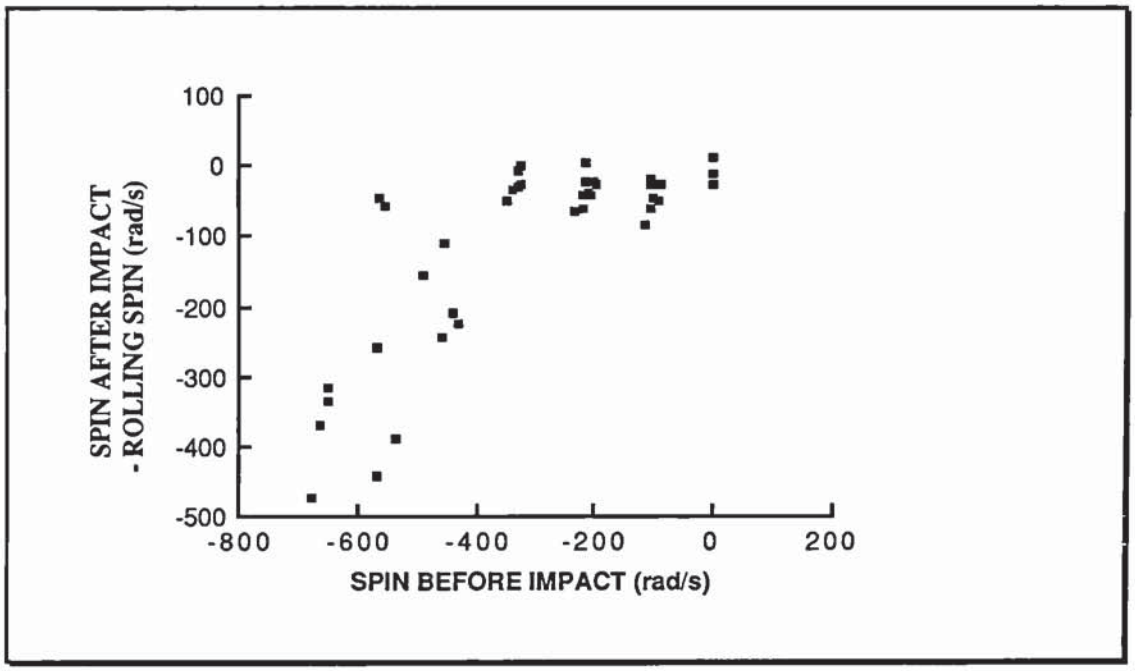

FIGURE 3.9. A graph showing the difference between the actual spin after impact and the spin required for rolling versus the spin before impact for Ganton golf club.

All impacts involve slip to some extent. Only in some of the impacts, however, does the ball slip throughout. It is possible for a ball to rebound with topspin and still to have slipped off the surface. In this case, the topspin of the ball will be lower than that required for the ball to roll across the surface. The larger the difference between the spin of the ball after impact and the spin required for rolling (i.e. the further the impact is away from the line in Figure 3.6) the more likely it is that the ball slipped throughout impact. Figure 3.9 shows a graph of this difference against the initial backspin for the impacts studied at Ganton golf club (Table 3.4). At low backspins the balls leave the

surface with spins comparable to that required for rolling, i.e. the difference between the spin after impact and that for rolling is small. At higher backspins, the balls tended to rebound from the turf with spins much lower than that required for rolling. This indicates that slipping must have taken place. In Figure 3.9 this occurs at a value of about -350rads^{-1}.

Graphs similar to Figure 3.9 were plotted for each green (Appendix F) and balls that slipped throughout impact were chosen arbitrarily as points below the line y = -100rads^{-1}. The sets of results for each green (Appendix E) were then altered so that they contained only impacts where the ball was considered to have rolled off the surface. Stepwise regression were used to observe the effect of the removal of these slipping impacts from the data set. The coefficients of the regressions are shown in Appendix G. It was not possible to carry out statistical analysis on the slipping impacts alone as there were so few slipping occurrences on each green.

Removing the slipping occurrences caused some variables (e.g. spin, velocity) to be removed from the regressions described by equations 3.4, 3.5 and 3.6. In other cases, the form of the regression stayed the same but the value of the coefficients were changed. The individual effects of removing the "slipping " impacts from regressions are too numerous to discuss here. Therefore, the important effects will be described by considering the effect of slip on two different greens.

Figures 3.10 and 3.11 show the results of the impacts on the greens at Austerfield Park and Ganton respectively. The points represent the means of the impacts studied with a single setting of the ball firing device. For example, the average velocity of rebound for impacts at 17ms^{-1} at 45° to the horizontal and with zero spin for Ganton (the first three rows in Table 3.4) is 6.4ms^{-1}. The standard error was 0.3ms^{-1}. To increase the legibility of the graphs in Figures 3.10 and 3.11, the maximum standard error found at each velocity is shown instead of the standard error for each point.

Figure 3.10 shows, in graphical form, the results from the stepwise regressions for Austerfield Park (similar to those in equations 3.4, 3.5 and 3.6) but with the angle of incidence fixed at 45°. At a fixed velocity, an increase in the backspin causes the velocity of the rebounding ball to decrease, the angle of rebound to increase and the positive spin to decrease (i.e. tend more towards backspin). The graphs for Ganton in Figure 3.11 are similar to those for Austerfield but differ at higher backspins. There appears to be a discontinuity in the mid spin range. It is likely that on the green at Ganton the ball slipped off the surface at higher backspins.

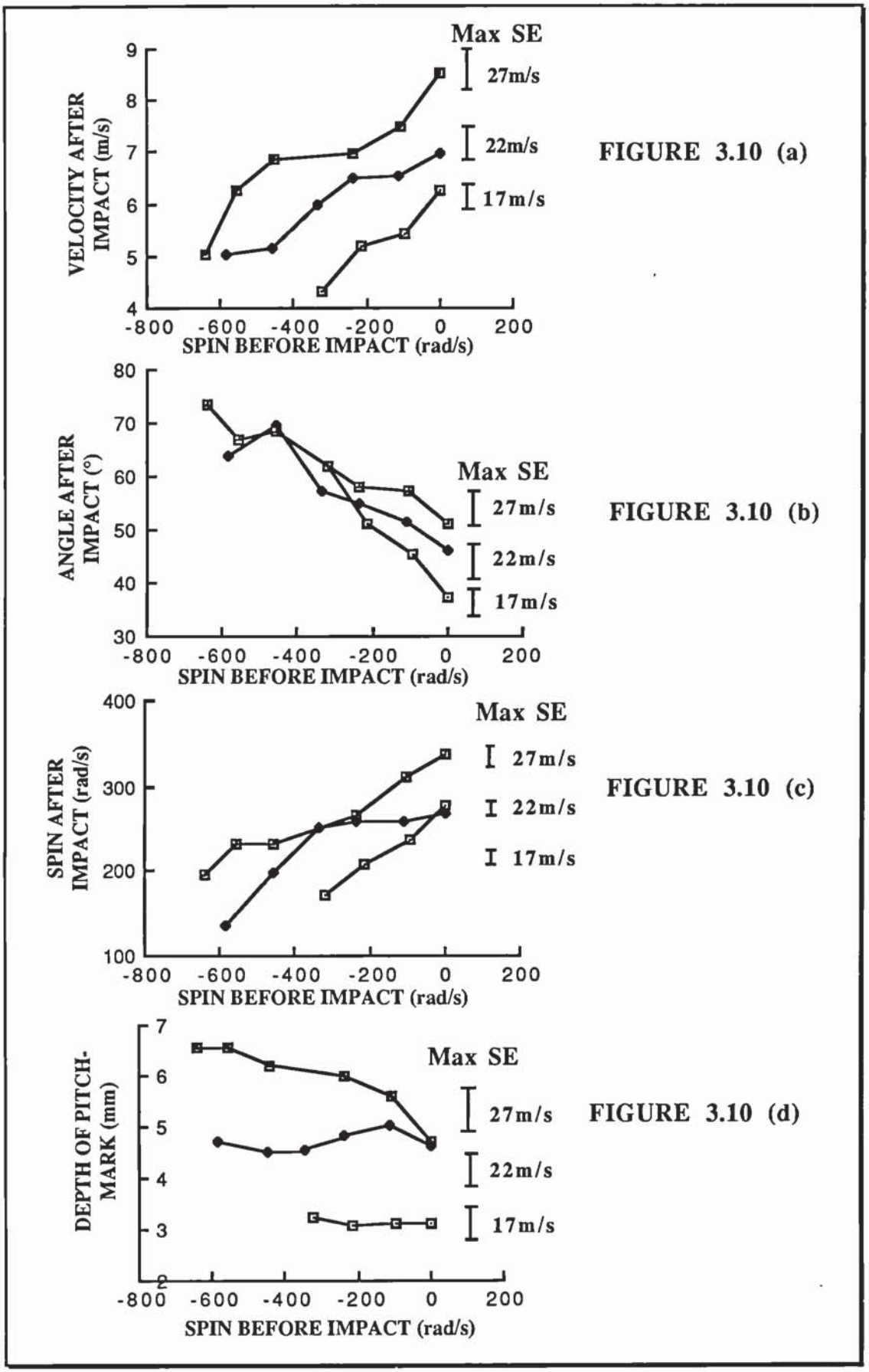

FIGURE 3.10. A series of graphs showing the effect of an increase in spin on the velocity, angle, spin after impact and the depth of the pitchmark for different initial velocities at Austerfield Park.

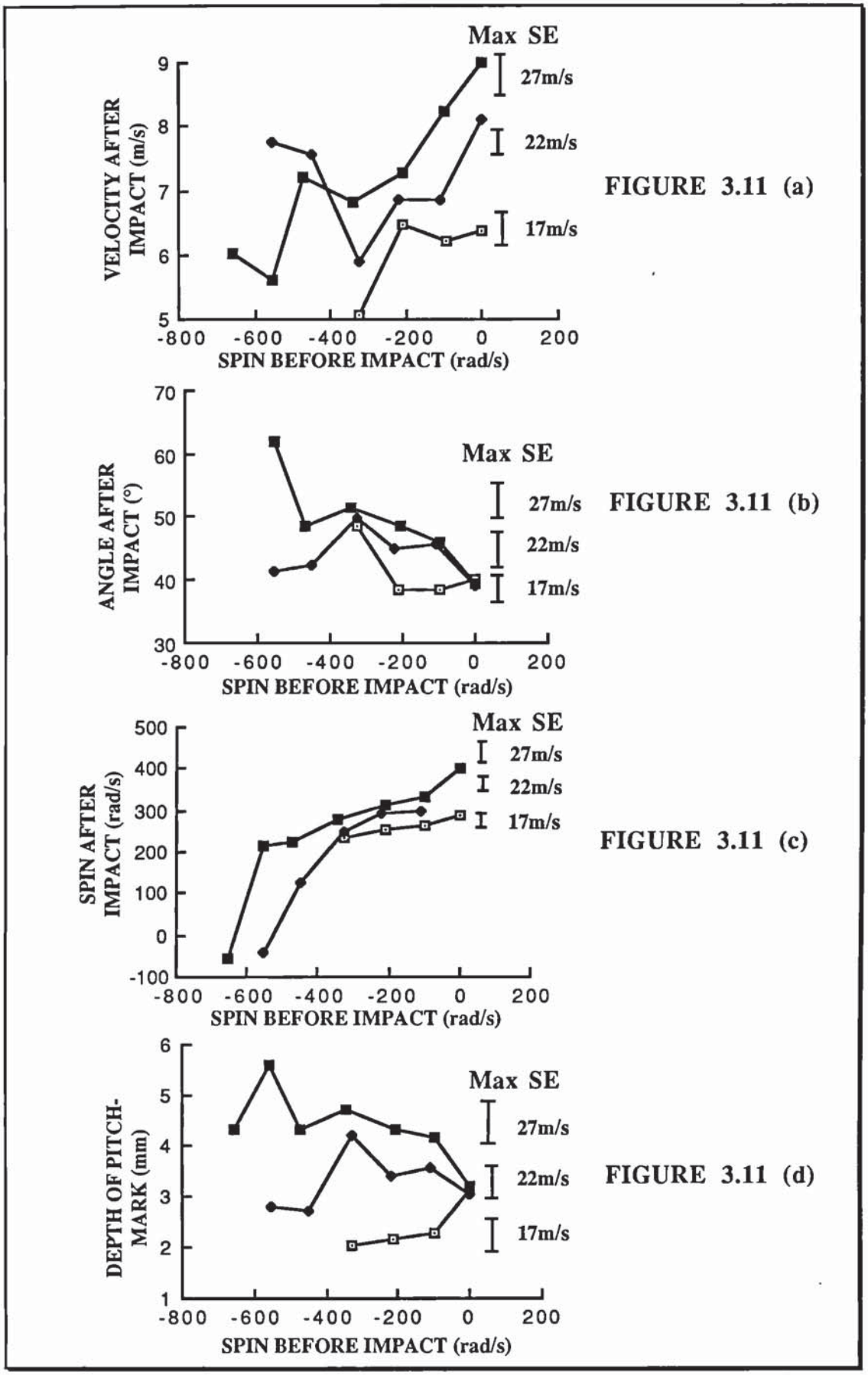

FIGURE 3.11. A series of graphs showing the effect of an increase in spin on the final velocity, angle and spin and the depth of the pitchmark for different initial velocities at Ganton.

This agrees with Figure 3.9 in which it was seen that gross slip started to occur at backspins greater than about -350rads^{-1}. Thus at Ganton, the relationships similar to those in equations 3.4, 3.5 and 3.6 are not strictly valid since they are no longer linear.

Apart from the stroboscope photographs, the only other information of the impact is the pitchmark that was created. This was measured using the green hardness tester described Chapter 2. The effects of the velocity, angle and spin of the incoming ball on the depth of the pitchmark were investigated using multiple regressions. The coefficients are shown in Table 3.9.

Depth of the pitchmark									
Course	**Int**	C_V^2	dC_V^2	C_θ	dC_θ	C_ω^2	dC_ω^2	**r**	**p**
Austerfield	1.60	.0059	.0008	FIXED ANGLE				.71	0.0001
Belfry	-1.84	.0024	.0003	.07	.02			.75	0.0001
Crewe	-0.97	.0030	.0003	.033	.008			.84	0.0001
Ganton	1.17	.0043	.0008	FIXED ANGLE				.65	0.0001
Hill Valley	0.03	.0029	.0005					.70	0.0001
Lindrick	0.70	.0066	.0013	FIXED ANGLE		4.1×10^{-6}	1.4×10^{-6}	.82	0.0001
Moor Hall	-0.23	.0094	.0008	FIXED ANGLE		3.4×10^{-6}	1.3×10^{-6}	.90	0.0001
Newcastle	0.25	.0029	.0002			1.5×10^{-6}	0.5×10^{-6}	.88	0.0001
Sandmoor	1.68	.0046	.0010	FIXED ANGLE				.60	0.0001
Sutton Park	-2.05	.0033	.0003	.05	.01	1.3×10^{-6}	0.4×10^{-6}	.89	0.0001

TABLE 3.9. The coefficients of the stepwise regressions for the depth of the pitchmark created during impact. The depth was measured in mm.

These regressions suggested that the pitchmark depth was directly related to the square of the velocity before impact and in some cases to the initial spin squared. The square of the velocity is a measure of the translational energy of the ball while the spin squared is a measure of the rotational energy of the ball. The regressions coefficients shown in Table 3.9 agree with observations in the field; increasing the incoming energy of the ball increased the depth of the pitchmark.

It was observed that the shape of the pitchmark changed between impacts. Figure 3.12 shows the shape of a pitchmark created by a golf ball with a large amount of spin. At high backspins the grass and roots were sheared through so that the bottom of the pitchmark was bare. The loose material was pushed towards the front of the pitchmark forming part of the ridge seen in Figure 3.12. This material was very loose and on some occasions was projected away from the pitchmark by the impacting ball. These facts suggest that the turf acts as two separate layers, the top layer consisting of grass roots and the lower layer consisting of soil and thatch (dead plant material). This idea is pursued further in Chapter 5.

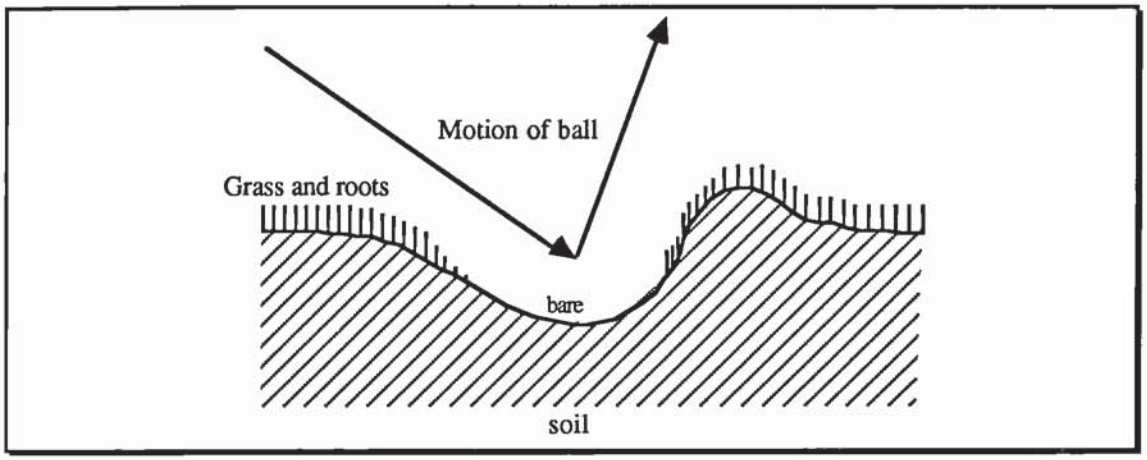

FIGURE 3.12. A schematic diagram of the pitchmark created by a golf ball with a large amount of backspin.

Differences in the pitchmark depth were also observed between greens. Figures 3.10 (d) and 3.11 (d) suggest that the pitchmarks were shallower at Ganton than at Austerfield Park. At Austerfield the depth of the pitchmark was approximately constant at each velocity while on the green at Ganton the depth of the pitchmark appeared to decrease at high backspins. It was observed that this decrease in depth was accompanied by an increase in length and was probably caused by the ball slipping across the surface. This tends to agree with earlier findings which showed that gross slip started to occur on the green at Ganton at these high backspins.

In can be seen in Figure 3.11(a) that the velocity tends to increase when the ball slips throughout impact and that the angle of rebound decreases at high incident backspins. This may be explained by considering the variation in the shape of the pitchmark. As just described, the pitchmark tends to become long and shallow at these high backspins. The front inclined face of the pitchmark is therefore less steep and the ball would tend to rebound at a lower angle. Since the horizontal motion of the ball is opposed less, the ball rebounds at a higher velocity.

It was found that the results from the greens could be split into two categories; (1) those that were like Austerfied Park and mostly had impacts in which the ball rolled off the surface, and (2) those like Ganton in which the ball slipped throughout impact if the backspin exceeded a certain threshold. The numbers of slipping and rolling impacts on each green were determined using the graphs similar to that in Figure 3.9 (Appendix F). Table 3.10 shows numbers of impacts on each green that rolled and those that slipped. The letters "R" and "S" indicate greens on which impacts were likely to roll off the surface at the end of impact and on which the ball could slip off the surface at the end of impact if the backspin was high enough. On eleven of the greens most of the impacts studied rolled at the end of impact, while on five greens there was gross slip occurred in a large number of impacts. It should be stressed that the ball

must slip initially in all the impacts since the peripheral velocity of the ball is not the same as that required for rolling.

Course	Rolling	Slipping	
Austerfield	61	2	R
Belfry	25	33	S
Bingley	36	1	R
Crewe	37	25	S
Formby	37	3	R
Ganton	33	12	S
Hallowes	23	0	R
Hill Valley	23	14	S
Keighley	33	4	R
Lindrick	28	5	R
Moor Allerton	36	0	R
Moor Hall	49	1	R
Moortown	41	2	R
Newcastle	48	3	R
Sandmoor	36	7	R
Sutton Park	39	24	S

TABLE 3.10. The relative numbers of rolling and slipping impacts that occurred on each green. The letter "R" indicates that an impact is likely to roll throughout impact while the letter "S" shows that there was a possibility of slip if the backspin was high enough.

(iv) The effect of slip on subsequent bounces

Table 3.10 shows how greens can be categorised into "rolling" and "slipping" greens. The former is characterised by impacts which rebound at low velocities and at high angles and predominantly with topspin. On the latter type of green the balls rebound at higher velocities and at lower angles. For spins exceeding the "slip threshold" an increase in backspin causes a direct decrease in positive spin after impact. For spins beneath this threshold, the spin after impact does not vary much and depends upon the velocity of the rebounding ball (since $v=\omega r$).

These results become more significant if we consider what is likely to happen to the ball on the second bounce for a ball arriving on a rolling green and on a slipping green with a backspin in excess of $-350 rads^{-1}$. A ball rebounding from the rolling green would tend to have topspin. On the second bounce, the ball would bounce onwards since it already has a spin equivalent to its rolling spin. On the slipping green, the ball would tend to bounce forwards with backspin. This would tend to check or even stop

the ball on the second bounce due to the frictional forces at the point of impact opposing the forward motion of the ball and trying to reduce its backspin. If the backspin is high enough, the retarding frictional forces may overcome the forward motion of the ball and cause it to "screw back" along the ground.

These effects are frequently seen by golfers and the ability of the ball to stop on the green is perceived as its "holding power". What may surprise golfers is that this perception may have different meanings on different greens. For instance, on the rolling green, the ball comes to almost a dead stop on the first bounce and can even rebound in the direction from which it came. Since the ball has topspin after impact, it rolls forwards. On the slipping green, if the backspin on the ball is high enough, the ball can rebound forwards, while retaining some backspin, and "check" on the second bounce. In both cases the ball may end up in the same position relative to the initial impact, but will have arrived there by different means. The golfer may consider, therefore, that both types of green "held" the ball equally as well.

The results in Figure 3.11 also explains the frustration felt by some golfers who find that their shots tend to bounce forwards on the green ending up far from the flag, while professional golfers can play the same green and cause their shot to "screw back" every time. In Figure 3.11 (c) it was seen that, for low amounts of backspin, the ball rebounds with positive rolling spin, i.e. a spin proportional to the velocity of the ball. Thus, a golfer applying spins in this range, will find that the ball bounces forwards after rebounding. Once the golfer applies backspins to the ball exceeding -350rads^{-1}, however, it becomes much easier to cause the ball to screw back. Any increase in the backspin given to the ball produces a corresponding increase in the backspin retained by the ball after impact. It becomes much easier for the golfer to create impacts in which the ball can screw back if backspins are applied above this threshold.

3.5 Summary

One of the conclusions found in this chapter that may have surprised some golfers was that the construction of the ball had little effect on the ball/turf impact (at least for impacts at the velocities, angle and spins tested). Many golfers find that the impact of the ball with the green *is* affected when different golf balls are used and it is concluded that this is due to the differences in the initial spin acquired by the ball on impact with the club face. This causes the trajectories of the balls to be different with the result that the ball arrives at the green with different velocities, angles and spins resulting in dissimilar rebounds. As already stated, the result of this is that the ball can be considered as a rigid solid and will simplify the models of impact which shall be considered later in Chapter 5.

High speed films of the impacts showed that the time of contact of the ball with the turf was approximately 6 to 9msecs and that the forces experienced by the ball were consistent with the ball rebounding from the front forward inclined face of the pitchmark. It was also seen that the impacts tended to roll off the surface at the end of the impact. This fact was also evident in many of the 721 stroboscope photographs of impacts that were studied.

The results of the regressions carried out on the velocity, angle and spin of the ball after impact could be explained by the variation in the depth of the pitchmark created. A deepening of the pitchmark involved a steepening the front plane and this caused the ball to rebound at a high angle. It was found that some of the regressions for certain greens were dissimilar from the rest and that these differences were due to the golf balls slipping throughout impact. Two different types of green emerged. On the first type of green, the ball rolled off the turf and left the surface with a topspin equivalent to the ball rolling up the inside of the pitchmark. In these impacts, the ball invariably rebounded with a low velocity and at a large angle to the horizontal and may even have rebounded in the direction from which it came. On the second type of green, the golf balls always rebounded at a lower angle, at higher velocities and in some cases retained backspin after impact. It was found that there was a threshold for the backspin below which the ball rolled off the surface and above which the ball slipped off the surface. Once the spin of the ball was above this threshold, each additional amount of spin was retained after impact.

The results of this chapter give a clear indication of the effect of a change in velocity, angle or spin on the rebounding ball. These effects are used in the Chapter 5 in the formulation of a model of impact. One of the most important effects that has to be modelled is the discontinuity between impacts which roll or slip off the surface at the slip threshold of $-350 rads^{-1}$.

It is useful to identify the playing characteristics of the two types of green found in this section. A greenkeeper could then do a series of tests on the green to determine how it would play and the maintenance required to cause it to play in the manner requested by the members of the club. The next Chapter assesses the relationship between the impacts and the playing quality and distinguishes between the two types of green.

Chapter 4 - Results and statistical analysis of the tests to determine the characteristics of golf greens

4.1 Introduction

The effect of the characteristics of the green on the impact have not yet been discussed. However, the importance of the depth and shape of the pitchmark in the last chapter shows that the "hardness" of turf is an important factor in the impact. The ball would be expected to penetrate less on a green that is hard while the ball might "plug" into a surface that is very soft. The term "hardness" could have many different meanings, however. This chapter discusses the tests to measure the characteristics of the green. Each test is evaluated to determine its usefulness and its exact meaning. The complex relationships between different characteristics have to be understood in order to determine their exact effects on the ball/turf impact.

Golf courses were visited throughout the summer of 1987 and were chosen to give a variation in the construction and quality of greens and for their proximity to the Institute. One of the difficulties in carrying out research on golf greens was to arrange days during which play was minimal. Furthermore, the work had to be completed in a single day to avoid possible changes in the characteristics of the green. Some of the visits were aborted because of bad weather or because of equipment malfunction but, in total, 18 greens were tested, two of which were on the same course but on different days.

The tests described in Chapter 2 were carried out on each green. For convenience it is possible to separate them into three categories; the first contains tests to study directly the natural characteristics of the turf. These are the grass species composition, the moisture content, the organic matter content and the soil composition. The second and third categories contain tests on properties that are dependent upon these natural characteristics. These are the tests related to the hardness of the green (the Clegg Impact Hardness Tester, penetrometer, traction and ball bounce) and to the motion of the ball across the turf (surface evenness, stimpmeter and friction). For convenience, the first category will be referred to as Green Characteristics while the second and third categories will be referred to as Playing Quality Tests.

The results from each test are shown in Appendix G and the means shown in Tables 4.1 and 4.2. Some data points are missing due to equipment failure on the day or because the apparatus had not been developed when the tests were made. Table 4.1 contains tests concerned with the Green Characteristics and with the Playing Quality Tests related to the surface. Table 4.2 contains the results from the Playing Quality Tests related to hardness. The next section studies each test and examines and compares the measurement errors due

to tha apparatus with the errors inherent in the surface. This is necessary to ensure that the methods of measurement are neither too accurate nor too inaccurate.

4.2 Results

(i) Ground cover and species composition

Twenty frames of five readings were examined using the optical point quadrat frame. The random points located using the frame were identified as dead, bare or as a species of grass and expressed as a percentage of the total ground cover. The most common grasses were *Poa annua* (annual meadow grass) and *Agrostis* (Bent). The percentage of *Poa annua* in the sward is shown in Table 4.1 and varies from 5 to 100%. The errors involved in this analysis can be estimated using the binomial distribution (Woolhouse, 1976). If 100 points are identified and the ground cover of a particular type is 50% then the error is approximately ±10%. This error decreases as the ground cover increases.

(ii) Soil moisture content, organic matter content, soil composition

The results for the moisture content is displayed in Table 4.1. The range was found to be 14 to 43%. The average standard deviation from all the sites was about 2%.

In order to determine the organic matter content and the soil composition, the 10 samples from each green were grouped together. There is therefore only one calculation of organic matter content and soil composition and consequently no error estimation. The mechanical analysis carried out on the soil defined the composition in terms of particle size. Clay, silt and very fine sand are collectively known as fines and have diameters less than 0.125mm. Thus a soil which has very few fines is sandy while one with a high percentage of fines is of a silt or clay type. The percentage of fines present in the soil from each green varied from 11% to 64% (Table 4.1). The overall textural designation is determined on the basis of mass ratios of the sand, silt and clay. In order of increasing particle size, the relative numbers of greens in each classification are, 2 sandy clay loams, 1 loam , 4 sandy loams, 5 loamy sands and 4 sands. For example, the soil from Hallowes was classed as a loam while the soil from Austerfield Park was classed as a sandy clay.

(iii) Surface evenness/roughness

The surface evenness/ roughness was found using the profile gauge described in section 2.6. The standard deviation of the ten rod positions was found at ten positions on the turf and the mean calculated. The most level green had a mean standard deviation of 0.4mm while the roughest green had a value of 1.2mm. The average error in these values was found to be about 0.3mm. The highest and lowest values are, therefore, significantly different, but the range is not very large in comparison to the error. The deviations are

approximately the size of the largest sand grains. Together with the variation in the grass sward, this may be the cause of the irregularities producing the standard deviations. It is possible that these small scale irregularities could cause inconsistencies in the roll of the ball since a small deflection at the beginning of a roll would cause a large deviation.

(iv) Stimpmeter

The stimpmeter was used to roll a golf ball twenty times across the turf at each site. Two balls were rolled along the same path and the distances travelled and the distance between the final ball positions were measured. The latter measurement was used as a simple measure of the consistency of the green; the further apart the final resting points of the two balls the more inconsistent the green. Only two rolls were made along the same line since tracks started to appear if further rolls were made. The method above was repeated in the opposite direction to reduce the effects of minor slopes. The mean of the twenty rolls and the ten differences were calculated and expressed in metres. The consistency figures are presented as a percentage of the mean of the distance rolled under the column heading "% variation" in Table 4.1. Expressing the differences in metres would have been misleading since the balls rolled further on faster greens with a corresponding increase in the variation between rolls.

The slowest green had a "speed" of 1.8m while the fastest had a speed of 2.6m. The average standard deviation was 0.3m. The USGA green section has drawn up guide-lines for stimpmeter readings (Radko, 1977) and the readings above fall in the categories "medium" to "fast" for regular membership play. Cochran and Stobbs (1968) found that, on a good green, a putting machine hardly ever missed putts of around 1.8m. The "% variation" in the stimpmeter readings above was essentially a measure of the distance between the final resting points of two similar rolls across a green. In Cochran and Stobbs' results, the maximum percentage error of this kind occurred if the the ball just reached either side of the hole; in both cases the ball would have dropped into the hole. The distance apart of these two points (i.e the diameter of the hole) was taken as the maximum error allowed in the putts of 1.8m. This distance is about 110mm and corresponds to about 6% of the distance rolled by the ball. Thus, it can be considered, arbitrarily, that a percentage variation of 6% or less indicates a fairly consistent green. This was found on seven of the sites tested.

(v) Sliding friction and traction

Preliminary tests using the sliding friction and the traction apparatus showed that some damage to the greens would occur. Tests were carried out at different locations to study the effect of altering the weight of the apparatus since a lighter apparatus produced less damage to the green. Figure 4.1 (a) shows that the surface traction values for two different sites increased proportionally with the weight of the apparatus. An increase in

the downwards force produced greater penetration of the half golf balls attached to the bottom of the test disc which increased the torque required to twist the disc through the surface. There was hardly any penetration of the surface using a weight of 10kg and therefore the torque required to twist the disc was negligible. Using the friction apparatus it was possible to vary the weight of the apparatus from 10 to 40kg (Figure 4.1 (b)). At two different sites, an increase in weight produced a corresponding increase in the force required to pull the sled along at a constant speed, probably due to the increased penetration of the golf balls on the test sled into the turf. As the relationships between the weight of the apparatus and the traction and friction readings were found to be linear, it was possible to use the lowest weights possible to keep damage to the turf to a minimum. For the traction apparatus this was 20kg and for the friction apparatus this was 10kg. Limiting the tests to five measurements further reduced the damage to the green.

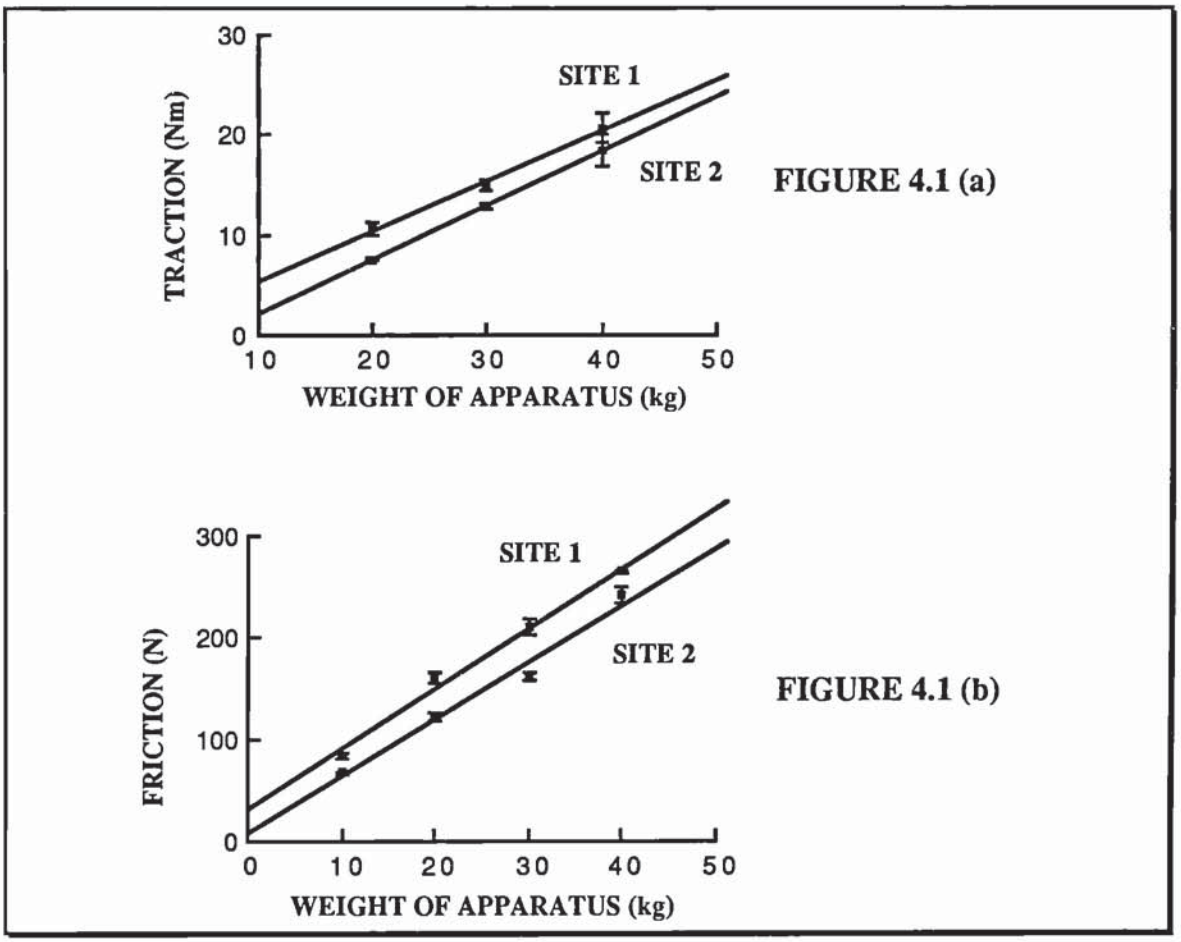

FIGURE 4.1. The effect of increasing the weight of (a) the traction apparatus and (b) the friction apparatus at two different sites.

The results from the traction apparatus varied from 10.1 to 17.7Nm while the average standard deviation was about 1.1Nm. This is consistent with the accuracy of ±1Nm in the reading of the measurement from the torque wrench used to twist the test disc through

TEST / NAME	POA ANNUA (%)	MOISTURE (%)	ORGANIC MATTER (%)	FINES (%)	SURFACE EVENNESS (mm)	STIMP-METER (m)	& VARIA-TION (%)	FRICTION (N)
Austerfield Park	79	24	12.2	48	1.2	1.8	4.3	72
Belfry	56	20	6.1	11	0.8	2.0	6.0	83
Bingley	79	26	7.7		1.0	2.2	7.4	81
Birkdale		25	6.1	18				
Crewe	34	24	3.7	29	0.8	2.3	6.7	93
Formby	43	27	5.9	13	0.6	2.5	4.2	87
Ganton	17	26	6.1	24	0.6	2.6	8.3	73
Hallowes	20	28	5.6	64	1.0			60
Hill Valley	5	17	2.8	11	0.8	2.3	8.5	79
Keighley	65	27	6.1		0.9	2.3	6.0	80
Lindrick (1)		33	8.4	53	0.6	2.4	5.7	71
Lindrick (2)	20	38	8.4	39	0.4	2.4	6.4	85
Moor Allerton	61	14	2.1	12	1.1	2.3	6.9	79
Moor Hall	67	25	6.5	31	0.6	2.4	6.6	87
Moortown	100	43	3.0	35	0.7	2.3	6.4	76
Newcastle-u-Lyme	37	36	7.3	33	0.6	2.1	4.5	85
Sandmoor	97	25	6.3	42	1.0	2.2	5.3	72
STRI green		23	6.9		0.5	2.0	9.3	49
Sutton Park	60	29	7.9	26	0.5	2.1	5.2	86

TABLE 4.1. A table showing the results of the tests used to describe the natural characteristics and four playing quality tests of sixteen golf greens and a test site at the Sports Turf Research Institute.

the turf. The range of values was large enough, compared to the average deviation, for the greens to be considered significantly different.

The highest value using the sliding friction apparatus was 93N and this indicated that it was difficult to pull the sled across the surface. The lowest value was 49N. The average standard deviation was calculated to be about 5N. This is consistent with the individual measurements from the newton meter used to pull the friction sled which were in discrete steps of 5N.

(vi) The Clegg Impact Soil Tester and the USGA penetrometer

Twenty measurements were made per green using each of the four indenters dropped from a height of 300mm. The mean is expressed in gravities (*g*) (Table 4.2). The measurements were taken in discrete steps of 10*g* so that a mean of 29*g* (for Austerfield

NAME \ TEST	CLEGG 0.5kg (gravities)	CLEGG RB (gravities)	CLEGG MB (gravities)	CLEGG 1.0kg (gravities)	PENETRO-METER $\frac{1}{16}$ in	TRACTION (Nm)	BALL BOUNCE (%)
Austerfield Park	29	4	2	20	7.8	17	5.2
Belfry	52	5	7	33	7.1	12	2.3
Bingley				40	5.6	12	3.7
Birkdale							3.9
Crewe	62	10	10	42	7.2	14	5.4
Formby	50	8	9	23	6.2	14	5.6
Ganton	73	22	17	48	7.0	13	4.1
Hallowes	83	20	17	56	7.7	15	5.5
Hill Valley	57	2	5	31	8.3	12	6.4
Keighley	33				7.1	12	8.1
Lindrick (1)	75	20	22	63	4.3	13	4.6
Lindrick (2)	60	12	15	44	5.7	15	4.1
Moor Allerton	66	7	8	43	9.8	13	
Moor Hall	44	7	7	33	6.3	17	4.2
Moortown	48	5	8	24	7.6	18	
Newcastle-u-Lyme	57	8	5	38	5.4	14	4.6
Sandmoor	56	6	6	35	8.9	16	
STRI green	70	23	33	62	11.4		
Sutton Park	61	2	9	39	6.3	14	4.6

TABLE 4.2. A table showing the results of the playing quality tests relating to hardness for sixteen golf greens and five test sites at the Sports Turf Research Institute.

Park for example) was composed of 10, 20 and 30*g* measurements. It was considered that the 0.5kg Clegg was the most suitable indenter to use since individual measurements gave the greatest accuracy. The average standard deviation for the 0.5kg indenter was found to be about ±10*g* which corresponds to the error in individual measurements. The average value for the Clegg 0.5kg indenter was found to be 57*g*. In Chapter 3 the accelerations from the high speed films were compared to the average value of the Clegg indenter above. It was found that the analogy of the impact as the motion of a mass on a spring was not correct. This was not surprising since there must be a damping component if the ball is to slow down during impact.

Twenty measurements were also made on each green using the USGA penetrometer and a range of 4.3 to 11.4 sixteenths of an inch was found. The lower value indicates a firm green where the penetration was low. The higher value indicates a green which was soft and therefore unresistant to penetration. In this case the penetration was almost the radius

of a golf ball. Individual measurements were read to an accuracy of ±1 sixteenth of an inch. The average standard deviation was 1.3 sixteenths of an inch.

(vii) Ball rebound resilience

A Titleist 384 tour wound golf ball was used for the ball rebound resilience tests as this was the type of ball used in the studies of golf ball impacts. A comparison was made, however, between the wound ball and a Pinnacle 384 solid golf ball, the constructions of which were described in Chapter 3. Ten drops of each ball were recorded at a single site and the rebound heights expressed as a percentage of the drop height. The mean and standard deviation of ten drops for the wound golf ball was 5.5 ± 0.4%. This corresponds to a rebound height of 28 ± 2cm. Using the solid golf ball, the mean and standard deviation was 5.2 ± 0.6%, corresponding to an average rebound height of 26 ± 3cm. If the means are compared using a t-test, it is found that there is no significant difference between the ball rebound resiliences for the two constructions of ball. Therefore, at this height, the rebound resilience depends upon the characteristics of the turf rather than the properties of the ball. This agrees with the tests in Chapter 3 in which it was found that the construction of the ball had little effect on the impact of the ball with the turf.

Using the Titleist wound golf ball, ten drops were recorded on each green and the mean of the values expressed as a percentage of the original drop height of 5m. The range of rebound heights found across the greens varied from 11cm to 41cm, corresponding to a rebound resilience of 2.3 to 8.1%. It was possible to measure the rebound heights to within approximately ±™cm which corresponds to an error in the ball rebound resilience of about 0.1%. It was found that the average of the standard deviations for all the greens was five times larger than this at approximately ±2™cm for the rebound height or 0.5% for the ball rebound resilience.

4.3 Analysis

(i) Introduction

The correlation matrix shown in Figure 4.2 contains correlation coefficients of the relationships between all the tests shown in Tables 4.1 and 4.2. A coefficient of zero indicates that there was no correlation between the variables while a value of plus or minus one indicates an exact linear relationship. The negative sign indicates an inverse relationship. The number of degrees of freedom in each correlation determines the level of significance of the relationship. For instance, it can be found using tables that a correlation with 20 occurrences and a correlation coefficient of 0.6 is significant at the 1% level of confidence. This indicates that there is a probability of only one in a hundred that this relationship occurred by chance. The values boxed in bold in Figure 4.2 are signifi-

	CLEGG 0.5 kg	CLEGG RB	CLEGG MB	CLEGG 1.0kg	PENETROMETER	TRACTION	% BALL BOUNCE	% POA ANNUA	% BENT	% MOISTURE	% ORGANIC	% FINES
CLEGG 0.5 kg	1											
CLEGG RB	0.727	1										
CLEGG MB	0.644	0.885	1									
CLEGG 1.0kg	0.841	0.844	0.843	1								
PENETROMETER	0.068	0.072	0.183	0.064	1							
TRACTION	-0.183	-0.28	-0.344	-0.408	0.222	1						
% BALL BOUNCE	-0.196	0.001	0.052	0.037	0.083	-0.304	1					
% POA ANNUA	-0.572	-0.468	-0.393	-0.476	0.175	0.549	-0.253	1				
% BENT	0.369	0.039	-0.108	0.022	-0.127	-0.432	0.185	-0.929	1			
% MOISTURE	-0.012	0.128	0.158	0.015	-0.453	0.185	0.239	-0.027	-0.112	1		
% ORGANIC	-0.240	0.135	0.151	0.042	-0.171	0.053	0.127	0.208	-0.243	0.347	1	
% FINES	0.217	0.505	0.44	0.433	-0.261	0.363	0.203	0.142	-0.544	0.511	0.556	1
LEVELS	0.386	0.468	0.296	0.509	0.127	-0.426	0.024	-0.417	0.291	-0.274	-0.417	0.122
STIMPMETER	0.399	0.35	0.159	0.241	-0.299	-0.309	0.256	-0.418	0.181	0.132	-0.359	-0.185
% VARIATION	0.230	0.001	0.348	0.398	0.001	-0.125	0.089	-0.305	0.246	-0.378	-0.167	-0.189
FRICTION	-0.385	-0.642	-0.647	-0.539	-0.56	-0.162	0.029	0.033	0.205	0.047	-0.135	-0.627

	LEVELS	STIMPMETER	% VARIATION	FRICTION
LEVELS	1			
STIMPMETER	0.211	1		
% VARIATION	0.269	0.001	1	
FRICTION	-0.283	0.27	-0.566	1

FIGURE 4.2. A correlation matrix showing the relationships between the tests for playing quality and the natural characteristics of the green. Relationships that correlated well have coefficients near to plus or minus unity. Negative values indicate an inverse relationship. The values boxed in bold are significant at the 5% confidence level and those that are boxed and underlined are significant at the 1% confidence level.

-cant at the 5% level of confidence and those that are boxed and underlined are significant at the 1% level of confidence. As with Tables 4.1 and 4.2, the Playing Quality Tests and the Green Characteristics are grouped together.

All of the playing qualities described in the previous section depend to some extent upon the recent weather experienced by the green. A recent drought may cause the green to become very dry and hard while a heavy storm may cause an abnormally high moisture content. In some cases the construction of the green or past maintenance regimes may affect the tests. The correlations shown in Figure 4.2 were analysed in more detail using regression analysis. The results of this, and their graphical representations are given in the following sections.

(ii) Green Characteristics

The correlations involving the naturally occurring turf characteristics were considered first since they were, in effect, the independent variables measured by the other tests.

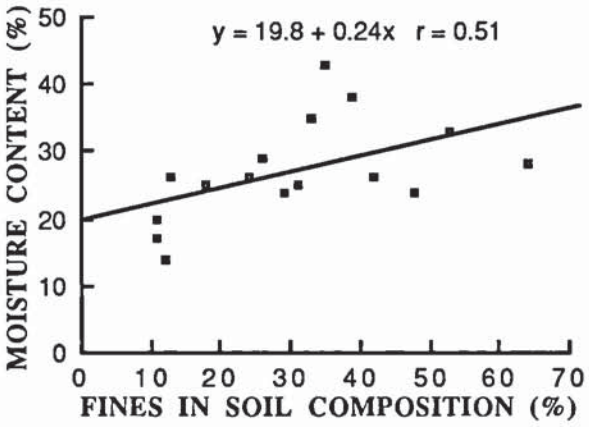

FIGURE 4.3 (a)

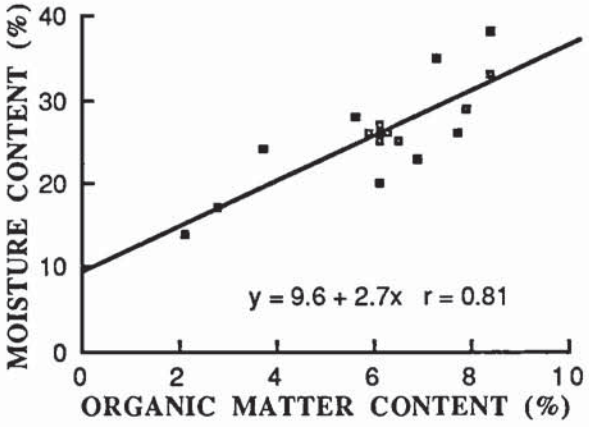

FIGURE 4.3 (b)

FIGURE 4.3. The relationships between (a) the moisture content and the percentage of fines in the soil composition and (b) the moisture content and the organic matter content of the soil from different golf greens.

The moisture content correlated with the percentage of fines present in the soil at the 5% level of significance. Figure 4.3 (a) shows that the moisture content increases as the percentage of fines increases.

It has been found (Buckman and Brady, 1971) that soil water drains from large pore spaces first and remains in small pore spaces longest. Clay soils have very small particles and the resultant pore spaces between them are also small. A smaller, additional factor is that the clay particles have surface charges which attract water molecules. Soils with a high amount of clay, therefore, tend to have higher moisture contents than soils with a high sand composition.

Figure 4.3 (b) shows that the moisture content is positively correlated with the organic matter content at the 1% level of significance. This, however, was not found in the correlation matrix since two spurious points were found either side of a central band and were consequently omitted. One of the occurrences was that for Moortown and at this green the drainage was very poor. It is possible that the poor drainage of the green affected the moisture content more than the amount of organic matter present in the soil to produce an abnormally high reading. The other occurrence was that for Austerfield Park. This green was constructed on an old waste site and it is possible that this caused the organic matter to be abnormally high. Excluding these two values increases the correlation coefficient to 0.81 at the 1% level of significance. If this is a true correlation then it suggests that a soil with a high organic matter content has a high soil moisture content. This could be caused by a number of factors and it is not clear which is cause and which is effect. Organic matter *is* very water absorbent, but wet soils hinder the breakdown of organic matter due to their anaerobic nature. This fact links high organic matter contents to high moisture contents. In Figure 4.3 (a) it was seen that high moisture contents occurred on soils with high clay and silt contents. Clay contains water molecules that are only released during the high temperatures experienced during loss on ignition (determination of organic matter content). This contributes to the organic matter content reading giving a larger value than might be expected. The relationships shown in Figure 4.3 (a) and (b) are, therefore, closely linked. Soils with a high percentage of fines tend to have high moisture contents and large organic matter contents. All three measures may be mutually dependent and so it is necessary to state the value of each when determining the characteristics of a turf.

The species of grass prevalent on the green also has an effect on the organic matter and moisture content. Two dominant species of grass were found on the greens visited, *Poa annua* and *Agrostis*. *Poa annua* prefers moist conditions while *Agrostis* is much more drought resistant and is able to live in drier conditions. Thus, where one predominates the

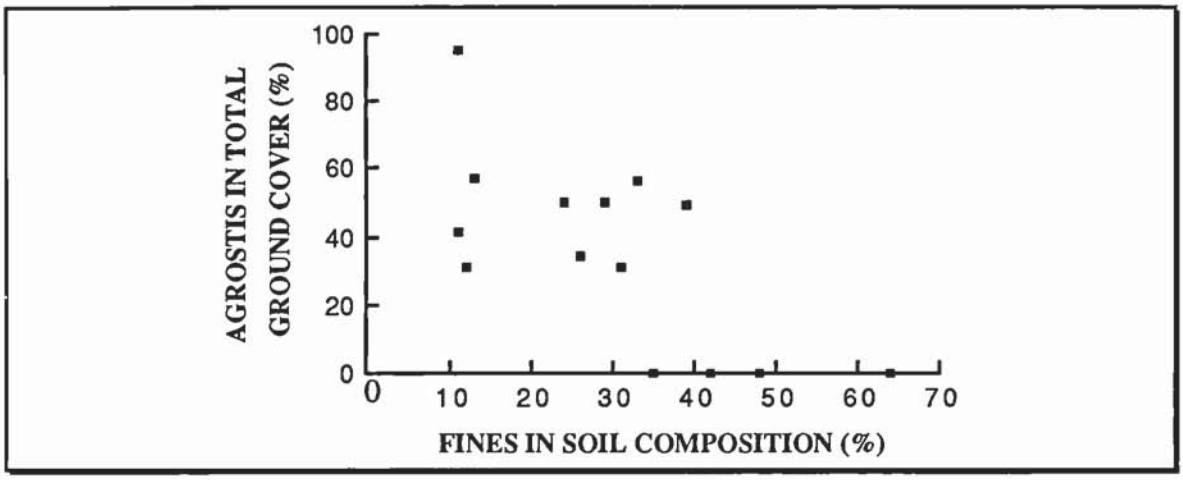

FIGURE 4.4. The relationship between the percentage of *Agrostis* in the total ground cover and the percentage of fines in the soil.

other is insignificant and, in most of the cases studied, the *Poa annua* and the *Agrostis* provided the total ground cover.

Figure 4.4 shows that the trend is for *Agrostis* to live on sandy soils. Since *Agrostis* is drought resistant, it is able to live on the free draining sandy soils where other grasses such as *Poa annua* would die. The *Agrostis* is therefore linked with the soils that have low clay compositions, low moisture contents and low organic matter contents. As with the graphs in Figure 4.3 (b), it is not clear which is cause and which is effect. It may be that the dominant species of grass present is not just an indicator of the characteristics of the green but also contributes to those characteristics.

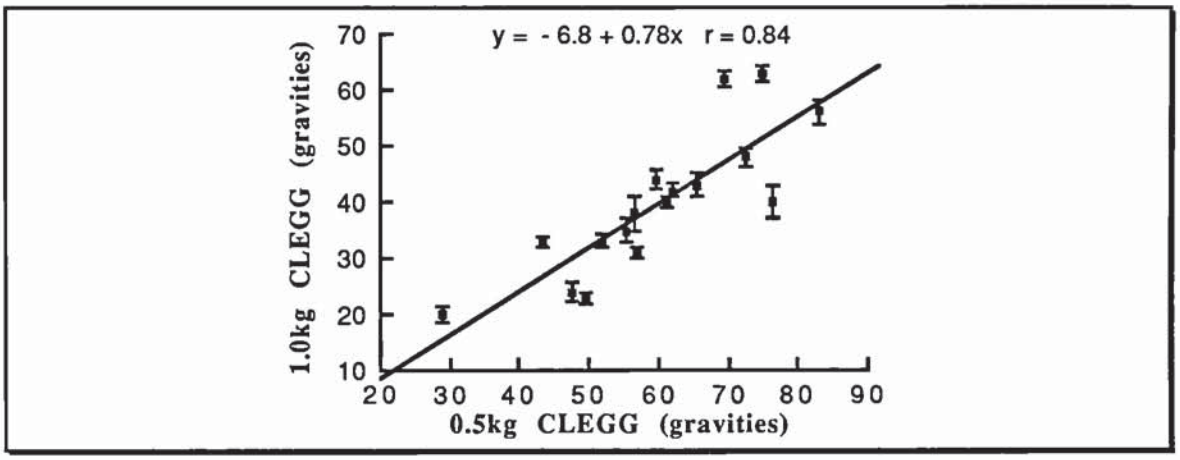

FIGURE 4.5. The relationship between the 1.0 and 0.5kg cylindrical indenters used with the Clegg Impact Hardness Tester.

(iii) Playing Quality Tests relating to the hardness of the surface

As might have been expected, the correlations between the different indenters used with the Clegg Impact Hardness Tester were all significant at the 1% level of confidence (Figure 4.2). The relationship between the maximum decelerations measured using the

1.0kg and the 0.5kg cylindrical indenters is shown in Figure 4.5. The measurements from the indenters are proportional to each other and this fact indicates that they are probably measuring the same property of the soil. There is little, if any, difference between the readings taken with the indenter with a metal golf ball shaped end and that with a real golf ball adhered to its end. As with the results from the ball rebound resilience earlier in this chapter, this implies that the elastic properties of the ball play a minor role in the impacts.

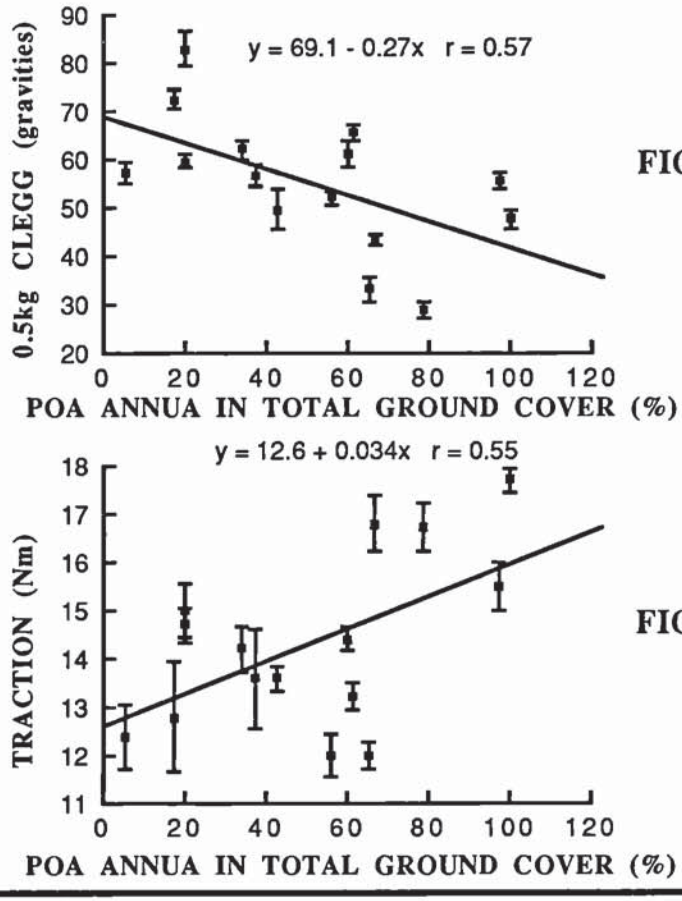

FIGURE 4.6 (a)

FIGURE 4.6 (b)

FIGURE 4.6. The relationships between (a) the 0.5kg Clegg indenter and (b) the traction with the percentage of *Poa annua* in the sward.

The 0.5kg Clegg and the amount of *Poa annua* present in the grass sward were correlated at the 1% level of significance with a correlation coefficient of 0.57 (Figure 4.6 (a)). The maximum deceleration of the indenter measured by the Clegg Impact Hardness Tester decreases as the amount of *Poa annua* in the sward increases. It is known that the above ground biomass is higher for *Poa annua* than for *Agrostis* mown at 25mm (Canaway 1983). This increase in biomass with an increase in *Poa annua* would cause the Clegg values to be decrease since the ground would be softer. An additional factor may be due to the fact that *Poa annua* prefers moist conditions and so tends to live on soils with a high clay and organic matter content where the soil is likely to be soft anyway. The 0.5kg

Clegg, therefore, indicates that the ground is likely to produce a lower deceleration when the amount of *Poa annua* in the sward is high.

The traction values were found to correlate positively with the percentage of *Poa annua* at the 5% level of significance, i.e. the higher the amount of *Poa annua* the harder it is to twist the disc through/across the surface. This relationship could be caused by the nature of the soil reflected by the species composition. *Poa annua* prefers clay soils which are "heavy" and bind together well. Sandy soils, on the other hand, have little *Poa annua* on them and are easy to shear through. If soils with a high clay content are soft then the test disc on the traction apparatus is likely to penetrate into the soil. This would produce high traction readings. On a firm sandy soil, on the other hand, the test disc may not penetrate into the soil and may interact more with the top layer of grass and organic matter. This may result in a lower traction reading. Thus, Figure 4.6 indicates that a turf with a large amount of *Poa annua* in its sward reflects, and to some extent causes, conditions that are soft to a vertical impact but quite resistant to shear through the surface. Conversely, soils with a small amount of *Poa annua* are likely to be sandy and appear firm to a vertical impact but relatively weak to horizontal motion of a ball through the surface.

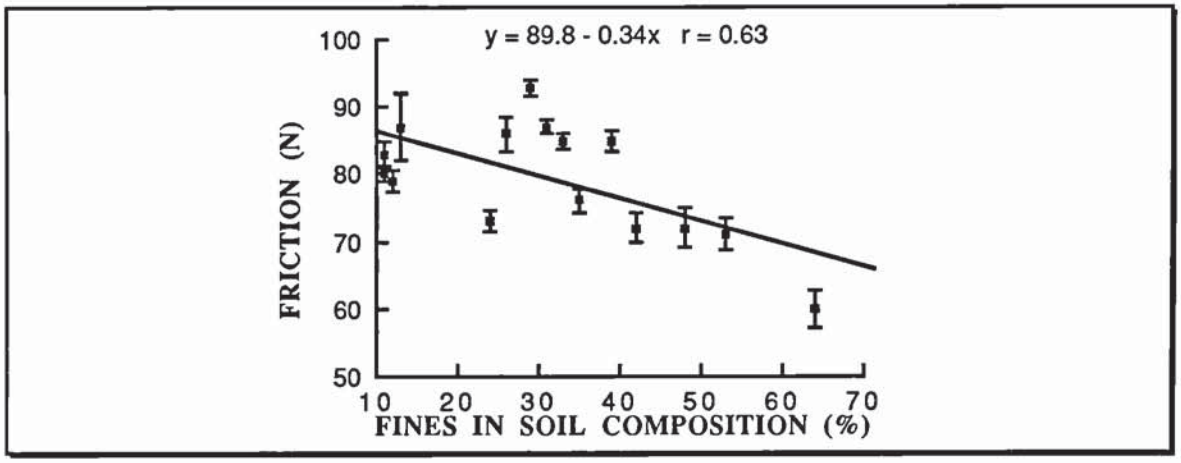

FIGURE 4.7. The relationship between the friction of the surface and the percentage of fines in the soil.

(iv) Playing quality tests relating to the surface characteristics

The percentage of fines present in the soil was negatively correlated with the friction of the soil at the 5% significance level, i.e. the friction of the surface tended to decrease as the percentage of fines increased (Figure 4.7).

The fines are particles less than 0.125mm in diameter and a golf ball sliding across a soil composed mostly of particles of this size would experience little resistance. The particles in a sandy soil, on the other hand, could be as large as 2mm and would resist the motion of the golf ball over the surface therefore increasing the frictional force measured by the friction apparatus. This hypothesis assumes that the test apparatus is sliding across the

bare soil and does not account for the effect of the the grass on the frictional force. Another possible explanation is that clay soils tend to have a higher moisture contents and that this affects the moisture on the surface. This moisture then produces surfaces that have a lower friction than their dryer counterparts.

The purpose of this section was to gain an understanding of the relationships between the different Green Characteristics and Playing Quality Tests. It is now possible to use them to determine their effect on the ball/turf impact. The relationships between the Green Characteristics and the impacts described in Chapter 3 are discussed in the following section.

4.4. The effect of Green Characteristics on Ball/turf impacts

It is useful to understand the effects of different characteristics of the green on golf ball impacts with the turf so that the effect of different maintenance regimes and constructions can be assessed. The relationships between the velocity, angle and spin of the rebounding ball and those of the incident ball were shown in Chapter 3. If Tables 3.6, 3.7 and 3.8 are reconsidered, for instance, it can be seen that the coefficients of the regressions for the velocity, angle and spin vary from one green to another. The most likely cause of these differences is the variation in the characteristics of the green. The following method compares regression coefficients with Green Characteristics. These relationships will be beneficial to our understanding of the ball/turf impact.

Consider again the regression coefficients in Tables 3.6 to 3.8. These coefficients were correlated with the results from the playing quality tests in Tables 4.1 and 4.2. For instance, the relationship between the spin coefficients for the rebound velocity in Table 3.7 and the penetrometer readings for each green had a correlation coefficient of 0.235. This was not significant at the 5% level of confidence and was therefore rejected.

Five significant relationships were found and each one is considered individually. Figures 4.8, 4.9 and 4.10 show the relationships between three regression coefficients and the percentage of fines in the soil. Figure 4.8 shows the relationship between the coefficient for the angle of incidence in the regression for the velocity after impact (Table 3.6) and the fines in the soil. This correlated at the 5% level of significance. It is important to realise that this relationship indicates that the percentage of fines influences the *manner* in which the angle of incidence effects the velocity after impact. There are only five points on the graph since the angle of incidence was varied on only five greens. The errors shown are the standard errors of the coefficients and can be found in Table 3.5.

At this stage the meaning of the relationship is fairly abstract. It can be explained, however, if Figure 4.8 (b) is considered. A pure sand has zero fines present in it and, using the equation in Figure 4.8 (a), the angle regression coefficient would be $-0.3ms^{-1}$ per degree. As the percentage of fines in the soil increases the angle regression coefficient also increases and reaches zero when the percentage of the fines in the soil is about 60%. Thus a soil with 60% fines would have zero slope while a pure sand would have a slope of $-0.3ms^{-1}$ per degree.

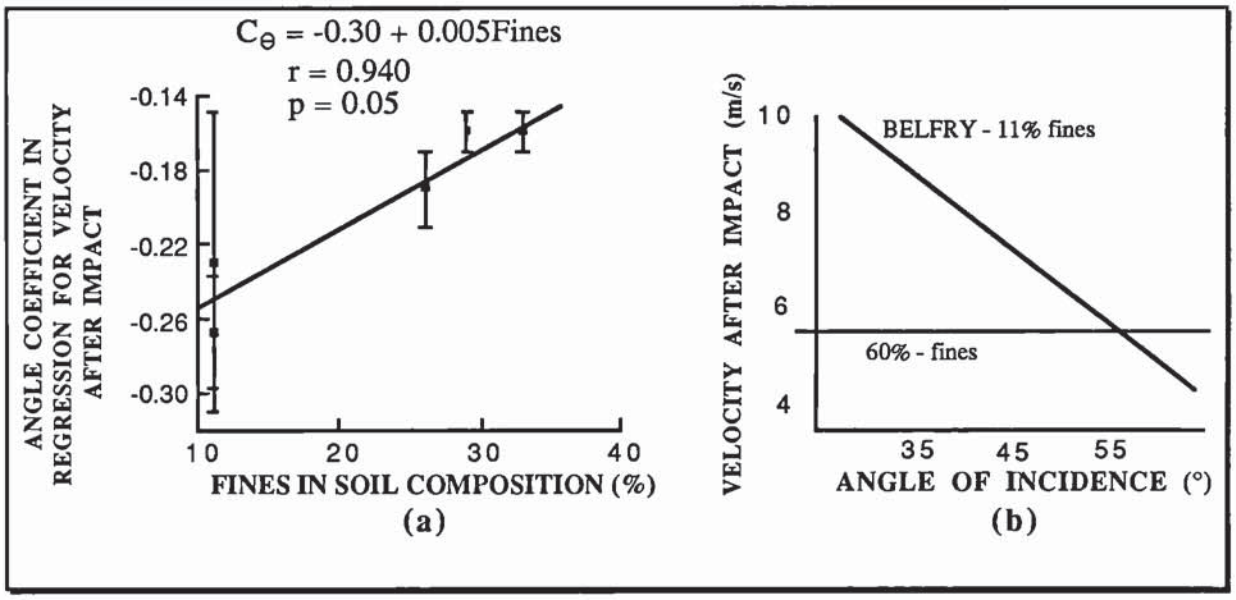

FIGURE 4.8. Graphs showing (a) the relationship between the angle coefficient in the regressions for the velocity after impact and the percentage of fines in the soil composition and (b) the relationship this implies between the velocity after impact and the angle of incidence.

An increase in the angle of incidence on a sandy green, therefore, produces a large decrease in the velocity of the rebounding ball. An increase in the angle of incidence on a clay green, however, has little effect on the velocity of the ball after impact. It tends to have the same rebound velocity independent of the incoming angle. The intercept of the lines in Figure 4.8 (b) were found to decrease as the slope approached zero. The velocity of rebound on a clay green was, therefore, lower for most angles of incidence than on a sandy green.

Figure 4.9 (a) shows the relationship between the spin coefficient in the regressions for the spin after impact with the fines present in the soil. It was significant at the 5% level of significance and shows that, as the percentage of fines in the soil increases, the spin regression coefficient decreases. Thus, on a pure sand soil, the spin coefficient would be at its maximum. On a soil containing about 60% of the fines the slope is zero. These facts are translated onto Figure 4.9 (b). An increase in backspin (i.e a decrease in the positive spin, since backspin is negative) produces a large increase in the final backspin

on sandy greens but has little effect on clay greens since the topspin of the rebounding ball remains approximately constant, independent of the initial spin.

If Figures 3.10 (c) and 3.11 (c) are reconsidered, it can be seen that the variation of the spin after impact with the incident spin is less for Austerfield Park than for Ganton. At Austerfield Park the spin of the rebounding ball is predominantly related to the rebound velocity. Thus, the spin after impact varies little with the incident spin. At Ganton, however, gross slip occurs and and since the rebound spin is proportional to incident spin, the variation in the spin after impact is much greater. In effect, therefore, Figure 4.9 is stating that the ball will slip throughout impact on a green with a low percentage of fines and not on a green with a high percentage of fines. Further evidence for this will be shown in the next section.

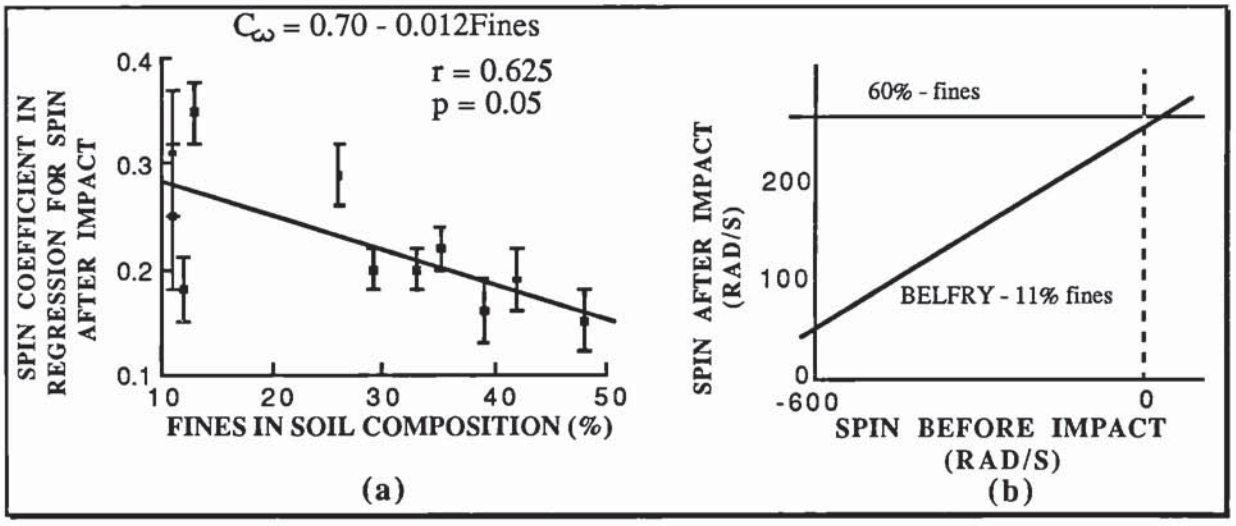

FIGURE 4.9. Graphs showing (a) the relationship between the spin coefficient in the regressions for the spin after impact and the percentage of fines in the soil composition and (b) the relationship this implies between the spin before and after impact.

During the analysis of the impacts, the energy loss of the ball during impact was calculated. This was done by summing the kinetic energy of the ball with its rotational energy before and after impact using,

$$\text{Energy of ball} = \frac{1}{2}m\,v^2 + \frac{1}{2}I\omega^2 = \frac{1}{2}m\,v^2 + \frac{1}{2}(0.4mr^2)\omega^2$$

where m is the mass of the ball, v is its velocity, I is the moment of inertia, r is its radius and ω is its spin. The calculation of the moment of inertia approximates the ball to a homogeneous solid. The effect of the percentage of fines in the soil on the energy lost during impact is considered in Figure 4.10. Figure 4.10 (a) shows that an increase in the percentage of fines in the soil composition produces an increase in the spin coefficient for the regressions for the loss of energy of the ball as it impacts with the turf. The spin coefficient is, therefore, low on sandy greens and high on greens with a large clay content. This is described schematically by Figure 4.10 (b) in which the energy lost by

the ball is little affected by a change in the spin on sandy greens. On a clay green, however, an increase in the initial backspin produces a large increase in the energy lost by the ball.

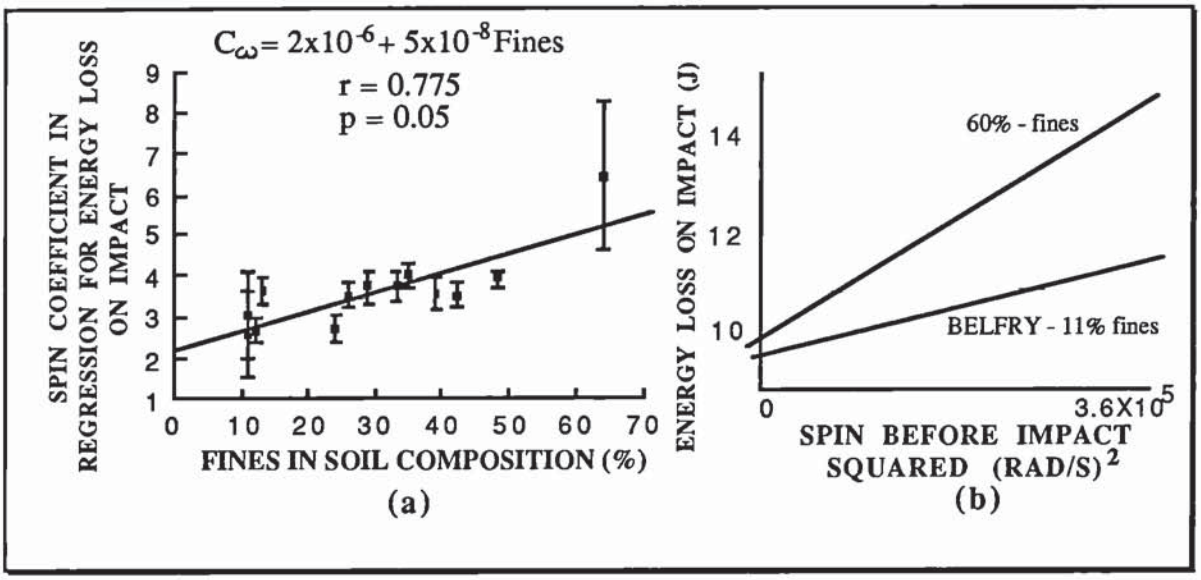

FIGURE 4.10. Graphs showing (a) the relationship between the spin coefficient in the regressions for the energy lost by the ball during impact and the percentage of fines in the soil composition and (b) the relationship this implies between the energy loss and the spin before impact.

The effects described by Figures 4.8, 4.9 and 4.10 can be explained by the differences found between clay and sandy greens found earlier in this chapter. Greens with a high clay content are often moist and tend to be unresistant to vertical forces but resistant to horizontal motion of the ball across the turf. Greens with a high sand content, on the other hand, tend to be dryer and much firmer. The result is that sandy greens are resistant to vertical forces and, since the pitchmark is much shallower, the forces opposing horizontal motion are less. On clay soils, there does not tend to be much difference between impacts since the ball rebounds with roughly the same low velocity and with the same amount of topspin regardless of the initial impact. Sandier greens are much more receptive to changes in the angle of incidence and the initial backspin since the pitchmark changes more in depth as the impacts vary.

4.5 The characteristics of greens that allow backspin to be retained

The basic characteristics of the greens on which slip is likely to occur can be determined if we redraw some of the graphs found earlier in this chapter. Figure 4.11 shows the information contained in Figure 4.3, the letter "s" indicates the greens on which the ball was likely to slip off the surface if the initial backspin was high enough. Table 3.10 shows the greens that were considered to allow backspin to be retained if the incident spin exceeded -350rads^{-1}. It can be seen in Figures 4.11 (a) and (b) that these greens are

characterised by a fairly low percentage of fines, a low organic matter content and a low moisture content. If Figure 4.6 is also reproduced in Figure 4.12 it can be seen that the greens on which slipping occurred had fairly low percentages of *Poa annua* in their sward, high Clegg Impact Hardness Tester measurements and low traction values. Therefore, slipping occurred on fairly sandy greens that were well drained and had a low organic matter content. These were quite resistant to vertical impacts. Horizontal motion through the turf was fairly unimpeded.

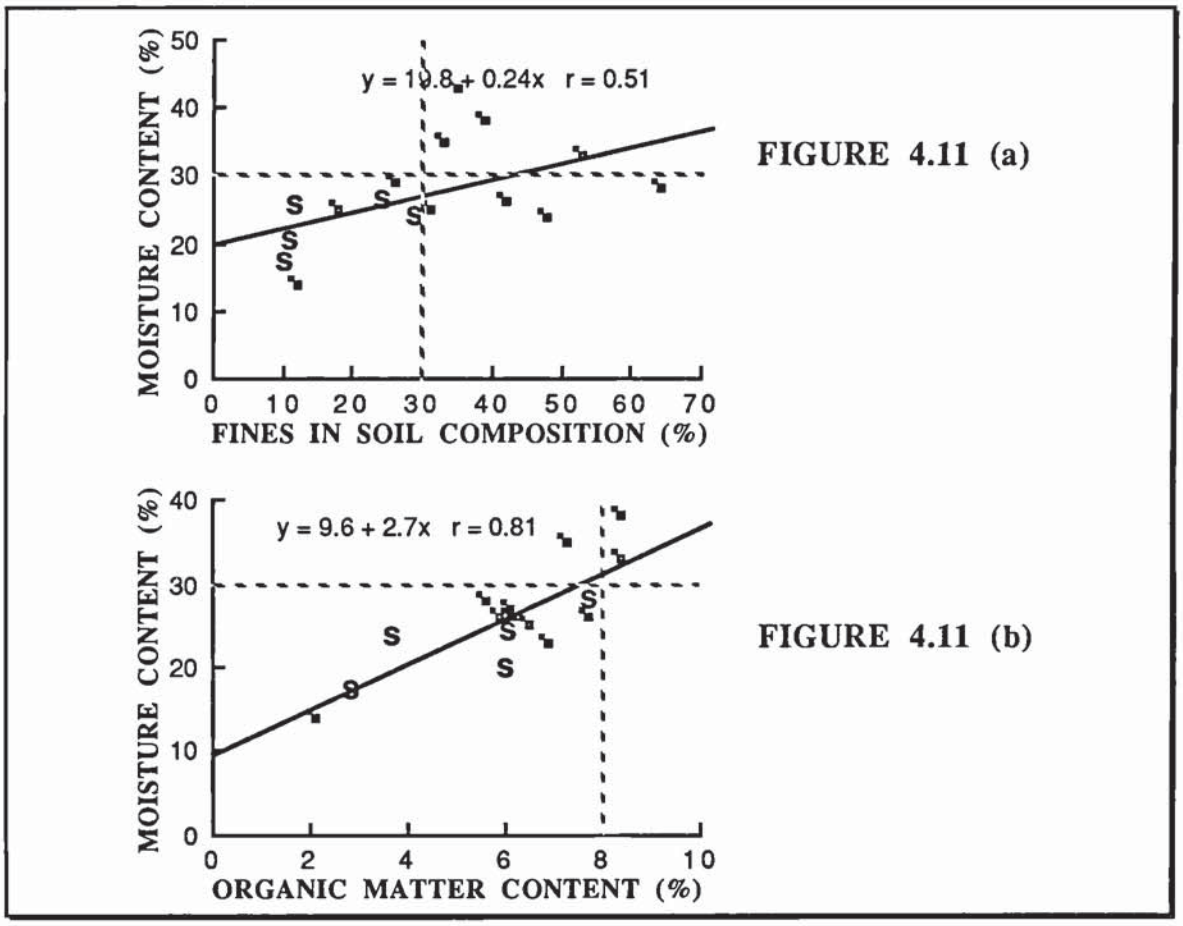

FIGURE 4.11 (a)

FIGURE 4.11 (b)

FIGURE 4.11. Graphs to show the relationship between greens where golf balls are likely to slip when rebounding from the surface and the natural characteristics of the turf. These greens are indicated by the letter "s".

Using these graphs, limits of all the tests can be suggested to indicate the likelihood of the ball slipping at the end of impact on a particular green. For slip to take place, the upper limit for the percentage of fines and the moisture content of the soil should be about 30% while the maximum organic matter possible should be about 8%. Slip throughout impact is most likely to occur if the percentage of *Poa annua* in the sward is less than 60% and if the measurements using the Clegg Impact Hardness Tester (0.5kg indenter) are greater than about 50*g*. The lowest desirable traction value for slipping to occur throughout impact is about 15N.

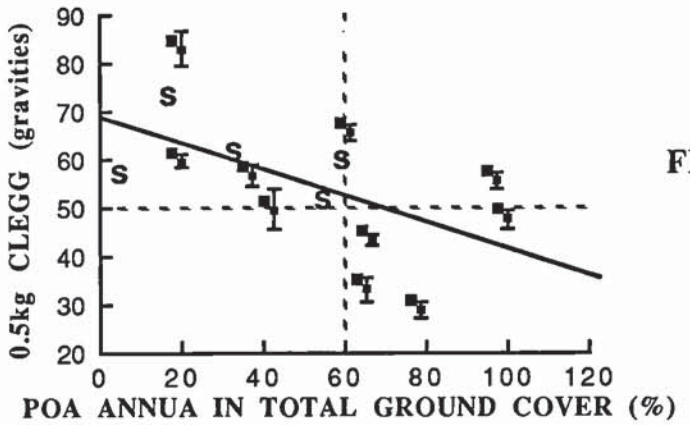

FIGURE 4.12 (a)

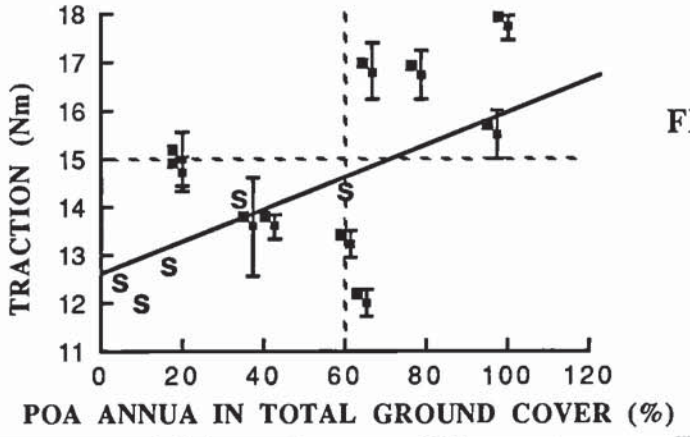

FIGURE 4.12 (b)

FIGURE 4.12. The graphs from Figure 4.6 showing the greens on which the ball was likely to slip off the surface (indicated by the letter "s").

These guidelines could be used by greenkeepers to determine whether impacts on a particular green would always roll off the surface or whether slip throughout impact would be possible. If the greenkeeper wanted the ball to retain some backspin then maintenance regimes could be implemented that would satisfy the conditions above. Although this would not guarantee the retention of backspin, it would make its occurrence more probable.

4.6 Summary

This chapter analysed the results of the tests to determine the characteristics of golf greens. Some tests were found to relate significantly to other tests while others were found to be relatively independent. Although the Stimpmeter had already been used in golf research, it did not relate to any of the other tests. The differences between greens showed up well, however, and the results agreed with previous Stimpmeter tests in this country (Downes 1982) which concluded that greens in this country were too slow for tournament play.

The ball rebound resilience was not found to correlate with any of the other tests. However, it was found that the construction of the ball played little part in impacts from this height. It is possible that balls dropped from 5m only interacted with a top layer consisting of grass and roots. Other tests, such as the Clegg Impact Hardness Tester, probably interacted with the soil layer beneath the grass.

It was found in this chapter that the soil composition, the organic matter content and the moisture content were all inter-related. A sandy soil is likely to be dry and have a low organic matter content. A clay soil is generally more moist and has a higher organic matter content. It is not clear whether it is the organic matter that retains the moisture or the moisture content that aids the build up of the organic matter. The species of grass present provides a good indication of the characteristics of the green since *Poa annua* tends to live on moist clay soils with a high organic matter content while *Agrostis* tends to live on dry sandy soils with a low organic matter content..

Results of some of the tests were found to vary significantly within errors between greens but were not found to relate significantly to any other tests. It is possible that more observations may have produced a significant correlation but it is equally possible that the differing physical nature of the tests caused the lack of significance. The three extra indenters developed for the Clegg Impact Hardness Tester were slightly disappointing because the readings obtained with them were in such large discrete steps. This caused the Tester to be inaccurate when taking individual readings. Once a more accurate indenter was used, however, differences between greens showed up clearly. It was found that the Clegg Impact Hardness Tester could be used to determine the effect of the green composition (soil composition, organic matter content etc.) on the vertical deceleration experienced by an impacting body. The traction readings showed the effect of the green composition on the forces in the horizontal direction.

The Clegg 0.5kg indenter was found to provide a realistic measure of the *Poa annua* present on the greens, the "softer" surfaces indicating higher *Poa annua* contents. The traction values were also found to correlate significantly and this highlighted an important characteristic of greens containing a lot of *Poa annua*, that is, that they are fairly unresistant to vertical impacts but are resistant to horizontal shearing through the surface.

The greens studied in this project were categorised in Chapter 3 into those on which the ball slipped throughout impact if the backspin was high enough and those on which the ball always rolled off the surface. The playing characteristics of the two types of green were determined and it was found that the greens on which gross slipping was possible were sandy in composition. These were characterised by low moisture and organic matter contents and *Poa annua* contents of less than 60%. As a consequence, these greens

tended to have high Clegg Impact Hardness Tester values and moderate to low traction values. It was possible, therefore, to suggest limits of these playing quality tests which could be used to determine the playability of a particular green. These could be used by greenkeepers to determine the correct maintenance regimes required for a certain type of green.

There was no significant difference between the rebound heights of two different constructions of golf ball. This agreed with earlier findings in Chapter 3 which showed that the construction of the ball played a minor roll in impacts. As stated earlier, this simplifies the model of impact considered in the next Chapter since the ball can be considered as a rigid solid.

Chapter 5. Physical models of impact

5.1 Introduction

This chapter describes the development of the model to simulate the impact of golf balls on turf. The aim of such a model is to increase the understanding of the forces involved and consequently of the impact as a whole. To simplify the impact, the model should have as few input parameters as possible. In this case they could involve the characteristics of the green described in Chapters 2 and 4. If the model is accurate, then the need for extensive testing using stroboscope photography would be reduced. The effect of different maintenance regimes on the impact of the golf ball with the turf could then be determined by the model rather than by testing. Experiments would only be needed to verify that the model was correct. This would be the ideal position at the end of this chapter. First, however, models found in the literature review are re-evaluated.

Daish (1972) used classical mechanics to predict the rebound of sports balls on a rigid surface while Hutchings *et al.* tried to predict the variation in crater volume with impact angle for a rigid sphere impacting against a rigid plastic half space. Cochran (1974a) used viscoelastic models to simulate the forces experienced by a golf ball impacting with a golf club face. These models are used in the following sections as a basis from which to create a model of the ball/turf impact.

5.2. The Newtonian model of impact

(i) An ideal solution

A treatment used by Daish (1972) assumed that the sphere and the surface on which it impacted were perfectly rigid and did not deform during impact. Daish realised that two simple cases were possible, that the ball could roll off the surface or slide throughout impact. It was assumed in the analysis that the coefficient of restitution and the coefficient of friction were both independent of the impact and were related simply to the surface. Consider, therefore, Figure 5.1 which depicts a ball impacting with the surface from the left. The conventions for the direction of velocity and spin before and after impact are shown. The components in the horizontal and vertical directions are denoted by "x" and "y" while the subscripts "i" and "f" indicate initial and final values respectively.

The coefficients of friction and restitution are represented by μ and e respectively and are constants related to the characteristics of the ground. For the case in which the ball slides throughout impact, the equations of the velocity and spin of the ball after impact, using Newton's laws, were found to be,

$$Vx_f = Vx_i - \mu Vy_i(1 + e) \qquad \text{eqn. 5.1}$$

$$Vy_f = eVy_i \qquad \text{eqn. 5.2}$$

$$\omega_f = \frac{5\mu Vy_i}{2a}(1 + e) - \omega_i \qquad \text{eqn. 5.3}$$

where a is the radius of the ball. For the case in which the ball rolls throughout impact, the equations are,

$$Vx_f = \frac{5Vx_i - 2a\omega_i}{7} \qquad \text{eqn. 5.4}$$

$$Vy_f = eVy_i \qquad \text{eqn. 5.5}$$

$$\omega_f = \frac{Vx_f}{a} = \frac{5Vx_i - 2a\omega_i}{7a} \qquad \text{eqn. 5.6}$$

The angle of rebound to the horizontal is found using,

$$\tan\Theta_f = \frac{Vy_f}{Vx_f} \qquad \text{eqn. 5.7}$$

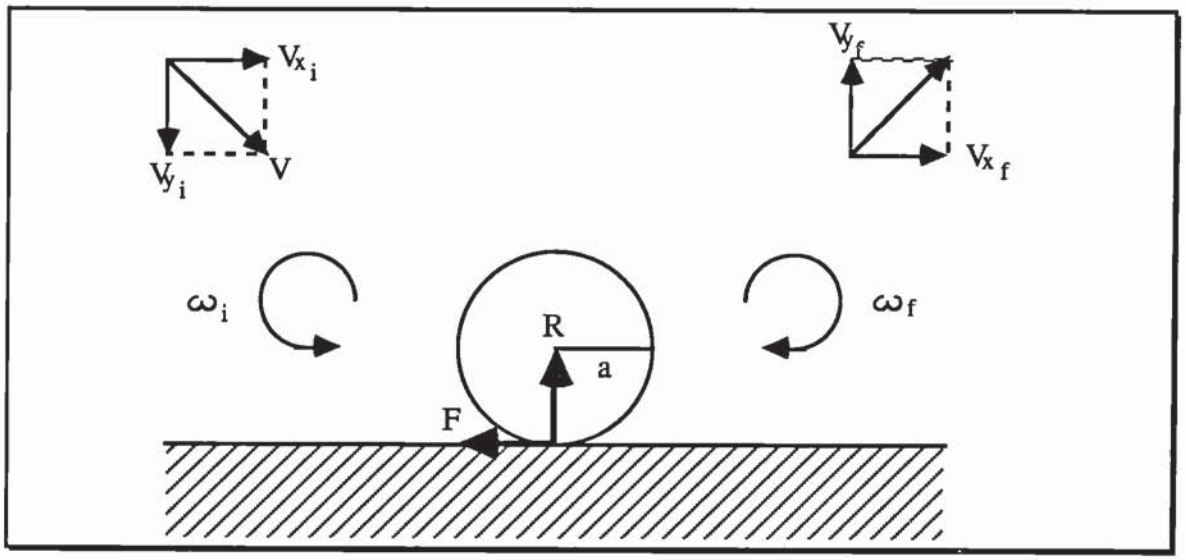

FIGURE 5.1. A diagram showing the conventions used in the analysis of a rigid sphere impacting with a rigid surface. The subscripts "i" and "f" are used to denote the incoming and rebounding ball respectively.

(ii) Application of the theory to golf ball impacts

Let us first consider impacts which roll off the surface and in which the initial backspin of the ball is zero. Equations 5.4, 5.5 and 5.6 become,

$$Vx_f = \frac{5Vx_i}{7},\ Vy_f = eVy_i \text{ and } \omega_f = \frac{5Vx_i}{7a}.$$

The equation for the angle of rebound is given by $\tan\Theta_f = \frac{Vy_f}{Vx_f} = \frac{7eVy_i}{5Vx_i} = \frac{7e\tan\Theta_i}{5}$. If the angle of incidence is fixed at 45°, say, then $\tan\Theta_f = \frac{7e}{5}$. In the analysis carried out by Daish the coefficient of restitution was considered to be a constant. Thus, the model predicts that balls impacting with the turf at an angle of 45° (and indeed at any fixed angle) to the horizontal and with zero spin rebound at an angle that is independent of the incoming velocity. In practice, this is not the case since the regression coefficients in Table 3.7 show that the angle of rebound increases as the velocity of the incoming ball

increases. If a similar analysis is carried out for the case when the ball slips throughout impact, then the equation for the angle of rebound is, using equations 5.1 and 5.2, $\tan\Theta_f = \frac{e}{1 - \mu(1 + e)}$. This also shows that, if the coefficients of restitution and spin are fixed, then the angle of rebound is fixed.

The model predicts a fixed rebound angle because it assumes that the ground and the ball do not deform. This may be true for the ball but in Chapter 3 it was found, using high speed film, that the ground can deform to up to half the diameter of the golf ball during impact. This deformation causes the ball to rebound from the front inclined plane of the pitchmark created causing an increase in the rebound angle.

The model could be made more realistic by introducing a tilt angle to allow for the modification of the pitchmark during impact. The tilt angle would modify the angle of incidence to give the correct values of velocity and spin for the rebounding ball. Using the regression equations in Chapter 4, consider a ball impacting with the green at Austerfield Park at a velocity of $22ms^{-1}$ at an angle of 45° to the horizontal and with zero spin. It would rebound with a velocity of about $6.3ms^{-1}$ at an angle of approximately 50° to the horizontal. The ball bounce measurement for the green at Austerfield was 5.2%. This corresponds to a coefficient of restitution of 0.23. Using equations 5.4 and 5.5 it is possible to calculate the components of the incident velocity required to produce a ball rebounding at 6.3 ms^{-1} and at an angle of 50° to the horizontal. It was found that the ball would have to arrive at the green at an angle of about 75° to the horizontal for the angle of rebound to be 50°. The ball actually arrives at 45°, however, and this introduces a tilt angle of about 30° into the equations. It is difficult to determine the variation of the tilt angle with the velocity and angle of the incoming ball, but it is possible to produce an equation that gives the correct tilt angle at the extremes of velocity and angle. Such an equation could be, for instance,

$$\Theta_{tilt} = (90 - \Theta_i)(1 - \exp\{-kV_i\sin\Theta_i\}) \qquad \text{eqn. 5.8}$$

where k is a constant related to the surface. The tilt angle approaches zero at angles of incidence of zero and 90°. As the velocity increases the tilt angle also increases. The equation for the tilt angle has no physical basis, however, except to facilitate an increase in the angle of rebound as the depth of the pitchmark increases.

It is considered, therefore, that this model is unsuitable for predicting the impact of golf balls on turf. A good feature of this model, however, was that only three external parameters were required, the coefficient of restitution, the coefficient of friction and the constant k.

5.3. A model in which the forces are proportional to the area of contact

(i) The equations of motion

The use of two external parameters was also a feature of the next model considered. It was used by Rickerby and Macmillan (1980) and later by Hutchings *et al.* (1981) to calculate the volume of the crater caused by the impact of a steel sphere on a rigid-plastic surface. An iterative numerical procedure was used to solve the equation of motion. It was assumed that all the forces experienced by the sphere could be approximated to one dynamic force related to the area of contact of the sphere with the surface. This was called the "dynamic hardness".

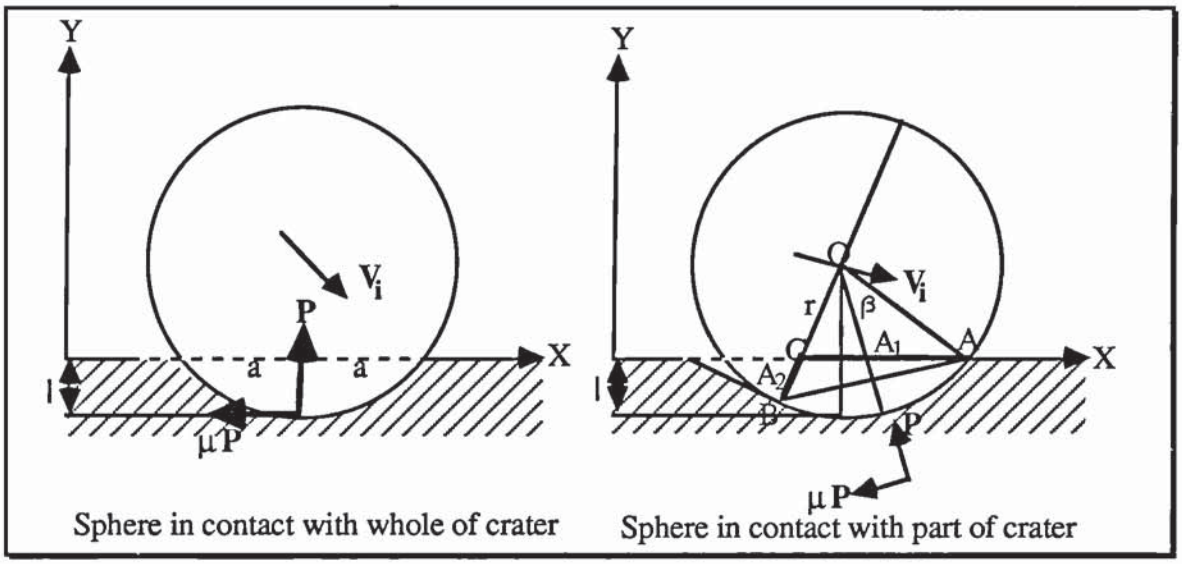

FIGURE 5.2. A diagram showing a steel sphere impacting with a rigid-plastic surface and modeled by Hutchings *et al.* The two cases when the sphere is in contact with the whole of the crater and just part of the crater are shown.

Figure 5.2 shows the direction of the forces on the sphere during the incoming and outgoing stages of the impact. Near the beginning of the impact the sphere is in contact with the whole of the surface of the crater formed by the impact and the equations of motion are,

$$m\frac{d^2x}{dt^2} = -\mu P \qquad \text{eqn. 5.9}$$

$$m\frac{d^2y}{dt^2} = P \qquad \text{eqn. 5.10}$$

where $P = \pi a^2 P_d$. P_d is the "dynamic hardness" and is related to the properties of the surface. The crater elongates during the impact and the ball is no longer in contact with the whole of the crater surface. The contact area is consequently more complex and, provided that the sign convention used by Hutchings *et al.* is observed, then the equations of motion become,

$$m\frac{d^2x}{dt^2} = -P\sin(\Theta_i + \beta) - \mu P\cos(\Theta_i + \beta) \qquad \text{eqn. 5.11}$$

$$m\frac{d^2y}{dt^2} = P\cos(\Theta_i + \beta) - \mu P\sin(\Theta_i + \beta) \qquad \text{eqn. 5.12}$$

where $$P = P_d(A_1\sin(\gamma - \Theta_i) + A_2\cos\gamma \qquad \text{eqn. 5.13}$$

and where A_1, A_2, β and γ are calculated in terms of the depth of the crater l, the radius of the ball r and the angle of incidence Θ_i (Appendix J).

(ii) Application of the model to golf ball impacts

A computer program was written to calculate the equations of motion using a simple integration routine employing the trapezium rule. This is shown in Appendix J. The diameter and mass of a golf ball were used and the value of P_d altered until contact times comparable with those in section 3.3 were found. It was then possible to study the effect of changing the incoming velocity on the velocity and angle of rebound.

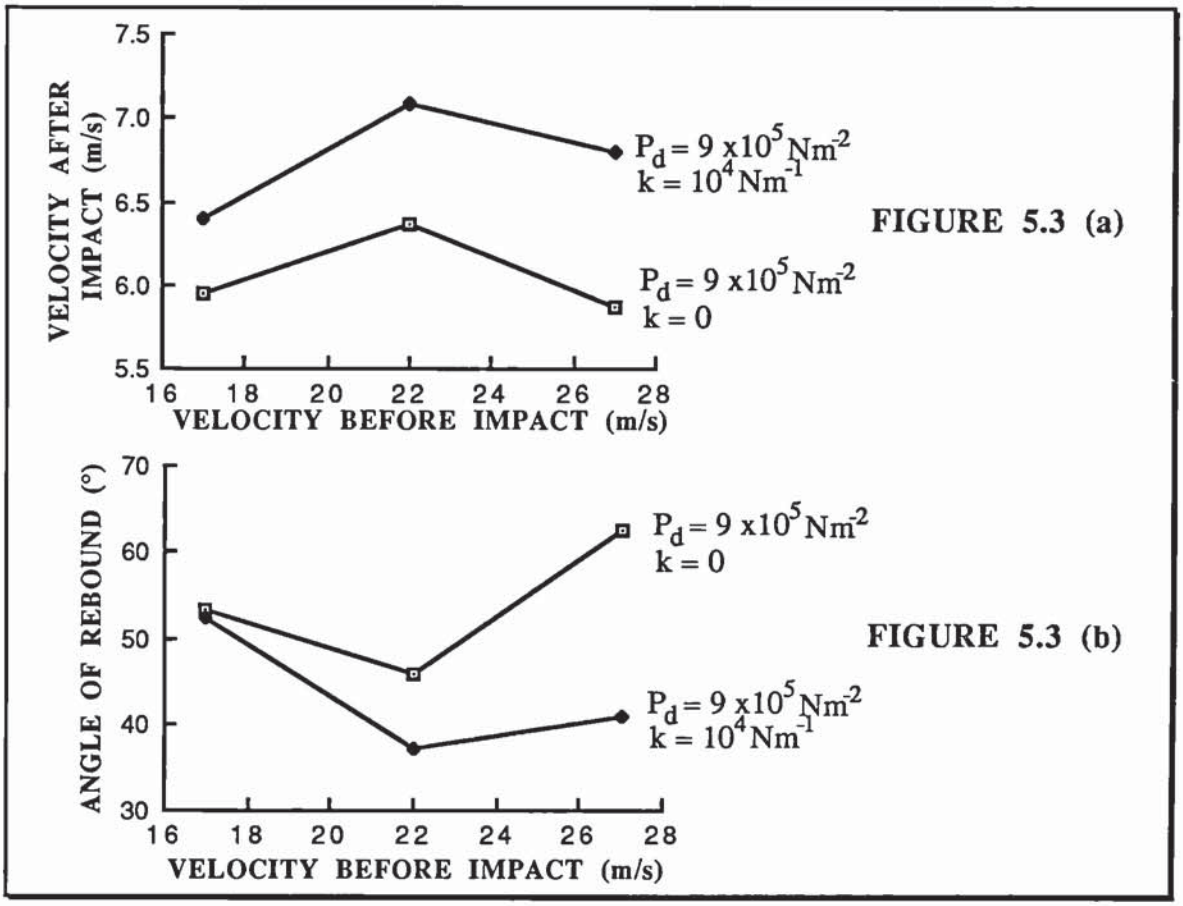

FIGURE 5.3 (a)

FIGURE 5.3 (b)

FIGURE 5.3. Graphs showing the predictions of (a) the velocity after impact and (b) the angle of rebound using the model used by Hutchings *et al.* and modified for a golf ball impacting with a rigid-plastic surface. A spring constant *k* was also introduced to allow for some recovery of the surface.

The model was modified slightly by introducing a spring element into the equations so that equation 5.13 became,

$$P = P_d(A_1\sin(\gamma - \Theta_i) + A_2\cos\gamma + kl \qquad \text{eqn. 5.14}$$

where *k* was a spring constant. The depth of the crater was used as an estimate of the displacement and the force from the spring acted in the same direction as the dynamic

force P. This was used to try to allow for the recovery of the surface indicated in the high speed films in section 3.3.

The variation in the velocity and angle of rebound with the velocity before impact for the model with and without the spring constant are shown in Figure 5.3. A suitable value of P_d was found to be $9x10^5$Pa while a value of 10^4Nm^{-1} was used for the spring constant. It can be seen in Figure 5.3 (a) that the velocity of rebound increases for both versions of the model between 17 and 22ms^{-1} but decreases as the velocity exceeds 22ms^{-1}. In Figure 5.3 (b) it can be seen that the angle of rebound decreases for velocities below 22ms^{-1} and increases above 22ms^{-1}.

Neither model, therefore, predicts correctly the variation in the velocity and angle of the rebounding ball from the surface as the incoming velocity increases. There were no values of the constants with which the model predicted the correct rebound velocity and angle. One of the probable reasons for the discrepancies of the model was that it did not account for the effects of spin. Nor did it account for the build up of material ahead of the sphere during impact. This would cause the model to underestimate the angle of rebound. The model was originally developed for impacts at speeds of over 200ms^{-1} and it may be, therefore, that it is not valid at low velocities where the elastic strains are comparable to the plastic strains.

The model had several good attributes, however. Only two input parameters were used, the dynamic hardness P_d and the coefficient of friction μ. The model assumed that the force experienced by the ball was proportional to the area of contact with the surface. In Chapter 3 it was found that balls that penetrated deeply into the surface, consequently having a large area of contact, usually rebounded with topspin and with low velocities. Impacts in which the depth of the pitchmark was shallow, however, tended to rebound faster and were likely to retain backspin. This indicates that the forces experienced by the ball were larger when the contact area was larger.

The model in this section was not considered to be suitable for describing the behaviour of a golf ball impacting with turf. It was also thought that a model of vertical impacts needed to be developed before the more difficult case of oblique impacts were considered. The next section describes the results of experiments to study normal impacts on golf greens. The results will be then used in section 5.5 to verify a model to simulate normal impacts.

5.4 Vertical impacts on golf greens

(i) Introduction

The impact of the ball on the green was simplified by considering only normal impacts. Golf balls were fired at, or dropped onto, four greens. The rebound heights were recorded against a scale using a video camera (similar to the method of recording the ball rebound resilience in Chapter 2). To achieve low velocities, golf balls were dropped from 25cm, 50cm, 1m, 2.5m and 5m. The impact velocities were then calculated using $\sqrt{2gh}$ where h is the height of drop. Higher velocities were achieved by directing the ball projection device directly downwards and projecting the balls with zero spin. The actual velocities at the individual wheel settings were known from the stroboscope photographs. Thus, velocities up to about $30ms^{-1}$ were used with discrete steps of about $2ms^{-1}$. Five impacts were carried out at each velocity and the depth of each pitchmark was measured using the green hardness tester described in Chapter 2.

(ii) Results

Vertical impacts were studied on four greens. Graphs of the rebound velocity and the depth of the pitchmark created versus the impact velocity are shown in Figure 5.4. The maximum standard error found for each variable is also shown. Initially, the rebound velocity increases with the impact velocity but between 10 and $15ms^{-1}$ it reaches a fixed value. At a higher incoming velocity, the velocity of rebound suddenly drops and the ball "plugs" into the surface. It can be seen in Figure 5.4 that the pitchmarks become measurable at between 10 and 15 ms^{-1} (except for Moortown which is measurable at about $5ms^{-1}$). This is the velocity at which the rebound velocity reaches its upper limit. The depth of the pitchmark then rises almost exponentially with the increasing velocity until the ball stops rebounding and sticks in the turf.

It can be seen in Figure 5.4 that the maximum velocity of rebound is roughly the same for all the greens at approximately $2.5ms^{-1}$. The impact velocity at which this maximum is reached and the impact velocity at which the ball no longer returns are different for each green. These facts may help to distinguish between the greens when a model is formulated.

The effects shown in Figure 5.4 can be explained by considering the turf as a multi-layered surface. At low velocities the ball only penetrates the top layer of soil and roots. This layer is quite "springy" and therefore an increase in the impact velocity increases the velocity of rebound. As the velocity is increased, the ball starts to penetrate the next layer which is probably a mixture of thatch, soil and roots. Thatch is the organic matter that builds up as the grass on the green grows and dies. It is quite spongy in appearance and tends to absorb water (Chapter 4). This layer tends to reduce the velocity of rebound and

an increase in the impact velocity no longer produces an increase in the rebound velocity. As the ball penetrates further it starts to interact more with the soil layer. This has the effect of reducing the rebound velocity even further until the impact velocity is so high that all the energy is lost on impact.

In practice the turf does not have distinct boundaries between the layers as one layer tends to merge into another. This factor, along with the variation of the thickness of the layers across the green, explains the variation in the rebound velocities for a given impact velocity and hence the magnitude of the standard errors shown in Figure 5.4.

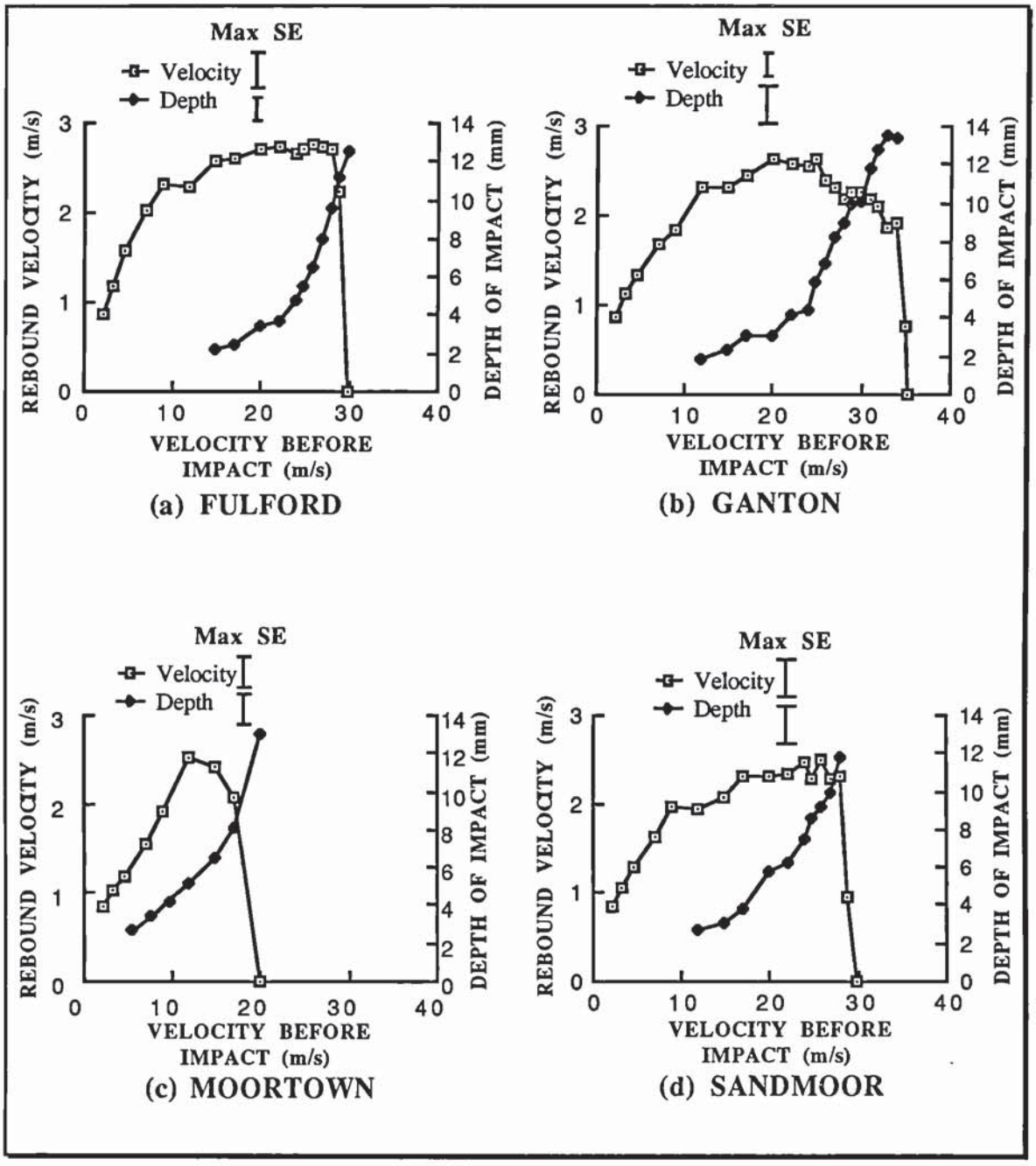

FIGURE 5.4. Graphs showing the relationship between the rebound velocity and the depth of the pitchmark created and the velocity before impact on four different greens. The maximum standard error for each variable is shown for each green.

The purpose of these experiments was to assimilate information on vertical impacts with which to verify models of normal impact. These models are studied in the next section.

5.5 Visco-elastic models of impact

(i) Introduction

Cochran (1974a) used visco-elastic models to simulate the impact of a golf ball with a golf club face. Visco-elastic models simulate forces in term of two elements, springs and dampers. For example, a car suspension can be modeled in terms of the Kelvin-Voigt model shown in Figure 5.5. This involves a spring and a damper in parallel. When a car goes over a bump in the road, the spring provides the force to return the wheel. The damper slows the motion of the wheel down so that it does not overshoot the normal equilibrium position. The elastic forces are proportional to the displacement of the spring while the damping forces are proportional to the speed at which the displacement occurs. The equation of motion in the Kelvin-Voigt model is,

$$\frac{d^2y}{dt^2} = - C_1y - C_2\frac{dy}{dt} \qquad \text{eqn. 5.15}$$

where C_1 is the spring constant, C_2 is the damping constant and y is the displacement of the mass.

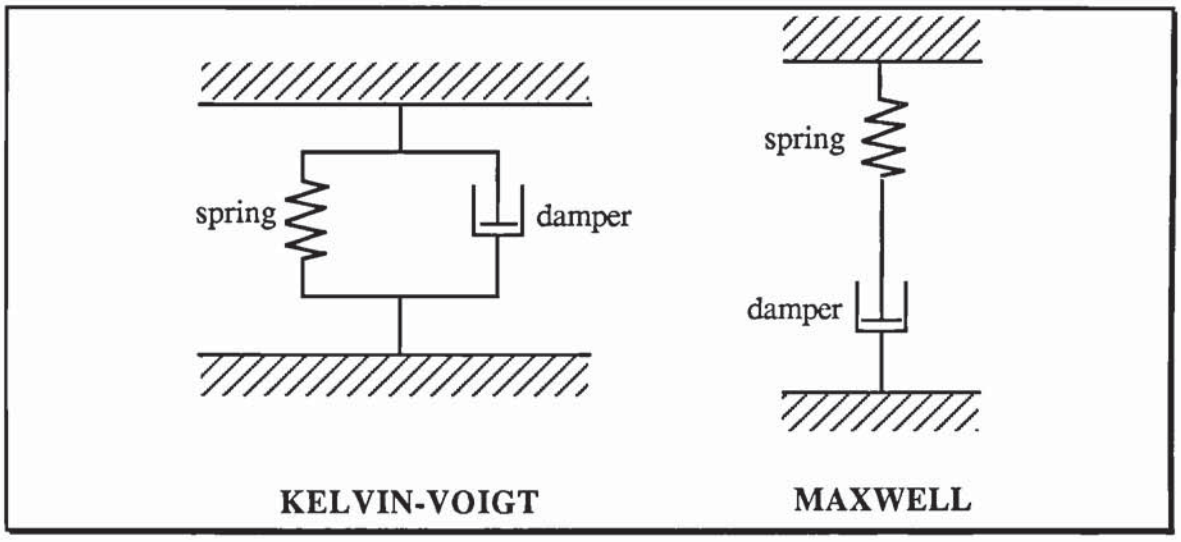

FIGURE 5.5. A diagram showing two viscoelastic models, the Kelvin-Voigt and the Maxwell solids. The models use two elements, springs and dampers, to simulate the characteristics of an impact.

In the case of golf ball impacts, the model has to contain a damping coefficient since the ball rebounds at a lower velocity than its impact velocity. Of the two models in Figure 5.5, the Kelvin Voigt model is more realistic in relation to golf ball impacts. The Maxwell model is not considered suitable since it compresses indefinitely under a sustained force. The next sections use the Kelvin-Voigt model as a basis for simulating the impact of a

golf ball with the turf. In Chapter 4 it was found that the construction of the ball had little effect on the ball/turf impact. The ball will therefore be considered as a rigid solid in the models discussed here. The results of the previous section are used to verify the model as it is developed.

(ii) Vertical impacts using the Kelvin-Voigt model

A BASIC program was used to calculate the equations of motion of the ball while in contact with the surface. Equation 5.15 was used to simulate the acceleration experienced by the ball. The differential equations were solved using the Runge-Kutta fourth order set of equations, the program for which is shown in Appendix K. The equations describing the forces involved in the impact are located at the end of the program in the form of a subroutine.

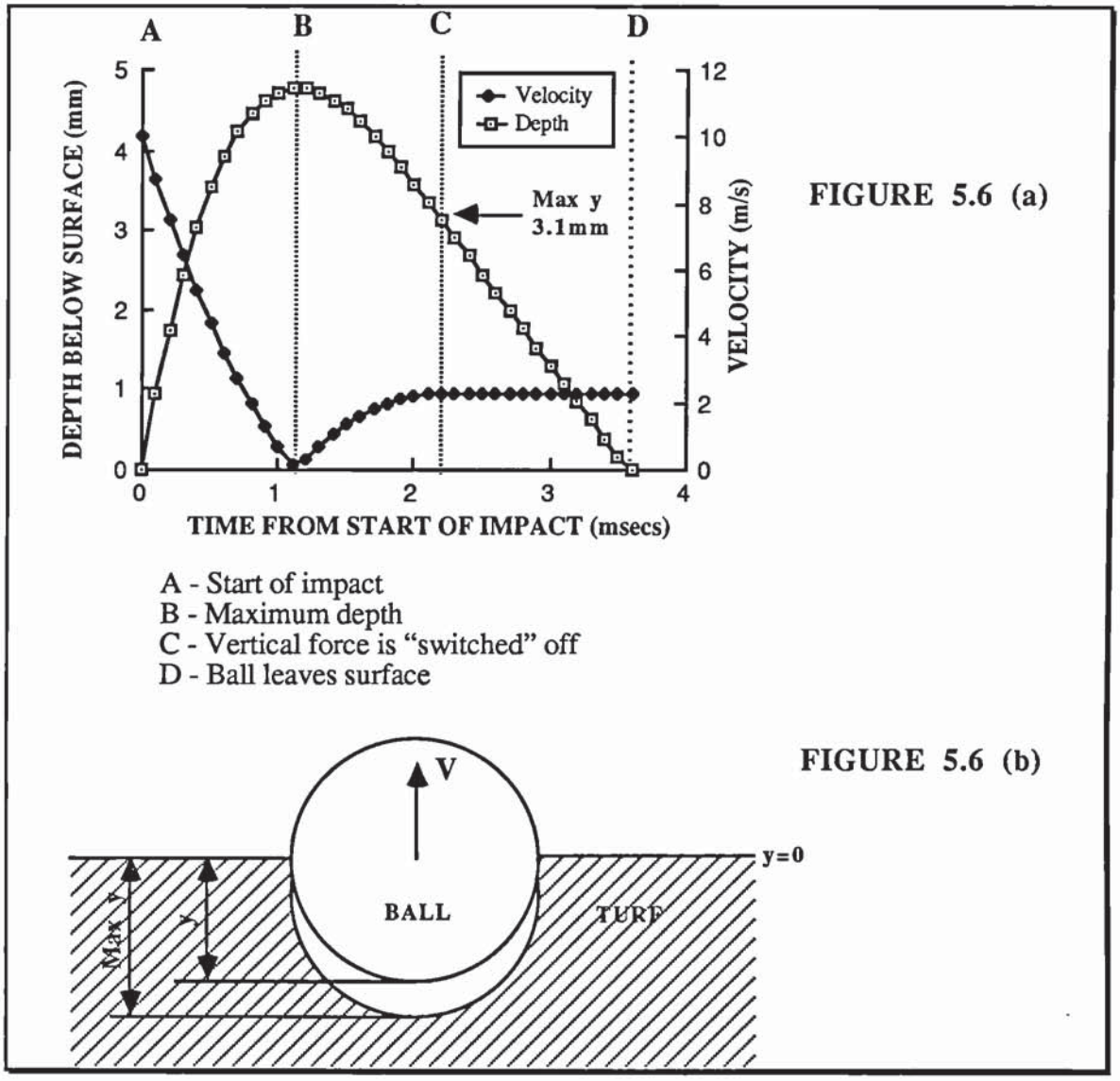

FIGURE 5.6 (a)

FIGURE 5.6 (b)

FIGURE 5.6. A graph showing the velocity and position of a golf ball during impact with a surface described by the Kelvin-Voigt model. The figure below shows the position of the ball in its rebound phase and the pitchmark allowed for by the model.

The results from a single run of the program are shown in Figure 5.6 in which the initial velocity was $10ms^{-1}$ and the spring and damper constants were 10^6s^{-2} and $1.3x10^2s^{-1}$ respectively. These values were chosen to give a realistic rebound velocity of about $2.3ms^{-1}$ and a contact time of around 4msecs. The calculation step length determines the number of steps used in the calculation of the final velocity. A suitable value was found by gradually decreasing the step length until the final answer was the same each time. The step length was subsequently fixed at 0.1msecs. The results shown in Figure 5.6 were calculated in 36 steps.

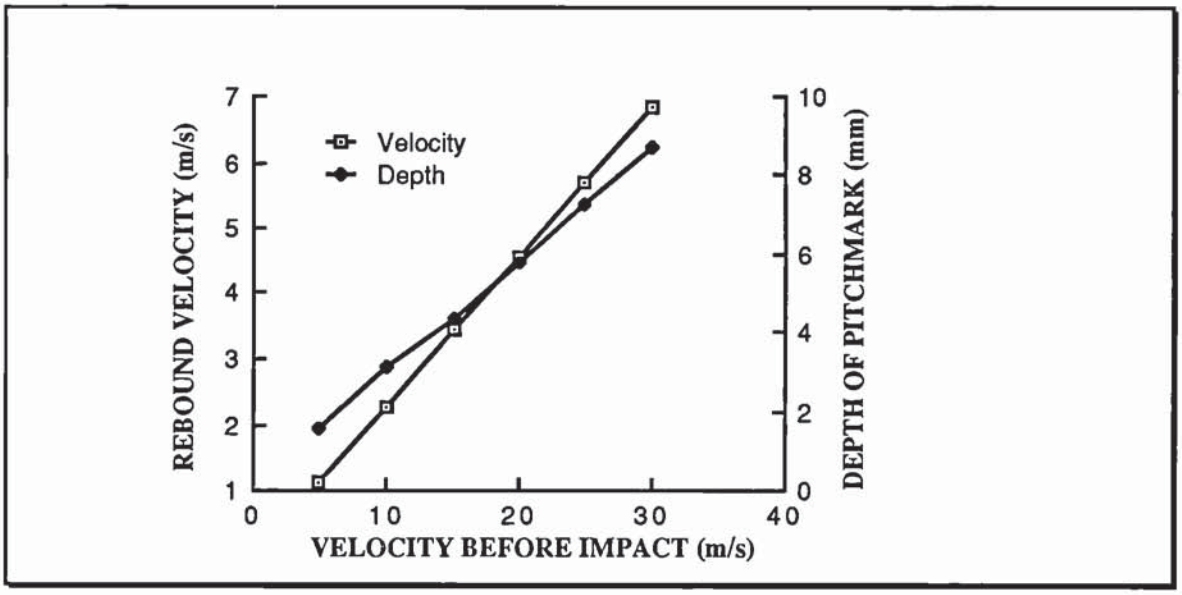

FIGURE 5.7. The rebound velocity and the depth of the pitchmark predicted using the Kelvin-Voigt model of impact.

Figure 5.6 (a) shows how the predicted velocity and depth of the ball below the surface vary during the impact. If permanent deformation of the surface occurs, as happens in practice, then at some point the ball must lose contact with the surface before it rises above the level of the turf (Figure 5.6 (b)). To facilitate this in the program, the vertical force is "switched off" if it becomes less than zero, i.e if it pulls the ball back towards the ground. The ball then continues upwards at a fixed velocity until it reaches y=0, indicating that it had left the surface. In Figure 5.6 (a), the maximum deformation of the surface is 4.8mm and occurs at B after 1.1msecs. The surface recovers until the ball leaves a permanent pitchmark with a depth of 3.1mm at 2.2msecs. The ball is predicted to leave the surface at 3.6msecs.

In this manner, the program was used to calculate the velocity of rebound and the depth of the pitchmark created for velocities between 0 and $30ms^{-1}$ and compared with the experimental data in section 5.4. The rebound velocities predicted by the Kelvin-Voigt model are shown in Figure 5.7. It can be seen that the rebound velocity and the depth of the pitchmark increases indefinitely as the impact velocity increases.

Since this did not agree with the experimental data, the model was modified so that the vertical force was proportional to the area of contact of the ball with the surface. As stated earlier, it was considered that this was more realistic since impacts in which the ball penetrated quite deeply experienced high forces. This implied that the area of contact was an important feature of the impact.

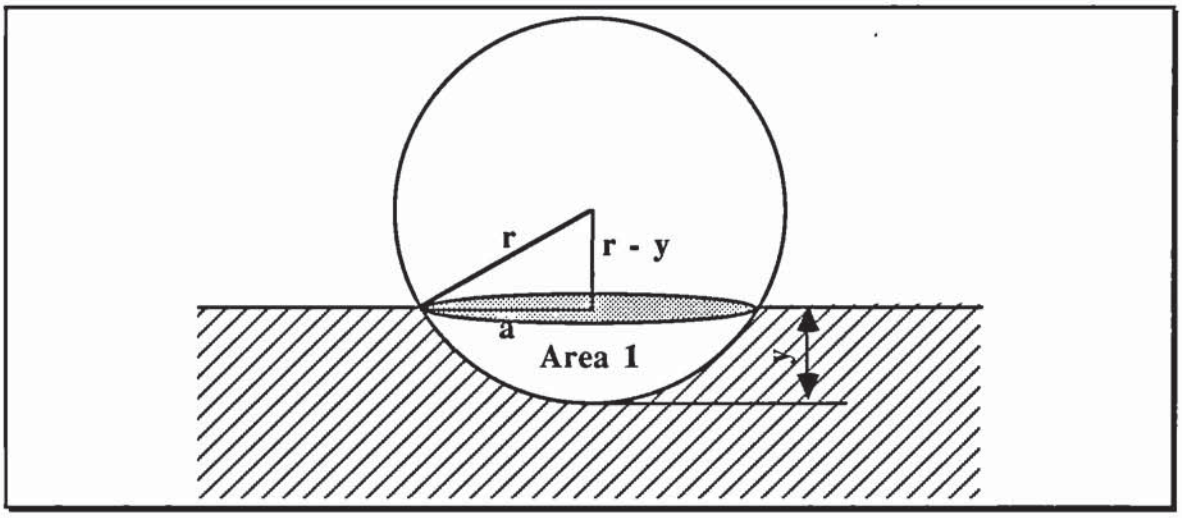

FIGURE 5.8. A diagram showing the contact area (Area 1) between the ball and the surface.

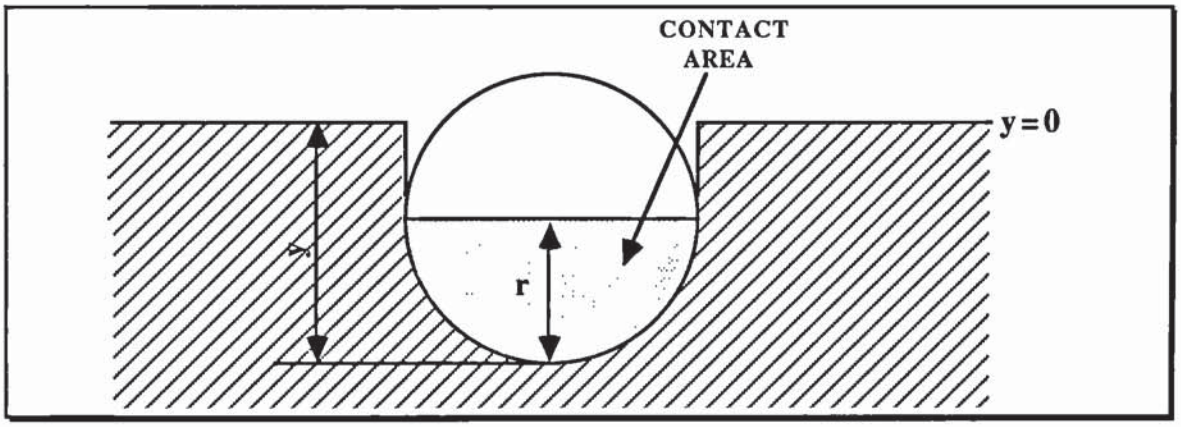

FIGURE 5.9. A diagram showing the contact area of the ball with the surface if the centre of the ball is below ground level.

The area of the circle of radius a in Figure 5.8 was used as a measure of the area of contact of the ball with the surface. It can be shown that the vertical force derived from a uniform pressure on this area is equal to the vertical force derived from the same pressure on the contact area of the sphere with the surface. The projected area of contact between the ball and the ground is,

$$\text{Area} = (2r - y)\pi y \qquad \text{eqn. 5.16}$$

Thus, the force in equation 5.15 was multiplied by the area in equation 5.16 to give,

$$\frac{d^2y}{dt^2} = (- C_1 y - C_2 \frac{dy}{dt})(2r - y)\pi y \qquad \text{eqn. 5.17}$$

where C_1 and C_2 have now changed in value from the Kelvin-Voigt model and are now in units of $s^{-2}m^{-2}$ and $s^{-1}m^{-2}$ respectively.

A feature of this model is that if the centre of the ball drops below the level of the ground, the contact area is limited to the lower half of the ball (Figure 5.9). This is because the vertical faces of the pitchmark above its centre are no longer in contact with the ball. The area of contact of the ball with the surface is then πr^2 and the displacement of the surface is considered as r. Equation 5.17 therefore becomes,

$$\frac{d^2y}{dt^2} = (- C_1 r - C_2 \frac{dy}{dt})\pi r^2 \qquad \text{for } y \geq r \qquad \text{eqn. 5.18}$$

The velocities and depths of the pitchmark predicted using this model are shown in Figure 5.10. Values of $10^9 s^{-2}m^{-2}$ and $2x10^6 s^{-1}m^{-2}$ were used for C_1 and C_2 to give approximately the same values for the rebound velocity as the Kelvin-Voigt model described by equation 5.15. It can be seen that causing the force to be proportional to the area of contact produced little change in the variation of the rebound velocity or the depth of the impact. The Kelvin-Voigt model, with or without the modification for the area of contact, does not agree with the variation in the rebound velocity found experimentally. It was found, however, that the rebound velocity was predicted to increase linearly with the impact velocity up to $10ms^{-1}$. At these lower velocities the model may be realistic. The results found experimentally indicate that there is a discontinuity in the surface when the energy of the impact exceeds that of a ball impacting at $10ms^{-1}$. This may be accounted for by considering the surface as a two-layered system. This is considered in the following section.

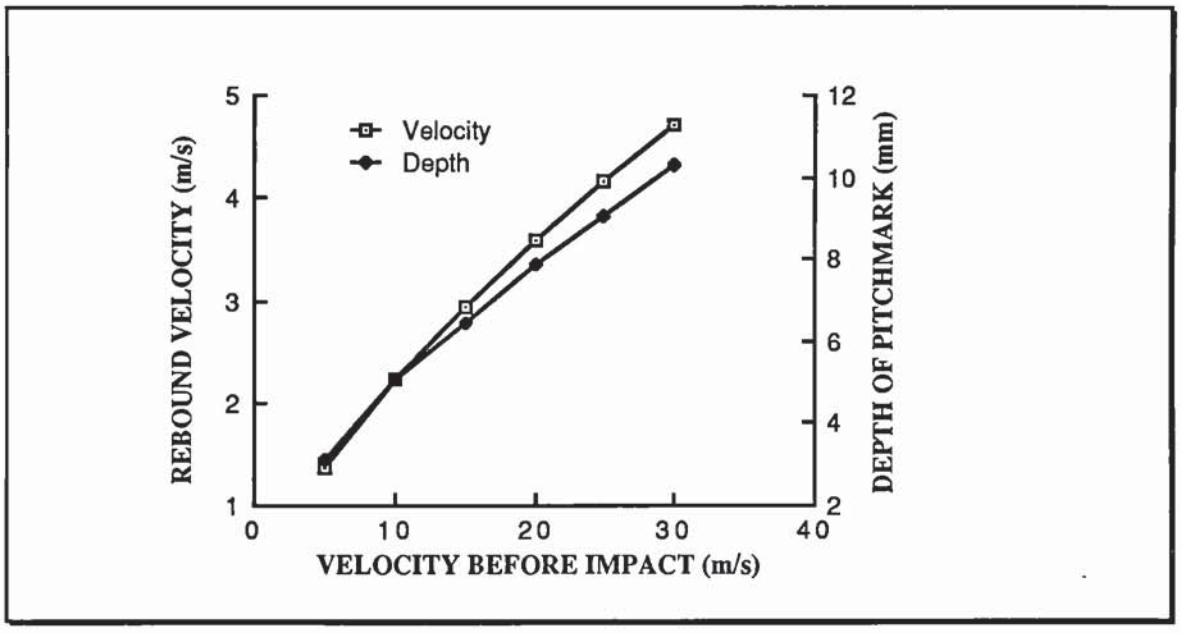

FIGURE 5.10. A graph showing the velocity and depth of the pitchmark predicted by the Kelvin-Voigt model in which the force was proportional to the area of contact of the ball with the surface.

(iii) A two layered viscoelastic model of impact

In line with experimental results, the model was modified so that the surface consisted of two layers. Two sets of equations existed within the program, one set for when the ball was in contact with just the first layer and another for when the ball was in contact with both layers. Figure 5.11 shows a diagram of the ball in contact with the two layers. Consider the first layer to have a thickness L. The equation of motion is the same as that in equation 5.18 when the ball is in contact with the first layer only. When the ball is in contact with both layers the total force is composed of the forces from the two layers. The effective area of contact with both the layers has to be calculated. The projected area of contact below y=L is,

$$\text{Area } 2 = \{2r - (y - L)\}\pi(y - L) \qquad \text{eqn. 5.19}$$

The effective area in contact with the upper layer is ,

$$\text{Area } 1 = (2r\text{-}y)\pi y - \text{area } 2 = (2r\text{-}y)\pi y - \{2r - (y - L)\}\pi(y - L)$$

$$= \pi L(L - y) \qquad \text{eqn. 5.20}$$

The second layer was considered to be a single damper since the experiments on normal impacts suggested that it was a retarding layer only and contributed little to the springiness of the turf. The equation for the vertical force is, therefore,

$$\frac{d^2y}{dt^2} = \{- C_1L - C_2\frac{dy}{dt}\}(\text{area } 1) - C_3\frac{dy}{dt}\text{area } 2 \qquad \text{eqn. 5.21}$$

where C_3 is the damper coefficient in the lower layer. When the ball is in contact with both layers, the deformation of the upper layer is taken as L. The velocity of the ball through both layers is $\frac{dy}{dt}$. As in the previous section, the areas of contact and the deformations used are modified if the centre of the ball drops below the level of the ground. A similar modification is used if the centre of the ball drops below the boundary of the two layers.

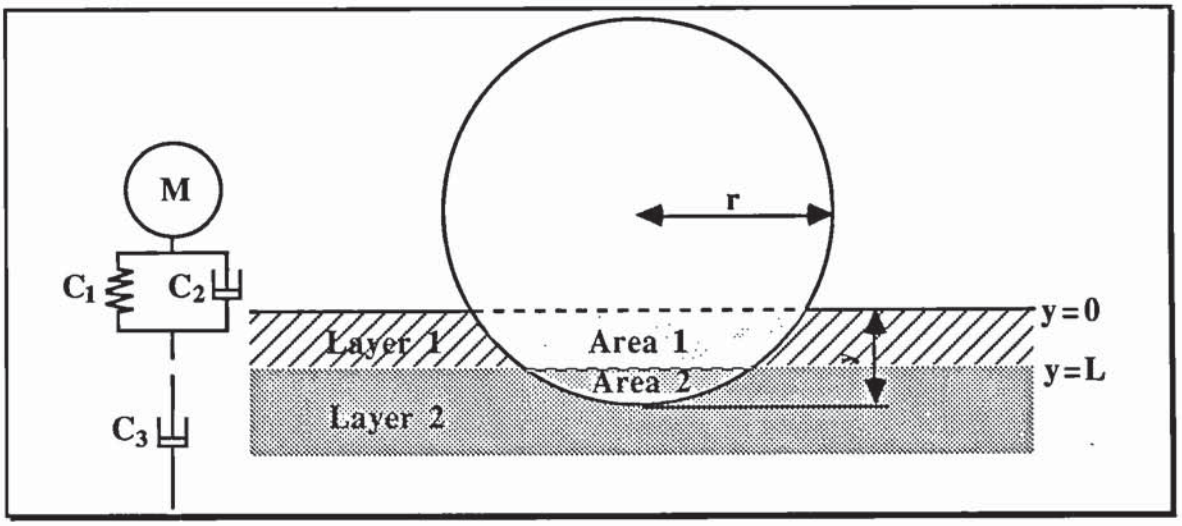

FIGURE 5.11. A diagram showing the areas used in the model of impact incorporating two layers into the surface. The viscoelastic representation of the surface is also shown.

The model was used to predict the velocity of rebound at incident velocities up to $30ms^{-1}$. The previous values of the spring and damper constants were used, i.e. $10^9s^{-2}m^{-2}$ and $2x10^6s^{-1}m^{-2}$ respectively while the thickness of the layer was varied from 3 to 8mm. The simulated rebound velocities versus the initial velocity for different thicknesses of the top layer are shown in Figure 5.12. In comparison with the experimental data in section 5.4, it can be seen that a top layer thickness of 8mm gives the approximate upper limit for the

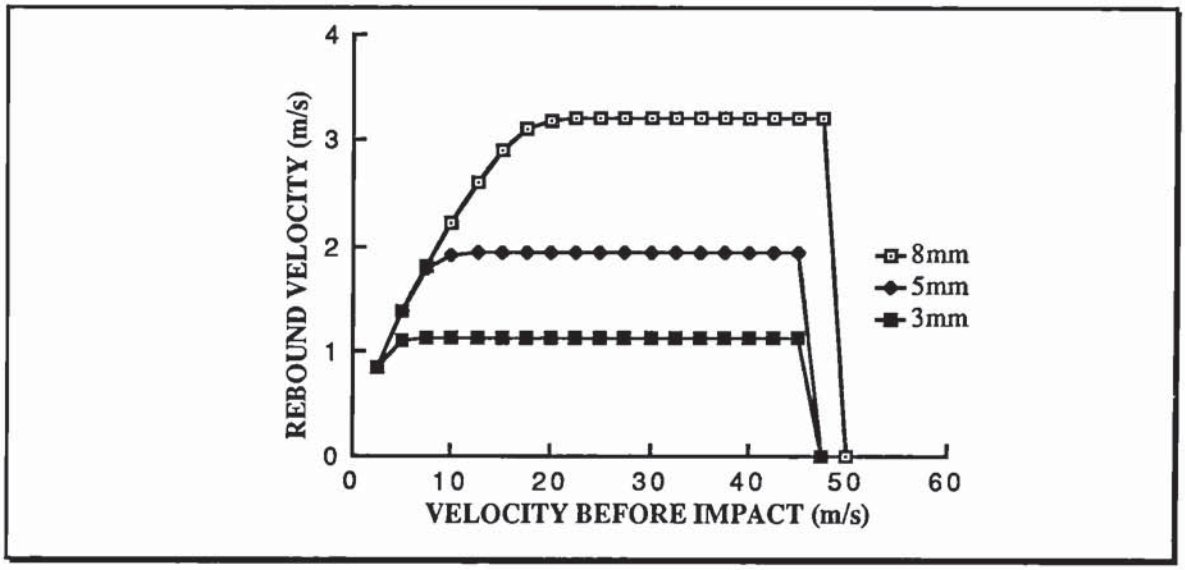

FIGURE 5.12. The variation of the rebound velocities with the impact velocity for different thicknesses of the top layer in the two-layered model of the surface. The bottom layer of the surface was considered to be a single damper.

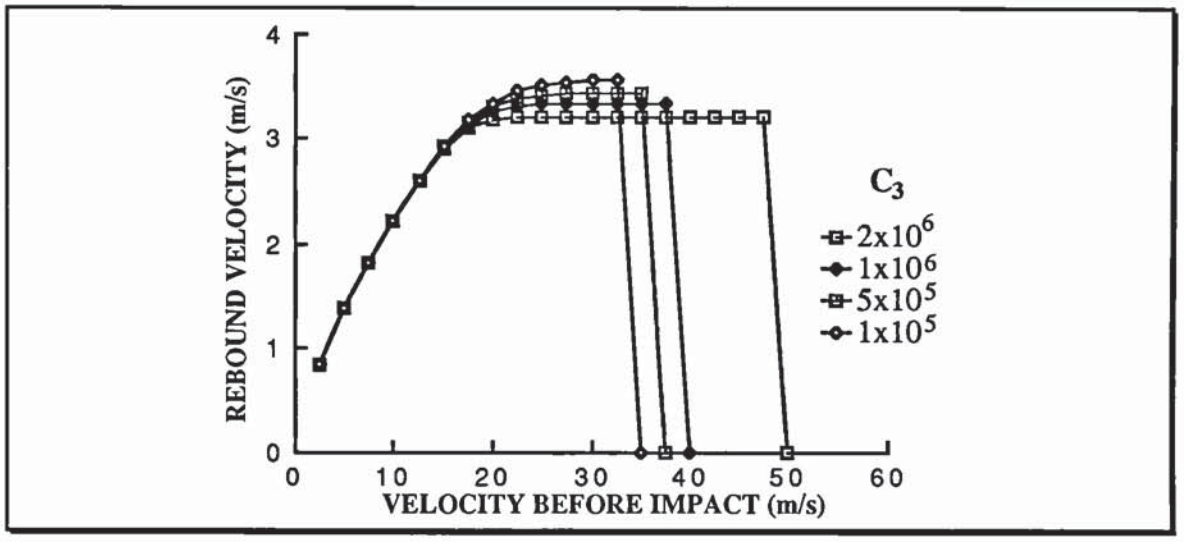

FIGURE 5.13. A graph showing the effect of varying the damper constant of the second layer on the rebound velocities in the two-layered model of the surface. The first layer was fixed at a thickness of 8mm.

rebound velocity. The impact velocity at which the ball was predicted to plug into the surface is too high since, experimentally, it was found to be nearer $35ms^{-1}$.

The value of the damper constant in the second layer (C_3) was varied to see its effect on the variation in the rebound velocity. The simulated rebound velocities are shown graphically in Figure 5.13. It can be seen that a decrease in the damper constant of the second layer causes the upper limit of the rebound velocity to increase. The impact velocity above which the ball no longer returns decreases with the value of the damper constant. With a value of $10^5 s^{-1}m^{-2}$, the model predicts an impact velocity limit of $35ms^{-1}$. At this stage it was thought that the model predicted adequately the results shown in Figure 5.4. A suitable value of the depth L was found to be 8mm and values of $10^9 s^{-2}m^{-2}$, $2x10^6 s^{-1}m^{-2}$ and $10^5 s^{-1}m^{-2}$ for C_1, C_2 and C_3 gave predictions similar to the results found experimentally.

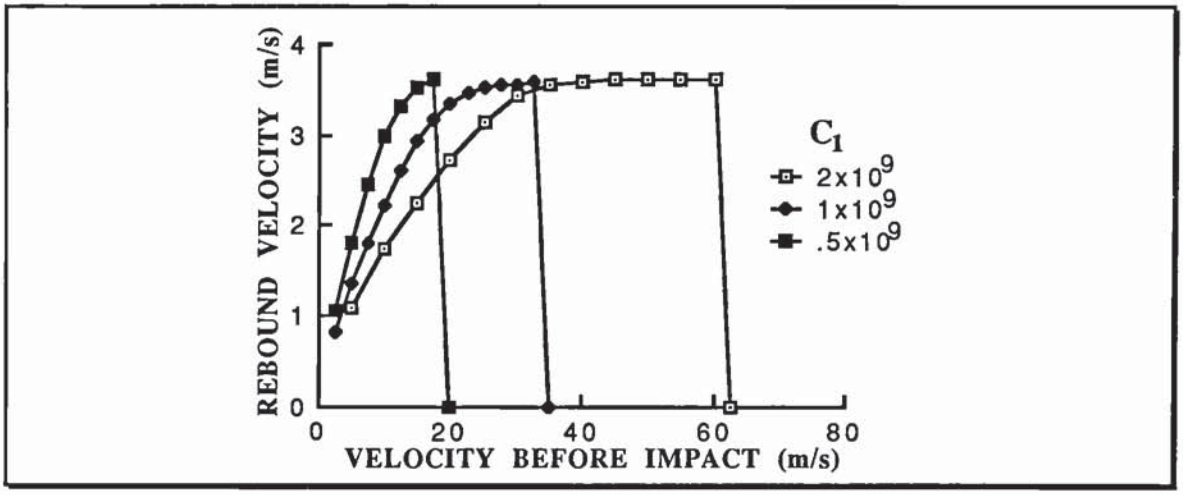

FIGURE 5.14. A graph showing the effect of changing the constants C_1 and C_2 such that the ratio of their values remains the same. The thickness of the top layer was 8mm and the damper constant for the second layer was fixed at $10^5 s^{-1}m^{-2}$.

Figure 5.14 shows the effect of varying the spring and damper constants of the first layer in a fixed ratio. The ratio was taken as the values of C_1 to C_2 previously used (i.e. $454s^{-1}$ to 1). The damper constant for the second layer was fixed at $10^5 s^{-1}m^{-2}$. It can be seen that decreasing the value of both constants simultaneously caused the impact velocity at which the ball no longer returned to decrease. The maximum rebound velocity, however, remained approximately the same. This is a similar effect to that seen in Figure 5.4. The values of all the constants may, therefore, relate to the characteristics of the green in some way. The thickness of the top layer and the value of the damper constant for the second layer appear to determine the approximate ranges for the maximum velocity of rebound and for the impact velocity at which the ball no longer returns. The value of the spring constant for the top layer (and hence the damper constant for the top layer if their ratio is fixed) appears to determine the thresholds more exactly within these ranges.

An analogy could be drawn between these constants and the characteristics of the turf. A dry clay green, for instance, would be very hard while a wet clay green would be very

soft. The maximum thickness of the upper layer and the damper constant C_3 would be analogous to the soil composition as they would define the range of possible rebound values. The values of the spring and damper constants for the top layer would be analogous to the moisture content since this would determine the rebound velocities more exactly.

For instance, if the constant C_1 (and hence C_2) is low, this implies a turf high in moisture and this would only be able to withstand low impact velocities. This can be seen in Figure 5.4. The green at Ganton was well drained and reasonably dry while the green at Moortown was very poorly drained. The maximum impact velocity on the green at Ganton was $35ms^{-1}$ while that on the green at Moortown was $20ms^{-1}$. This agrees with the results found in Chapter 4, i.e. that a soft wet green is less resistant than a firm dry green.

Figure 5.15 shows the simulated rebound velocity and maximum penetration as the impact velocity is increased using the values of the constants given above. The predicted maximum penetration of the ball into the surface has the same variation as the depth of the pitchmark found experimentally. The depth at which the vertical force was "switched off" is also shown. This does not have the same variation as the maximum depth and may not be a good estimate of the depth of the pitchmark as previously thought since it is probable that the pitchmark recovers after the ball has left the surface. The correct pitchmark depth may be a combination of the maximum depth and the depth at which the vertical force reduced to zero.

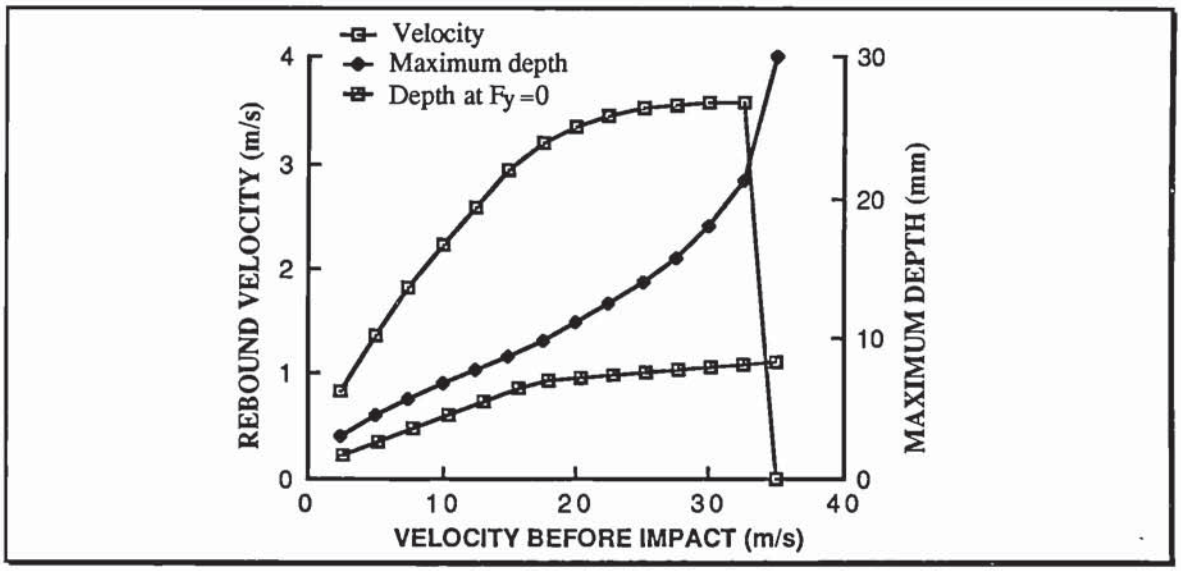

FIGURE 5.15. A graph showing the variation in the predicted rebound velocity, the predicted maximum penetration of the ball and the depth at which the vertical force was "switched off". The thickness of the first layer was 8mm and the constants C_1, C_2 and C_4 were $10^9 s^{-2}m^{-2}$, $2x10^6 s^{-1}m^{-2}$ and $10^5 s^{-1}m^{-2}$ respectively.

The model for normal impacts shown here predicted the correct variation of the rebound velocity as the impact velocity was increased. Values of the constants were found such that the rebound velocities were realistic. In the next stage of the modelling process, the equations were modified to account for oblique impacts.

5.6 A viscoelastic model of oblique impacts

(i) Equations of motion

The final program for normal impacts was modified so that oblique impacts could be considered. Equations 5.18 and 5.21 were used to simulate the vertical forces using the values of the constants found in the previous section. The horizontal forces were formulated in the same manner as the vertical forces. The top layer was composed of a spring and a damper in parallel while the bottom layer was composed of a single damper. The horizontal force from each layer was proportional to the cross sectional area of the ball in contact with the surface (Figure 5.16). The areas are segments of the diametrical circle of radius r and are given by the equations,

$$\text{Area } 3 = r^2\tan^{-1}\left(\frac{w_2}{w_1} - w_1 \times w_2\right) - \text{area } 4 \qquad \text{eqn. 5.22}$$

$$\text{Area } 4 = r^2\tan^{-1}\left(\frac{w_4}{w_3} - w_3 \times w_4\right) \qquad \text{eqn. 5.23}$$

where $w_1 = \left(1 - \frac{y}{r}\right)$, $w_2 = (1 - w_1^2)$, $w_3 = \left(1 - \frac{(y - L)}{r}\right)$ and $w_4 = (1 - w_3^2)$.

Thus, the equation of motion in the horizontal direction given by the viscoelastic properties is,

$$\frac{d^2x}{dt^2} = \left\{- C_1x - C_2\frac{dx}{dt}\right\}(\text{area } 3) - C_3\frac{dx}{dt}\text{area } 4 \qquad \text{eqn. 5.24}$$

where C_1, C_2 and C_3 have the same values as in the normal impact.

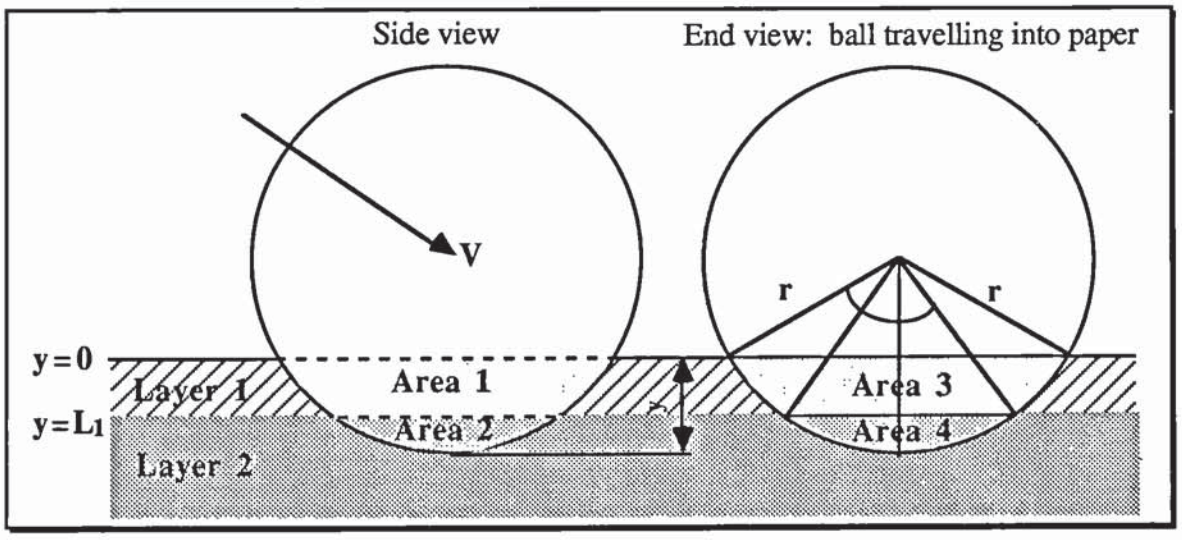

FIGURE 5.16. The areas of contact for the vertical and horizontal forces used in the viscoelastic model of oblique impact.

The spin of the ball has also to be considered in the case of oblique impacts. The force causing the ball to tend towards rolling spin was considered to be the torque produced by the reaction of the surface on the ball (Figure 5.17). The torque τ produced by the force μR acting at a distance r from the centre of the ball produces an angular acceleration which modifies the spin. The angular acceleration is found using,

$$\tau = \mu Rr = I\frac{d^2\Theta}{dt^2}$$

where μ is the coefficient of friction, r is the radius of the ball and I is the moment of inertia of the ball about its centre.

Thus, $$\frac{d^2\Theta}{dt^2} = \frac{\mu Rr}{I}$$ eqn. 5.25

The reaction R is calculated assuming that all the force components in the z-direction (i.e into or out of the paper) cancel each other out. The reaction therefore lies in a vertical plane through which the centre of the ball passes. R is calculated by taking components of the horizontal and vertical forces (equations 5.21 and 5.24) along the direction perpendicular to the motion of the ball Figure 5.17 (a).

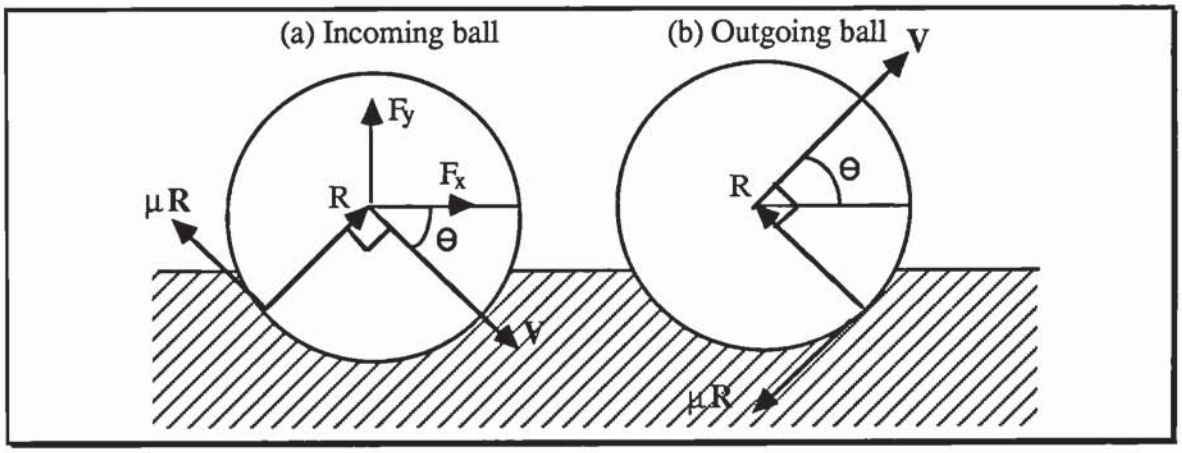

FIGURE 5.17. A diagram showing the spin force μR on the incident and rebounding ball in the oblique model of impact.

This gives an equation for R of,

$$R = F_x\sin(\Theta) + F_y\cos(\Theta)$$ eqn. 5.26

where F_x and F_y are the horizontal and vertical components of the force arising from the viscoelastic properties of the surface. When the spin matches that required for rolling, the coefficient of friction drops to zero and the angular acceleration becomes zero.

The forces so far described in this section arise from the viscoelastic properties of the surface. Other forces must also act on the ball since the results in Chapter 3 (eg. Figure 3.10) showed that a change in the initial backspin of the ball caused a change in the behaviour of the rebounding ball. A retarding force arising from the spin of the ball must act during impact since, for impacts which roll off the surface, an increase in the backspin causes the ball to rebound at higher angles and with lower velocities. This additional

force was estimated to be the component of the frictional force μR acting in a direction parallel to the motion of the ball (Figure 5.17). The horizontal and vertical components of this spin force were added to equations 5.21 and 5.24. The final equations of motion were therefore,

$$\frac{d^2x}{dt^2} = \{- C_1x - C_2\frac{dx}{dt}\}(\text{area } 3) - C_3\frac{dx}{dt}\,\text{area } 4 + \mu R\sin(\Theta) \qquad \text{eqn. 5.27}$$

$$\frac{d^2y}{dt^2} = \{- C_1(y - L_1) - C_2\frac{dy}{dt}\}(\text{area } 1) - C_3\frac{dy}{dt}\,\text{area } 2 - \mu R\cos(\Theta) \qquad \text{eqn. 5.28}$$

$$\frac{d^2\Theta}{dt^2} = \frac{\mu Rr}{I} \qquad \text{eqn. 5.29}$$

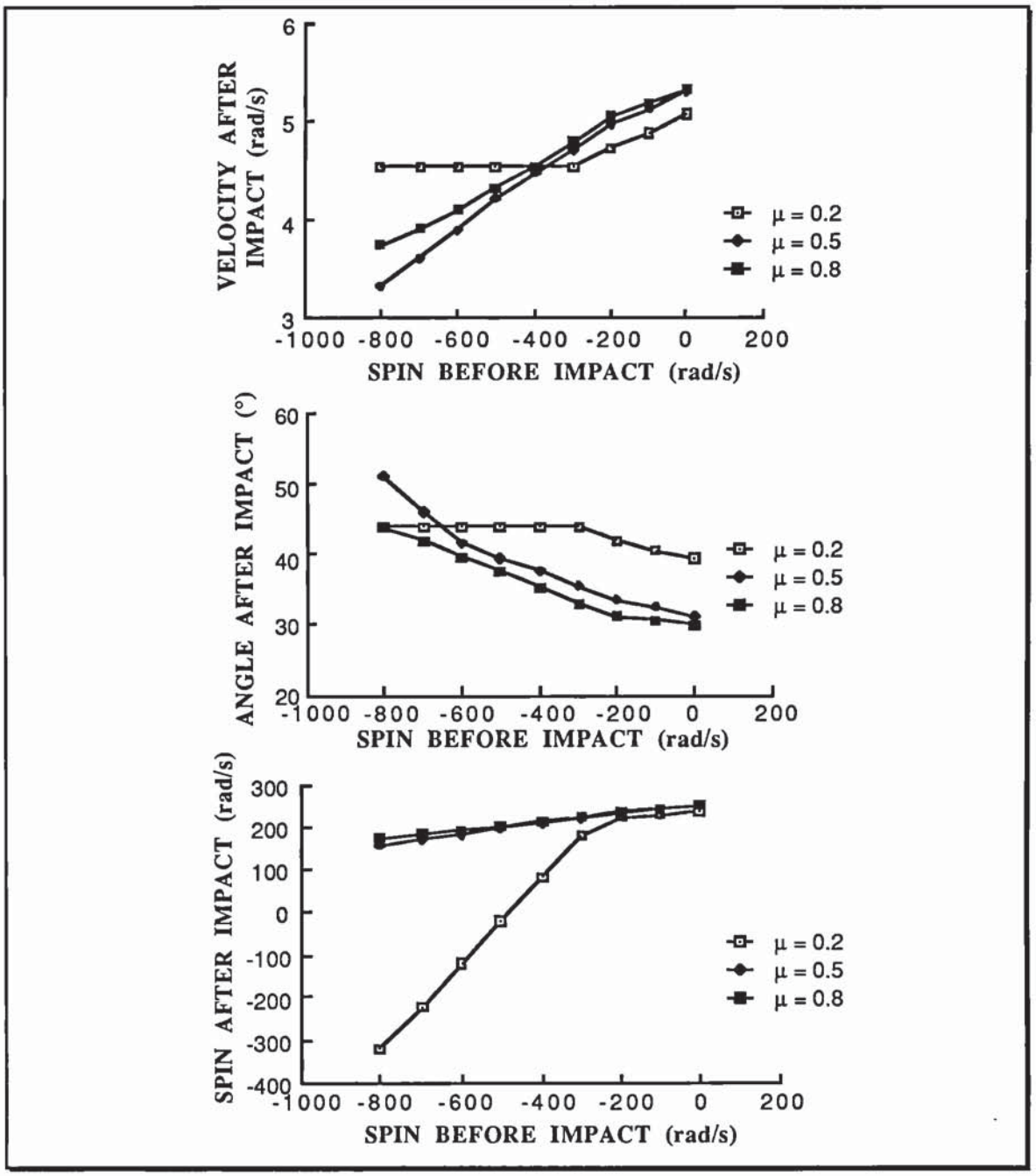

FIGURE 5.18. The rebound velocities, angles and spins for increasing backspin and for different values of the coefficient of friction predicted by the model of oblique impact. The angle of incidence was 45° and the incoming velocity was 22ms^{-1}.

A problem arises in the selection of the appropriate displacement x in equation 5.27. If the displacement used is the total displacement from the initial contact point, the ball tries to return to the original impact point. This is clearly not what happens in practice since the ball moves horizontally through the turf. It was considered, therefore, that a constant force was more realistic. This was actually created using the same equations as those in equation 5.27 but using the displacement between increments instead of the total horizontal displacement. This caused the horizontal force to drop to zero at the beginning of each increment, essentially giving a constant force.

As in the previous sections, the areas of contact of the ball with each layer were modified if the centre of the ball dropped below the level of the ground or below the boundary between the layers.

(ii) Predictions of the model

The effect of the coefficient of friction μ has so far not been considered. Figure 5.18 shows the predicted velocities, angles and spins of the rebounding ball for increasing backspin and for different values of μ. The impacting velocity was $22ms^{-1}$ and the incoming angle was 45°. The thickness of the top layer of the surface was fixed at 8mm and the values of the spring and damper constant were the same as in the previous section. Three values of the coefficient of friction were used, 0.2, 0.5 and 0.8. It can be seen in Figure 5.18 (a) that the model predicts a continuous drop in the rebound velocity with increasing backspin for values of the coefficient of friction of 0.5 and 0.8. For a coefficient of friction of 0.2, however, the rebound velocity reaches a static value as the backspin exceeds $-300rads^{-1}$. A similar effect occurs with the rebound angle: the model predicts an increase in the angle of rebound with backspin but, for a coefficient of friction of 0.2, reaches a discontinuity at $-300rads^{-1}$. The reason for the differences between the graphs for coefficient of frictions of 0.8 and 0.5 and that of 0.2 can be seen in Figure 5.18 (c). For the higher values of the coefficient of friction the ball rebounds with a topspin that is proportional to the velocity of rebound, i.e. the ball rolls off the surface. For a coefficient of friction 0.2, however, the ball slips off the surface for backspins greater than about $300rads^{-1}$. As might have been expected, the value of the coefficient of friction, therefore, determines whether the ball rolls or slips off the surface.

The model was used to simulate the behaviour of the rebounding ball for different velocities and with a coefficient of friction of 0.2. The rebound velocities, angles and spins predicted by the model as the backspin was increased are shown in Figure 5.19. The form of this graph is similar to that for the experimental data shown in Figures 3.10 and 3.11. If the simulated values in Figure 5.19 are compared to the results in Figure 3.11, it can be seen that similarities exist between the two sets of graphs. The model

predicts the initial decrease in the velocity and the increase in the angle of rebound at low backspins.

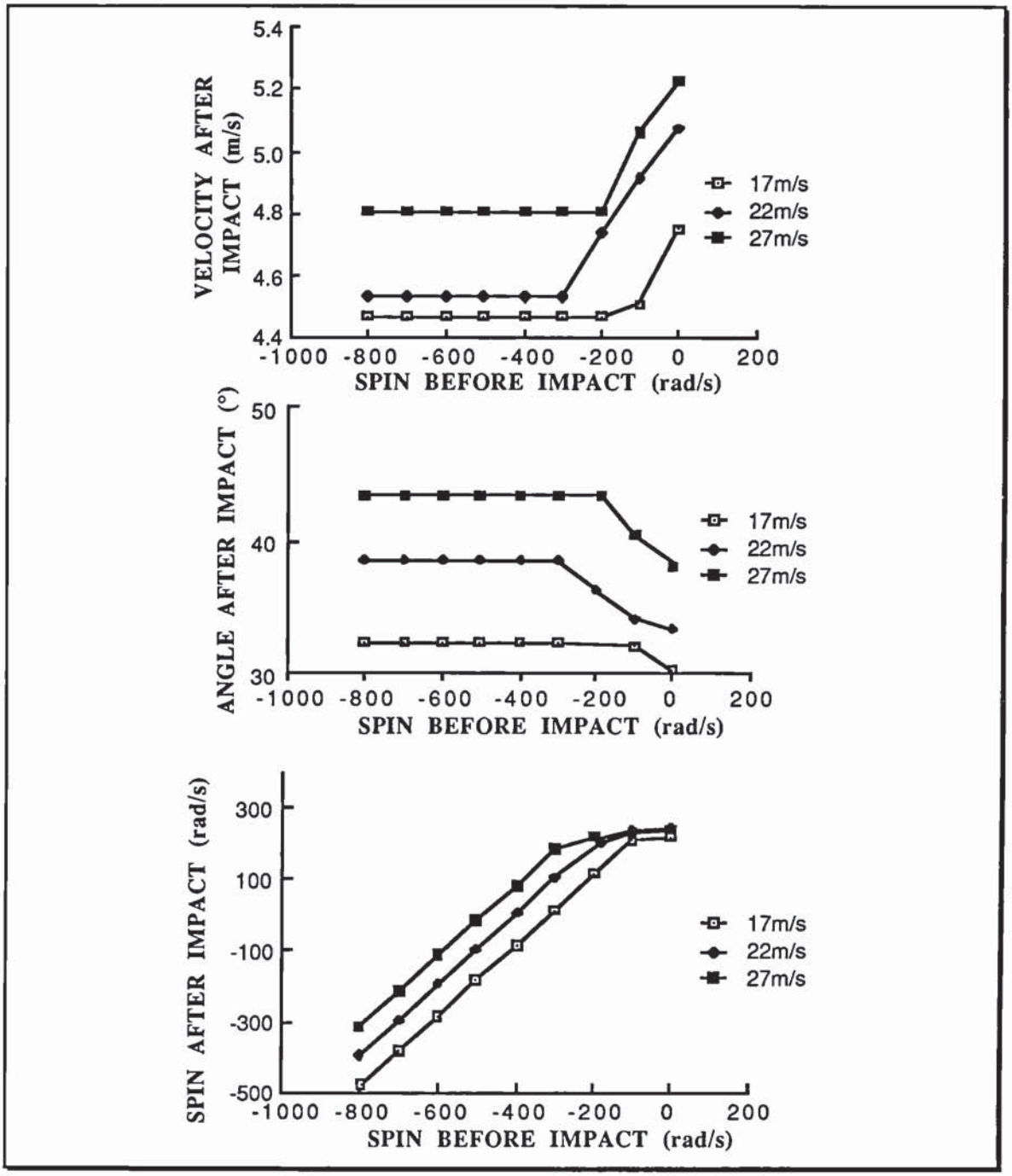

FIGURE 5.19. Graphs showing the velocities, angles and spins predicted by the model of oblique impact for increasing impact velocities and backspins.

At these low backspins the ball rolls off the surface while at higher backspins the ball slips off the surface. The model predicts that, if slip occurs throughout impact, then the backspin retained varies linearly with the spin before impact. This was found in Figure 3.11 (c) for velocities of 22 and 27ms^{-1}.

As found experimentally, the model shows a discontinuity in the velocity and angle of rebound when the incoming backspin exceeds a certain threshold. As the backspin is increased further, however, the model becomes less consistent with experimental data. The model predicts that the velocity and angle of rebound have fixed values above a threshold of about -300rads^{-1}. This could be explained by the fact that, for slipping to occur, the coefficient of friction had to be lower than the value suggested by the sliding friction test. The lowest experimental value found on the greens was about 0.45. It is a possibility that the coefficient of friction is not independent of the velocity of the impact and may be dependent upon the relative velocity between the periphery of the ball and the surface. This fact was used in a simple way in the model above, to the extent that the coefficient of friction was reduced to zero when the spin matched the spin required for the ball to roll off the surface.

(iii) Application of oblique model to shots using different clubs

The final model described in the previous section was applied to impacts of golf balls on greens arising from different golf shots. The velocities, angles and spins of balls arriving at the green due to shots from a 9-iron and a 5-iron were shown in Figure 1.1.

The viscoelastic model described in the previous section was used to determine the behaviour of the golf ball on the first bounce on each green. The trajectory of the ball after the first bounce was calculated assuming that lift and drag were negligible. The values of the velocity, angle and spin after the first bounce were used for the second bounce and the subsequent trajectory was determined. The visco-elastic model was not verified at low velocities and high angles of incidence and was therefore not used to simulate the third bounce. At this point it was assumed that the ball travelled over the surface in some manner. The ball may have done a number of things during this phase of the impact. If the model calculated that the ball had topspin as it arrived on the third bounce, then it would have rolled forwards. If the ball had backspin, it may have "checked" or "screwed back". The most useful piece of information to know is the distance travelled by the ball after the third impact. This can be determined if the ball's velocity across the surface is known. The average deceleration, found using the stimpmeter, can then be used to determine the distance travelled. An equation for the velocity of the ball across the surface is found in the following manner.

Firstly, let the normal reaction of the ball to surface at a time t be R(t). Thus, if slipping occurs, then,

$$m\frac{d^2x}{dt^2} = -\mu R(t) \qquad \text{eqn. 5.30}$$

where m is the mass of the ball, and μ is the coefficient of friction. Equation 5.30 can be written as,

$$Vx = -\frac{\mu}{m}R(t) \qquad \text{eqn. 5.31}$$

If this is then integrated, then we get,

$$Vx_f = Vx_i - \frac{\mu}{m}\int R(t)dt \qquad \text{eqn. 5.32}$$

Similarly, for the spin of the ball,

$$\omega_f = \omega_i + \frac{5\mu}{2mr}\int R(t)dt \qquad \text{eqn. 5.33}$$

where r is the radius of the ball. If we consider that the deformation of the ground is negligible, then the rotational velocity of the ball will match the horizontal velocity of the ball at the point at which slipping ceases. This will occur at $Vx_f = \omega r$. Using this relationship, equation 5.32 becomes,

$$Vx_f = \frac{1}{1.4}(Vx_i + 0.4r\omega_i) \qquad \text{eqn. 5.34}$$

This gives the horizontal velocity of the ball at the moment that slipping ceases.

Using the viscoelastic model of oblique impacts, the behaviour of the ball after the first two bounces were determined. On the third bounce it is assumed that the ball starts to travel over the surface in some manner determined by the spin and velocity of the ball. If the backspin is great enough then the velocity in 5.34 is negative and the ball travels back in the direction from which it came when it ceases to slip. If the ball has topspin, then the velocity in equation 5.34 is positive and the ball travels forwards at the end of slipping. What is not known, however, is the behaviour of the ball during the slipping phase of the the third impact. It is assumed, however, that the ball does not travel very far during this phase and that the velocity in equation 5.34 applies from the point of the third impact.

Using information from the use of the Stimpmeter, it is possible to get an estimate of the deceleration experienced by the ball as it rolls across the surface. The average distance rolled was about 2.3m (Appendix G). The velocity of the ball as it leaves the end of the Stimpmeter is estimated to be about $2ms^{-1}$. This gives an average deceleration of $0.9ms^{-2}$. This can be used to calculate the distance rolled by the ball once it has ceased slipping. For instance, a ball impacting at $3ms^{-1}$ at 70° to the horizontal and with $300rads^{-1}$ backspin would have a horizontal velocity of about $-1.1ms^{-1}$ once slipping had stopped. This would cause the ball to "screw back" and would finish about 60cm behind the original impact point.

This complete model was used to show the behaviour of different shots on different greens. Two different greens were simulated using the visco-elastic model. Both greens had a top layer depth of 8mm and a damper coefficient for the bottom layer of $10^5 s^{-1}m^{-2}$. The first green (Green 1) was considered to be firm ($C_1=10^9 s^{-2}m^{-2}$, $C_2=2x10^6 s^{-1}m^{-2}$) and had a low coefficient of friction (0.2). It was thought that this green would be well drained and have a low moisture content. The second green (Green 2) was less resistant

to impacts ($C_1=0.5x10^9s^{-2}m^{-2}$, $C_2=10^6s^{-1}m^{-2}$) and had a higher coefficient of friction (0.8). If the analogy with the Green Characteristics mentioned in section 5.5(iii) is again considered, this green would be less well drained than the first and would have a higher moisture content.

Impacts from a 5-iron and a 9-iron shot were simulated using the model. Using the correct incoming velocities and angles for each, the amount of backspin before impact was varied. Two bounces were determined and it was assumed that the ball travelled across the surface on the third bounce. The distance travelled by the ball was then calculated. Comparisons for the 5-iron shot on the two different greens for each spin are shown in Figure 5.20. Three spins were used, -750, -500 and -250rads^{-1}. The final positions of the ball on each green for each shot are also shown. In Figure 5.20 (a), it can be seen that the ball bounces further on Green 1 than on Green 2 after the first impact. After the second bounce, the ball on Green 1 retains some backspin and the ball "screws back" on the third bounce to finish about 1.4m in front of the initial impact point. The bounces of the ball on Green 2 are higher and shorter than on Green 1. On the third impact, however, the ball does not retain enough backspin to check it and consequently rolls forwards, finishing 1.3m in front of the initial impact point. On both greens, therefore, the ball is predicted to finish at approximately the same point but arrive there by different means.

If the initial backspin is reduced to -500rads^{-1} (Figure 5.20 (b)) then the ball tends to travel forwards on both greens after the third impact. The ball on Green 1 retains backspin after the second bounce but is not enough to check it. On green 2, the ball has topspin after the second bounce and the ball rolls forwards across the green on the third impact. Again, the balls finish in similar positions approximately 2m in front of the initial impact point.

If the backspin is reduced further to -250rads^{-1}, then the balls rebound with topspin after the second bounce on both greens. However, because the velocity of the ball is larger on Green 1, it travels further, finishing nearly 4m from the initial point of impact.

On Green 1, therefore, large amounts of spin are required to stop the ball. If the ball has only a low amount of spin, then the ball rolls forwards a long way. On Green 2 the spin has less effect on the final resting point of the ball. Even with low amounts of spin, the ball finishes only 2.5m away from the initial impact point.

Figure 5.21 shows the simulated impacts for the 9-iron for the two different greens. (Note that the horizontal scale is different from that in Figure 5.20). Three spins were used, -930, -680 and -430rads^{-1}. It can be seen that the ball bounces a lot further on

Green 1 than on Green 2 in all cases. The ball retains large amounts of backspin after the second bounce on both greens for an initial backspin of -930rads^{-1} (Figure 5.21 (a)).

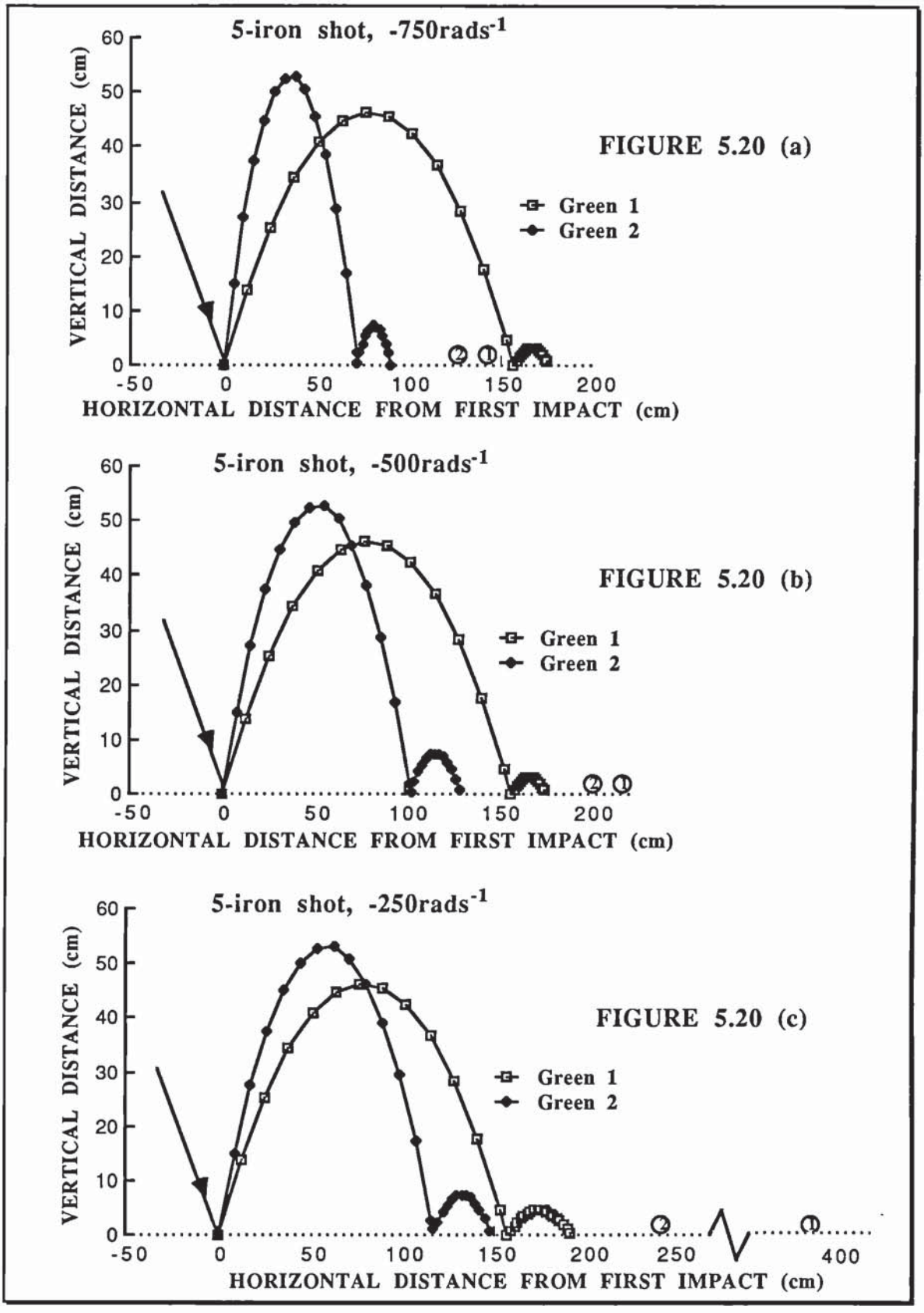

FIGURE 5.20. Diagrams showing the simulated behaviour of 5-iron type shots with different amount of backspins on a "hard" and a "soft" green using the visco-elastic model of oblique impact. The estimated final resting point of the ball is shown for each green.

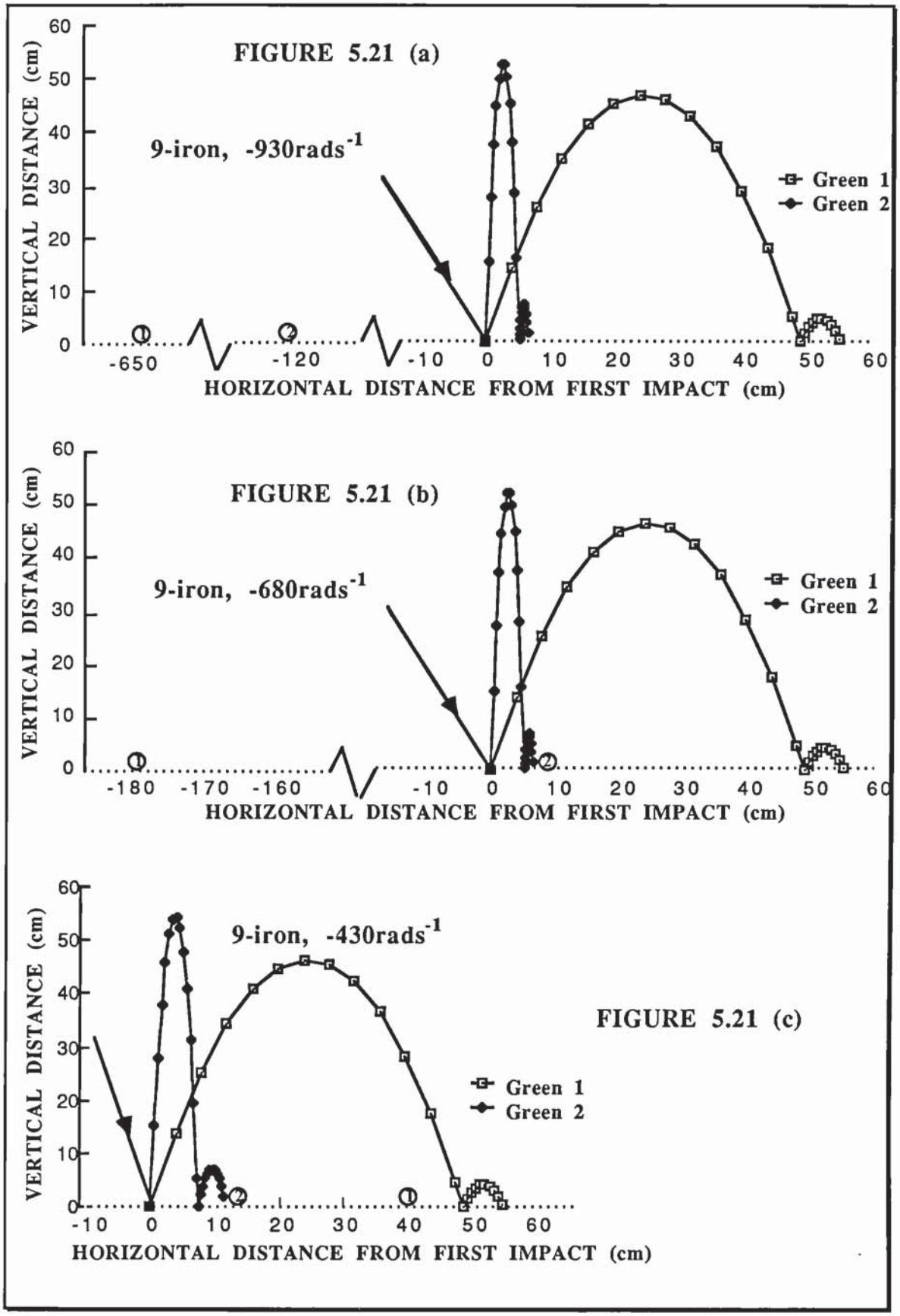

FIGURE 5.21. Diagrams to show the simulated behaviour of 9-iron type shots with different amounts of backspin on a "hard" (green 1) and a "soft" (green 2) green using the visco-elastic model of oblique impact. The estimated final resting point of the ball is shown for each green.

However, the ball on Green 1 retains much more backspin than on Green 2 and consequently screws back much further, finishing almost 6.5m behind the first impact point. If the spin is reduced to -680rads^{-1}, then the ball retains just enough backspin after the second bounce on Green 2 to check it on the third. On Green 1 the ball retains backspin and screws back. The result is that ball finishes 1.8m behind the first impact point on Green 1 and 10cm in front of it on Green 2.

At the lowest rate of spin that was simulated, the ball on Green 2 is again checked on the third bounce. On Green 1 the ball bounces further but still screws backs a small distance. The result is that both balls finish in front of the first impact point.

As with the 5-iron shot, the impact of the ball on Green 2 is affected less by backspin than the impact of the ball on Green 1. There is little difference between impacts on Green 2 at the two lower rates of spin and the ball only screws back if the backspin is very large. On Green 1, however, the final resting point is very dependent upon the initial spin. The spin could be adjusted so that the ball screws back to the region of the initial impact.

These predictions show what might be expected of such shots on the two types of green distinguished in Chapter 4. On the first type of green, the ball retained backspin if the initial spin was high enough, while on the second type of green the ball nearly always rebounded with topspin. The first type of green tended to be well drained, have low amounts of organic matter and have low moisture contents. The second type of green tended to be less well drained, have high organic matter contents and high moisture contents. As stated in the previous section, it is possible that the constants required for this model are related to the tests for playing quality. The thickness of the top layer and the damper constant for the bottom layer may be related to the fixed characteristics of the green, such as the soil composition and organic matter content. The visco-elastic constants for the top layer and the coefficient of friction may relate to the constantly changing characteristics of the green such as the moisture content.

The coefficient of friction used to allow the retention of backspin was 0.2. This is smaller than the coefficient of friction measured using the friction sled. It was assumed that the coefficient of friction was independent of the velocity of the ball, but this difference might suggest the opposite. It is possible that the coefficient of friction reduces substantially when the backspin is such that the ball slips throughout impact. It was seen during the study of impacts that the pitchmark tended to increase in length and decrease in depth as the ball started to slip throughout the impact. This would account for the decrease in the rebound angle as the ball started to slip throughout impact. The increase in the length of the pitchmark could be due to a decrease in the coefficient of friction. The ball would tend

to be impeded less horizontally and would therefore tend to move across the surface rather than penetrate into it.

5.7. Summary

It was found in this chapter that a model of impact based purely on the classical law of elastic impacts did not suitably describe the impact of golf balls on turf. This was because the deformation of the ground was not taken into account during the impact.

A model used to predict high velocity plastic impacts was modified to simulate the impact of a golf ball on turf. This model did not agree with the results described earlier in this thesis and was probably because it was originally developed for impacts at much higher velocities.

In order to simplify the formulation of the model, experiments were carried out on vertical impacts. It was found that, above a given impact velocity, the velocity of rebound was constant. At velocities greater than about $30ms^{-1}$ the ball no longer rebounded from the surface. An explanation for this was that the surface was acting like a two-layered surface. The top layer consisted of grass and roots which was quite springy. At low velocities an increase in the impact velocity caused a proportional increase in the rebound velocity. At higher impact velocities the ball interacted with the lower layer. This layer retarded the motion of the ball and an increase in the impact velocity produced a corresponding increase in the reduction in the rebound velocity. Using this information, vertical impacts with the turf were simulated using visco-elastic models.

These simulated the characteristics of the surface in terms of springs and dampers, the first layer consisted of a spring and a damper in parallel while the second layer consisted of a single damper. The resultant model had several notable characteristics. Firstly, the force on the ball was proportional to the area of contact. The force causing the ball to rebound was composed of the forces from the two layers with each force proportional to the area of contact of the ball with the layer. Another feature of the model was that it allowed for the centre of the ball dropping below the level of the ground or below the boundary between the layers.

The model required five input parameters, the thickness of the first layer, the spring and damper constants for the first layer, the damper constant for the second layer and the coefficient of friction. These constants were varied until agreement with experiment was found. These values were then used in a modification of the vertical model to simulate the oblique impacts of golf balls on turf. The horizontal force in the model of oblique impact were composed in a similar manner to the vertical force just described, i.e. they were proportional to the area of contact and were composed of the force contributions from the

two layers. The spin of the ball was modified by the torque caused by the frictional force of the turf on the ball. The rotational force from this torque tended to cause the ball to roll off the surface and instantaneously reduced to zero if the topspin of the ball matched the spin required for rolling.

The predictions from the model agreed fairly well with the results in Chapter 3 for the values of the constants found in the model of vertical impact. However, there were certain discrepancies. Above a certain backspin threshold the ball was predicted to slip across the surface. As the backspin was increase further, the ball rebounded at a fixed angle and velocity, a relationship that was not found experimentally. Since the model predicts non-spinning vertical impacts it is likely that the error in the model arises in the interaction of the spin with the translational motion of the ball. The coefficient of friction used in the model was much smaller than the values found using the sliding friction apparatus described in Chapter 2. It is possible that the the coefficient of friction is not a constant and that it varies with the velocity of the periphery of the ball (relative to the surface). The coefficient of friction may have lower values at higher backspins allowing the ball to slip throughout impact.

The aim of this chapter was to produce a model of the ball/turf impact in order to increase the understanding of the processes of impact. Although the model of oblique impact does not agree precisely with experiment, the model of normal impacts gives a fair representation of the effects found on golf greens. This indicates that the simplification of the surface to two layers is justified.

The final version of the model of oblique impact was used to simulate the different golf shots onto two contrasting types of green. It was assumed that the ball travelled across the turf (i.e. "rolled") on the third impact. Even with the inaccuracies in the model, the effects predicted were similar to those seen in play.

Chapter 6 - Final discussion

6.1 The study of impacts

The purpose of this chapter is to review the contents of this thesis and highlight the results that have emerged from it. First of all, it is useful to view the project as a whole. One of the aims of a PhD project is to increase the knowledge of the subject studied. The project has provided information on a previously ignored topic within impacts, that of spinning rigid sports balls on a turf that can be deformed permanently. This chapter reviews the aims of the project to see how well they have been fulfilled. The efficiency of the system of projecting and recording impacts is considered in order to aid the design and development of future projects. The main results of the project are restated and linked to the management of golf courses.

6.2 The golf ball projection device

One of the main aims of the project was to design and develop an apparatus to project golf balls with variable speed, spin and angle on to a golf green and to record the impacts of the ball with the turf. The first part of this objective was carried out with the modification of the "Jugs" bowling machine. Since the flight of the ball before and after each impact was recorded, it was not necessary to have a ball projection device that was calibrated exactly. There has to be a certain degree of accuracy in the use of the projection device so that the operator can set it, with confidence, to give the approximate speeds, spins and angles required. Figure 6.1 shows the speeds attained by golf balls with the wheels on the projection device set at different values. These values were found from the repeated use of the device throughout the project. The horizontal and vertical axes give the projection device wheel speeds in mph as stated on the device control panel. As stated in Chapter 2, these values are for reference only since a value of 40mph on the dials, say, actually projects the ball at about 55mph due to a zero error of 15mph. Thus the units here are referred as "mph units" to distinguish them from absolute values.

With the device in a vertical orientation, the bottom wheel was varied up to 75mph units while the top wheel was varied up to 40mph units. The values shown in the boxes in Figure 6.1 are mean velocities in ms^{-1} attained by golf balls. The contour lines show the wheel speeds required for velocities between $10ms^{-1}$ and $32.5ms^{-1}$. Setting the top wheel on 20mph units and the bottom wheel on 60mph units, for instance, projected a golf ball at about $25.1ms^{-1}$ (56.5mph). Figure 3.4 and Table 3.5 give an idea of the consistency of the bowling machine. For instance, it was seen that the mean speed of many impacts at a single setting of the projection device (both wheels set at 25mph units) gave $17.2ms^{-1}$. The mean standard deviation was $0.6ms^{-1}$. Any inconsistencies in the speeds attained by the ball at different wheel settings can probably be attributed to moisture on the ball or

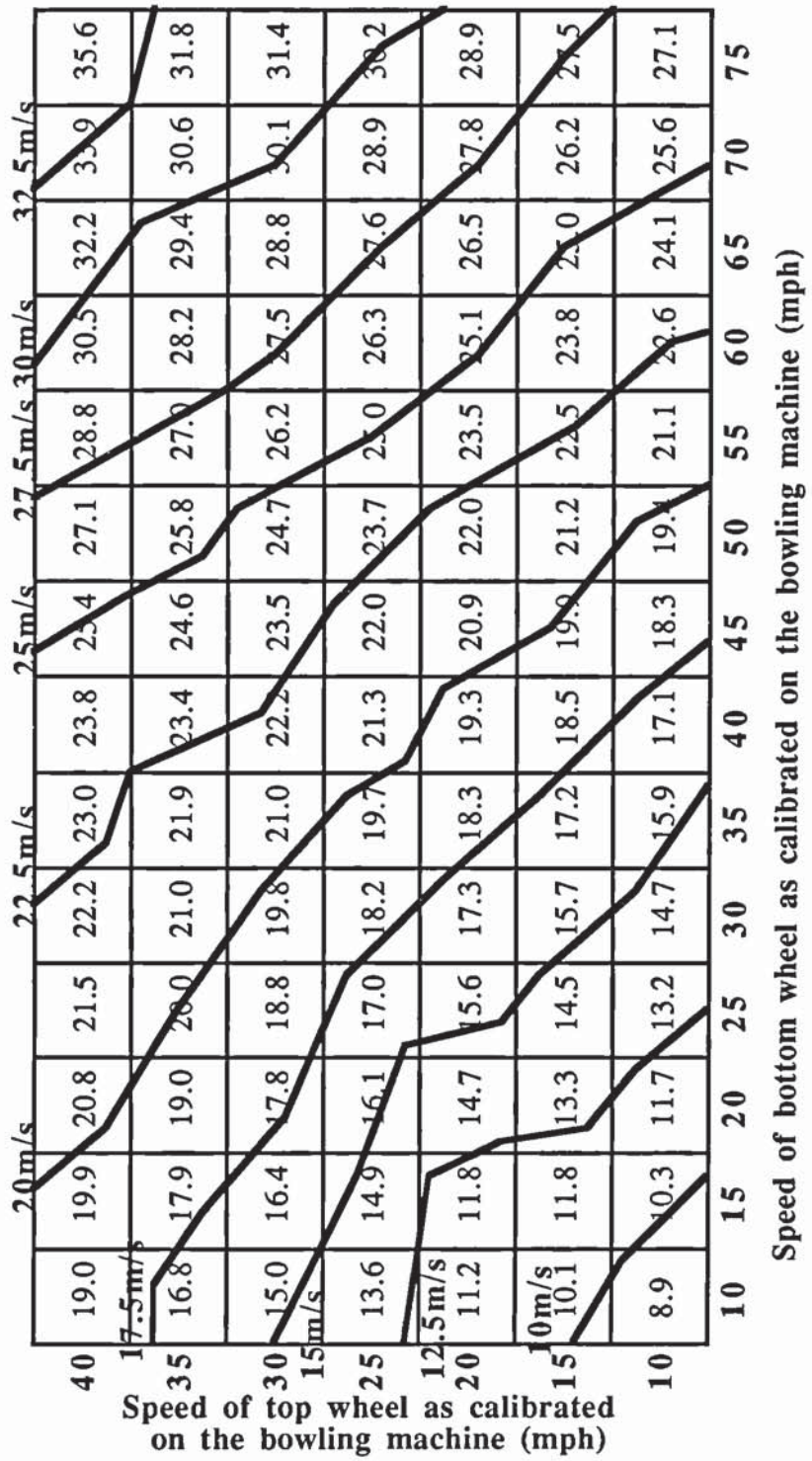

FIGURE 6.1. A diagram showing the speeds attained by a golf ball projected using the modified "Jugs" bowling machine. The axes show the speeds marked on the projection device while the speed of the projected golf ball is given in ms^{-1}.

wheels causing slip, an error in the actual setting of the wheel speeds or errors in the calculation of the ball velocity.

It is also useful to know the consistency with which the ball acquires spin from the projection device. Figure 6.2 shows the spins gained by a golf ball for an increasing difference in the wheel speeds. The discrepancy between the wheel speed setting and the actual velocity of the projected ball is the same for each wheel. Thus, the horizontal axis

in Figure 6.2 gives actual speed differences in mph. The errors given are the standard deviations of the means. The values shown in Figure 6.2 were found during the use of the machine during the project. It can be seen that the spin imparted to the ball increases linearly with the difference between the speeds of the wheels. For instance, if the difference between the speeds of the wheels is 20mph, then the ball acquires a spin of approximately 220rads^{-1}. Theoretically, this spin should equal the difference between the the wheel speeds divided by the diameter of the ball fired (Figure 2.2). The spin in this case would be 209rads^{-1}. The theoretical spin, therefore, almost matches the actual spin acquired by the golf balls.

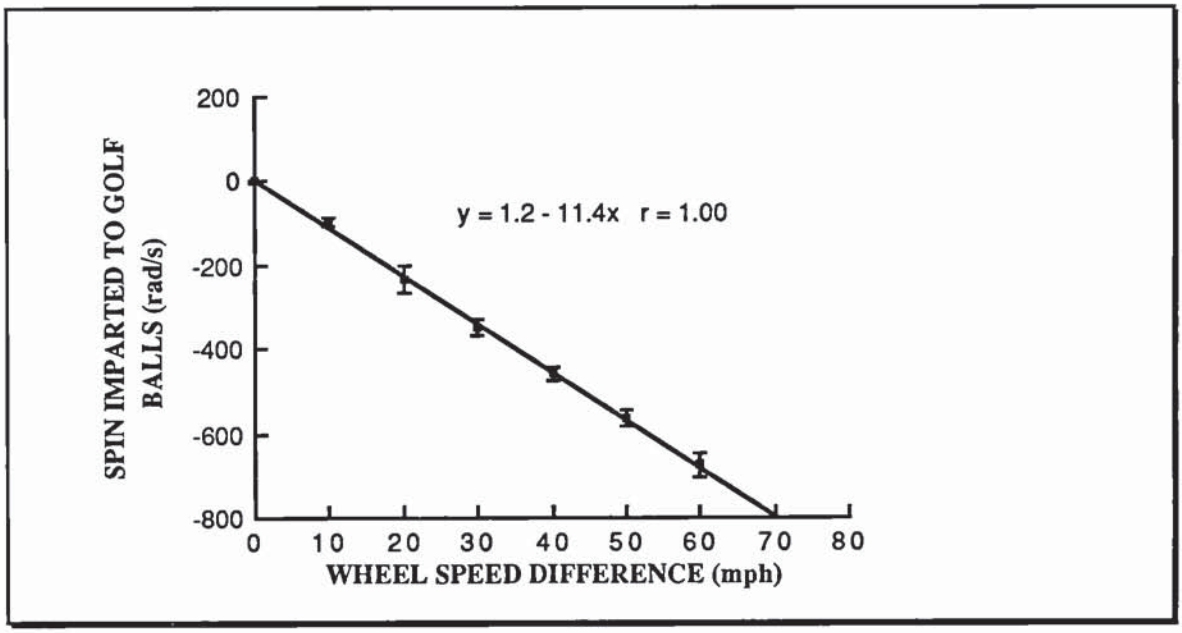

FIGURE 6.2. A graph showing the spins attained by a golf ball for increasing differences in the speeds between the wheels on the projection device.

If Figure 3.4 and Table 3.5 are studied again, it can be seen that the angle of projection was very consistent with a maximum standard deviation of about 1.6°. It was found, therefore, that the projection device could be relied upon to give consistent values of speed, spin and angle.

The wheels on the ball projection device had maximum and minimum speeds and this meant that the possible spins were limited. For instance, projecting a ball at 17ms^{-1} and with a spin higher than about 350rads^{-1} was not possible. This was because the top wheel was at its minimum speed. An increase in the speed of the bottom wheel would have increased the spin but would have also increased the velocity of the ball. A similar limitation occurred when the wheels of the bowling machine reached their upper limit. These higher spins could be achieved if the wheels were able to rotate in both directions, although the spin would still be limited by their maximum speeds. The projection apparatus worked well, however, and still appears to be the only suitable method of projecting golf balls at a variable speed, spin and angle.

6.3 The method of recording impacts

The method of recording impacts which produces the most information is that using high speed film. Using this method, the impacts can be viewed dynamically and measurements can be made at any part of the impact depending upon the speed of the film through the camera. As stated in Chapter 2, however, its major fault is its cost and the length of time required to set up an impact. The only information that is not present in the stroboscopic photographs is the time of contact of the ball with the turf.

The method of stroboscope photography worked well and achieved its purpose of recording the motion of the ball before and after impact. The electronics used, however, needed to be kept as dry as possible and the infra-red trigger mechanism had to be shielded from direct sunlight.

It was found during testing that strict concentration was required so that the impacts were recorded correctly. In effect, the tests were carried out blind since it was not known whether the tests were successful until the films were developed at a later date. During the evaluation of recording techniques, a high speed video camera was considered. This had the advantages of the method using high speed film and the immediate play back facilities of video. Unfortunately, its cost was in excess of £40,000, well above the finance for the whole project. However, the cost of a similar system marketed in late 1988 was just less than £10,000. This brings the apparatus almost within the budget of a project such as this and is well worth considering in future impact studies. The main disadvantage with the video system is that the frequency of the images is fixed at 50Hz. Its main advantage is that the camera is gated so that the exposure time for each frame is short enough to stop a moving ball. Consecutive images of a ball travelling at $20ms^{-1}$, however, would be 40cm apart making analysis difficult. At present, the use of a still camera coupled to a stroboscope is still the most effective system of recording ball/turf impacts.

6.4 The physical characteristics of the turf

The second aim of the project was to identify the measurable characteristics of the turf and to relate the results of the impacts to them. Eleven characteristics of the turf were studied and the relationships between them found in Chapter 4. Four measures of the natural characteristics of the turf were used, the moisture content, the organic matter content, the soil composition and the grass species prevalent on the turf. If was found that these characteristics were all closely inter-related and that stating the value of one often implied the value of another. Any measurement is dependent upon the recent history of the green; for instance a recent storm may have caused the moisture content to be abnormally high.

Thus, stating all four of these characteristics ensured that the correct nature of the surface was determined.

Some of the measurements of the natural characteristics were closely related to measurements of the playing quality of the turf. It was found that the dominant species of grass present on the green was a good indicator of the condition of the turf. Greens with a large amount of *Poa annua* in their ground cover tended to be resistant to horizontal motion across the turf but less so to vertical impacts. Since the amount of *Poa annua* was found to be inversely related to the percentage of *Agrostis* in the ground cover, greens with a large amount of *Agrostis* tended to be resistant to vertical impacts but unresistant to horizontal motion.

The relationships between the tests for playing quality were used to explain the differences between similar golf ball impacts on different greens.

6.5 Golf ball impacts

From the results of the golf ball impacts it was found that the depth of the pitchmark played an important role in the behaviour of the ball after impact. An increase in the incident angle or velocity tended to increase the depth of the pitchmark resulting in an increase in the rebound angle.

The variable that appeared to affect the impacts most, however, was the backspin of the ball before impact. An increase in backspin, in general, caused a decrease in the rebound velocity and an increase in the angle of rebound. As the backspin exceeded 350rads^{-1}, however, differences emerged between greens. This showed that there were two basic types of green studied. On the first, backspin was hardly ever retained after impact and the ball rolled off the surface. On this type of green the rebound angle tended to be large and the velocity after impact small. If the initial backspin is large enough then the ball may rebound back on itself, but still with spin likely to cause the ball to roll forwards. On the second type of green, the ball nearly always rebounded forwards and, if the initial backspin was large enough, retained backspin after impact. The ball slipped throughout impact. Once the backspin had reached the threshold for this slipping to occur, then each extra amount of backspin before impact produced an equivalent amount of backspin retained after impact.

It was then found that the characteristics of the greens were related to the impacts to determine their effect on individual greens. On greens with a large clay content, increasing the angle of incidence or the spin before impact produced little change in the behaviour of the rebounding ball. This was because the ball tended to penetrate quite far with the result that the ball rolled off the surface at the end of impact.

Green Characteristics and Playing Quality Tests were used to determine the nature of the greens on which the ball predominantly rolled off the surface and on which the ball slipped off the surface if the backspin was large enough. It was found that the greens on which slipping could occur tended to have less than 30% of clay in their composition, an organic matter content less than 8% and a moisture content below 30%. There also tended to be less than 60% of Poa annua in the ground cover. These results indicated that for slipping to occur in a large proportion of the impacts, the green has to be fairly resistant to vertical impacts but less so to horizontal motion across the turf. These greens tend to be free draining with low *Poa annua* contents (or high *Agrostis* contents).

An interesting fact that emerged from the measurement of the ball rebound resilience was that, at the velocity tested, the construction of the ball had little effect on the impact. In the impacts studied using stroboscope photography, it was found that the construction of the ball had no significant effect on the behaviour of the rebounding ball. In these types of impact, therefore, the ball could be considered as a rigid solid. This made the modelling of the ball/turf impact simpler since the properties of the ball could be ignored.

From the golfer's point of view, this fact may seem wrong since the impact of the golf ball with the green is seen to be affected by the construction of the golf ball. Different constructions, however, acquire different amount of spins when hit with a golf club. This alters the trajectory of the ball with the result that the balls land on the green with different velocities, angles and spins. If different golf balls hit the green at the same velocity, angle and spin, however, they tend to rebound in the same way.

6.5 Models of impact

During the literature review it was found that there were no models of impact that were immediately applicable to ball/turf impacts. In some cases this was because the deformation of the ground was ignored.

It was considered that the ball/turf impact had to be simplified and, hence, studies of vertical impacts on golf greens were studied. It was found during tests of vertical impacts that, below a certain velocity, an increase in the impact velocity caused the ball to rebound with a higher velocity. Above this velocity, however, the ball rebounded at the same velocity regardless of the incoming velocity. This suggested that the ball was impacting with a surface that was composed of two separate layers. It was considered that the surface could probably be modelled as a visco-elastic surface consisting of two layers. The top layer was considered to be a spring and a damper in parallel while the lower layer was modelled as a damper. The force on the ball was proportional to the area of surface contact of the ball with each layer. The model also allowed for the case in which the

centre of the ball dropped below the level of the surface or the level of the boundary between the two layers.

It was found that the model could predict the velocities of rebound for non-spinning vertical impacts quite well. This depended upon four input parameters; the spring and damper constant of the top layer, the damper constant of the lower layer and the thickness of the top layer. Suitable values of these constants were determined and the model of vertical impact used as a basis for the simulation of oblique impacts.

Several additions were required to the model in order to simulate oblique impacts since a mechanism was needed for the interaction between the backspin of the ball and the surface. This interaction not only caused the tendency for the modification of the backspin to topspin but also changed the angle and velocity of rebound. This was required since experiments showed that if the ball slipped throughout impact, then it tended to rebound at a lower angle and with a higher velocity than if it had rolled off the surface.

The model was used to simulate the impacts of shots from a 5-iron and a 9-iron. A simple calculation of the distance (and direction) rolled by the ball after the initial bounces was also performed. The result of this was that the ball was predicted to screw back on on a hard green if the spin was high enough but not on a soft green. Another interesting feature of this model was that, if the spin was quite low in the impacts onto the hard green, then the shot bounced on and rolled forwards quite far. Thus, a golfer on this theoretical green would be penalised if the backspin before impact was not large enough. In Chapter 5, the constants in this model were related to various characteristics of the green. From a greenkeeper's point of view it is useful to know the effects of certain maintenance regimes on the characteristics of the green - this is considered in the following section.

6.6 Golf course management

For this project to be truly successful, the results have to be useful to those who have to maintain the golf greens, i.e. the greenkeepers. But first, the type of green required has to be decided upon. Some writers of golfing literature advocate the use of fertilizers and the watering of greens with the aim of producing soft lush surfaces that "hold" golf shots. By "hold" they mean that the ball creates a large pitchmark on the green and loses most of its energy during impact. On this type of green the ball would tend to rebound with topspin and would therefore roll forwards after impact. Other writers prefer the absence of both water and fertilizers with the hope of producing deep rooting *Agrostis* and *Festuca* grasses. If the green is fairly firm then the ball would tend to bounce further but its backspin would cause it to check or screw back on subsequent bounces. Thus the fact

that the ball "held" has different meanings on different greens. It might be considered that the former type of green would hold most shots while the latter would hold only those with large amounts of backspin. Thus, the first type of green would be preferred by the less able golfer while the second would be preferred by professionals.

The two types of green mentioned in the last paragraph emerged quite distinctly from the results of the project. One of the most important characteristics of a golf green was found to be its drainage. A green with a large amount of sand in its composition tended to drain well and have a predominance of *Agrostis* in its sward. This was due to the ability of the grass to withstand drought conditions. These greens tended to be firm and allow the possibility of the retention of backspin after impact. Therefore, if this type of green is required then maintenance should be carried out to ensure that drainage is good enough to encourage the growth of *Agrostis*. The removal of thatch through scarification could also reduce the moisture retained by the green thus improving drainage.

Some golfing enthusiasts prefer greens composed purely of a *Fetsuca/Agrostis* mixture to encourage the firm dry conditions of the backspin retaining greens. It has been shown in this project, however, that greens with as much as 60% of *Poa annua* in its composition can still allow the retention of backspin. This, however, does not take into account other considerations; for instance, *Poa annua* tends to die out in dry conditions or in the winter and this leaves an inconsistent putting surface. These greens also tend to have a high clay content and therefore tend to dry out during summer droughts. This causes them to be very hard and shots become unstoppable on them. It must be stressed, therefore, that the results of this project were taken during the summer and conclusions for the whole of the year can not be drawn. It may be that more *Agrostis* is required, or that the drainage has to be better during the winter months to produce the same conditions found during the summer months.

6.7 The future

The apparatus developed during this project worked well in the study of golf balls. It could work equally well, however, for other sports. In Chapter 4, a method of calculating three dimensional spin from two dimensional photographs was formulated. It was found that, due to the accumulation of errors, the method was not suitable for golf. It could, however, be used for sports such as cricket or tennis in which side or rifling spin is much more important. The ball projection device could easily be modified to fire these larger balls by increasing the gap between the projector wheels.

The model produced in this thesis assumes that the ball does not deform. This would not therefore apply to other sports balls such as tennis, since the ball clearly deforms on

impact with the surface. This might be allowed for in the model by introducing other visco-elastic elements to simulate the elastic properties of the ball.

This project was the first of its type on the subject of golf. The experiments that were carried out on the golf greens were designed to test the apparatus and at the same time to investigate the properties of the green. Now that some results have been obtained it is possible to carry out further studies on specific points of interest. For instance, an important factor for the model is the effect of the velocity of impact on the coefficient of friction. This could be done by carefully investigating the threshold at which spin is retained on different greens. The coefficient of friction could also be investigated using a friction shoe similar to that used by Stuurman and Koenigs (1968). This used a shoe attached to the end of a pendulum. The length of the pendulum could be varied to give different velocities as it swung down to hit the turf. In this case, a rotating golf ball could be attached to the end of the pendulum. The ball could be rotated at different speeds and the resulting reduction in the velocity of the ball as the pendulum swung past the turf would give an indication of the coefficient of friction.

Experiments similar to those in this project could be carried out on more golf greens. This would give a clearer indication of the effect of the characteristics of the turf on the impact of the ball/turf impact. A modification of these experiments could include the removal of the top layer of the surface to determine the characteristics of the lower soil layer. This would give better estimates of the visco-elastic properties of the surface.

A further series of experiments could be carried out on recently constructed fine turf plots at the Sports Turf Research Institute. Experiments to determine the effects of type of drainage and construction of the green are just beginning. This would be the ideal opportunity to use the apparatus developed in this project to determine in detail the effect of the characteristics of the green on the ball/turf impact.

References

Bailey, N.T.J. (1959). *Statistical methods in Biology.* The English Universities Press Ltd., London, 160pp.

Baker, S.W. (1985). The selection of topsoil to be used for sand-soil rootzone mixes: A review of current procedures. *J. Sports Turf Res. Inst.* **61**, 65-70.

Bearman, P.W. & Harvey, J.K. (1976). Golf ball aerodynamics. *Aeronaut. Q.*, **27**, 112-122.

Bell, M.J., Baker, S.W. & Canaway, P.M. (1985). Playing quality of sports surfaces: a review. *J. Sports Turf Res. Inst.*, **61**, 9-35.

Bowers, K.D. & Martin, R.B. (1974). Impact absorption , new and old Astroturf at West Virginia University. *Med. & Sci. in Sports*, **6**, 3, 217-221.

Briggs, L.J. (1945). Methods for measuring the coefficient of restitution and the spin of a ball. *J. of Nat. Bur. of Standards*, **34**, Research paper RP1624.

Buchanan W.G. (1984). Why don't the greens hold? *USGA Green Section Record,* **22**, 4, 1-5.

Buckman, H.O. & Brady, N.C. (1971). *The nature and properties of soils.* Macmillan Company, New York, 653pp.

Briggs, L.J. (1945). Methods for measuring the coefficient of restitiution and the spin of the ball. *J. Res. Nat. Bur. Standards,* **34**, Research paper RD1624.

Canaway, P.M. (1975). Fundamental techniques in the study of turfgrass wear: An advance report in research. *J. Sports Turf Res. Inst.*, **51**, 104-115.

Canaway, P.M. (1981). Wear tolerance of turfgrass species. *J. Sports Turf Res. Inst.*, **57**, 65-83.

Canaway, P.M. (1983). The effect of rootzone construction on the wear tolerance and playability of eight turfgrass species subjected to football type wear. *J. Sports Turf Res. Inst.*, **59**, 107-123.

Clegg, B. (1976). An impact testing device for *in situ* base course evaluation. *Australian Road Res. Bureau Proc.*, **8**, 1-6.

Clegg, B. (1978). An impact soil test for low cost roads. *Proc. 2nd Conf. Road Eng. Assoc. of Asia and Australasia*, Manila, Phillipines, Oct. 1978, pp. 58-65.

Colclough, T. & Canaway, P.M. (1988). Fertilizer nutrition of sand golf greens II. 1987 results. *Amenity grass research conference, Aberystwyth.* In press.

Cochran, A.J. (1974a). The impact of an imperfectly elastic sphere on a hard plane surface: Part 1: Normal impact. Confidential Acushnet Company report, AJC/P1/74.

Cochran, A.J. (1974b). The impact of an imperfectly elastic sphere on a hard plane surface: Part 2: Oblique impact. Confidential Acushnet Company report, AJC/P3/74.

Cochran, A.J. & Stobbs, J. (1968). *The Search for the Perfect Swing.* Heinemann, London, 256pp.

Daish, C.B. (1972). *The Physics of Ball Games.* English University Press, London, 180pp.

Davies, J.M. (1949). The aerodynamics of golf balls. *J. Appl. Phys.*, **20**, 821-828.

DIN 18035 Part 6(1978). Sports grounds - Synthetic surfacings (Requirements, tests, maintenance). Beuth-Verlag, Berlin, 28pp.

Dury, P. & Dury, P.L.K. (1983). *A study of natural materials (dynamic/particulate) in the provision of synthetic non-turf sports facilities, particularly for soccer and other winter games.* Nottinghamshire County Council Education Department, Playing Fields Service, 78pp.

Engel, R.E., Radko, A.M. & Trout, R.J. (1980). Influence of mowing procedures on rollspeed of putting greens. *USGA Green Section Record* **18**, 1, 7-9.

Goldsmith, W. (1960). Impact. Edward Arnold, London.

Granelli, U. (1983). Materials testing in the design and construction of road bases. *Le Strade*, **LXXXV**, 99-105.

Haggar, R.J., Stent, C.J. & Isaac, S. (1983). A prototype hand-held patch sprayer for killing weeds, activated by spectral differences in crop/weed canopies. *J. Agric. Engng. Res.* **28**, 349-358.

Haggar, R.J. & Isaac, S. (1985). The use of a reflectance ratio meter to monitor grass establishment and herbicide damage. *Grass & Forage Sci.* **40**, 331-334.

Hertz, H. (1881). *J. Math.* **92**, 156.

Holmes, G. & Bell, M.J. (1986a). The playing quality of bowling greens: a survey. *J. Sports Turf Res. Inst.*, **62**, 50-66.

Holmes, G. & Bell, M.J. (1986b). A pilot study of the playing quality of football pitches. *J. Sports Turf Res. Inst.*, **62**, 74-91.

Holmes, G. & Bell, M.J. (1987). Standards of playing quality for natural turf. *Sports Council/Sports Turf Research Institute Contract report.* 67pp.

Hoos, D.D. & Faust, W.W. (1979). Putting greens - The height of cut. *USGA Green Section Record,* **17**, 1-4.

Hutchings, I.M., Macmillan, N.H. & Rickerby, D.G. (1981). Further studies of the oblique impact of a hard sphere against a ductile solid. *Int. J. Mech. Sci.*, **23**, 11, 639-646.

Hutchings, I.M., Winter, R.E. & Field, J.E. (1976). *Proc. Roy. Soc. London.*, **A348**, 379.

Langvad, B. (1968). Sambandet mellan fotbollens studshöjd och klipphöjden på sportturf. *Weibulls Gräs-tips*, **10-11**, 355-357.

Laycock, R.W. & Canaway, P.M. (1980). A new optical point quadrat frame for the estimation of cover in close mown turf. *J. Sports Turf Res. Inst.*, **56**, 91-92.

Lush, W.M. (1985). Objective assessment of turf cricket pitches using an impact hammer. *J. Sports Turf Res. Inst.*, **61**, 17-79.

Maw, N., Barber, J.R. and Fawcett, J.N. (1976). The oblique impact of elastic spheres. *Wear*, **38**,1, 101-114.

Maw, N., Barber, J.R. & Fawcett, J.N. (1981). The role of elastic compliance in oblique impact. *J. Lub. Tech., Trans ASME,* **103**, 74-79.

Mehta, R.D. (1985). Aerodynamics of sports balls. *Ann. Rev. Fluid Mech.*, **17**, 151-189.

Piper, C.S. (1950). *Soil and Plant Analysis.* Univ. of Adelaide, Australia.

Putnam, C.A. & Baker, J.A.W. (1984). Spin imparted to a tennis ball during impact with conventionally and diagonally strung rackets. *Research Quarterly for Exercise and Sport,* **55**, 261-266.

Quale, P.P. (1924). Spark photography and its application to some problems in ballistics, *BS Sci .Pap.*, **20**, 237.

Radko, A.M. (1977). How fast are your greens? *USGA Green Section Record,* **15**, 5, 10-11.

Radko, A.M. (1978). How fast are your greens? - An update. *USGA Green Section Record,* **16**, 2, 20-21.

Rayleigh, L. (1906). On the production of vibrations by forces of relatively long duration, with applications to the theory of collisions. *Phil. Mag.*, **11**, 6, 283-291.

Rickerby, D.G. & Macmillan, N.H. (1980). On the oblique impact of a rigid sphere against a rigid-plastic solid. *Int. J. Mech. Sci.*, **22**, 491-494.

Shildrick, J.P., Laycock, R.W. & Dunn, R. (1983). Multi-centre trials of turfgrass cultivars in the UK: 3.Fine-leaved fescues, 1978-81. *J. Sports Turf Res. Inst.*, **59**, 51-72.

Snedecor, G.W. & Cochran, W.G. (1974). *Statistical methods.* The Iowa State University Press, Ames, Iowa, U.S.A., 593pp.

Sports Council (1984a). *Specification for artificial sports surfaces. Part 1 - General principles and classification,* Sports Council, London, 22pp.

Sports Council (1984b). *Specification for artificial sports surfaces. Part 2 - Surfaces for general sports use,* Sports Council, London, 22pp.

Stanitiski, C.L., McMaster, J.H. & Ferguson, R.J. (1974). Synthetic turf and grass - a comparative study. *J. Sports Medicine,* **2** (1), 22-26.

Stewart, V.I. & Adams, W.A. (1968). County cricket wickets. *J. Sports Turf Res. Inst.*, **44**, 49-60.

Stewart, V.I. & Adams, W.A. (1970). Soil factors affecting the control of pace on cricket pitches. *Proc. 1st Int. Turfgrass Res. Conf.*, Harrogate, England, July 1969 (Ed. Sports Turf Res. Inst.), pp. 533-546, Sports Turf Res. Inst., Bingley.

Stimpson, E.S. (1974), Putting greens - how fast? *USGA Golf J.*, **27**,2,28-29.

Stuurman, F.J. & Koenigs, F.F.R. (1968). Een apparaat voor het meten van de sterkte van de zode van grassportvelden. *Tidschrift Koninklijke Nederlandsche Heidemaatschappij,* **79**, 376-381.

Tabor, D. (1955). Elastic work involved in rolling a sphere on another surface. *Brit. J. Appl. Phys.*, **6**, 79-81.

Tait , P.G. (1896). *Trans Roy. Soc. Edinburgh,* **39**, pt.II, 494 (1896-1899).

Tatara, Y. (1983). The behaviour of soft spheres during impact by high speed photography. *J.Eng. Mat. Technol., Trans. ASME,* **105**, 1, 67-73.

Thomas, F. (1978). The Stimpmeter and the Open. *USGA Green Section Record,* **16**, 6, 7-9.

Thomas & Guérin, J.P. (1981). A method of measuring the quality of sports turf. *Proc. Fourth Int. Turfgrass Res. Conf.*, Guelph, Canada, July 1981 (Ed. R.W. Sheard), 151-154, Ontario Agric. College.

Thorpe, J.D. & Canaway, P.M. (1986a). The performance of tennis court surfaces, 1. General principles and test methods. *J. Sports Turf Res. Inst.,* **62**, 92-100.

Thorpe, J.D. & Canaway, P.M. (1986b). The performance of tennis court surfaces, 2.Photometric methods for measuring pace and bounce under playing conditions. *J. Sports Turf Res. Inst.,* **62**, 101-117.

Throssel, C.S. & Duich, J.M. (1981). Management factors affect golf course green speeds. *Science in Agriculture,* **28**, 4, 9.

Winterbottom, W. (1985). *Artificial grass surfaces for Association Football*, Sports Council, London, 127pp.

Wolf, P.R. (1974). *Elements of Photogrammetry*. McGraw Hill, London, pp115-124.

Woolhouse, A.R. (1976). Estimation of ground cover in turfgrass communities. *J. Sports Turf Res. Inst.* **52**, 64-76.

Appendix A - A model to predict the trajectories of golf balls hit with different clubs

The following program calculates the landing velocity, angle to the vertical and spin of a golf ball projected from the ground with a velocity angle and spin introduced manually by the operator. The model estimates the drag and lift coefficients of the ball from information gained from wind tunnel tests on a Titleist golf ball by the Acushnet Company. Thus, the calculations performed can only be estimates since the information in the drag and lift calculations are for a single type of golf ball in a range of velocities. The model may, therefore, not be suitable for trajectories in which the initial backspin is extremely large or in which the angle of ascent is large. Information from the program should not be used without the consent of Dr. A. J. Cochran.

```
PRINT "This program calculates the trajectory of a spinning golf ball"
PRINT "COPYRIGHT A.J.Cochran, revisions 1985,1986"
PRINT "Lift and drag supplied confidentially by Acushnet Co., New Bedford, USA"
PRINT
FOR J=1 TO 200
K=J
NEXT J
PRINT "ENTER INITIAL SPEED (fps), spin (rpm), Angle (degrees)"
INPUT R,N,PO
CLS:PRINT "The program can deal with headwind (-) or tailwind (+)"
PRINT "ENTER WINDSPEED IN fps (+/-)"
INPUT WIND
CLS:PRINT "The program uses a calculation steplength of 0.1sec, prints trajectory
details at intervals of 1 second and terminates after 10 seconds if the ball has not returned
to the ground by then."
PRINT "Do you wish to use different values for any of these?"
PRINT "Answer (Y)es or (N)o"
INPUT ANSWER$
IF ANSWER$="N" THEN GOTO 280
PRINT "Enter calculation step length, print interval and termination time you wish (in
seconds)"
INPUT H,H1,T1
GOTO 290
280 H=0.1:H1=1:T1=10
290 PRINT "If drag and lift are standard please type 0 otherwise type 1"
INPUT Q2
IF Q2=0 THEN GOTO 420
PRINT "Enter the factors by which drag and lift are to be multiplied (e.g. 1.1, 0.9)"
INPUT C1,C2
GOTO 560
420 C1=1: C2=2
GOTO 550
440 PRINT "Launch conditions"
PRINT "SPEED ="R"fps;  SPIN ="N" rpm;  ANGLE = "PO" degrees;  WIND =
"WIND" fps"
GOTO 610
550 IF Q2=0 THEN  580
560 CLS:PRINT "DRAG ="C1"times standard;  LIFT="C2"times standard"
GOTO 590
580 PRINT "DRAG and LIFT standard"
590 PRINT "Calculation step length = "H" sec"
600 GOTO 440
610 READ M,GO,W,A
READ A0,A1,A2,A3
READ B0,B1,B2,B2
T=0:X=0:Y=0
```

```
P0=P0*ATN(1)/45
U=R*COS(P0)-WIND
V=R*SIN(P0)
PRINT "    T(sec)        X(ft)        Y(ft)        U(fps)        V(fps)"
I=0
J=0
FOR T=0 TO T1-H STEP H
I=I+1
R=SQR(U*U+V*V)
REM**The next twenty or so steps give functional approximations to DRAG and LIFT
measured for a particualr Titleist ball
D1=A0+A1*R+A2*R*R+A3*R*R*R
D=D1+(N-1570)*.000007)*(1-EXP(-.03*R))
D=D*C1
L1=B0+B1*R+B2*R*R+B3*R*R*R
L=L1+(.000244)*R*(1-EXP(-W*(N-1570)))
L=L*C2
F=G0*(-D*U-L*V)/(M*R)
G=G0*(-D*U+L*V)/(M*R)-G0
U5=U+.5*H*F
V5=V+.5*H*G
N5=N*EXP(=A*H/2)
R5=SQR(U5*U5+V5*V5)
D5=A0+A1*R5+A2*R5*R5+A3*R5*R5*R5
D5=D5+(N5-1570)*.000007)*(1-EXP(-.03*R5))
D5=D5*C1
L5=B0+B1*R5+B2*R5*R5+B3*R5*R5*R5
L5=L6+(.000244)*R5*(1-EXP(-W*(N5-1570)))
L5=L5*C2
F5=G0*(-D5*U5-L5*V5)/(M*R5)
G5=G0*(-D5*U5+L5*V5)/(M*R5)-G0
U1=U+H*F5
V1=V+H*G5
X9=X:Y9=Y
X=X+.5*H*(U+U1)
Y=Y+.5*H*(V+V1)
U9=U:V9=V
T9=T
U=U1:V=V1
N=N*EXP(-A*H)
P2=V*V9
IF P2<0 THEN1380
1110 Q1=0
IF Y>=0 THEN 1150
Q1=1
GOTO 1320
1150 IF I*H<J*H1 THEN 1280
1160 J=J+1
DIM O(4)
1170 O(0)=INT(100*(T*H)+.5)/100
O(1)=INT(100*(X+(T*H)*WIND)+.5)/100
O(2)=INT(100*Y+.5)/100
O(3)=INT(100*(U+WIND)-.5)/100
O(3)=INT(100*(U+WIND)-.5)/100
FOR K=0 TO 4
        @%=131594
        PRINT;O(K);
NEXT K
IF Q1=1 THEN 1400
1270 RESTORE
```

```
1280 NEXT T
1290 DATA 0.10125,32.2,.000636,.05
DATA 0,.0001,.000003,2.7E-9
DATA -.212,.0044,-.000025,5.28E-8
X=(X*Y9-X9*Y)/(Y9-Y)
T=-H+((T+H)*Y9-T9*Y)/(Y9-Y)
Y=0
U=(U*Y9-U9*Y)/(U9-Y)
V=(V*Y9-V9*Y)/(V9-Y)
GOTO 1170
1380 Y7=Y9+.5*H*V9^2/(V9-V)
GOTO 1110
1400 A9=45*ATN(-V/(U+WIND))/ATN(1)
V7=SQR((U+WIND)^2+V*V)
PRINT "Landing speed = "INT(100*V7+.5)/100" fps"
PRINT "Angle = "INT(100*Y7+.5)/100"degrees"
PRINT "Spin = "INT(N)"rpm"
END
```

Appendix B - Errors involved in the analysis of the photographs of ball impacts

B.1. Errors in the method using points representing the co-ordinates of the ball

(i) Errors of measurement

The smallest squares on the grid on Figure 2.10 are 5mm x 5mm and the horizontal and vertical lines are marked at 1mm intervals. It was estimated that a single co-ordinate had an error of ±1mm since this was the greatest accuracy possible. Figure B.1 shows the propagation of an error ε through the calculation of the velocity in equation 2.1, assuming that the error in all the co-ordinates is the same. An initial error in placing a co-ordinate of 1mm produces a final error of 2mm. The minimum distance between images of the incoming ball was found to be approximately 70mm and therefore, the greatest error produced in calculating the initial velocity of the ball was about 3%. The speed of the outgoing ball was calculated by measuring the distance across a number of images; 6 or 7 images usually measured about 70mm. The error in this measurement is the same as that for the incoming ball so that the percentage error was again about 3%.

Expression	Accumulated error
h, k	ε
h^2, k^2	$2\varepsilon h,\ 2\varepsilon k$
$h^2 + k^2$	$\sqrt{(4\varepsilon^2(h^2+k^2))}$
$\sqrt{(h^2+k^2)}$	ε

TABLE B.1. The propagation of an error ε through equation 4.1. An initial error of 1mm produces a final error of 2mm. The greatest error in calculating the incoming velocity was found to be 3% while that for the outgoing velocity was often less than 1%.

An error in reading the co-ordinates of the ball was also present throughout the calculations of the angle of arrival and departure of the ball (equations 2.3 and 2.4). When two co-ordinates with an initial error of ε are subtracted the combined error is $\pm\varepsilon\sqrt{2}$ (Figure B.1). Thus, a maximum and minimum of Θ_i and Θ_f were calculated and this gave a range of possible angles. These were interpreted as an error $\pm\, d\Theta_i$ and $\pm d\Theta_f$ in Θ_i and Θ_f respectively. Thus,

$$d\Theta_i = \pm \frac{1}{2} x \left(\Theta_{i_{max}} - \Theta_{i_{min}} \right)$$

$$= \pm \frac{1}{2} x \left(\text{TAN}^{-1} \frac{(Y_1 - Y_2 + \varepsilon\sqrt{2})}{(X_1 - X_2 - \varepsilon\sqrt{2})} - \text{TAN}^{-1} \frac{(Y_1 - Y_2 + \varepsilon\sqrt{2})}{(X_1 - X_2 - \varepsilon\sqrt{2})} \right) \qquad \text{eqn. B.1}$$

and,

$$d\Theta_f = \pm x \left(\Theta_{f_{max}} - \Theta_{f_{min}} \right)$$

$$= \pm \frac{1}{2} x \left(\text{TAN}^{-1} \frac{(Y_3 - Y_4 + \varepsilon\sqrt{2})}{(X_3 - X_4 - \varepsilon\sqrt{2})} - \text{TAN}^{-1} \frac{(Y_3 - Y_4 + \varepsilon\sqrt{2})}{(X_3 - X_4 - \varepsilon\sqrt{2})} \right) \qquad \text{eqn. B.2}$$

If the distance between two images is about 70mm and the ball is travelling at 45° to the horizontal, then an error of 1mm in each of the co-ordinates gives a range of 43.36° to 46.64° for the calculation of the angle. This is represented as an error of ± 1.64°.

(ii) Systematic errors

Figure B.1 (a) shows a diagram of a series of images of the ball 100mm apart and with the grid misplaced at an angle σ to the true impact plane. Due to the angled grid the distance between images appears as d' to the left of the centre of the photograph and as d" to the right of the centre of the photograph. d' and d" can be estimated as,

$$d' \approx OA' + A'B = d\cos(\sigma) + AA'\tan(\sigma + \psi) = d\cos(\sigma) + d\sin(\sigma)\tan(\sigma + \psi) \qquad \text{eqn. B.3}$$

and,

$$d'' \approx OD - DC' = \frac{d}{\cos(\sigma)} - \frac{EF}{\cos(\sigma)} \approx \frac{d}{\cos(\sigma)} - \frac{d\psi\sin(\psi)}{\cos(\sigma)} \qquad \text{eqn. B.4}$$

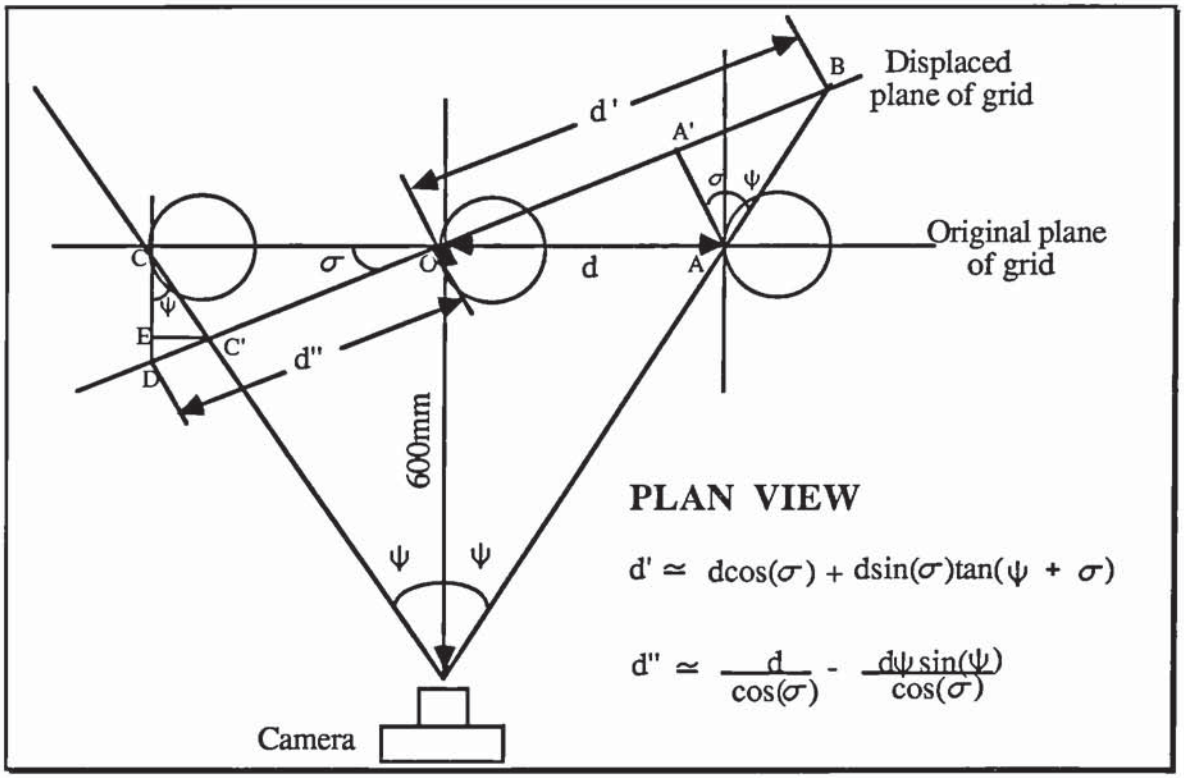

FIGURE B.1 (a). The effect of placing the grid accidentally at an angle σ to the true impact plane. The distance d would appear to be d' to the right of the centre of the photograph and d" to the left of the centre of the photograph. The equations give approximate calculations for the apparent distances between images, some estimates of which are given in Figure C.1 (b).

σ (°)	d' (mm)	d" (mm)
1	100.3	99.7
5	102.3	98.6
10	106.1	97.1

FIGURE B.1(b). Some estimates of the apparent distances d' and d" as the angle between the scale and the true plane of impact increases for an actual distance between impacts of 100mm.

Equations B.3 and B.4 are used to give some estimates of d' and d'' as σ increases in Figure B.1 (b). These were calculated for an initial distance between images of 100mm. At angles of 10° the error in d' is 6.1mm longer than the true value and d'' is 2.9mm shorter than the true value. It was possible to see errors of this magnitude when placing the grid since it required misplacing both ends of the scale by about 45mm - more than one golf ball diameter. It was estimated that systematic errors of this sort were kept to less than 3%, requiring the scale to have been misplaced by less than half a golf ball diameter on either side of the true impact plane.

Figure B.2 (a) shows the effect of moving the grid a distance ∂ to a plane parallel to that of the true plane of impact. The distance d is modified by $\pm\partial\tan(\alpha)$ and the apparent lengths of d' and d'' with increasing ∂ are shown in Figure B.2 (b) if the actual distance between images is 100mm. The error reaches a value of 5% when ∂ is approximately 30mm. This is one and a half times the radius of a golf ball and it was estimated that the scale could be placed well within this distance either side of the pitch marks.

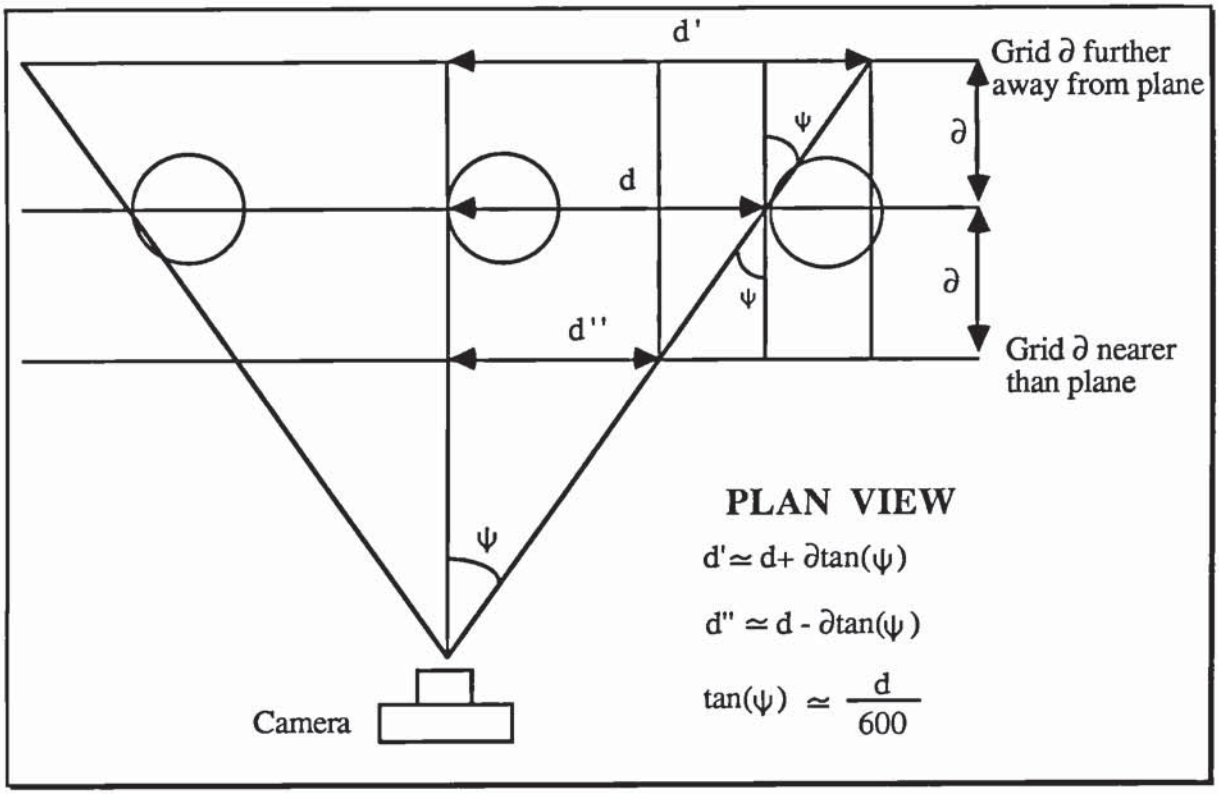

FIGURE B.2 (a). The effect of misplacing the grid nearer or further away than the true plane of impact.

δ (mm)	d' (mm)	d''(mm)
10	101.7	98.3
20	103.3	96.7
30	105.0	95.0

FIGURE B.2 (b). The variation of the app distances d' and d'' as the distance ∂ of the from the true plane of impact increases.

Appendix C - The calculation of spin in three dimensions using two dimensional images

C.1. Introduction

During the analysis of the pictures using the co-ordinate method described in Appendix B above it was considered that estimates of the side spin would help to explain odd results that occurred. The method described in this appendix was developed to calculate the three dimensional spin of the ball using the images on the two dimensional photographs. It consists of three stages, the first modifies the two dimensional co-ordinates from the photographs to points in three-dimensional space. The second calculates the spin axis of the ball and the third stage calculates the magnitude of the spin and hence the spin in the three dimensions.

C.2. Relief displacement

The relief displacement is the shift in the position of an image on a photograph caused by the height of the object above a selected datum. The relief displacement, with respect to a datum, is outwards from the centre of the photograph (the principal point) for points whose elevations are above the datum. As an example, consider Figure C.1 which shows a schematic diagram of an aerial view of a set of office buildings. Consider a co-ordinate system that is at ground level and that we wish to determine the position of the buildings. Since the bases of the buildings can not be seen on the photograph, the co-ordinates of the tops of the buildings have to be used. The building at the principal point is seen straight on and the co-ordinates of the top of this building are the same as those at the ground. However, an office block away from the centre of the photograph is seen from an angle and the point representing the top of the building appears further from the principal point than its base. It is necessary to reduce the distance R by a small amount δ to ensure that the co-ordinate we measure is correct.

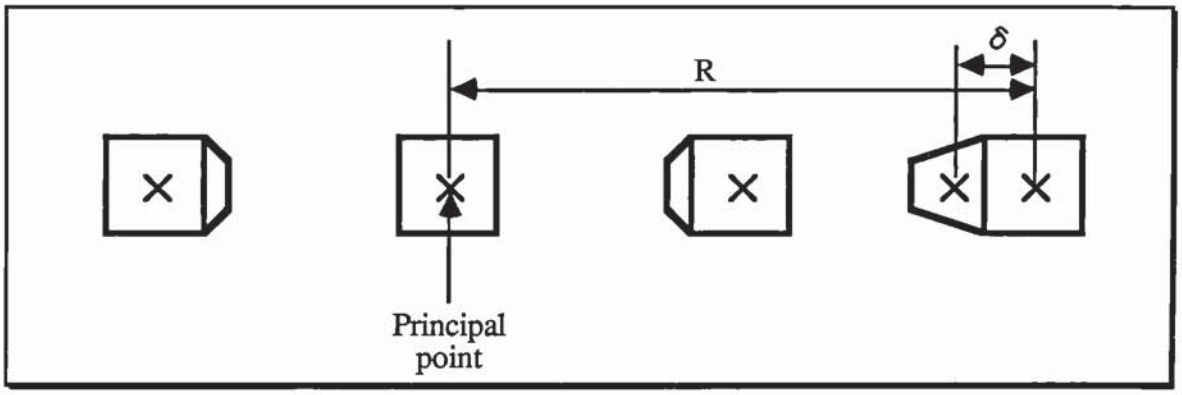

FIGURE C.1. A schematic diagram showing an aerial view of a set of office buildings with a co-ordinate system at ground level. If the co-ordinates of the tops of the buildings are used to pinpoint the position of the buildings then the buildings to the right would appear too far to the right and the co-ordinates would have to modified by a small amount δ.

This modification can also be used to alter the photographs of the golf ball impacts where the co-ordinate system is in the plane of the impact and the "tops of the buildings" are points on the balls surface away from this plane (Figure C.2).

The modification of the two dimensional co-ordinates to three dimensional ones and the alteration for relief displacement takes place as follows. From the photograph of an impact (Figure 2.10 for example) the Y and Z co-ordinates of a point are measured. The X co-ordinate is calculated assuming that the radius of the ball is 21.3mm using,

$$X = \sqrt{(21.3^2 - (Y - Y_0)^2 - (Z - Z_0)^2)} \qquad \text{eqn. C.1}$$

The distance R is the distance, as measured on the photograph, from the principal point to the point P (Figure C.2). It can be shown (Wolf, 1974) that R, X and δ are related by,

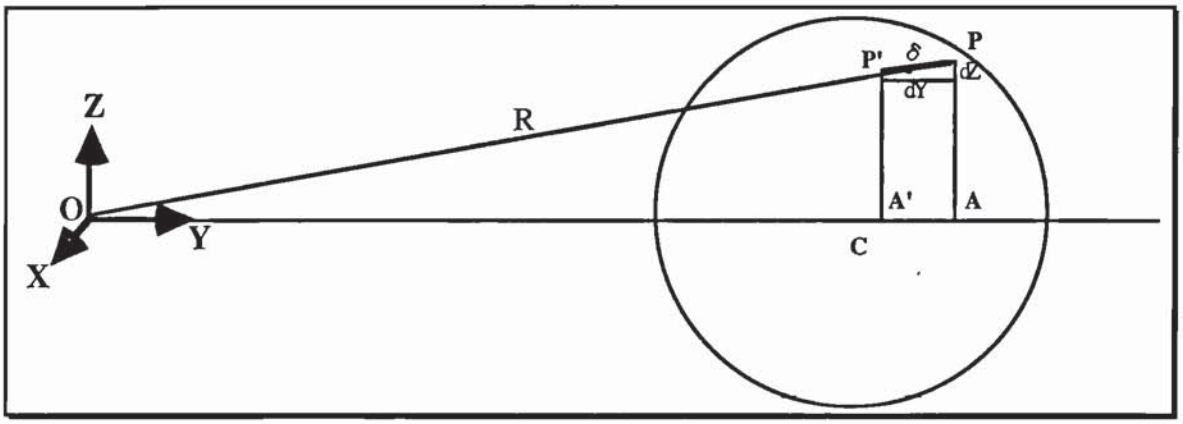

FIGURE C.2. A schematic diagram of a golf ball whose centre lies in a plane containing the principal point (0,0,0). The distance from the principal point to the point P is modified by a distance δ to the new point P'.

$$\delta = \frac{R \times X}{L} \qquad \text{eqn. C.2}$$

where L is the distance of the camera from the impact plane. The triangles OPA and OP'A' in Figure 3.8 are similar and therefore we have the equations,

$$\frac{Y}{R} = \frac{Y - dY}{R - \delta} \text{ and } \frac{Z}{R} = \frac{Z - dZ}{R - \delta} \qquad \text{eqn. C.3}$$

which, rearranged, give $dY = Y(1 - \kappa)$ and $dZ = Z(1 - \kappa)$, where $\kappa = (1 - \frac{\delta}{R})$. Thus we have equations for the modified set of co-ordinates which are,

$$Y' = Y - Y(1 - \kappa) = Y\kappa \qquad \text{eqn. C.4}$$

$$Z' = Z - Z(1 - \kappa) = Z\kappa \qquad \text{eqn. C.5}$$

$$X' = \sqrt{(21.3^2 - (Y' - Y_0) - (Z' - Z_0))} \qquad \text{eqn. C.6}$$

where $\kappa = (1 - \frac{\delta}{R})$ eqn. C.7

As an example, consider a photograph of a ball where the principal point is at (0, 0, 0), the centre of the ball is at (0, 250, 0) and a point on its surface is at (X, 264, 14). This represents a ball 250mm to the right of the centre of the photograph (as read on the scale on the picture) with a point 14mm up and 14mm to the right of the centre of the ball. The X co-ordinate is,

$$X = \sqrt{(21.3^2 - (264 - 250) - (14 - 0))} = \sqrt{(453.69 - 392)} = \sqrt{(61.69)} = 7.85\text{mm}.$$

The distance R would can be calculated as $\sqrt{(Y^2 + Z^2)} = \sqrt{(264^2 + 14^2)} = 264.37$mm. If the camera is approximately 600mm from the plane of impact then, using equation C.2, the relief displacement is,

$$\delta = \frac{264.37 \times 7.85}{600} = 3.46\text{mm and } \kappa = (1 - \frac{3.46}{264.37}) = 0.9869$$

Using equations 3.9, the modified co-ordinates are,

$Y' = 260.55$

$Z' = 13.82$

and $X' = \sqrt{(21.3^2 - (260.55 - 250)^2 - (13.82 - 0)^2)} = 12.30.$

The original co-ordinates of (7.85, 264, 14) have been modified for their relief displacement to (12.3, 260.55, 13.82). It should be noted that this modification was not

required when using the co-ordinates for the calculations in Appendix B since the points used lay in the impact plane where X = 0 and hence $\delta = 0$.

C.3. Method

Once the co-ordinates have been modified they can be used to calculate the spin axis of the ball and hence the spin in the three dimensions. The vectors $\mathbf{r_1}$, $\mathbf{r_2}$ and $\mathbf{r_3}$ in Figure C.3 represent a point on the surface of a ball, with respect to its centre, at times T_1, T_2 and T_3 respectively. The direction cosines of the vectors are written as,

$$\cos\alpha_1 = \frac{X_1}{r_1}, \cos\beta_1 = \frac{Y_1}{r_1}, \cos\gamma_1 = \frac{Z_1}{r_1} \qquad \text{eqn. C.8}$$

$$\cos\alpha_2 = \frac{X_2}{r_2}, \cos\alpha_2 = \frac{Y_2}{r_2}, \cos\alpha_2 = \frac{Z_2}{r_2} \qquad \text{eqn. C.9}$$

$$\cos\alpha_3 = \frac{X_3}{r_3}, \cos\alpha_3 = \frac{Y_3}{r_3}, \cos\alpha_3 = \frac{Z_3}{r_3} \qquad \text{eqn. C.10}$$

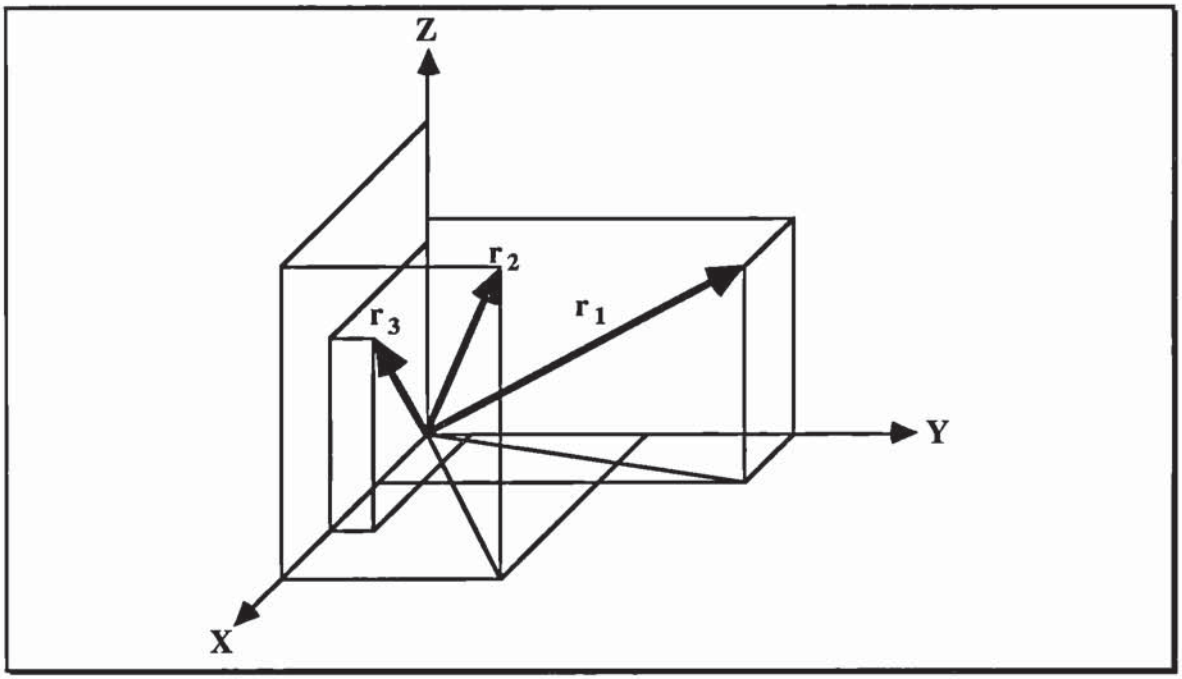

FIGURE C.3. The vectors $\mathbf{r_1}$, $\mathbf{r_2}$ and $\mathbf{r_3}$ are representations (with respect to the centre of the ball) of a point on its surface at times T_1, T_2 and T_3. The direction cosines of the vectors can be used to calculate the spin axis of the ball and hence the spin in the three dimensions.

These equations do not uniquely define the spin axis since the ± sign indicates a choice of spin direction. If the direction of rotation is known before any calculations are made then the signs of $\cos\alpha$, $\cos\beta$ and $\cos\gamma$ are known. Once the spin axis is found it is relatively simple to find the magnitude of the spin and hence the components in each direction. Figure C.4 shows points P_1 and P_2 at times T_1 and T_2.

The vectors $\mathbf{r_1}$, $\mathbf{r_2}$ and $\mathbf{r_3}$ are equidistant from the spin axis since they represent the same point on the surface of the ball at different times. Their magnitudes are the same and are equal to the radius of the ball. Using this fact, it can be shown that the direction cosines of the spin axis are,

$$\cos\alpha = \pm\sqrt{(C)},\ \cos\beta = \pm B\sqrt{(C)},\ \cos\gamma = \pm\sqrt{(1 - C(1 + B^2))} \qquad \text{eqn. C.11}$$

where,

$$A = \frac{(\cos\gamma_1 - \cos\gamma_2)}{(\cos\gamma_1 - \cos\gamma_3)} \qquad \text{eqn. C.12}$$

$$B = \frac{\{(\cos\alpha_1 - \cos\alpha_2) - A(\cos\alpha_1 - \cos\alpha_3)\}}{\{A(\cos\beta_1 - \cos\beta_3) - (\cos\beta_1 - \cos\beta_2)\}} \qquad \text{eqn. C.13}$$

and

$$C = \frac{(\cos\gamma_2 - \cos\gamma_1)}{\{(1+B_2)(\cos\gamma_2 - \cos\gamma_1)^2 + ((\cos\alpha_1 - \cos\alpha_2) + B(\cos\beta_1 - \cos\beta_2))^2\}}$$

eqn. C.14

Since the points are both equidistant from the spin axis then the angles between the vectors representing P_1 and P_2 and the spin axis are the same and can be calculated using the identity,

$$\cos\Theta = \cos\alpha\cos\alpha_1 + \cos\beta\cos\beta_1 + \cos\gamma\cos\gamma_1 \qquad \text{eqn. C.15 (a)}$$

$$\cos\Theta = \cos\alpha\cos\alpha_2 + \cos\beta\cos\beta_2 + \cos\gamma\cos\gamma_2 \qquad \text{eqn. C.15 (b)}$$

Since,

$$\sin\frac{1}{2}\phi_{rot} = \frac{\frac{1}{2}(P_2 - P_1)}{OP_2} = \frac{P_2 - P_1}{2r\sin(\Theta)}$$

then,

$$\phi_{rot} = 2\sin^{-1}\frac{\sqrt{((X_2 - X_1)^2 + (Y_2 - Y_1)^2 + (Z_2 - Z_1)^2)}}{2r\sin(\Theta)} \qquad \text{eqn. C.16}$$

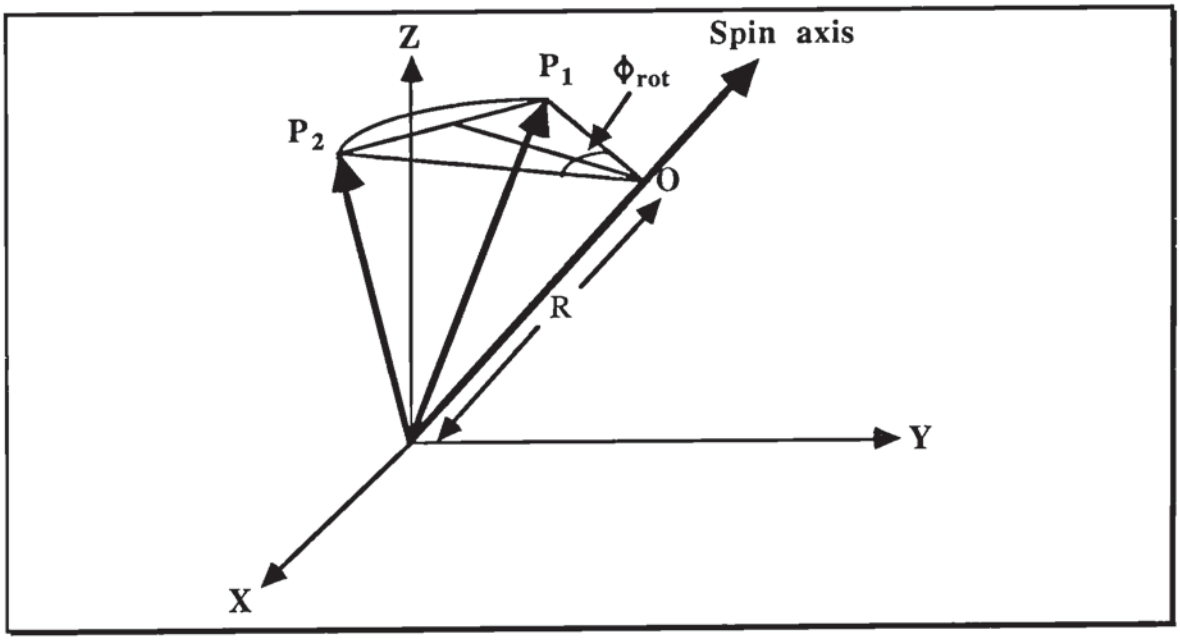

FIGURE C.4. The points $\mathbf{P_1}$ and $\mathbf{P_2}$ represent a point on the ball at times T_1 and T_2 and are equidistant from the spin axis. Using simple geometry the rotation ϕ_{rot} can be calculated and, using the spin axis direction cosines, the spin in the three dimensions can be found.

This is the angle rotated through in the time (T_2 - T_1). Multiplying this by each of the spin axis direction cosines ($\cos\alpha$, $\cos\beta$, $\cos\gamma$) give the components of spin in the three dimensions.

As an example, Figure C.5 shows a sphere of unit radius at times T_1, T_2 and T_3. The ball is rotating in a clockwise direction and the co-ordinates of a point on the surface of the sphere at successive time intervals are (0.707, 0.5, 0.5), (0.707, 0.5, -0.5) and (0.707, -0.5, -0.5).

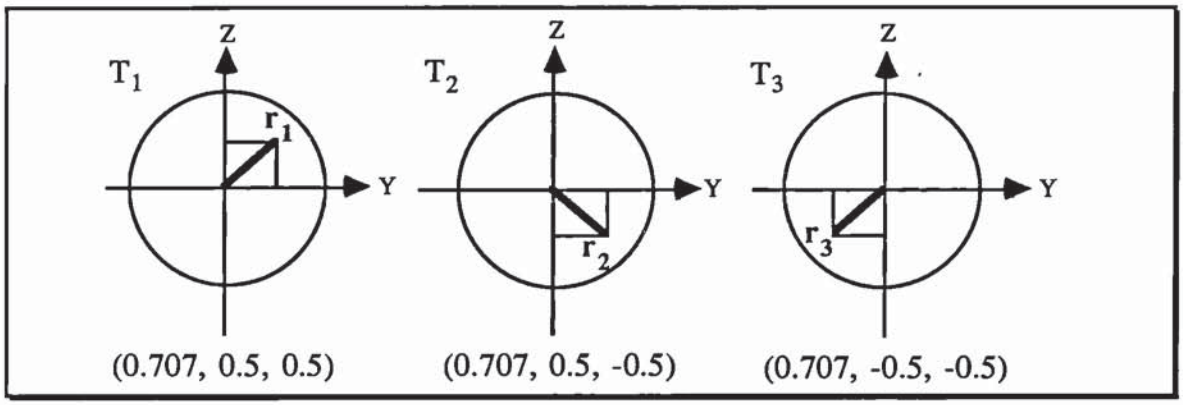

FIGURE C.5. The co-ordinates of the points P_1, P_2 and P_3 with respect to the centre of a sphere of unit radius represented by $\mathbf{r_1}$, $\mathbf{r_2}$ and $\mathbf{r_3}$ at times T_1, T_2 and T_3. This represents the sphere rotating in a clockwise direction by a quarter of a revolution per image.

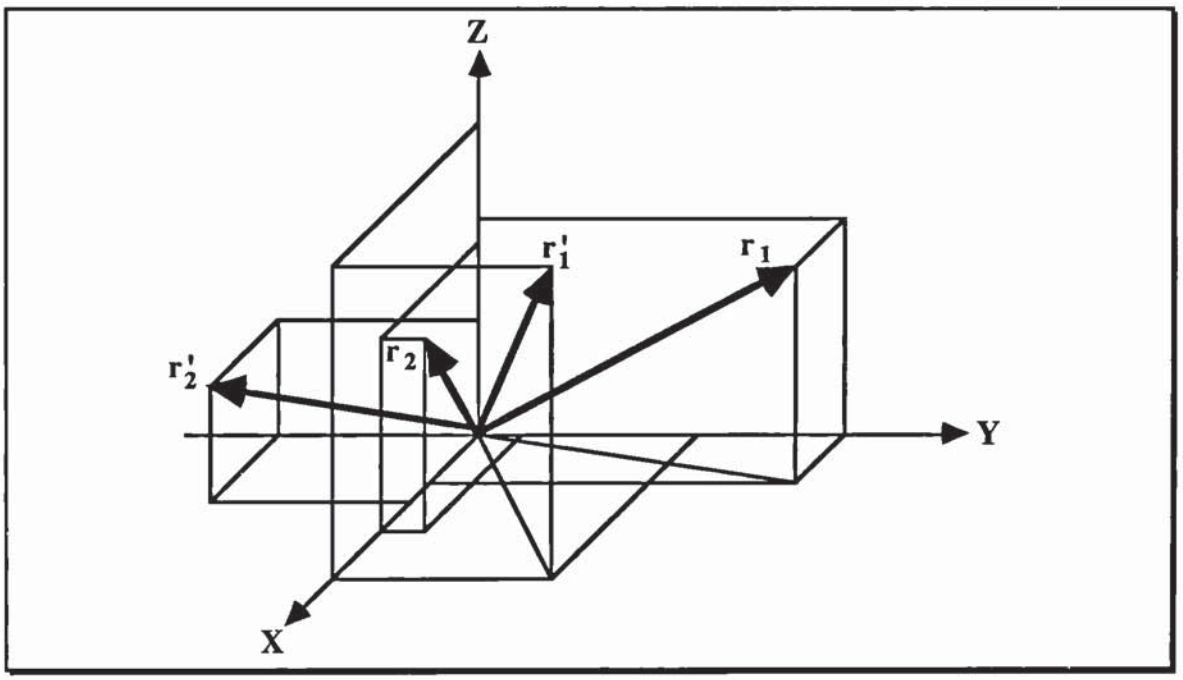

FIGURE C.6. The four vectors $\mathbf{r_1}$, $\mathbf{r_2}$, $\mathbf{r'_1}$ and $\mathbf{r'_2}$ represent (with respect to the centre of the ball) two points on the surface of the balls at times T_1 and T_2. $\mathbf{r_1}$ and $\mathbf{r'_1}$ make the same angle with the spin axis, as do $\mathbf{r_2}$ and $\mathbf{r'_2}$, and this fact enables the calculation of the three dimensional spin.

Using equations C.8, C.9 and C.10 the direction cosines of the three points are,

$\cos\alpha_1 = 0.707$, $\cos\beta_1 = 0.5$, $\cos\gamma_1 = 0.5$

$\cos\alpha_2 = 0.707$, $\cos\beta_2 = 0.5$, $\cos\gamma_2 = -0.5$

and $\cos\alpha_3 = 0.707$, $\cos\beta_3 = -0.5$, $\cos\gamma_3 = -0.5$.

From equations C.11 to C.14 the direction cosines of the spin axis are, $\cos\alpha = 1$, $\cos\beta = 0$ and $\cos\gamma = 0$. The magnitude of the spin can be calculated using equations D.15 and D.16 as follows,

$$\cos\Theta = 1 \times 0.707 + 0 \times 0.5 + 0 \times 0.5 = 0.707$$

$$\therefore \quad \Theta = 0.7854\text{rad}$$

$$\sin\frac{1}{2}\phi_{rot} = \frac{\sqrt{((0.707 - .0707)^2 + (0.5 - 0.5)^2 + (0.5 + 0.5)^2)}}{2\sin(0.7854)} = 0.707$$

$$\therefore \quad \frac{1}{2}\phi_{rot} = 0.7854\text{rad}$$

$$\text{and} \quad \phi_{rot} = 1.5708\text{rad} \equiv 90°$$

Multiplying this by the direction cosines of the spin axis gives $\phi_\alpha = 90°$, $\phi_\beta = 0°$ and $\phi_\gamma = 0°$. If the time between images is 0.002 seconds, say, then the magnitude of this spin is 50 revolutions per second about the X-axis.

C.4. Limitations of the method

Initially, the spin calculation was not possible since there were only two images of the incoming ball in most of the photographs (Figure 2.10). A simple modification made it possible to employ the above method using two points on two successive images of the ball. The method is the same but four points are now used (Figure C.6) and only the subscripts change in equations C.8 to C.16.

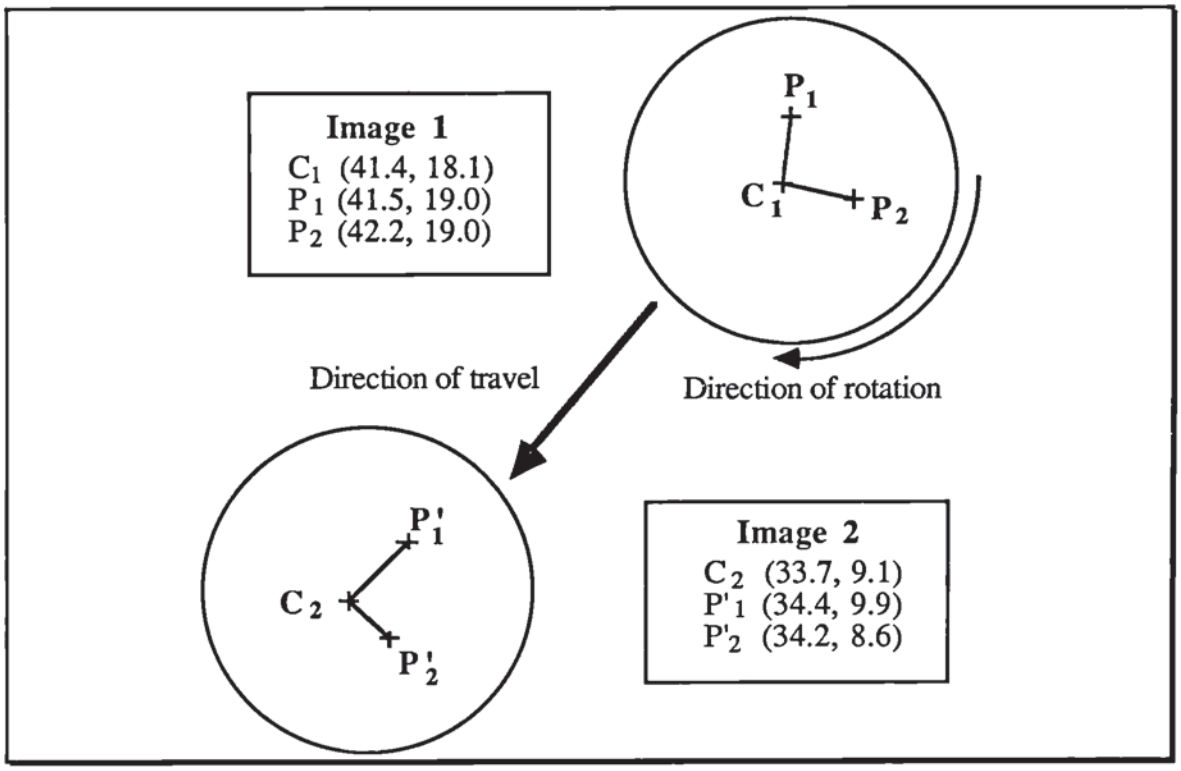

FIGURE C.7. A diagram showing the two dimensional co-ordinates of two points on consecutive images of a golf ball from the photograph of an impact. The points represent exactly the points seen on the photograph although the distance between images is not to scale.

involved subtracting the co-ordinates of the centre of the ball from the co-ordinates of the points. Since these were fairly near to each other, the combined error was large compared to the result. In the calculation of the direction cosines for the spin axis there are many subtractions, all increasing the error relative to the result. Section 5 of this appendix

describes a BASIC program which calculates the three dimensional spin of a golf ball using two points on two consecutive images. This program was used to analyse some images of a golf ball impact, one of which is shown in diagrammatic form in Figure C.7.

Due to the large number of steps in the calculation of the spin it was not viable to calculate exactly an error for each result that was output. In order to get an estimate of the accuracy of the calculations the co-ordinates of the points were altered by the error in their measurement, i.e. ± 1mm. The co-ordinates were altered by ± 1mm so that all combinations were accounted for and the effect on the calculation of the final spin noted. The co-ordinates of the centre of the first image were altered by ± 1mm and the magnitude of the total spin varied from 54.74 to 135.8rads^{-1}. Keeping the value of the centre constant and varying the co-ordinates of the two points on image 1 in turn by ±1mm had the effect of altering the total spin from 55.65 to 165.29 rads^{-1}. When the co-ordinate error was reduced to ±0.5mm the range of spin was 109.0 to 151.0rads^{-1} and if it was reduced still further to ±0.1mm the range was 132.50 to 138.46rads^{-1}. The errors in the calculation of the final spin are too large to rely on the result when the error in each co-ordinate is ±1mm. With an error of ±0.1mm, however, the range of values for the total spin is small enough for the calculations to be considered accurate. This implies that the images of the balls have to be considerably bigger and the scale a lot finer if the calculations of three dimensional spin are to be accurate. It is therefore possible that this method would be more suitable for studying impacts of larger balls such as tennis, cricket or football.

C.5. A BASIC program to perform the three dimensional spin calculations

A large number of mathematical steps are required to perform the calculations above so the mathematics were written into a BASIC program to increase the speed of the process; this is shown below. The language used was Microsoft BASIC for the Apple MacintoshPlus.

```
REM***************THREE DIMENSIONAL SPIN ANALYSIS***************
REM****************************(3DSPIN.2P)****************************
REM*****************************By S.J.Haake*****************************
REM**This program calculates the spin of a sphere about its origin and gives the answer
REM**as spin about the three dimensional axes. The program uses the two dimensional
REM**co-ordinates of two points at successive times from photographs of ball impacts.
REM**The program initially alters the co-ordinates to allow for the relief displacement
REM**(i.e the distortion of the image on the photograph due to the distance of the object
REM**away from the principal axis of the camera lens).

REM**Y,Z is the principle point
REM**YO(1),ZO(1) is the centre of the first image
REM**Y(1,1),Z(1,1) is the first node on the first image
REM**Y(2,1),Z(2,1) is the second node on the first image
REM**The coordinates for the successive images are similar but with the second array
REM**variable as 2,3 and 4.

REM**Dimension the arrays
DIM YO(4),ZO(4),Y(2,4),Z(2,4)

REM**Read in the data
FOR J%=1 TO 4
        READ YO(J%),ZO(J%)
                FOR I%=1 TO 2
                READ Y(I%,J%),Z(I%,J%)
        NEXT I%
NEXT J%
READ Y,Z,F
```

```
REM**Adjust the data to allow for the relief displacement
FOR I%=1 TO 2
        FOR J%=1 TO 4
        IF 4.536901-(Y(I%,J%)-YO(J%))^2-(Z(I%,J%)-ZO(J%))^2<0 THEN
        X(I%,J%)=0:GOTO 5
        X(I%,J%)=SQR(4.536901-(Y(I%,J%)-YO(J%))^2-(Z(I%,J%)-ZO(J%))^2)
5       R(I%,J%)=SQR((Y(I%,J%)-Y)^2+(Z(I%,J%)-Z)^2)
        D(I%,J%)=X(I%,J%)*R(I%,J%)*.0154
        YO(J%)=YO(J%)-Y:Y(I%,J%)=Y(I%,J%)-Y
        ZO(J%)=ZO(J%)-Z:Z(I%,J%)=Z(I%,J%)-Z
        K(I%,J%)=1-D(I%,J%)/R(I%,J%)
        Y(I%,J%)=Y(I%,J%)*K(I%,J%)
         Z(I%,J%)=Z(I%,J%)*K(I%,J%)
        Y(I%,J%)=Y(I%,J%)-YO(J%):Z(I%,J%)=Z(I%,J%)-ZO(J%)
        IF 4.536901-Y(I%,J%)^2-Z(I%,J%)^2<0 THEN X(I%,J%)=0:GOTO 6
        X(I%,J%)=SQR(4.536901-Y(I%,J%)^2-Z(I%,J%)^2)
6       NEXT J%
NEXT I%

REM**Modify cartesian coordinates to direction cosines
FOR J%=1 TO 4
        FOR I%=1 TO 2
        X(I%,J%)=X(I%,J%)/2.13
        Y(I%,J%)=Y(I%,J%)/2.13
        Z(I%,J%)=Z(I%,J%)/2.13
        NEXT I%
NEXT J%

REM**Calculate spin vector before impact
        IF Z(2,1)-Z(2,2) = 0 THEN A=1E+20:GOTO 10
        A=(Z(1,1)-Z(1,2))/(Z(2,1)-Z(2,2))
10      IF A*(Y(2,1)-Y(2,2))-Y(1,1)+Y(1,2)=0 THEN 20
        B=(X(1,1)-X(1,2)-A*(X(2,1)-X(2,2)))/(A*(Y(2,1)-Y(2,2))-Y(1,1)+Y(1,2))
        C=1+B*B+((X(1,1)-X(1,2)+B*(Y(1,1)-Y(1,2)))/(Z(1,2)-Z(1,1)))^2:GOTO 30
20      B=1E+20:C=1E+20
30      Xb=SQR(1/C)
        Yb=B*Xb
        Zb=SQR(1-(1+B*B)*Xb*Xb)

REM**Calculate rotation before impact
        ANGb=Xb*X(1,1)+Yb*Y(1,1)+Zb*Z(1,1)
        ANGb=-ATN(ANGb/SQR(-ANGb*ANGb+1))+1.570796
        R=4.26*SIN(ANGb)
        D=SQR((X(1,1)-X(1,2))^2+(Y(1,1)-Y(1,2))^2+(Z(1,1)-Z(1,2))^2)
        ROTb=D/R
        ROTb=2*ATN(ROTb/SQR(-ROTb*ROTb+1))

REM**Calculate spin vector after impact
        IF Z(2,3)-Z(2,4) = 0 THEN A=1E+20:GOTO 10
        A=(Z(1,3)-Z(1,4))/(Z(2,3)-Z(2,4))
10      IF A*(Y(2,3)-Y(2,4))-Y(1,3)+Y(1,4)=0 THEN 20
        B=(X(1,3)-X(1,4)-A*(X(2,3)-X(2,4)))/(A*(Y(2,3)-Y(2,4))-Y(1,3)+Y(1,4))
        C=1+B*B+((X(1,3)-X(1,4)+B*(Y(1,3)-Y(1,4)))/(Z(1,4)-Z(1,3)))^2:GOTO 30
20      B=1E+20:C=1E+20
30      Xa=SQR(1/C)
        Ya=B*Xa
        Za=SQR(1-(1+B*B)*Xa*Xa)

REM**Calculate rotation after impact
        ANGa=Xa*X(1,3)+Ya*Y(1,3)+Za*Z(1,3)
```

```
        ANGa=-ATN(ANGa/SQR(-ANGa*ANGa+1))+1.570796
        R=4.26*SIN(ANGa)
        D=SQR((X(1,3)-X(1,4))^2+(Y(1,3)-Y(1,4))^2+(Z(1,3)-Z(1,4))^2)
        ROTb=D/R
        ROTb=2*ATN(ROTb/SQR(-ROTb*ROTb+1))

REM**Output of data
PRINT "*****Before impact*****"
PRINT "Spin Vector is ";:PRINT USING "+#.##,";Xb;Yb;Zb
PRINT "ROTx = ";:PRINT USING "+###.##";ROTb*Xb*F;:PRINT" rad/s, ROTy
= ";:PRINT USING "+###.##"; ROTb*Yb*F;:PRINT" rad/s, ROTz = ";:PRINT
USING "+###.##";ROTb*Zb*F;:PRINT " rad/s."
PRINT "Total rotation is ";:PRINT USING "+###.##";ROTb*F;:PRINT " rad/s"

PRINT "*****After impact*****"
PRINT "Spin Vector is ";:PRINT USING "+#.##,";Xa;Ya;Za
PRINT "ROTx = ";:PRINT USING "+###.##";ROTa*Xa*F;:PRINT" rad/s, ROTy
= ";:PRINT USING "+###.##"; ROTa*Ya*F;:PRINT" rad/s, ROTz = ";:PRINT
USING "+###.##";ROTa*Za*F;:PRINT " rad/s."
PRINT "Total rotation is ";:PRINT USING "+###.##";ROTa*F;:PRINT " rad/s"

END
DATA 41.4,18.1
DATA 41.5,19.0
DATA 42.2,17.9
DATA 33.7,9.1
DATA 34.4,9.9
DATA 34.2,8.6
DATA 41.3,18.0
DATA 41.5,19.2
DATA 42.2,17.9
DATA 33.8,9.2
DATA 34.4,9.9
DATA 34.2,8.6
DATA 31.0,14.5,250
```

Appendix D - Data on the impacts of two-piece and wound golf balls

The following results were taken on a natural green at Austerfield Park. The *Poa annua* content of the green was 79%, the moisture content was 24%, the organic matter content was 12.2% and the percentage of fines in the soil was 48%.

D.1 Two-piece golf balls

VELOCITY (ms^{-1})		ANGLE (°)		SPIN ($rads^{-1}$)		DEPTH
initial	final	initial	final	initial	final	(mm)
16.8	6.2	45	36	0	264.9	
16.8	6.2	45	36	0	264.9	3.3
16.9	5.7	45	46	-86.8	226.3	3.3
17.1	5.9	45	43	-96.4	242.9	1.8
16.8	5.0	46	52	-223.0	199.5	1.5
16.5	5.2	45	51	-213.1	219.3	2.3
16.9	4.4	46	54	-322.3	191.3	4.1
16.9	4.4	45	59	-322.3	180.3	3.3
21.4	6.7	45	49	-8.8	282.6	4.8
21.9	7.2	45	45	0	304.7	4.1
21.8	6.6	45	52	-109.3	247.3	3.6
21.8	6.9	46	59	-110.4	235.5	6.6
21.7	6.9	45	52	-236.2	272.7	4.8
21.4	6.9	45	52	-234.0	272.7	2.8
20.9	5.6	47	57	-344.4	251.7	3.8
22.6	4.4	45	86	-464.7	150.8	5.1
23.1	5.1	45	67	-453.5	206.0	3.8
23.0	6.1	45	53	-580.8	87.1	2.8
23.2	4.9	45	70	-603.2	65.7	4.3
27.7	9.1	44	44	0	380.5	3.6
27.3	8.7	45	51	4.4	357.4	5.3
27.3	7.3	47	57	-107.2	335.1	5.9
25.8	5.8	50	65	-245.7	227.9	5.9
27.2	7.2	47	70	-464.7	287.4	5.3
26.6	7.0	48	62	-455.4	254.7	4.3
27.7	6.4	45	64	-580.8	254.7	6.6
27.2	5.9	43	72	-536.2	223.4	7.4
28.1	4.8	48	74	-641.2	178.7	5.3
27.5	4.7	47	69	-647.9	250.2	7.6
26.8	6.9	48	57	-223.4	272.6	4.8
25.0	5.9	47	64	-293.8	223.4	6.9
27.1	6.5	46	68	-227.9	245.7	7.6

TABLE D.1. A table showing the velocities, angles and spins before and after impact using a two-piece golf ball.

D.2 Wound golf balls

VELOCITY (ms^{-1})		ANGLE (°)		SPIN ($rads^{-1}$)		DEPTH
initial	final	initial	final	initial	final	(mm)
16.3	6.5	45	36	0	315.7	3.8
16.4	6.1	46	42	4.4	262.0	2.0
16.8	4.2	46	46	-93.8	242.9	4.8
16.9	5.9	45	46	-103.8	234.0	2.5
17.3	5.3	46	54	-213.4	192.1	3.8
16.8	5.3	45	48	-217.5	214.2	3.3
17	4.2	45	67	-317.9	160.1	2.8
21.4	7.3	45	42	4.4	251.7	4.8
21.7	6.8	45	50	0	234.0	4.1
21.0	7.3	45	46	-114.8	287.0	3.6
21.4	5.3	46	49	-110.4	259.2	6.4
21.5	6.0	45	58	-229.6	241.1	5.6
21.8	6.2	45	57	-249.5	244.2	6.1
21.4	5.7	45	61	-344.0	216.7	3.8
22.8	5.5	45	64	-451.3	212.7	2.8
22.6	5.7	45	62	-460.2	225.6	3.1
23.0	5.0	44	64	-577.5	196.6	3.8
23.5	5.3	45	69	-567.4	193.5	5.1
26.8	7.9	45	55	8.9	319.5	5.6
27.2	8.3	47	53	0	299.4	4.3
27.2	7.8	47	55	-105.0	299.4	5.6
27.2	7.6	47	59	-102.8	279.3	5.1
26.6	7.3	46	56	-230.1	294.9	7.6
27.7	8.2	45	54	-232.0	324.7	6.9
28.2	6.6	45	73	-440.1	227.9	7.1
28.4	6.6	45	70	-460.2	214.5	6.1
26.1	7.0	43	61	-558.5	252.4	6.1
27.3	5.7	45	71	-554.0	201.1	6.1
30.5	5.3	48	76	-638.9	175.7	6.6
26.5	8.0	46	53	-248.0	268.1	5.6
28.2	8.3	46	58	-234.6	308.3	5.9

TABLE D.2. A table showing the velocities, angles and spins before and after impact using a wound golf ball.

Appendix E - results of the photographs of impacts

TABLE E.1. A table containing the results from the 721 photographs of impacts. The subcsripts "i" and "f" denote the initial and final values respectively. Blank spaces occur where the variable was not measured.

	VELOCITY		ANGLE		SPIN		D
	ms^{-1}		degrees		$rads^{-1}$		mm
COURSE	i	f	i	f	i	f	
AUSTERFIELD	16.8	6.2	45	36	0	264.9	
AUSTERFIELD	16.8	6.2	45	36	0	264.9	3.3
AUSTERFIELD	16.9	5.7	45	46	-86.8	226.3	3.3
AUSTERFIELD	17.1	5.9	45	43	-96.4	242.9	1.8
AUSTERFIELD	16.8	5.0	46	52	-223.0	199.4	1.5
AUSTERFIELD	16.5	5.2	45	50	-213.1	219.3	3.8
AUSTERFIELD	16.9	4.4	46	54	-322.3	191.3	4.1
AUSTERFIELD	16.9	4.4	45	59	-322.3	180.3	3.3
AUSTERFIELD	21.4	6.7	45	49	-8.8	282.6	5.6
AUSTERFIELD	21.9	7.2	40	45	0	304.7	4.1
AUSTERFIELD	21.8	6.6	45	52	-109.3	247.3	3.6
AUSTERFIELD	21.8	6.9	46	59	-110.4	235.5	6.6
AUSTERFIELD	21.7	6.8	45	52	-236.2	272.7	4.8
AUSTERFIELD	21.4	6.9	45	52	-234.0	272.7	2.8
AUSTERFIELD	20.9	5.6	47	57	-344.4	251.7	3.8
AUSTERFIELD	22.6	4.4	45	86	-464.7	150.8	5.1
AUSTERFIELD	23.1	5.1	45	67	-453.5	206.0	3.8
AUSTERFIELD	23.0	6.1	45	53	-580.8	87.1	2.8
AUSTERFIELD	23.2	4.9	45	70	-603.2	65.7	4.3
AUSTERFIELD	27.7	9.1	44	44	0.0	380.5	3.6
AUSTERFIELD	27.3	8.7	45	51	4.5	357.4	5.3
AUSTERFIELD	27.4	7.3	47	57	-107.2	335.1	5.9
AUSTERFIELD	25.8	5.8	50	65	-245.7	227.9	5.9
AUSTERFIELD	27.2	7.2	47	70	-464.7	287.4	5.9
AUSTERFIELD	26.6	7.0	48	62	-455.7	254.7	4.3
AUSTERFIELD	27.7	6.4	45	64	-580.8	254.7	6.6
AUSTERFIELD	27.2	5.9	43	72	-536.2	223.4	7.4
AUSTERFIELD	28.1	4.8	48	74	-641.1	178.7	5.3
AUSTERFIELD	27.5	4.7	47	69	-647.9	250.2	7.6
AUSTERFIELD	26.8	6.9	48	57	-223.4	272.6	4.8
AUSTERFIELD	25	5.9	46	64	-293.8	223.4	6.9
AUSTERFIELD	27.1	6.5	46	68	-227.9	245.7	7.6
AUSTERFIELD	16.3	6.5	45	36	0	315.7	3.8
AUSTERFIELD	16.4	6.1	46	42	4.4	262.0	2.0
AUSTERFIELD	16.8	4.2	46	46	-93.8	242.9	4.8
AUSTERFIELD	16.9	5.8	45	46	-103.8	234.0	2.5
AUSTERFIELD	17.3	5.3	46	54	-213.4	192.1	3.8
AUSTERFIELD	16.8	5.3	45	48	-217.5	214.2	3.3
AUSTERFIELD	17.0	4.2	45	67	-317.9	160.1	2.8
AUSTERFIELD	21.4	7.3	45	41	4.4	251.7	4.8
AUSTERFIELD	21.6	6.8	45	50	0	234	4.1
AUSTERFIELD	21.0	7.3	45	46	-114.8	287	3.6
AUSTERFIELD	21.4	5.3	47	49	-110.4	259.2	6.4
AUSTERFIELD	21.5	6.0	45	58	-229.6	241.1	5.6
AUSTERFIELD	21.8	6.2	45	57	-249.5	244.2	6.1

	VELOCITY		ANGLE		SPIN		D
	ms^{-1}		degrees		$rads^{-1}$		mm
AUSTERFIELD	20.9	5.6	47	57	-344.4	251.7	3.8
AUSTERFIELD	22.8	5.5	45	64	-451.3	212.7	2.8
AUSTERFIELD	22.6	5.7	45	62	-460.2	225.6	3.1
AUSTERFIELD	23.0	5.0	44	64	-577.5	196.6	3.8
AUSTERFIELD	23.5	5.3	45	69	-567.4	193.5	5.1
AUSTERFIELD	26.8	7.9	45	55	8.9	319.4	5.6
AUSTERFIELD	27.2	8.3	47	53	0	299.4	4.3
AUSTERFIELD	27.2	7.8	47	55	-105	299.4	5.6
AUSTERFIELD	27.2	7.6	47	60	-102.8	279.2	5.1
AUSTERFIELD	26.6	7.3	46	56	-230.1	294.9	7.6
AUSTERFIELD	27.7	8.2	45	54	-232	324.7	6.9
AUSTERFIELD	28.2	6.6	45	73	-440.1	227.9	7.1
AUSTERFIELD	28.4	6.6	45	70	-460.2	214.5	6.1
AUSTERFIELD	26.1	7.0	43	61	-558.5	252.4	6.1
AUSTERFIELD	27.3	5.7	45	71	-554	201.1	6.1
AUSTERFIELD	30.5	5.3	48	76	-638.9	175.7	6.6
AUSTERFIELD	26.5	8	46	53	-248	268.1	5.6
AUSTERFIELD	28.1	8.3	46	58	-234.6	308.3	5.9
BELFRY	26.7	9.6	34	40	0	402.1	2.3
BELFRY	26.2	9.8	35	38	0	430.0	1.9
BELFRY	26.9	8.2	35	42	-111.7	390.9	2.4
BELFRY	26.7	9.6	34	37	-122.9	379.8	2.3
BELFRY	26.4		35		-122.9		2.3
BELFRY	28.4	11.1	31	33	-240.2	128.4	2.3
BELFRY	27.6	8.4	35	40	-223.4	229	2.5
BELFRY	26.2	10.9	35	32	-363.0	8.4	2.5
BELFRY	27.3	11.2	35	31	-363.0	27.9	2.1
BELFRY	27.2	11.7	34	29	-402.1	-39.1	2.0
BELFRY	26.9	9.6	35	40	-446.8	-44.7	2.8
BELFRY	28.8	10.8	35	37	-485.9	-100.5	1.9
BELFRY	26.9	9.1	35	39	-502.6	-111.7	2.2
BELFRY	29.2	8.2	35	48	-552.9	-128.4	3.2
BELFRY	27.9	10.9	37	32	-519.4	-223.3	2.5
BELFRY	30.7	9.4	34	35	-586.4		2.3
BELFRY		7.9		47	-603.2	-231.8	2.9
BELFRY	28.4	9.6	37	42	-776.3	-307.1	2.5
BELFRY	28.1	10.2	37	39	-647.9	-312.8	2.2
BELFRY	21.1	9.1	36	32	0	229.0	2.0
BELFRY	20.4	7.6	35	33	-11.7	312.8	2.0
BELFRY	22.0	7.2	36	49	-128.4	307.2	1.4
BELFRY	22.7	9.2	35	36	0	374.2	2.0
BELFRY	22.8	8.1	34	38	-251.3	147	1.4
BELFRY	23.0	8.0	35	43	-240.2	122.9	2.0
BELFRY	22.1	9.2	34	29	-323.9	-61.4	1.1
BELFRY	20.8	8.5	37	32	-296	117.3	1.1
BELFRY	21.7	8.1	34	37	-446.8	-60.0	2.3
BELFRY	23.1		34		-452.4	-5.6	1.8
BELFRY	22.3	8.0	35	39	-430	-41.9	
BELFRY	23.1	8.9	36	37	-558.5	-145.2	
BELFRY	21.1	8.1	32	38	-642.3	-203.8	2.2
BELFRY	21.5	8.2	37	39	-569.7	156.4	1.9
BELFRY	16.3	6.7	36	34	5.6	335.1	.6
BELFRY	16.7	7.4	36	30	0	301.6	1.0

	VELOCITY		ANGLE		SPIN		D
	ms^{-1}		degrees		$rads^{-1}$		mm
BELFRY	16.5	6.6	36	39	0	329.5	.8
BELFRY	17.3	6.1	36	41	-111.7	284.8	2.0
BELFRY	16.5	5.7	36	41	-111.7	301.6	1.9
BELFRY	16.8	6.7	36	35	-111.7	321.1	.9
BELFRY	17.4	5.8	36	41	-223.4	279.2	1.2
BELFRY	17.7	5.9	35	37	-212.2	223.4	1.5
BELFRY	17.0	6.0	36	37	-217.8	310.0	1.6
BELFRY	16.3	5.0	36	45	-318.3	270.9	1.6
BELFRY	16.4	5.7	37	44	-329.5	78.2	1.0
BELFRY	17.0	5.3	36	46	-335.1	175.9	1.5
BELFRY	17.0	5.1	44	40	0	258.9	1.0
BELFRY	17.5	3.6	46	67	-322.0	112.5	2.8
BELFRY	17.8		44		-333.2	166.6	2.5
BELFRY	22.4	6.1	45	45	0	283.7	1.1
BELFRY	23.2	5.8	44	46	-4.5	263.4	2.6
BELFRY	22.8	5.5	45	49	-585.4	-186.8	2.5
BELFRY	22.8	4.5	45	59	-585.4	-177.9	2.5
BELFRY	27.8	5.4	43	59	-4.5	252.2	3.5
BELFRY	26.4	3.8	45	70	-639.4	-216.1	3.5
BELFRY	27.6	3.9	45	67	-639.4	-186.9	3.5
BELFRY	27.8	10.5	35	32	6.3	413.3	2.2
BELFRY	23	8.7	35	35	-117.3	279.2	1.4
BELFRY	21.9	6.0	33	54	-335.1	284.8	2.1
BINGLEY	12.0	5.3	46	38	-10.5	222.5	
BINGLEY	12.1	5.3	44	38	-7.8	243.5	
BINGLEY	12.5	5.5	45	38	-5.2	227.8	
BINGLEY	11.2	5.6	44	34	5.2	209.4	
BINGLEY	11.2	5.6	45	36	-7.8	246.1	
BINGLEY	12.0	4.6	44	38	-130.9	214.7	
BINGLEY	12.2	4.5	44	41	-130.9	191.1	
BINGLEY	12.0	5.1	46	38	-130.9	199.0	
BINGLEY	12.1	4.8	45	38	-125.7	206.8	
BINGLEY	12.7	6.0	45	48	-204.2	185.9	
BINGLEY	12.4	4.2	45	49	-214.7	170.2	
BINGLEY	12.9	4.6	45	44	-219.2	185.9	
BINGLEY	12.4	4.9	45	38	-217.3	209.4	
BINGLEY	16.4	6.1	45	44	-3.5	286.2	
BINGLEY	16.6	6.6	44	38	-3.5	286.2	
BINGLEY	17.0	7.9	45	36	3.5	300.2	
BINGLEY	16.6	6.9	45	36	-10.5	296.7	
BINGLEY	17.0	6.9	45	36	-10.5	296.7	
BINGLEY	17.1	7.0	44	39	-118.7	279.2	
BINGLEY	16.6	6.2	44	45	-101.2	254.8	
BINGLEY	17.1	7.0	45	40	-219.9	268.8	
BINGLEY	17.3	5.5	44	46	-226.9	240.8	
BINGLEY	16.4	5.8	46	43	-223.4	244.3	
BINGLEY	16.8	5.5	43	33	-205.1	268.8	
BINGLEY	23.0	8.5	43	43	-32.4	344.7	
BINGLEY	21.1	6.4	43	51	0	270.5	
BINGLEY	21.1	7.8	43	37	0	410.1	
BINGLEY	22.1	8.2	44	40	-17.4	336.0	
BINGLEY	21.9	8.6	43	38	13.1	384.0	
BINGLEY	20.9	7.6	42	44	-117.8	318.5	

	VELOCITY		ANGLE		SPIN		D
	ms^{-1}		degrees		$rads^{-1}$		mm
BINGLEY	22.5	7.4	41	48	-122.2	305.4	
BINGLEY	21.4	7.1	45	51	-113.5	292.3	
BINGLEY	22.5	8.2	43	40	-117.8	331.6	
BINGLEY	21.6	6.0	42	52	-240.0	274.9	
BINGLEY	22.1	7.4	44	45	-240.0	279.2	
BINGLEY	22.1	6.8	43	54	-240.0	253.1	
BINGLEY	21.6	6.2	43	53	-239.8	292.3	
CREWE	18.1	8.5	37	33	0	347.1	1.2
CREWE	15.9	7.3	36	36	0	311.5	
CREWE	16.8	7.0	36	33	-284.8	111.3	1.2
CREWE	17.0	6.0	36	43	-320.4	173.6	2.1
CREWE	21.9	8.9	36	39	0	391.6	1.7
CREWE	22.6	7.9	36	45	0	338.2	2.3
CREWE	21.9	6.7	36	50	-329.3	267.0	1.8
CREWE	22.5	7.4	35	41	-333.8	311.5	1.0
CREWE	21.9	6.0	39	57	-338.2	235.9	1.7
CREWE	22.6	6.1	40	53		148.2	1.8
CREWE	21.9	6.9	39	42	-600.8	49.0	2.0
CREWE	22.7	6.6	39	47	-534.1	74.1	1.9
CREWE	28.6	9.6	37	42	-4.5	400.5	2.2
CREWE	27.1	8.7	37	45	-8.9	356.0	2.6
CREWE		6.2		64		278.2	
CREWE		6.2		62		278.2	3.6
CREWE		7.2		56		5.6	2.9
CREWE	17.2	6.1	45	44	0	305	1.3
CREWE	17.6	6.7	45	40	0	327.4	1.7
CREWE	18.8	5.8	45	45	-322.9	219.8	1.0
CREWE	18.3	5.3	44	49	-336.4	208.6	1.0
CREWE	18.6	5.5	46	46	-314	226.5	1.1
CREWE	23.3	7.8	44	38	4.5	340.9	1.7
CREWE	21.6	7.2	45	44	0	331.9	1.7
CREWE	23.3	8.6	45	41	13.5	336.4	
CREWE	23.4	5.8	46	59	-354.4	228.8	2.0
CREWE	23.3	5.3	46	65	-372.3	201.8	1.9
CREWE	23.4	5.8	46	59	-354.3	228.8	2.0
CREWE	23.3	5.3	46	65	-372.3	201.8	1.9
CREWE	23.5	5.2	47	58	-569.6	82.5	1.9
CREWE	24.0	5.9	46	65	-569.6	32.9	2.1
CREWE	22.6	4.7	51	65	-565.2	74.0	0
CREWE	28.0	8.2	46	45	0	340.9	2.4
CREWE	27.3	7.5	46	56	9	297.2	3.2
CREWE	28.0	5.9	46	63	-345.4	242.2	2.7
CREWE	28.0	6.0	46	62	-345.4	219.8	2.8
CREWE	28.0	5.3	46	70	-345.4	213.0	3.6
CREWE	27.8	6.0	47	64	-619	9.0	3.5
CREWE	28.5	5.6	45	63	-650.4	168.2	2.3
CREWE	28.2	5.3	45	63	-547.2	94.2	3.1
CREWE	17.0	5.1	53	50	0	215.3	1.4
CREWE	16.5	5.0	56	53	0	213.1	2.1
CREWE	17.1	5.4	53	49	0	213.1	1.2
CREWE	18.0	4.1	54	61	-314	161.5	1.7
CREWE	17.6	3.8	54	67	-331.9	143.5	2.2
CREWE	18.3	4.2	53	62	-322.9	152.5	2.0

	VELOCITY		ANGLE		SPIN		D
	ms^{-1}		degrees		$rads^{-1}$		mm
CREWE	23.7	6	56	52	4.5	255.9	1.5
CREWE	21.2	5.4	54	54	9.0	224.3	2.1
CREWE	22.6	6.7	54	55	4.5	231.0	2.5
CREWE	22.5	4.2	54	70	-345.4	160.0	2.2
CREWE	23.4	3.3	57	77	-578.6	105.4	2.2
CREWE	22.4	3.4	57	82	-560.7	100.9	3.0
CREWE	23.1	4.4	58	85	-583.1	98.7	2.6
CREWE	27.2	5.3	56	60	-9	211.7	3.3
CREWE	27.6	5.6	56	64	0.0	204.1	3.1
CREWE	26.5	4.9	56	67	0.0	197.4	3.3
CREWE	27.3	4.8	55	75	-345.4	166.0	2.9
CREWE	27.9	4.5	55	72	-354.4	103.1	3.3
CREWE	26.7	4.5	56	74	-345.4	130.1	3.4
CREWE	28.4	3.8	55	88	-538.2	154.7	3.2
CREWE	26.9	4.0	52	77	-654.9	148.0	2.6
CREWE	27.7	3.6	52	86	-628	100.9	3.2
FORMBY	12.4	5.4	45	40	-5.3	195.0	
FORMBY	13.1	5.5	45	42	2.6	195.0	
FORMBY	12.5	4.9	47	43	5.3	231.9	
FORMBY	12.6	5.1	45	40	-2.6	224.0	
FORMBY	12.6	5.0	44	41	-2.6	237.2	
FORMBY	12.5	4.4	45	46	-121.2	179.2	
FORMBY	11.8	4.3	45	45	-121.2	173.9	
FORMBY	12.6	4.7	44	42	-116	187.1	
FORMBY	11.9	4.5	48	45	-123.9	200.3	
FORMBY	13.0	4.1	42	48	-105.4	166.0	
FORMBY	12.9	4.7	45	45	-197.7	181.8	
FORMBY	13.1	4.7	45	48	-200.9	168.7	
FORMBY	12.5	4.2	45	49	-205.6	150.2	
FORMBY	13.0	5.8	45	57	-195	166.0	
FORMBY	16.4	7.0	42	35	-2.6		
FORMBY	17.1	7.0	42	41			
FORMBY	16.0	6.6	44	37	-2.6	242.5	
FORMBY	16.4	6.8	44	37	-5.3	260.9	
FORMBY	17.3	6.4	43	31	-105.4		
FORMBY	17.1	7	42				
FORMBY	17.1	6.3	44	42	-110.7	218.7	
FORMBY	17.2	6.4	45	41	-97.5	266.2	
FORMBY	16.4	5.9	44	44	-105.4	258.3	
FORMBY	17.1	5.7	45	46	-216.1	229.3	
FORMBY	17.1	5.7	44	44	-216.1	237.2	
FORMBY	17.5	5.7	44	48	-229.3	221.4	
FORMBY	22.4	7.2	44	44	14.0	335.1	
FORMBY	22.9	7.6	44	45	0	310.7	
FORMBY	23.3	7.9	45	43	-10.5	321.1	
FORMBY	22.7	7.1	41	45	-108.2	307.2	
FORMBY	22.7	7.4	44	43	-122.2	300.2	
FORMBY	23.3	7.9	43	43	-111.7	300.2	
FORMBY	22.7	6.0	42	53	-237.4	233.9	
FORMBY	21.8	6.7	44	49	-233.9	275.8	
FORMBY	21.8	6.7	44	51	-226.9	268.8	
FORMBY	35.4	9.0	44	49	0	350.5	
FORMBY	32.1	7.7	44	47	-16.2	404.5	

	VELOCITY		ANGLE		SPIN		D
	ms^{-1}		degrees		$rads^{-1}$		mm
FORMBY	32.4	8.8	43	55	-5.4	350.5	
FORMBY	31.9	6.8	44	60	-701.1	37.8	
FORMBY	31.2	5.6	44	71	-749.6	140.2	
GANTON	17.5	6.4	44	41	0	277	3.8
GANTON	17.7	5.8	45	41	0	245.7	3.1
GANTON	17.6	6.9	45	38	0	339.6	2.5
GANTON	17.1	6	45	36	-102.8	259.1	2.3
GANTON	17.4	6.3	46	39	-89.4	268.1	2.0
GANTON	17.7	6.4	45	37	-205.5	259.1	1.8
GANTON	22.0	8.1	44	39			3.1
GANTON	22.3	6.8	45	46	-107.2	290.4	3.1
GANTON	21.7	6.6	43	47	-107.2	292.6	4.3
GANTON	22.5	6.5	43	49	-216.7	308.3	
GANTON	22.1	7.3	44	40	-232.3	277.0	4.3
GANTON	22.2	6.8	44	46	-214.5	296.4	1.8
GANTON	22.6	5.9	43	52	-328.4	247.5	4.1
GANTON	22.0	5.9	44	48	-326.2	249.5	4.3
GANTON	22.6	7.5	44	43	-458.0	107.2	3.1
GANTON	21.7	7.6	43	40	-428.9	134.0	2.5
GANTON	22.7	7.6	43	43	-437.9	147.4	2.5
GANTON	22.8	7.5	43	44	-536.2	-37.4	2.3
GANTON	22.4	8	44	38	-567.4	-69.2	3.3
GANTON	26.9	9.1	42	39	0	402.3	3.3
GANTON	27.5	8.8	45	39	0	402.3	3.1
GANTON	26.7	7.9	43	45	-99.5	325.5	5.3
GANTON	28.5	8.3	44	44	-106.2	330	4.1
GANTON	27.1	7.3	45	50	-221.5	305.1	3.8
GANTON	27.5	5.7	44	63	-212.5	230.5	7.4
GANTON	26.4	7.1	45	48	-203.4	311.9	5.1
GANTON	27.5	7.3	44	48	-198.9	316.4	4.1
GANTON	26.7	6.6	45	51	-348.1	262.2	4.8
GANTON	28.4	7.1	45	52	-339.0	297.8	4.6
GANTON	27.7	7.3	44	54	-452.0	230.5	5.1
GANTON	27.8	7.8	44	44	-565.0	103.9	2.5
GANTON	28.0	5.7	44	61	-551.5	212.4	5.9
GANTON	28.2	5.5	44	63	-560.5	212.4	5.4
GANTON	17.5	6.3	45	40	-98.3		2.5
GANTON	17.7	6.5	45	40	-218.9	245.7	2.5
GANTON	17.7	5.0	45	50	-326.2	234.6	2.3
GANTON	17.6	5.2	45	47	-328.4	234.6	2.0
GANTON	21.8	7.2	44	44	-116.2	254.7	3.3
GANTON	27.0	8.5	45	48	-90.4	346.9	3.1
GANTON	28.4	8.0	43	43	-488.2	219.2	4.1
GANTON	26.9	6.6	45	51			3.8
GANTON	26.9	6.2	45	54	-664.5	-78.5	
GANTON	27.5	8.2	44	42	-678.1	-88.2	4.1
GANTON	25.9	5.9	44	55	-650.9	-59.3	4.6
GANTON	25.5	6.0	44	54	-650.9	-35.3	
HALLOWES	18.4	7.5	46	42	0	268.3	
HALLOWES	18.5	7.6	46	37	-22.0	307.9	
HALLOWES	18.2	7.1	46	37	0	285.9	
HALLOWES	17.9	6.7	46	43	4.4	268.3	
HALLOWES	17.9	6.7	48	37	-105.6	285.9	

	VELOCITY		ANGLE		SPIN		D
	ms^{-1}		degrees		$rads^{-1}$		mm
HALLOWES	17.6	6.2	46	43	-118.8	255.1	
HALLOWES	18.2	7	46	44	-110	263.9	4.7
HALLOWES	18.2	6.5	46	51	-110	263.9	
HALLOWES	18.2	6.6	46	43	-241.9	255.1	
HALLOWES	18.4	5.9	47	47	-228.7	241.9	
HALLOWES	17.5	5.9	46	47	-285.9	228.7	4.6
HALLOWES	25.5	8.2	48	45	54.8	338.7	
HALLOWES	23.0	7.3	46	49	0	272.7	5.1
HALLOWES	22.3	8.2	46	43	8.8	343.1	
HALLOWES	22.4	7.5	47	42	-96.8	316.7	
HALLOWES	21.8	7.0	47	49	-110	285.9	3.6
HALLOWES	21.4	7.3	45	48	-114.3	263.9	
HALLOWES	22.6	6.7	44	44	-246.3	307.9	2.8
HALLOWES	22.0	6.8	47	45	-250.7	303.5	2.5
HALLOWES	21.9	7.3	45	41	-241.9	329.9	
HALLOWES	28.8	11.0	45	50	-5.7	369.8	4.1
HALLOWES	26.9		43				
HALLOWES	26.7		44				
HILL VALLEY	17.2	7.6	36	37	0	340	1.7
HILL VALLEY	16.9	7.9	36	33	0	0	.9
HILL VALLEY	17.4	7.7	36	34	0	317.9	1.3
HILL VALLEY	17.8	7.9	36	36	-335.6	66.2	.6
HILL VALLEY	17.0	7.8	36	36	-313.5	66.2	.7
HILL VALLEY	17.3	7.8	34	36	-313.5	66.2	1.0
HILL VALLEY	22.2	9.6	35	34	4.4	434.9	.5
HILL VALLEY	20.5	8.7	35	36	8.8	379.7	1.1
HILL VALLEY	22.3	10.3	35	32	0	379.7	1.3
HILL VALLEY	21.8	9.2	35	32	-322.3	220.8	1.0
HILL VALLEY	22.5	9.3	35	33	-326.8	163.4	.9
HILL VALLEY	21.9	8.4	34	38	-331.2	198.7	1.1
HILL VALLEY	22.2	8.8	35	38	-538.7	-159	1.6
HILL VALLEY	22.2	8.3	35	33	-547.5	0	1.3
HILL VALLEY	22.3	9.2	35	37	-552	-70.6	
HILL VALLEY	22.4	8.9	37	35	-543.1	-105.9	1.4
HILL VALLEY	26.0	10.9	34	28	0	538.7	2.0
HILL VALLEY	26.6	10.6	34	37	70.7	463.6	1.5
HILL VALLEY	26.7	9.3	35	45	35.3	410.6	2.3
HILL VALLEY	27.3	8.5	34	46	-335.6	335.6	1.6
HILL VALLEY	26.1	7.0	36	57	-335.6	269.4	2.7
HILL VALLEY		6.7		54		331.2	2.2
HILL VALLEY		7.6		47		344.4	2.6
HILL VALLEY	25.6	8.5	35	48	-631.4	4.4	1.9
HILL VALLEY		8.6		50		22.1	1.5
HILL VALLEY		9.4		43		-103.8	2.5
HILL VALLEY	17.4	6.5	46	46	0	273.8	.6
HILL VALLEY	17.0	6.7	46	41	0	295.9	.5
HILL VALLEY	17.6	6.8	45	43	4.4	264	.9
HILL VALLEY	17.5	5.6	44	48	-344.4	141.2	1.3
HILL VALLEY	22.8	5.9	45	56	0	238.4	.9
HILL VALLEY	22.9	5.0	49	61	-547.5	53.0	
HILL VALLEY	21.4	7.2	45	49	0	295.8	1.7
HILL VALLEY	22.0	5.2	46	58	-340	181.0	2.1
HILL VALLEY	22.4	5.7	47	52	-348.8	220.8	2.4

	VELOCITY		ANGLE		SPIN		D
	ms^{-1}		degrees		$rads^{-1}$		mm
HILL VALLEY	27.2	4.8	47	72	-340	198.7	2.4
HILL VALLEY	26.9	4.6	45	80	-348.8	172.2	2.8
KEIGHLEY	16.4	6.0	47	42	8.7	274.9	
KEIGHLEY	17.7	6.0	47	45	13.1	244.3	
KEIGHLEY	16.8	5.8	47	47	0	183.3	
KEIGHLEY	16.4	5.3	46	53	13.1	187.6	
KEIGHLEY	17.2	5.7	48	49	-100.3	222.5	
KEIGHLEY	18.0	6.5	46	43	-96.0	270.5	
KEIGHLEY	17.1	6.0	46	45	-96.0	248.7	
KEIGHLEY	16.8	5.3	46	53	-104.7	213.8	
KEIGHLEY	17.3	6.0	45	42	-91.6	226.9	
KEIGHLEY	16.3	4.6	46	55	-235.6	200.7	
KEIGHLEY	17.0	6.2	45	43	-226.9	104.7	
KEIGHLEY	13.8	5.7	46	45	-122.2	213.8	
KEIGHLEY	17.7	6.4	46	45	-436.3	21.8	
KEIGHLEY	17.8	7.2	45	43	-445.1	4.4	
KEIGHLEY	24.4	7.3	47	46	4.4	307.9	
KEIGHLEY	24.8	7.3	45	46	13.2	316.7	
KEIGHLEY	24.8	6.7	46	53	13.2	281.5	
KEIGHLEY	25.7	5.4	46	79	-144.3	180.3	
KEIGHLEY	25.1	6.9	45	54	-110	241.9	
KEIGHLEY	24.2	6.5	46	54	-118.8	255.1	
KEIGHLEY	24.8	6.0	46	57	-219.9	255.1	
KEIGHLEY	24.1	5.6	47	63	-224.3	219.9	
KEIGHLEY	24.2	5.0	43	72	-118.8	197.9	
KEIGHLEY	32.8	6.5	45	63	0	314.7	
KEIGHLEY	32.3	6.5	46	70	0	230.4	
KEIGHLEY	32.3	7.8	46	52	11.2	325.9	
KEIGHLEY	33.2	8.4	45	43	-5.6	151.7	
KEIGHLEY	34.6	5.4	44	73	-101.2	207.9	
KEIGHLEY	32.8	5.2	45	83	-140.5	174.2	
KEIGHLEY	34.8	4.5	45	90	-95.5	179.8	
KEIGHLEY	31.4	4.2	46	90	-224.8	151.7	
KEIGHLEY	35.5	5.7	46	74	-224.8	179.8	
KEIGHLEY	32.8	6.1	44	72	-213.6	196.7	
KEIGHLEY	32.6	4.2	45	90	-573.2	129.3	
KEIGHLEY	32.8	2.8	46	111	-590.1	134.9	
KEIGHLEY	32.8	2.1	45	116	-578.9	45.0	
KEIGHLEY	27.1	3.2	45	84	-578.9	123.6	
LINDRICK	16.7	6.6	45	36	0	263.6	2.5
LINDRICK	16.7	6.7	45	40	0	299.4	2.3
LINDRICK	17.0	6.3	45	42	4.5	270.3	2.3
LINDRICK	17.2	5.7	45	48	-116.2	241.3	3.3
LINDRICK	17.4	6.3	46	42	-107.2	256.9	2.3
LINDRICK	17.6	6.2	45	43	-100.5	248.7	2.8
LINDRICK	16.6	6.4	45	38	-111.7	268.1	1.5
LINDRICK	16.9	5.8	48	45	-214.5	250.2	2.8
LINDRICK	17.3	6.0	45	42	-218.9	236.8	2.8
LINDRICK	17.3	6.0	45	42	-218.9	236.8	2.8
LINDRICK	17.6	5.9	45	44	-216.7	245.7	2.5
LINDRICK	17.6	4.4	47	59	-323.9	172.0	4.1
LINDRICK	17.8	5.2	46	51	-319.5	210.0	3.3
LINDRICK	16.8	5.0	46	45	-330.6	225.6	4.1

	VELOCITY		ANGLE		SPIN		D
	ms^{-1}		degrees		$rads^{-1}$		mm
LINDRICK	21.4	7.8	45	38	0	294.9	3.3
LINDRICK	22.5	7.2	46	41	-4.5	290.4	3.8
LINDRICK	22.3	6.2	48	50	-4.5	259.1	4.8
LINDRICK	21.8	6.6	45	49	-98.3	254.7	4.8
LINDRICK	21.7	6.2	46	49	-120.6	256.5	4.3
LINDRICK	21.1	6.9	45	40	-116.2	306.1	4.3
LINDRICK	21.4	6.0	45	48	-245.7	256.9	4.6
LINDRICK	22.8	4.2	46	80	-227.9	134.0	
LINDRICK	21.9	6.2	45	51	-241.3	239.0	4.1
LINDRICK	22.4	6.6	45	46	-223.4	268.1	5.1
LINDRICK	22.6	6.1	45	50	-330.6	254.7	3.3
LINDRICK	21.6	5.8	46	56	-326.2	218.9	3.8
LINDRICK	22.1	6.0	46	51	-326.2	252.4	3.1
LINDRICK	22.6	5.1	45	58	-460.2	198.8	4.6
LINDRICK	23.2	6.6	47	49		89.3	4.3
LINDRICK	22.3	5.5	45	54	-460.2	239.0	3.8
LINDRICK	23.0	5.1	47	57	-558.5	147.4	6.1
LINDRICK	22.4	5.5	46	55	-569.7	138.5	5.6
LINDRICK	22.6	4.7	47	59	-563	126.6	5.6
M. ALLERTON	16.8	5.0	44	49	224.3		
M. ALLERTON	16.2	5.2	44	47	0	224.3	
M. ALLERTON	17.3	5.5	46	43	4.4	237.5	
M. ALLERTON	17.8	5.3	44	45	-92.4	219.9	
M. ALLERTON	17.3	4.8	46	47	-92.4	228.7	
M. ALLERTON	17.5	5.6	43	36	-96.8	268.3	
M. ALLERTON	17.5	5.2	44	47	-118.8	206.7	
M. ALLERTON	17.8	4.7	46	49	-189.1	193.5	
M. ALLERTON	18.4	4.3	44	48	-219.9	171.5	
M. ALLERTON	17.3	4.8	44	47	-211.1	215.5	
M. ALLERTON	21.7	5.7	44	49	4.4	193.5	
M. ALLERTON	23.4	4.8	44	43	0	215.5	
M. ALLERTON	21.9	5.5	42	56	8.8	224.3	
M. ALLERTON	23.0	5.5	44	51	-96.8	193.5	
M. ALLERTON	21.9	5.3	44	58	-118.8	211.1	
M. ALLERTON	23.7	4.3	42	57	-118.8	184.7	
M. ALLERTON	21.9	3.5	43	82	-200.7	174.5	
M. ALLERTON	23.5	4.7	46	65	-205.1	178.9	
M. ALLERTON	22.7	4.7	43	58	-222.5	196.3	
M. ALLERTON	27.4	4.7	42	72	13.1	222.5	
M. ALLERTON	28.5	5.5	45	66	0	183.3	
M. ALLERTON	27.6	3.5	43	90	0	152.7	
M. ALLERTON	27.1	4.7	44	72	-109.1	218.2	
M. ALLERTON	27.6	4.8	42	81	-109.1	174.5	
M. ALLERTON	28.3	7.1	44	82	-231.2		
M. ALLERTON	27.1	5.9	45	70	-240	196.3	
M. ALLERTON	27.8	4.3	44	83	-218.2	178.9	
M. ALLERTON	28.3	2.6	43	107	-375.2	96	
M. ALLERTON	29.2	3.1	45	83	-375.2	144	
M. ALLERTON	26.7	2.8	48	117	-370.9	56.7	
M. ALLERTON	27.8	2.0	45	120	-449.4	100.3	
M. ALLERTON	27.9	2.8	44	95	-480	122.2	
M. ALLERTON	27.9	2.1	44	112	-488.7	82.9	
M. ALLERTON	27.6	3.1	45	104	-558.5	126.5	

	VELOCITY		ANGLE		SPIN		D
	ms^{-1}		degrees		$rads^{-1}$		mm
M. ALLERTON	27.6	4.6	44	68	-584.7	174.5	
M. ALLERTON	26.9	4.0	46	83	-545.4	157.1	
MOOR HALL	16.9	6.1	44	42	0	264.0	2.5
MOOR HALL	17.7	6.2	44	46	8.7	257.4	2.0
MOOR HALL	17.1	6.5	45	41	6.5	261.8	2.5
MOOR HALL	17.2	5.5	45	46	-101.4	243.3	2.8
MOOR HALL	17.6	5.5	46	47	-97.1	231.3	4.1
MOOR HALL	17.9	5.9	44	44	-96	240.0	2.0
MOOR HALL	17.6	5.2	45	51	-196.3	202.9	2.5
MOOR HALL	17.5	5.3	45	54	-197.4	203.6	3.8
MOOR HALL	17.4	4.7	44	53	-312.7	196.3	3.8
MOOR HALL	17.3	4.4	45	57	-309.8	176.7	3.8
MOOR HALL	17.1	4.8	44	51	-314.2	199.8	3.1
MOOR HALL	22.5	6.7	44	49	-4.4	285.8	5.9
MOOR HALL	22.1	7.5	44	45	8.7	281.4	2.5
MOOR HALL	22.1	6.3	43	49	-104.7	266.2	5.1
MOOR HALL	21.8	6.3	43	51	-104.7	253.1	4.6
MOOR HALL	21.6	6.8	44	47	-109.1	292.3	4.1
MOOR HALL	21.8	6.0	44	52	-240	244.3	5.6
MOOR HALL	21.9	6.7	42	44	-222.5	277.1	4.3
MOOR HALL	22.1	7.1	43	42	-248.7	296.7	4.3
MOOR HALL	21.9	5.8	45	54	-229.1	226.9	4.6
MOOR HALL	23.1	5.3	44	60	-314.2	205.1	
MOOR HALL	21.7	5.9	45	48	-331.6	261.8	2.8
MOOR HALL	22.5	4.9	48	61	-427.6	202.1	4.8
MOOR HALL	21.7	4.5	45	66	-421.1	174.5	3.8
MOOR HALL	22.3	4.6	45	63	-432	183.3	4.3
MOOR HALL	23.3	4.4	45	69	-514.9	152.7	5.3
MOOR HALL	23.4	4.0	48	72	-545.4	196.3	5.9
MOOR HALL	23.5	5.1	45	58	-536.7	196.3	4.6
MOOR HALL	27.9	8.2	45	43	0	314.2	5.1
MOOR HALL	27.2	6.8	45	56	0	261.8	5.9
MOOR HALL	27.8	7.5	43	54	0	301.1	7.9
MOOR HALL	26.7	5.9	45	63	-78.5	253.1	6.9
MOOR HALL	26.7	6.6	44	56	-96.0	283.5	8.1
MOOR HALL	27.9	5.8	44	56	-122.2	270.5	7.1
MOOR HALL	26.9	6.0	44	62	-202.9	244.3	6.6
MOOR HALL	26.0	5.3	45	62	-213.8	240.0	6.1
MOOR HALL	26.7	5.4	45	70	-226.9	207.3	7.1
MOOR HALL	27.4	4.9	45	74	-340.3	181.1	7.6
MOOR HALL	26.9	4.4	45	74	-322.9	165.8	7.6
MOOR HALL	27.2	5.3	44	66	-340.3	178.9	6.4
MOOR HALL	27.2	5.4	44	72	-449.4	200.7	6.9
MOOR HALL	27.0	4.1	45	79	-445.1	163.6	8.9
MOOR HALL	27.6	4.5	45	75	-449.4	167.2	6.9
MOOR HALL	26.9	3.1	44	96	-530.1	123.3	8.1
MOOR HALL	27.0	3.5	45	90	-541.0	128.0	9.4
MOOR HALL	27.6	5	45	61	-558.5	174.5	
MOOR HALL	27.9	4.1	45	83	-593.4	144.0	8.9
MOOR HALL	17.6	4.3	46	47	-198.5	224.7	2.5
MOOR HALL	26.9	3.5	46	81	-645.8	132.3	8.1
MOOR HALL	27.9	4	45	76		52.4	7.6
MOORTOWN	17.0	6.7	46	44	24.1	281.8	

	VELOCITY		ANGLE		SPIN		D
	ms^{-1}		degrees		$rads^{-1}$		mm
MOORTOWN	16.4	6.8	45	39	21.9	291.3	
MOORTOWN	16.8	5.9	47	43	10.9	280.4	
MOORTOWN	16.3	6.7	46	43	32.9	302.3	
MOORTOWN	16.6	6.7	45	43	32.9	295.7	
MOORTOWN	17.3	5.9	46	48	-87.6	254.1	
MOORTOWN	17.3	6.2	45	46	-92	278.6	
MOORTOWN	16.5	7.4	46	51	-84.7	288.0	
MOORTOWN	16.2	5.4	45	49	-190.6	257.6	
MOORTOWN	17.1	5.3	47	55	-208.1	223.4	
MOORTOWN	17.5	5.7	45	49	-186.2	244.2	
MOORTOWN	16.1	5.7	45	49	-238.8	216.8	
MOORTOWN	21.8	8.1	45	44	0	350.5	
MOORTOWN	21.6	8.1	45	45	-4.4	340.6	
MOORTOWN	22.2	8.8	46	41	13.6	359.2	
MOORTOWN	22.0	7.4	45	43	-103	315.4	
MOORTOWN	21.0	7.2	45	47	-109.5	323.1	
MOORTOWN	21.7	7.6	45	47	-105.1	325.3	
MOORTOWN	22.0	6.6	45	52	-219	273.4	
MOORTOWN		6.0		56		243.0	
MOORTOWN	21.7	6.0	45	55	-214.7	261.1	
MOORTOWN	28.0	8.1	46	50	5.2	332.5	
MOORTOWN	25.7	7.5	47	50	0	329.9	
MOORTOWN	27.3	8.6	46	41	0	395.3	
MOORTOWN	25.9	6.5	47	61	-83.8	307.2	
MOORTOWN	26.3	7.3	47	54	-94.2	312.1	
MOORTOWN	26.8	7.7	46	54	-91.6	316.8	
MOORTOWN	27.6	7.1	47	51	-235.6	318.3	
MOORTOWN	27.5	7.4	46	55	-225.1	295.0	
MOORTOWN	26.3	7.6	44	51	-227.8	316.2	
MOORTOWN	27.3	6.5	46	57	-345.6	284.2	
MOORTOWN	27.9	7.1	46	56	-356.0	296.4	
MOORTOWN	29.1	5.5	45	61	-371.8	261.8	
MOORTOWN	27.6	6.0	45	66	-358.7	251.3	
MOORTOWN	29.1	6.1	46	60	-460.8	240.8	
MOORTOWN	29.1	4.9	48	77	-450.3	211.2	
MOORTOWN	26.9	5.1	45	80	-471.2		
MOORTOWN	28.8	4.9	46	73			
MOORTOWN	29.1	4.5	46	90		157.1	
MOORTOWN	27.2	4.4	46	78		188.5	
MOORTOWN	28.4	3.6	46	91	-717.3	75.4	
MOORTOWN	28.3	3.6	46	89	-701.6	151.8	
MOORTOWN	27.1	4.2	46	84	-696.4	170.2	
NEWCASTLE	17.8	6.5	48	42	0	327	1.0
NEWCASTLE	17.2	6.2	47	41	0	283.2	1.0
NEWCASTLE	18.5	4.9	47	53	-332.4	202.3	1.3
NEWCASTLE	18.9	4.7	48	57	-370.9	192.7	1.8
NEWCASTLE	18.6	4.6	46	55	-320.3	192.7	1.4
NEWCASTLE	24.0	7.3	46	47	0	337.2	1.8
NEWCASTLE	23.6	8.0	45	37	0	313.1	1.5
NEWCASTLE	23.0	7.0	46	46	0	274.6	1.8
NEWCASTLE	23.6	6.1	45	49	-529.9	264.9	2.0
NEWCASTLE		5.3		53			2.5
NEWCASTLE		5.1		60		199.9	2.1

	VELOCITY		ANGLE		SPIN		D
	ms^{-1}		degrees		$rads^{-1}$		mm
NEWCASTLE	29.9	7.7	45	49	0	308.3	2.5
NEWCASTLE	28.6	7.7	43	50	0	289.0	2.5
NEWCASTLE	29.1	5.5	45	65	-356.5	197.5	0
NEWCASTLE	29.1	5.8	46	60	-346.8	260.1	2.6
NEWCASTLE	19.3	5.7	53	51	0	264.9	1.0
NEWCASTLE	17.7	5.8	53	42	-24.1	221.5	1.0
NEWCASTLE	18.6	6.1	53	48	-9.6	240.8	1.0
NEWCASTLE	18.0	5.3	54	46	-101.2	202.3	1.0
NEWCASTLE	18.0	4.9	54	54	-115.6	183.0	1.3
NEWCASTLE	18.4	4.8	53	55	-221.6	168.6	1.2
NEWCASTLE	17.2	4.3	55	55	-224	202.3	1.4
NEWCASTLE	17.4	4.3	54	55	-236	161.4	.9
NEWCASTLE	16.9	3.8	55	63	-327.6	150.8	.9
NEWCASTLE	17.8	4.0	57	59	-322.7	154.1	1.5
NEWCASTLE	17.1	3.9	55	65	-308.3	192.7	1.6
NEWCASTLE	22.1	5.7	54	52	9.6	228.8	1.3
NEWCASTLE	21.5	5.5	53	54	0	207.1	1.9
NEWCASTLE	21.6	5.5	55	54	4.8	221.6	1.7
NEWCASTLE	22.4	5.4	55	53	-106	204.7	1.6
NEWCASTLE	22.0	5.4	54	58	-120.4	178.2	1.8
NEWCASTLE	23.1	4.5	54	68	-236	178.2	2.5
NEWCASTLE	22.0	4.7	55	63	-207.1	216.7	2.0
NEWCASTLE	23.0	4.8	54	60		168.6	1.9
NEWCASTLE	22.3	4.5	54	64	-332.4	183.0	2.1
NEWCASTLE	22.6	4.2	55	69	-327.6	163.7	1.8
NEWCASTLE	23.2	4.3	55	81		115.6	2.7
NEWCASTLE	22.8	4.0	54	70	-464.8	149.3	2.1
NEWCASTLE	23.4	3.7	55	82	-452.8	134.8	2.3
NEWCASTLE	23.0	3.3	56	73	-573.2	36.1	1.9
NEWCASTLE	22.4	2.8	55	81	-578	115.6	2.3
NEWCASTLE	22.5	3.1			-566	120.4	1.6
NEWCASTLE	28.3	6.2	55	58	-14.4	250.5	2.4
NEWCASTLE	28.6	6.2	54	63	4.8	252.8	2.2
NEWCASTLE	27.2	5.2	53	67	9.6	211.9	2.7
NEWCASTLE	26.1	5.3	54	64	-101.2	208.7	3.1
NEWCASTLE	27.4	5.6	53	60	-96.3	221.6	2.5
NEWCASTLE	27.7	5.7	54	59	-86.7	232.7	2.3
NEWCASTLE	27.9	4.7	54	67	-240.8	178.2	2.7
NEWCASTLE	27.2	4.8	52	69	-236	178.2	2.8
NEWCASTLE	27.5	3.8	54	82	-351.6	139.7	
SANDMOOR	16.0	6.6	45	41	0	279.2	2.0
SANDMOOR	16.5	6.6	46	40	13.1	266.2	
SANDMOOR	16	6.5	47	43	0	257.4	
SANDMOOR	17.4	6.4	45	48	-91.6	263.6	
SANDMOOR	17.4	6.7	47	38	-96.0	296.7	
SANDMOOR	18.0	6.2	46	48	-87.3	253.1	
SANDMOOR	17	4.7	45	49	-200.7	223.4	2.0
SANDMOOR	17.3	5.6	46	45	-198.5	248.0	2.3
SANDMOOR	17.2	5.7	46	45	-209.4	253.1	2.3
SANDMOOR	17.0	5.2	46	46	-327.2	231.3	
SANDMOOR	16.9	4.5	46	54	-340.3	200.7	4.6
SANDMOOR	17.7	4.6	45	55	-322.9	214.5	2.5
SANDMOOR	21.4	7.0	45	47			3.6

	VELOCITY		ANGLE		SPIN		D
	ms^{-1}		degrees		$rads^{-1}$		mm
SANDMOOR	21.6		45	44			4.1
SANDMOOR	22.1	7.0	46	51	0	253.1	3.8
SANDMOOR	21.5	7.1	46	49	-109.1	266.2	5.1
SANDMOOR	20.7	6.6	45	50	-96.0	261.8	4.6
SANDMOOR	20.8	6.2	46	50	-109.1	240	5.1
SANDMOOR	22.4	6.7	46	42	-229.1	281.4	3.3
SANDMOOR	22.1	6.1	44	52	-218.2	223.4	3.6
SANDMOOR	22.1	6.2	46	51	-234.6	232.3	4.3
SANDMOOR	22.6	6.1	47	54	-321.7	234.6	
SANDMOOR	22.9	5.9	46	56	-335.1	250.2	3.3
SANDMOOR	22.4	6.6	46	46	-339.6	272.6	4.3
SANDMOOR	27.6	8.3	46	46	0	351.7	8.4
SANDMOOR	27.7	7.2	46	47	0	363.0	3.3
SANDMOOR	28.6	8.9	46	40	0	334.7	4.1
SANDMOOR	27.4	7.3	46	50	-99.3	272.3	4.3
SANDMOOR	27.5	7.5	46	49	-90.8	323.3	5.3
SANDMOOR	27.7	7.6	46	48	-232.6	295.0	5.6
SANDMOOR	26.9	7.2	46	50	-243.9	270.9	3.3
SANDMOOR	26.7	6.8	46	58	-249.6	236.8	4.8
SANDMOOR	28.1	5.5	45	63	-346	209.9	5.1
SANDMOOR	28.2	6.7	45	57	-365.9	243.9	6.1
SANDMOOR	27.7	6.8	46	57	-351.7	273.7	5.1
SANDMOOR	28.8	7.3	45	48	-453.8	238.2	3.8
SANDMOOR	29.1	5.0	46	68	-476.5	158.8	7.4
SANDMOOR	29.1	6.9	46	56	-589.9	184.3	5.1
SANDMOOR	30.0	6.5	46	55	-578.6	160.2	3.6
SANDMOOR	28.8	5.5	46	71	-567.2	226.9	5.1
SANDMOOR	27.1	5.6	46	63	-669.3	-37.8	6.4
SANDMOOR	28.8	5.6	47	63	-709.0	66.7	6.9
SANDMOOR	27.7	5.9	47	71	-669.3	177.3	7.6
SUTTON PARK	17.0	6.7	40	41	4.7	292.3	1.0
SUTTON PARK	16.7	6.7	40	40	0	285.3	.5
SUTTON PARK	17.2	6.3	39	42	-154.3	304.0	1.0
SUTTON PARK	17.4	6.2	39	45	-157.5	280.6	1.1
SUTTON PARK	17.2	6.3	39	40	-148.1	292.3	1.1
SUTTON PARK	17.5	5.7	39	48	-229.2	252.6	1.4
SUTTON PARK	16.9	5.3	40	51	-210.5	243.2	
SUTTON PARK	17.3	5.8	39	45	-215.2	261.0	0
SUTTON PARK	17.7	5.2	39	48	-327.4	238.6	1.4
SUTTON PARK	16.9	4.7	40	52	-306.4	212.8	1.2
SUTTON PARK	16.8	6.1	38	45	-318.1	112.3	
SUTTON PARK	20.9	7.3	39	45	4.7	327.4	1.9
SUTTON PARK	21.6	6.9	39	47	-116.9	315.7	1.6
SUTTON PARK	21.5	7.3	39	43	-102.9	332.1	.9
SUTTON PARK	21.2	7.4	40	44	-109.9	304	1.3
SUTTON PARK	21.1	5.4	40	52	-219.8	254.9	1.3
SUTTON PARK	21.7	5.5	39	52	-243.2	266.6	2.1
SUTTON PARK	22.1	6.8	39	48	-226.8	292.3	1.1
SUTTON PARK	22.1	8.2	39	38	-336.8		1.5
SUTTON PARK	21.9	8	40	42	-404.6	-71.6	1.7
SUTTON PARK	22.1	7.5	39	44	-481.8	-43.5	1.9
SUTTON PARK	21.9	7.6	38	42	-444.4	-42.1	1.1
SUTTON PARK	21.5	7.4	40	46	-547.3	-171.2	1.9

	VELOCITY		ANGLE		SPIN		D
	ms^{-1}		degrees		$rads^{-1}$		mm
SUTTON PARK	21.3	6.9	40	48	-549.6	-88.9	2.2
SUTTON PARK	21.5	7.8	39	42	-556.6	-119.3	2.1
SUTTON PARK	26.8	8.7	37	40	0	328.7	2.5
SUTTON PARK	27.2	8.5	38	46	9.7	399.3	2.9
SUTTON PARK	27.9	9.5	41	45	9.7	316.5	2.0
SUTTON PARK	27.5	9.7	38	46	-82.8	360.3	2.2
SUTTON PARK	26.2	9.1	38	47	-90.1	428.5	2.3
SUTTON PARK	27.7	8.5	37	44	-82.8	409	2.5
SUTTON PARK	27.5	8.7	38	50	-248.3		2.7
SUTTON PARK	27.1	7.2	40	58	-238.6	316.5	
SUTTON PARK	26.1	7.5	40	55	-233.7	326.2	
SUTTON PARK	26.8	6.6	40	61	-233.7	305.8	2.9
SUTTON PARK	28.3	5.9	40	71	-370.1	228.9	2
SUTTON PARK	27.2	6.5	39	60	-365.2	183.8	2.8
SUTTON PARK	26.9	5.8	41	72	-474.8	243.5	2.7
SUTTON PARK	26.5	6.2	41	59	-462.6	60.9	3.1
SUTTON PARK	27.7	5.7	41	71	-491.8	214.2	3.1
SUTTON PARK	26.9	6.6	41	58	-555.1	-4.9	2.6
SUTTON PARK	27.4	7.3	39	47	-560	-53.6	2.8
SUTTON PARK	26.1	6.6	40	58	-603.8	-58.4	3.2
SUTTON PARK		5.9		64		69.8	2.9
SUTTON PARK	26.1	6.0	40	65	-672.0	-51.1	3.4
SUTTON PARK	27.5	6.3	38	61	-647.6	-24.3	2.2
SUTTON PARK	16.4	4.9	50	48	37.4	233.9	1.3
SUTTON PARK	16.0	5.3	50	52	0	208.1	1.5
SUTTON PARK	16.0	5.5	50	47	4.7	205.8	1.3
SUTTON PARK	16.9	4.6	50	64	0	161.4	1.2
SUTTON PARK	16.4	5.4	51	45	-327.4	161.4	2.0
SUTTON PARK	16.9	4.6	50	60	-285.3	161.4	1.1
SUTTON PARK	22.1	6.2	51	54	4.7	236.2	1.8
SUTTON PARK	21.6	6.2	51	54	-9.3	236.6	1.8
SUTTON PARK	22.5	4.3	51	77	-551.9	-121.6	3.2
SUTTON PARK	21.7	4.3	51	67	-542.6	-44.4	2.4
SUTTON PARK	22.3	4.8	51	67	-556.6	131.0	2.5
SUTTON PARK	26.4	5.8	50	61	9.3	252.6	3.4
SUTTON PARK	26.6	5.3	49	72	-9.3	208.1	3.3
SUTTON PARK	26.0	5.9	50	63	0	238.6	2.9
SUTTON PARK	26.8	3.4	50	91	-537.9	14.0	3.4
SUTTON PARK	28.0	2.7	50	101	-533.2	107.6	2.8
SUTTON PARK	26.7	3.1	51	92	-566.6	25.7	3.6

Appendix F - Graphs of the difference between the spin required for rolling and the actual spin after impact versus spin before impact

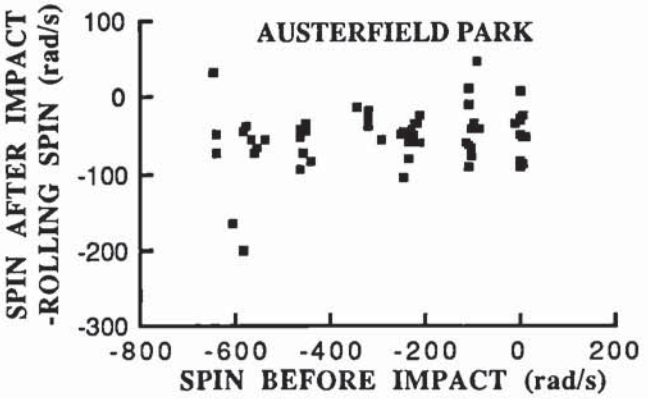

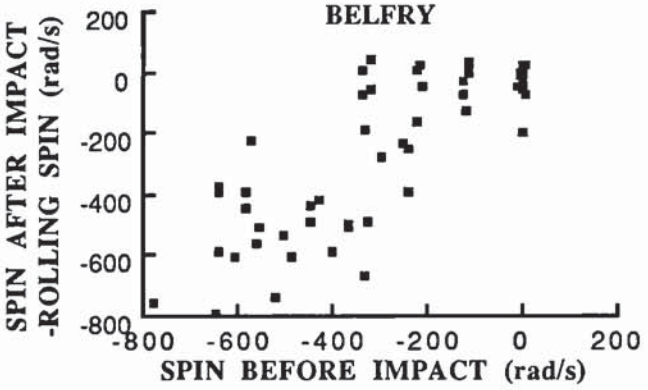

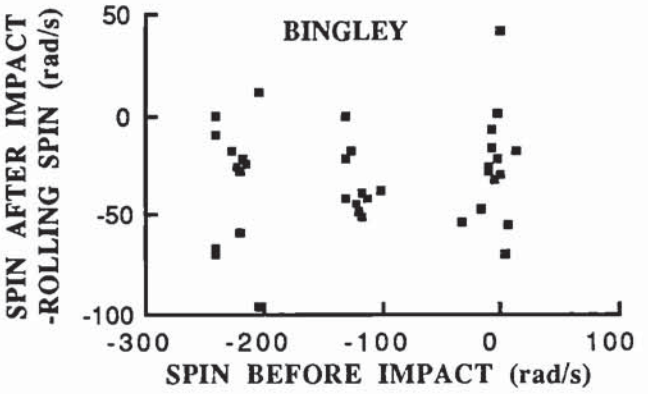

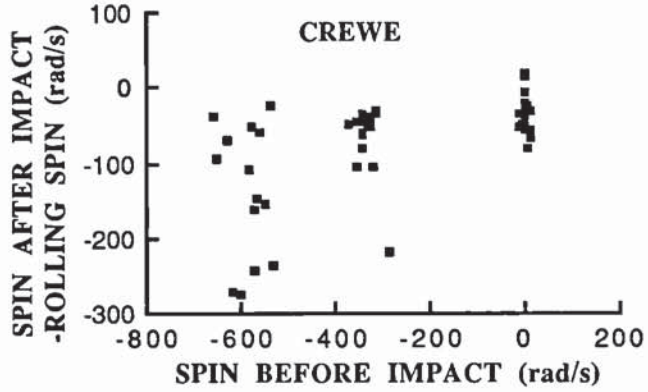

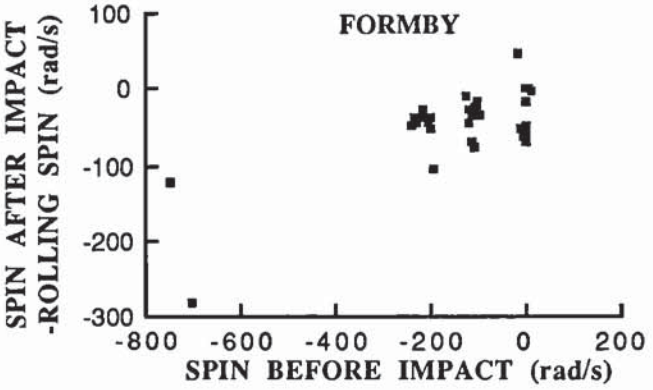
FORMBY
SPIN AFTER IMPACT -ROLLING SPIN (rad/s)
100
0
-100
-200
-300
-800 -600 -400 -200 0 200
SPIN BEFORE IMPACT (rad/s)

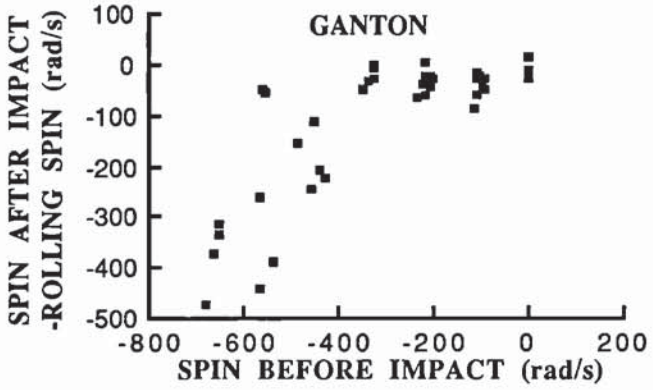
GANTON
SPIN AFTER IMPACT -ROLLING SPIN (rad/s)
100
0
-100
-200
-300
-400
-500
-800 -600 -400 -200 0 200
SPIN BEFORE IMPACT (rad/s)

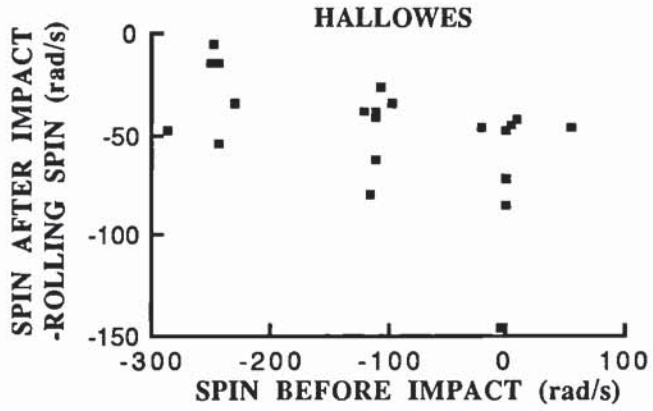
HALLOWES
SPIN AFTER IMPACT -ROLLING SPIN (rad/s)
0
-50
-100
-150
-300 -200 -100 0 100
SPIN BEFORE IMPACT (rad/s)

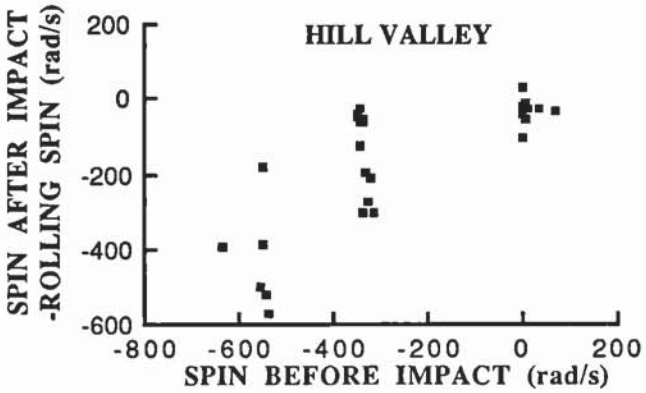
HILL VALLEY
SPIN AFTER IMPACT -ROLLING SPIN (rad/s)
200
0
-200
-400
-600
-800 -600 -400 -200 0 200
SPIN BEFORE IMPACT (rad/s)

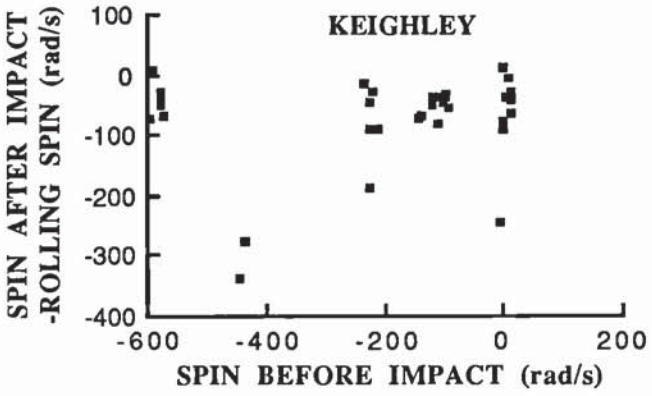
KEIGHLEY
SPIN AFTER IMPACT
-ROLLING SPIN (rad/s)
100
0
-100
-200
-300
-400
-600
-400
-200
0
200
SPIN BEFORE IMPACT (rad/s)

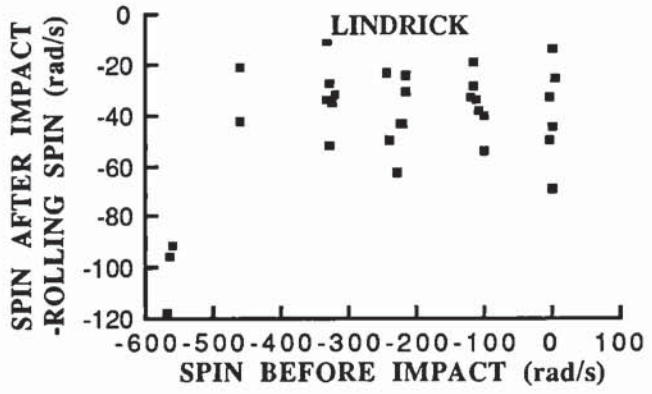
LINDRICK
SPIN AFTER IMPACT
-ROLLING SPIN (rad/s)
0
-20
-40
-60
-80
-100
-120
-600-500-400-300-200-100 0 100
SPIN BEFORE IMPACT (rad/s)

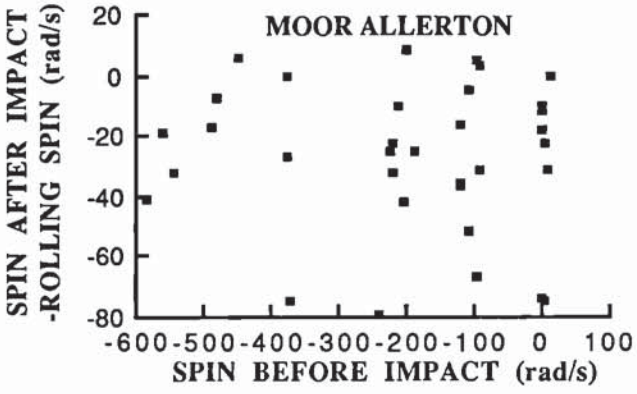
MOOR ALLERTON
SPIN AFTER IMPACT
-ROLLING SPIN (rad/s)
20
0
-20
-40
-60
-80
-600-500-400-300-200-100 0 100
SPIN BEFORE IMPACT (rad/s)

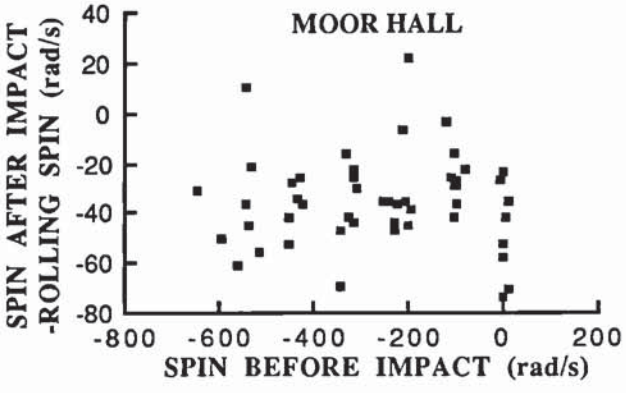
MOOR HALL
SPIN AFTER IMPACT
-ROLLING SPIN (rad/s)
40
20
0
-20
-40
-60
-80
-800 -600 -400 -200 0 200
SPIN BEFORE IMPACT (rad/s)

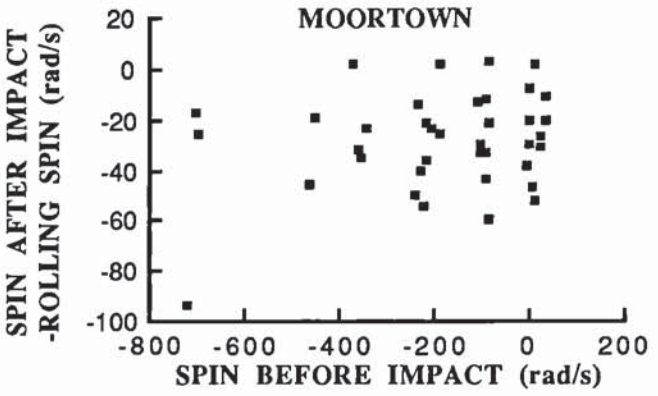
MOORTOWN
SPIN AFTER IMPACT -ROLLING SPIN (rad/s)
20
0
-20
-40
-60
-80
-100
-800 -600 -400 -200 0 200
SPIN BEFORE IMPACT (rad/s)

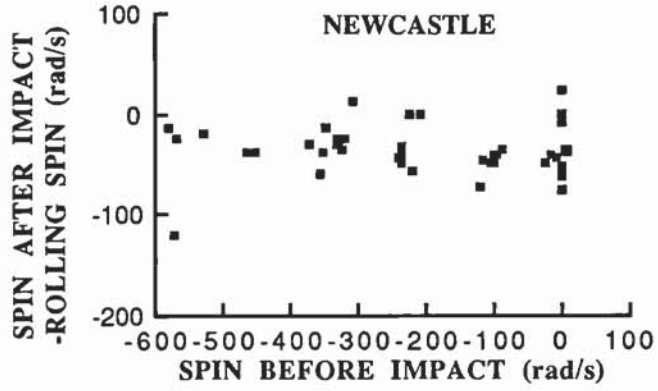
NEWCASTLE
SPIN AFTER IMPACT -ROLLING SPIN (rad/s)
100
0
-100
-200
-600-500-400-300-200-100 0 100
SPIN BEFORE IMPACT (rad/s)

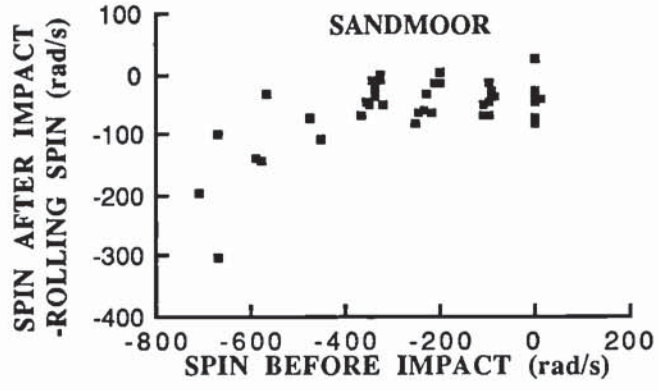
SANDMOOR
SPIN AFTER IMPACT -ROLLING SPIN (rad/s)
100
0
-100
-200
-300
-400
-800 -600 -400 -200 0 200
SPIN BEFORE IMPACT (rad/s)

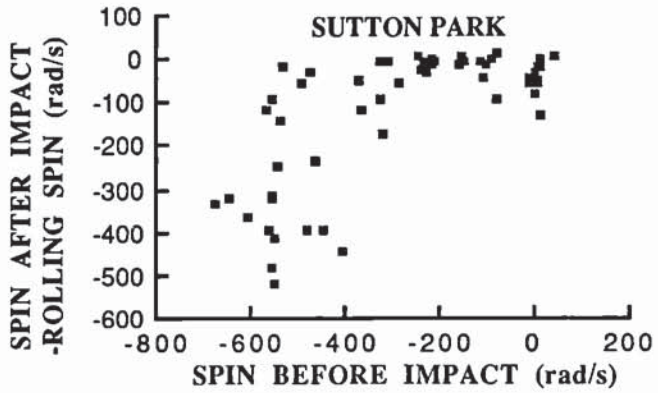
SUTTON PARK
SPIN AFTER IMPACT -ROLLING SPIN (rad/s)
100
0
-100
-200
-300
-400
-500
-600
-800 -600 -400 -200 0 200
SPIN BEFORE IMPACT (rad/s)

Appendix G - Playing quality test results

G.1 Clegg Impact Hardness Tester

This section contains the results from the Clegg Impact Hardness Tester using the four different indenters, i.e. the 0.5kg and 1.0kg cylindrical indenters, the indenter with a real golf ball attached to its end and the indenter with a metal end shaped like a golf ball. The readings are given in tens of graveties ($98.1 ms^{-2}$).

(i) Clegg 0.5kg

Austerfield Park	2, 2, 3, 3, 3, 4, 4, 3, 2, 3, 2, 3, 2, 2, 3, 3, 3, 4, 4
Belfry	5, 5, 5, 5, 5, 5, 6, 6, 6, 4, 4, 5, 5, 5, 5, 5, 5, 6, 6, 6
Bingley	No readings
Birkdale	No readings
Crewe	5, 5, 6, 6, 7, 6, 6, 6, 7, 7, 5, 6, 6, 7, 8, 5, 6, 6, 7, 7
Formby	4, 4, 4, 6, 8, 3, 4, 4, 4, 4, 4, 4, 4, 7, 8, 2, 4, 5, 7, 9
Ganton	6, 6, 6, 7, 7, 7, 7, 8, 8, 8, 6, 6, 7, 8, 8, 8, 8, 9, 7, 8
Hallowes	6, 8, 11, 12, 11, 9, 8, 8, 9, 8, 7, 7, 8, 7, 8, 8, 6, 7, 9, 9
Hill Valley	5, 5, 5, 5, 4, 4, 5, 5, 5, 6, 5, 5, 7, 7, 7, 5, 6, 7, 8, 8
Keighley	4, 3, 2, 3, 3, 4, 6, 3, 3, 3, 2, 2, 3, 3, 4, 3, 3, 6, 3
Lindrick (1)	7, 6, 8, 6, 6, 6, 6, 7, 7, 7, 8, 9, 10, 10, 8, 8, 8, 8, 8, 7
Lindrick (2)	6, 6, 6, 6, 6, 6, 6, 7, 7, 7, 5, 5, 5, 5, 6, 6, 6, 6, 6, 6
Moor Allerton	6, 7, 7, 5, 6, 7, 7, 8, 6, 6, 7, 6, 6, 7, 7, 6, 7, 7, 6, 7
Moor Hall	4, 4, 4, 4, 4, 4, 5, 5, 5, 5, 4, 4, 4, 4, 4, 4, 4, 5, 5, 5
Moortown	4, 4, 4, 5, 5, 6, 4, 5, 4, 4, 5, 3, 6, 5, 6, 5, 6, 5, 5, 4
Newcastle-u-Lyme	4, 4, 5, 5, 6, 6, 6, 6, 6, 7, 5, 5, 5, 5, 5, 6, 6, 6, 7, 8
Sandmoor	5, 4, 5, 5, 5, 6, 6, 6, 6, 5, 5, 5, 5, 5, 7, 6,7, 6, 6, 6
STRI Green	6, 6, 6, 6, 5, 6, 7, 7, 8, 8, 8, 8, 8, 8, 8, 6, 8, 6, 8, 6
Sutton Park	5, 5, 5, 5, 5, 6, 6, 7, 8, 9, 5, 5, 5, 6, 6, 7, 7, 7, 7

(ii) Clegg 1.0kg

Austerfield Park	3, 3, 2, 2, 2, 1, 2, 2, 3, 3, 1, 2, 2, 2, 2, 1, 2, 1, 2
Belfry	2, 3, 3, 3, 3, 3, 3, 3, 3, 3, 3, 3, 3, 3, 3, 4, 4, 4, 4, 4, 4
Bingley	No readings
Birkdale	No readings
Crewe	4, 4, 4, 4, 4, 4, 4, 4, 4, 4, 4, 4, 4, 4, 4, 3, 5, 5, 5, 5
Formby	2, 2, 2, 2, 2, 2, 2, 2, 2, 2, 2, 2, 2, 3, 3, 2, 2, 3, 3, 3, 3
Ganton	5, 5, 5, 5, 5, 5, 5, 5, 5, 5, 5, 4, 4, 4, 4, 4, 4, 4, 6, 7
Hallowes	6, 6, 5, 5, 5, 5, 5, 4, 5, 7, 6, 7, 6, 6, 6, 5, 5, 4, 6, 7
Hill Valley	3, 3, 3, 3, 3, 3, 3, 3, 3, 3, 3, 4, 4, 4, 2, 3, 3, 3, 3, 3, 3
Keighley	No readings
Lindrick (1)	7, 6, 6, 7, 7, 6, 6, 6, 6,6, 5, 5, 6, 7, 7, 6, 7, 6, 7, 6
Lindrick (2)	4, 4, 5, 5, 5, 5, 5, 5, 5, 6, 4, 4, 4, 4, 4, 4, 4, 5, 3, 3
Moor Allerton	5, 5, 5, 5, 4, 4, 6, 6, 3, 4, 4, 4, 5, 5, 3, 3, 4, 3, 4, 3
Moor Hall	3, 3, 3, 3, 3, 3, 3, 3, 3, 3, 3, 3,3, 3, 3, 4, 4, 4, 4, 4
Moortown	3, 4, 3, 3, 3, 3, 2, 2, 2, 1, 2, 1, 2, 2, 1, 2, 2, 3, 3, 3
Newcastle-u-Lyme	3, 3, 3, 3, 3, 3, 3, 3, 3, 3, 3, 3, 3, 3, 3, 4, 4, 6, 6, 6, 7
Sandmoor	3, 5, 4, 5, 5, 3, 3, 3, 3, 3, 4, 4, 4, 3, 4, 2, 3, 3, 2, 3
STRI Green	7, 7, 6, 7, 7, 7, 6, 6, 6, 7, 6, 5, 6, 6, 6, 6, 6, 5, 6, 6
Sutton Park	4, 4, 4, 4, 4, 4, 4, 4, 4, 4, 4, 4, 4, 4, 4, 4, 4, 3, 3, 3

(iii) Clegg RB

Austerfield Park	0, 0, 0, 0, 0, 1, 0, 1, 0, 0, 1, 0, 0, 0, 0, 0, 0, 0, 0, 1
Belfry	1, 1, 1, 1, 1, 1, 1, 1, 1, 1, 0, 0, 0, 0, 0, 0, 0, 0, 0, 0
Bingley	No readings
Birkdale	No readings
Crewe	1, 1, 1, 1, 1, 1, 1, 1, 1, 1, 1, 1, 1, 1, 1, 1, 1, 1, 0, 2

Formby	1, 1, 1, 1, 1, 1, 0, 0, 0, 0, 1, 1, 1, 1, 1, 1, 1, 0, 0, 2
Ganton	2, 2, 2, 2, 2, 2, 2, 2, 2, 2, 3, 3, 3, 3, 1, 1,1, 2, 2, 4
Hallowes	3, 1, 2, 1, 1, 2, 2, 2, 1, 2, 2, 2, 3, 3, 2, 3, 2, 2, 2, 2
Hill Valley	0, 0, 0, 0, 0, 0, 0, 0, 0, 0, 0, 0, 0, 0, 0, 0, 1, 1, 1
Keighley	No readings
Lindrick (1)	2, 2, 2, 2, 3, 2, 3, 2, 2, 2, 2, 2, 1, 1, 2, 1, 2, 2, 2, 2
Lindrick (2)	1, 1, 1, 1, 1, 1, 1, 1, 1, 1, 1, 1, 1, 1, 1, 1, 1, 2, 2, 2
Moor Allerton	1, 1, 1, 1, 0, 0, 1, 1, 1, 1, 0, 0, 1, 1, 1, 1, 0, 0, 1, 0
Moor Hall	0, 0, 0, 0, 0, 0, 1, 1, 1, 1, 1, 1, 1, 1, 1, 1, 1, 1, 1, 1
Moortown	1, 2, 1, 1, 1, 0, 0, 1, 0, 1, 0, 0, 0, 0, 0, 0, 0, 0, 0, 1
Newcastle-u-Lyme	0, 0, 0, 0, 0, 0, 0, 0, 0, 0, 1, 1, 1, 1, 1, 1, 1, 1, 1, 1
Sandmoor	0, 0, 0, 0, 0, 1, 1, 1, 0, 1, 1, 1, 0, 0, 1, 1, 1, 1, 1, 1
STRI Green	1, 2, 3, 2, 2, 2, 2, 1, 3, 3, 3, 3, 3, 3, 1, 2, 2, 2, 2, 2
Sutton Park	1, 1, 1, 1, 0, 0, 0, 0, 0, 0, 0, 0, 0, 0, 0, 0, 0, 0, 0, 0

(iv) Clegg MB

Austerfield Park	1, 1, 1, 1, 0, 1, 1, 0, 1, 1, 0, 0, 0, 0, 0, 0, 0, 0, 0, 0
Belfry	0, 0, 0, 0, 0, 0, 1, 1, 1, 1, 1, 1, 1, 1, 1, 1, 1, 1, 1, 1
Bingley	No readings
Birkdale	No readings
Crewe	1, 1, 1, 1, 1, 1, 1, 1, 1, 1, 1, 1, 1, 1, 1, 1, 1, 1, 1, 1
Formby	0, 0, 0, 0, 0, 1, 1, 1, 1, 1, 1, 1, 1, 1, 1, 1, 1, 2, 2, 2
Ganton	1, 1, 1, 1 ,1, 1, 1, 2, 2, 2, 2, 2, 2, 2, 2, 2, 2, 2, 2, 2
Hallowes	2, 2, 2, 1, 2, 2, 2, 3, 2, 1, 2, 1, 1, 1, 1, 2, 1, 3, 1, 1
Hill Valley	0, 0, 0, 0, 0, 0, 0, 0, 0, 0, 0, 0, 0, 0, 0, 0, 0, 0, 0, 1
Keighley	No readings
Lindrick (1)	2, 2, 3, 2, 3, 2, 3, 2, 3, 2, 3, 2, 1, 2, 2, 2, 2, 2, 2, 2
Lindrick (2)	1, 1, 1, 1, 1, 2, 2, 2, 2, 2, 1, 1, 1, 1, 1, 2, 2, 2, 2, 2
Moor Allerton	1, 1, 0, 1, 1, 0, 1, 1, 1, 1, 0, 1, 1, 1, 1, 1, 0, 1, 2, 1
Moor Hall	0, 0, 0, 0, 0, 0, 0, 1, 1, 1, 1, 1, 1, 1, 1, 1, 1, 1, 1, 1
Moortown	1, 1, 0, 1, 0, 0, 1, 0, 1, 0, 1, 1, 1, 1, 2, 1, 1, 1, 0, 1
Newcastle-u-Lyme	0, 0, 0, 0, 0, 0, 0, 0, 1, 1, 1, 1, 1, 1, 1, 1, 1, 1, 2, 3
Sandmoor	1, 0, 0, 0, 0, 0, 0, 0, 1, 1, 0, 1, 1, 1, 1, 1, 1, 1, 0, 0, 1
STRI Green	3, 3, 3, 3, 4, 4, 4, 4, 4, 4, 4, 2, 3, 3, 4, 3, 3, 2, 3, 3
Sutton Park	1, 1, 1, 1, 1, 1, 1, 1, 1, 1, 0, 0, 0, 0, 2, 1, 1, 1, 1, 1

G.2 Penetrometer

The following are readings for each green using the penetrometer described in Chapter 2. The units are dimensionless.

Austerfield Park	9, 7, 8, 8, 9, 7, 6, 7, 10, 7
Belfry	6, 7, 7, 8, 8, 7, 7, 7, 7, 7
Bingley	5, 4, 4, 6, 6, 6, 6, 8, 4, 6, 6, 5, 7, 6, 6, 7, 6, 5, 4, 4
Birkdale	No readings
Crewe	1, 6, 7, 7, 7, 7, 6, 7, 7, 8
Formby	6, 8, 6, 6, 7, 5, 5, 8, 5, 6
Ganton	5, 6, 7, 8, 9, 6, 7, 8, 8, 8, 6, 7, 7, 8, 9, 5, 6, 6, 7, 7
Hallowes	10, 6, 9, 10, 5, 6, 8, 8, 7, 8
Hill Valley	7, 7, 7, 9, 10, 8, 8, 9, 9, 9
Keighley	4, 6, 5, 7, 8, 9, 6, 7, 7, 7, 6, 12, 12, 4, 10, 4, 6, 9, 10, 6, 6, 6, 8, 7, 6, 6, 6, 8, 10
Lindrick (1)	3, 5, 4, 6, 5, 6, 6, 2, 3, 3
Lindrick (2)	8, 5, 6, 5, 6, 6, 5, 6, 5, 5
Moor Allerton	11, 11, 10, 10, 9, 9, 9, 8, 8, 10, 10, 10, 10, 11, 11, 11, 12, 6, 10, 10, 9, 8, 8, 12, 10, 9, 12, 11, 10, 9
Moor Hall	5, 6, 7, 7, 11, 4, 5, 5, 6, 7
Moortown	6, 6, 7, 8, 10, 9, 10, 9, 4, 6, 7, 4, 7, 7,7, 6, 11, 8, 10, 10
Newcastle-u-Lyme	5, 5, 6, 4, 5, 5, 5, 6, 7, 6

Sandmoor	5, 15, 16, 7, 9, 8, 14, 7, 9, 6, 6, 15, 10, 8, 6, 10, 5, 6, 9, 6
STRI Green	12, 13, 11, 10, 11
Sutton Park	5, 5, 5, 6, 7, 7, 6, 7, 7, 8

G.4 Traction

The following surface traction values are given in Newton metres.

Austerfield Park	17, 18, 20, 18, 16, 16, 16, 16, 15, 15
Belfry	11, 12, 11, 13, 12
Bingley	12, 14, 15, 16, 15,
Birkdale	No readings
Crewe	13, 13, 15, 15, 15
Formby	13, 14, 14, 14, 13
Ganton	10, 10, 15, 15, 14
Hallowes	14, 16, 14, 16, 16, 14, 14, 16, 14, 13
Hill Valley	10, 12, 13, 13, 14
Keighley	12, 11, 10, 10, 13, 13, 12, 10, 12, 13, 13, 12, 12, 13, 13, 11, 10, 12, 10, 11
Lindrick (1)	14, 10, 12, 12, 12, 12, 14, 14, 14, 14, 14
Lindrick (2)	14, 14, 15, 17, 15
Moor Allerton	12, 10, 12, 14, 12, 16, 14, 13, 14, 14, 13, 13, 14, 12, 13, 14, 13, 12, 14, 14
Moor Hall	15, 16, 17, 18, 18
Moortown	18, 19, 17, 18, 18, 18, 18, 17, 16, 18
Newcastle-u-Lyme	10, 13, 14, 15, 16
Sandmoor	14, 15, 17, 17, 14, 16, 13, 18, 16, 15
STRI Green	No readings
Sutton Park	15, 15, 14, 14, 14

G.4 Ball Bounce

This section contains the ball bounce values for each green. The numbers given are percentages of the drop height (5m).

Austerfield Park	5.5, 5.5, 4.8, 6.4, 5.2, 5.4, 5.8, 5.6, 5.2, 6.0 (Wound) 6.0, 4.8, 5.8, 5.4, 4.2, 5.6, 5.7, 5.0, 4.2, 5.2, 5.0 (Two-piece)
Belfry	2.5, 2.0, 2.8, 2.5, 2.1, 2.3, 2.6, 2.0, 2.2, 2.1, 2.3
Bingley	4.2, 4.0, 4.2, 4.0, 4.2, 4.0, 3.2, 2.5, 2.8, 3.4
Birkdale	3.8, 4.2, 3.8, 4.2, 4.4, 4.1, 3.7, 3.8, 3.8, 3.2, 3.8, 3.7
Crewe	4.9, 5.1, 4.9, 5.5, 5.8, 5.3, 5.2, 6.2, 5.6, 5.5, 5.6
Formby	4.7, 5.0, 6.6, 4.6, 7.0, 5.4, 5.4, 5.2, 6.2, 5.8
Ganton	4.0, 4.0, 4.5, 4.3, 3.8, 4.0, 4.0, 4.0, 4.5, 4.2, 4.2
Hallowes	6.8, 5.5, 5.3, 5.5, 5.6, 5.6, 5.2, 4.5, 5.3, 4.8, 5.8
Hill Valley	6.3, 6.8, 5.7, 5.2, 6.0, 7.0, 6.7, 6.8, 6.7, 6.3, 6.8
Keighley	9.0, 8.4, 7.2, 10.2, 6.8, 7.2, 8.6, 12.0, 9.0, 5.4, 5.8
Lindrick (1)	5.0, 4.8, 4.2, 4.5, 4.2, 4.5, 5.3, 4.2, 4.3
Lindrick (2)	4.0, 4.0, 3.7, 4.2, 4.2, 4.2, 4.3, 4.3, 4.0, 4.2
Moor Allerton	No readings
Moor Hall	4.2, 5.1, 4.5, 4.6, 4.0, 3.8, 3.8, 4.4, 4.0, 4.0
Moortown	No readings
Newcastle-u-Lyme	5.4, 5.4, 5.5, 4.6, 4.6, 4.4, 4.7, 4.0, 4.8, 4.2, 4.0, 4.1
Sandmoor	No readings
STRI Green	No readings
Sutton Park	5.3, 4.8, 4.7, 4.7, 5.0, 4.3, 4.1, 4.3, 4.3, 3.9, 4.6

G.5 Botanical analysis (optical point quadrat)

Austerfield Park	*Poa annua* -79%; Moss - 7%; Dead - 14%
Belfry	*Poa annua* - 56%; *Agrostis* - 41%; Dead - 3%

Bingley	*Poa annua* - 79%; *Agrostis* - 18%; Dead - 1%; Bare - 2%
Birkdale	No readings
Crewe	*Poa annua* - 34%; *Agrostis* - 50%; Yorkshire Fog - 16%
Formby	*Poa annua* - 43%; *Agrostis* - 57%
Ganton	*Poa annua* - 17%; *Agrostis* - 50%; Ryegrass - 3%; Clover - 1%
Hallowes	*Poa annua* - 20%; *Festuca* - 60%; Ryegrass - 15%; Dead - 5%
Hill Valley	*Poa annua* - 5%; *Agrostis* - 95%
Keighley	*Poa annua* - 65%; *Agrostis* - 28%; Dead - 7%
Lindrick (1)	No readings
Lindrick (2)	*Poa annua* - 20%; *Agrostis* - 49%; *Fescue* - 31%
Moor Allerton	*Poa annua* - 61%; *Agrostis* - 31%; Dead - 2%; Bare - 6%
Moor Hall	*Poa annua* - 67%; *Agrostis* - 31%; Dead - 1%; Bare - 1%
Moortown	*Poa annua* - 100%
Newcastle-u-Lyme	*Poa annua* - 37%; *Agrostis* - 56%; Dead - 2%; Ryegrass - 2%; Yorkshire Fog - 3%
Sandmoor	*Poa annua* - 97%; *Poa pretensis* - 3%
STRI Green	No readings
Sutton Park	*Poa annua* - 60%; *Agrostis* - 34%; *Fescue*- 2%; Dead - 2%

G.6 Moisture content

The following numbers are the moisture content of five sets of two cores taken on a single green at each course. The moisture contents are given as a percentage of the weight of the original mass of soil.

Austerfield Park	26.97, 18.21, 20.42, 24.19, 31.89
Belfry	22.18, 19.23, 22.01, 18.41, 19.33
Bingley	24.09, 27.67, 24.11, 29.57, 25.86
Birkdale	26.11, 22.96, 22.72, 26.17, 25.85
Crewe	24.81, 22.49, 23.90, 25.19, 23.17
Formby	26.41, 29.80, 28.69, 24.51, 26.40
Ganton	22.59, 25.12, 31.41, 24.09
Hallowes	25.13, 25.91, 27.19, 25.60, 34.86, 32.21
Hill Valley	12.69, 15.00, 18.27, 15.77, 21.32
Keighley	29.75, 30.57, 22.12, 21.30, 31.40
Lindrick (1)	33.06, 33.27, 33.26, 31.42, 32.35
Lindrick (2)	36.90, 35.22, 41.10, 38.62
Moor Allerton	12.96, 13.85, 14.10, 13.70, 13.35
Moor Hall	21.49, 24.33, 29.05, 26.58, 25.50
Moortown	44.97, 37.02, 42.53, 45.96, 42.80
Newcastle-u-Lyme	33.84, 35.93, 36.64, 33.13
Sandmoor	26.41, 25.35, 24.66, 24.90, 23.03
STRI Green	23.05, 24.66, 21.89, 21.33, 24.23
Sutton Park	30.84, 29.16, 31.55, 31.81, 22.59

G.7 Particle size Distribution

The following information details the particle size distribution of the ten cores taken from each green. The data is collated in the following order; stones (>8mm), coarse gravel (8 -4mm), fine gravel (4 - 2mm), very coarse sand (2 - 1mm), coarse sand (1 - 0.5mm), medium sand (0.50 - 0.25mm) fine sand (0.250 - 0.125mm), silt (0.050 - 0.002mm), clay (<0.002mm), loss on ignition (% of oven-dry fine-earth), calcium carbonate (% of air-dry fine earth), water dispersibility of the clay (%). The soil from each green is also classed in terms of texture. Fines are taken as fine sand, silt and clay and are written in italics for clarity.

Austerfield Park	0, 2, 1, 2, 6, 23, 21, *15, 12, 21*, 12.2, 0.1, 19. Sandy clay loam
Belfry	0, 5, 7, 4, 14, 38, 33, *8, 3, 0*, 4.1, 0, 0. Sand
Bingley	No readings

Birkdale	0, 0, 0, 0, 1, 20, 61, *4, 7, 7*, 6.1, 0.3, 0. Loamy sand
Crewe	0, 1, 2, 2, 3, 31, 32, *9, 11, 9*, 3.7, 0.1, 0. Loamy sand
Formby	0, 0, 0, 2, 5, 26, 54, *3, 5, 5*, 6.4, 0.2, 0. Sand
Ganton	0, 0, 0, 2, 9, 29, 36, *11, 5, 8*, 6.1, 0, 0. Loamy sand
Hallowes	0, 2, 1, 3, 9, 15, 9, *9, 31, 24*, 5.6, 0.1, 30. Loam
Hill Valley	0, 1, 1, 1, 7, 48, 33, *5, 3, 3*, 2.8, 0, 0. Sand
Keighley	No readings
Lindrick (1)	0, 0, 0, 2, 10, 20, 15, *10, 22, 21*, 8.4, 9.8, 18. Sandy clay loam
Lindrick (2)	0, 0, 0, 1, 11, 30, 19, *9, 17, 13*, 9.8, 3.0, 7. Sandy loam
Moor Allerton	0, 4, 11, 13, 38, 28, 9, *3, 4, 5*, 2.1, 0, 0. Sand
Moor Hall	0, 0, 1, 4, 11, 29, 25, *11, 12, 8*, 6.5, 0.2, 0. Loamy sand
Moortown	0, 1, 2, 7, 18, 20, 20, *5, 13, 17*, 3.0, 0.3, 21. Sandy loam
Newcastle-u-Lyme	0, 0, 1, 3, 8, 29, 27, *6, 14, 13*, 7.3, 0.1, 30. Sandy loam
Sandmoor	1, 0, 1, 4, 10, 20, 24, *16, 12, 14*, 6.3, 0.1, 46. Sandy loam
STRI Green	No readings
Sutton Park	0, 0, 1, 2, 7, 34, 31, *8, 12, 6*, 7.9, 0.1, 0. Loamy sand

G.8 Surface evenness (levels apparatus)

The following information details the ten readings of the vertical displacements of the ten rods located on the profile gauge described in Chapter 2. The readings are given in millimetres.

Austerfield Park

1. 2, 2, 1, 2, 0, 0, 1, 0, 0, 0
2. 0, 2, 3, 3, 4, 3, 4, 4, 2, 2
3. 0, 2, 1, 0, 1, 2, 3, 3, 2, 1
4. 3, 3, 3, 2, 2, 0, 2, 2, 1, -1
5. 1, 1, 2, 3,4, 3, 4, 3, 1, 1
6. 1, 1, 2, 2, 2, 3, 4, 3, 3, 0
7. 0, 1, 2, 1, 1, 0, 3, 2, 2, 2
8. 1, 2, 3, 2, 3, 2, 4, 3, 0, 0
9. 2, 0, 2, 1, 4, 2, 3, 4, 2, 2
10. 2, 3, 3, 1, 4, 3, 5, 3, 5, 2

Belfry

1. 1, 1, 1, -1, -1, 0, 0, 0, 2, 0
2. 0, 1, 1, 0, 0, 0, 1, 0, 1, 0
3. -1, 0, 0, 1, 0, 1, 1, 0, 1, 1
4. 0, 0, 1, 0, 0, 0, 1, 1, 1, 0
5. -1, 0, 1, 0, 0, 1, 3, 1, 1, 0
6. 0, 0, 1, 0, 0, 1, 3, 1, 0, 0
7. 0, 0, 0, 0, 0, 0, 1, 1, 3, 1
8. 0, 0, 1, 1, 1, 0, 1, 0, 1, 0
9. 2, 0, 1, 1, 0, 0, 1, 2, 2, 1
10. 0, 2, 2, 1, 2, 1, 1, -1, 0, 0

Bingley

No readings

Birkdale

No readings

Crewe

1. 1, 0, 1, 2, 1, 2, 1, 0, 1, 1
2. 0, 1, 0, -1, 0, 0, -1, 0, -1, -1
3. 0, 0, 1, -1, -1, -1, -1, 0, 0, 0
4. 1, 0, 1, 0, -1, -1, 0, 0, -1, 0
5. 0, 0, 2, 0, 0, -1, 0, -1, 0, -1
6. 2, 0, 0, 0, 0, -1, 0, -1, 0, 0
7. 0, 1, 2, 1, 1, 1, 1, 0, 0, 0
8. -1, 2, 2, 1, 2, 2, 1, 1, 0, 0
9. 0, 1, 1, 1, 0, 0, 1, 0, 0, 0
10. -1, -1, 0, 0, -1, -1, 1, 0, 0, 0

Formby

1. -2, 0, 0, -1, -1, 0, 0, 0, 0, 0
2. -1, 0, 0, 1, 1, 0, 0, 0, 1, 2
3. 0, 0, 0, 0, 0, 1, 1, 0, 1, 1
4. 0, 0, 0, -1, -1, 0, -1, -1, -2, -1
5. -1, 0, 0, 0, 0, 0, -1, 0, 0, 1
6. 0, 0, 1, 1, 0, 0, 0, 0, 2, 1
7. 0, 0, 0, 0, 0, 0, 0, 0, 0, 1
8. 1, 0, 0, -1, 0, 0, 0,0, 0, 0
9. 0, 0, 0, -1, -1, 0, 0, 0, 0, 0
10. -1, 0, -1, 0, -1, -1, 0, -1, 0, 1

Ganton

1. 0, 0, -1, 0, 0, 0, 0, 1, 0, 0
2. 1, -1, 0, -1, -1, 0, -1, -1, 0, 0
3. 0, 1, 0, 0, -1, -1, -1, -1, 0, -1
4. 0, 0, 0, 0, 0, 0, 0, -1, 1, 0
5. 0, 0, -1, -1, -1, -1, -1, 0, 0, 1
6. 0, 0, 0, 0, -1, 0, -1, 0, 0, 0
7. -1, 0, -1, -1, -1, -1, -1, 0, 0, 0
8. 0, 0, 0, 0, 0, -1,-1, 0, 0, 0
9. 0, 1, 0, 0, 0, 0, 0,0,0, 0, 0
10. 2, 2, 1, 1,0, 0, 1, 1, -1, 0

Hallowes

1. 2, 3, 4, 2, 2, 2, 1, 0, -1, 3
2. 0, 1, 2, 2, 2, 0, 1, 2, 2, 3
3. 3, 3, 1, 0, 3, 3, 3, 1, 0, 0
4. 1, 3, 5, 3, 3, 2, 2, 2, 2, 1
5. 2, 2, 3, 3, 2, 2, 2, 1, 0, 0
6. 1, 1, 1, 0, 1,0, -1, 0, 0, -1
7. 1, 1, 1, 1, 1, 0, 0, 1, 1, 1
8. -1, 0, 0, -1, 0, 0, 0, 0, 0, 0
9. 2, 2, 2, 0, 1, 0, 0, 0, -1, 0
10. 1, 0, 0, 0, 0, 0, 1, 3, 2, 0

Hill Valley

1. 0, -1, 0, -1, -1, -1, 1, 0, 0, 0
2. -1, -2, 0, 1, -1, -1, 0, 0, 0, 1
3. 0, 0, 0, 1, 1, 1, 0, -1, 1, 0
4. 0, 0, 0, 0, 0, 1, 2, 1, 0, 0
5. 0, 1, 1, 1, 0, 1, 0, 0, 1, 0
6. 0, -1, 0, 0, 1, 0, 0, 1, 1, 1
7. 0, -1, -1, -1, -1, -2, -1, 0, 0, 0, 0
8. -1, -1, 0, -1, -1, -1, 0, -1, 0, 1
9. -1, -1, -1, -1, -1, 0, 0, 0, 0, 1
10. 0, -1, -1, 0, 0, 0, 0, 0, 1, 0

Keighley

1. 2, 2, 0, 0, -1, -1, -1, -1, 0, -2
2. -1, -1, 0, -1, -2, -1, 0, -1, 0, -1
3. 0, 0, 1, 0, -1, 1, 1, 0, 0, 0
4. 1, 2, 1, 0, -1, -2, 1, -3, -1, 0
5. 1, 1, 1, 0, 1, 2, 2, 4, 2, 2
6. 0, 0, 0, -1, -1, 0, 1, 1, 2, 1
7. -1, -1, 0, -2, -1, -1, -1, -2, 0, -1
8. 0, 0, -1, -2, -2, -2, -1, 0, -2, 0
9. 0, 0, 0, 0, 0, -1, 0, -1, 1, 0,
10. 1, 1, 1, 0, 0, 0, 1, 1, 1, 0

Lindrick (1)

1. 0, 0, 1, 0, 0, 0, -1, -1, -1, 0
2. 2, 2, 0, 0, 0, 1, 0, -1, 0, 1
3. 0, 0, 1, 0, 0, 0, 0, 1, 1, 1, 1
4. 0, 1, 1, 0, 0, 0,0, 1, 0, 0
5. 1, 2, 2, 0, 1, 1, 1, 2, 1, 2

6. 0, 0, 0, -1, 0, -1, 0, 0, 0, 1
7. 0, 0, 0, 0, 0, 0, -2, 0, -1, 0
8. 0, 1, 1, 0, 0, 0,0, -1, -2, 0
9. 0, 0, 1, 0, 1, 0, 0, 0, 0, 1
10. 0, 0, 0, 0, 0, 0, 0, 0, -1, 0

Lindrick (2)

1. 0, 1, 0, 0, 0, 0, 0, 0, 0, 0
2. 0, -1, 0, -1, 0, -1, 0, -1, -1, -1
3. 1, 1, 0, 0, 0, 0, 0, 0, -1, 0
4. 0, 0, 0, 0, 0, 0, 0, 0, 0, 0
5. 0, 0, 1, -1, 0, 0, 0, 0, 0, 0
6. 1, 1, 0, 0, 0, 0, 0, 0, 1, 0
7. 0, 0, 0, 1, 0, 0, 0,0, -1, -2
8. 1, 0, 0, 0, 0, -1, 0, 0, 0,0
9. -1, 0, 0, 0, 0, 0, -1, 0, -1, 0
10. 0, 0, 0, 0, 0, 0, 0, -1, 0, 0

Moor Allerton

1. 1, 4, 3, 1, 1, 2, 3, 2, 2, 1
2. 4, 3, 2, 1, 2, 3, 4, 4, 3, 2
3. 0, 2, 1, 0, 1, 2, 0, 1, 1, 3
4. 3, 1, 1, 0, 1, 0, 2, 1, 3, 3
5. -1, 0, -1, -1, -1, -1, 0, 1, 1, 2
6. 0, 2, 3, 0, 3, 4, 2, 1, 1, 0
7. 0, 1, 0, 0, -1, -1, -1, -2, -1, 0
8. 2, 3, 3, 3, 2, 2, 2, 1, 1, 0, 0,
9. 1, 1, 2, 0, -1, -1, 3, -1, -2, 0
10. 1, 1, 2, 2, 1, 0, 0, 2, 1, 0

Moor Hall

1. 1, 1, 0, 0, 1, 0, 0, 1, 0, 0
2. 0, 0, 0, 0, 0, 0, 1, 0, 0, -1
3. 1, 1, 0, 0, 0, 0, 0, 0, 0, 0
4. 0, 0, -1, -1, 0, 0, -2, -1, 0, 0
5. 1, 0, 0, -1, 0, 0, -1, 0, 0, 0
6. 0, 0, 0, 0, 0, -1, -1, -1, 0, 0
7. 0, 0, 0, 1, 0, 0, 0, 1, 0, 0
8. 2, 0, 1, 2, 1, 1, 0, 1, 1, 0
9. 0, -1, 0, 0, -1, 0, 0, 1, 1, 0
10. -1, -1, 0, 0, -1, 0, 0, 1, 1, 0

Moortown

1. 0, 0, 0, 0, 1, 0, 0, 0, 0, 1
2. -1, 0, 0, 0, 0, 0, 0, 0, 1, 1
3. 1, 2, 1, 0, 1, 0, 1, 0, -1, 0
4. 1, 1, 1, 0 ,0, 0, 0, 0, -1, 0
5. 0, 1, 0, 1, 1, -1, 0, -2, -1, 0
6. -1, -1, 0, 2, -1, 0, 0, 0, 0, 0
7. 1, 2, 1, 0, 2, 2, 0, 0, -1, 0
8. 1, 0, 1, 1, 0, 1, 1, 1, 0, 1
9. 1, 3, 3, 1, 1, 1, 3, 1, 0, 1
10. -1, 2, 1, 0, 0, 0, 0, 0, 0, 1

Newcastle-u-Lyme

1. -1, -1, 0, 1, 0, 1, 1, 0, 0, 1
2. 0, 0, 0, 1, 1, 2, 1, 0, 1, 0
3. 1, 2, 1, 1, 1, 1, 1, 1, 1, 1
4. 0, 0, 1, 1, 1, 2, 1, 0, 1, 1
5. 0, 0, 0, 0, 0, 0, 0, -1, 0, 0
6. 0, 0, 0, 0, 0, 0, 0, 0, 1, 1
7. 0, -1, 0, 0, 0, -1, -1, 0, 1, 1
8. 1, 1, 0, -1, -1, 0, -1, -1, 0, 1
9. 2, 2, 1, 1, 2, 1, 2, 1, 1, 0
10. 1, 0, 0, 0, 0, 0, 0, 0, 0, 1

Sandmoor	1. 1, 0, 1, 0, 3, 3, 3, 2, 1, 2 2. 1, 1, 1, 0, 0, 0, 2, 2, 1, 1 3. 1, 1, 1, 0, 0, 0, 2, 2, 0, 0 4. 1, 1, 2, 1, 2, 2, 1, 2, 1, 2 5. 4, 3, 3, 1, 2, 1, 1, 1, 0, 0 6. 2, 2, 2, 2, 1, 0, 0, -1, 0, 0 7. 1, 1, 2, 2, 3, 2, 2, 1, 0, 0 8. 3, 2, 2, 1, 3, 1, 2, 1, 0, 0 9. 1, 1, 1, 1, 0, -1, 1, 3, 1, 1 10. 2, 4, 2, 0, 3, 1, 1, 2, 1, 1
STRI Green	1. 0, 1, 0, 1, 2, 1, 1, 1, 0, 1 2. 0, -1, 2, -1, 0, 0, 0, 1, 0, 1 3. 0, 2, 3, 2, 1, 2, 1, 0, 0, 1 4. 2, -1, 0, 1, 2, 1, 2, 0, 0, 1 5. -1, -1, 0, -1, -1, 0, 0, 0, 1, 0 6. 2, 3, 1, 0, 2, 0, 1, 0, 3, 0 7. 1, 2, 1, 0, 2, 2, 0, 0, 1, 1 8. 1, 1, 1, 1, 2, 1, 1, 0, 1, 1 9. 1, 0, 0, -1, -1, 1, 0, 1, 0, 1 10. -1, -2, 0, -1, 0, -1, 0, -1, 0, 1
Sutton Park	1. 0, 0, 1, 1, 1, 0, 0, 0, 0, 0 2. 1,1, 1, 1, 1, 0, 0, 1, 1, 1 3. 0, 0, 1, 0, 0, 0, 1, 1, 1, 1 4. 0, 1, 1, 1, 1, 1, 1, 1, 0, 0 5. 0, -1, 0, 0, 0, -1, -1, -1, 0, -1 6. 1, 1, 1, 1, 2, 1, 1, 1, 2, 1 7. -1, 0, 2, 1, 1, 1, 2, 2, 1, 1 8. 1, 0, 0, 0, 0, 0,1, 0, 0, 1 9. 0, -1, 0, 0, 0, 0, 0, 0, 0, 0 10. 0, 0, 1, 1, 0, 0, 0, 1, 1, 1

G.9 Stimpmeter

This section contains the distances rolled by golf balls across the green and set in motion using the stimpmeter. There are six readings on each line. The first two are the distances rolled by two balls travelling along exactly the same line while the third number indicates the distance between the resting positions of the two balls. The second set of three numbers on the same line is the replicate of the readings in the opposite direction.

Austerfield Park	1.98, 1.92, 0.10	1.90, 1.90, 0
	1.73, 1.79, 0.09	1.97, 1.80, 0.17
	1.42, 1.57, 0.17	2.22, 2.14, 0.10
	1.74, 1.67, 0.08	1.25, 1.36, 0.13
	1.70, 1.70, 0	1.91, 1.91, 0
Belfry	1.80, 2.09, 0.29	2.02, 1.99, 0.08
	2.00, 1.99, 0.08	2.06, 2.01, 0.10
	1.88, 1.98, 0.10	2.10, 1.92, 0.10
	2.15, 2.30, 0.15	2.00, 2.05, 0.12
	2.07, 2.15, 0.15	2.07, 2.06, 0.05
Bingley	2.80, 2.98, 0.23	1.71, 1.74, 0.10
	2.82, 2.68, 0.35	1.58, 1.63, 0.05
	2.77, 2.87, 0.12	1.70, 1.77, 0.07
	2.73, 2.93, 0.23	1.66, 1.77, 0.17
	2.57, 2.68, 0.35	1.62, 1.71, 0.10

Birkdale	No readings	
Crewe	2.21, 2.21, 0.11	2.43, 2.51, 0.08
	2.15, 2.23, 0.15	2.25, 2.07, 0.18
	2.38, 2.42, 0.04	2.33, 2.24, 0.09
	2.35, 2.34, 0.20	2.50, 2.41, 0.24
	2.39, 2.49, 0.12	2.20, 2.42, 0.34
Formby	2.39, 2.54, 0.25	2.42, 2.44, 0.07
	2.67, 2.73, 0.08	2.55, 2.62, 0.07
	2.41, 2.55, 0.08	2.41, 2.45, 0.04
	2.40, 2.40, 0	2.37, 2.39, 0.05
	2.43, 2.48, 0.18	2.13, 2.19, 0.14
Ganton	2.12, 2.15, 0.03	3.07, 3.14, 0.11
	2.19, 1.96, 0.28	3.24, 3.21, .021
	2.02, 2.05, 0.15	3.45, 3.46, 0.30
	1.98, 1.91, 0.19	2.99, 3.09, 0.36
	2.19, 2.21, 0.28	3.00, 3.26, 0.26
Hallowes	No readings	
Hill Valley	2.40, 2.62, 0.31	1.83, 2.08, 0.27
	2.50, 2.55, 0.22	1.87, 2.12, 0.25
	2.55, 2.42, 0.21	2.13, 2.13
	2.63, 2.66, 0.18	2.05, 2.18, 0.26
	2.76, 2.93, 0.17	2.00, 1.91, 0.09
Keighley	2.16, 2.17, 0.14	2.63, 2.74, 0.29
	2.19, 2.23, 0.10	2.37, 2.47, 0.10
	2.26, 2.36, 0.10	2.30, 2.40, 0.11
	2.11, 2.28, 0.17	2.29, 2.54, 0.29
	2.04, 2.06, 0.06	2.64, 2.68, 0.08
Lindrick (1)	2.90, 3.00, 0.10	1.91, 1.83, 0.09
	2.54, 2.91	1.75, 1.83
	2.54, 2.46, 0.20	1.21, 2.27
	2.87, 3.35, 0.10	1.99, 2.29, 0.26
	2.85, 3.04, 0.21	1.97, 2.00, 0.04
Lindrick (2)	2.05, 2.26, 0.25	1.89, 2.06, 0.18
	2.63, 2.63, 0.15	2.03, 2.05, 0.05
	3.00, 3.16, 0.16	2.12, 2.12, 0.12
	2.77, 2.74, 0.03	2.11, 2.11, 0.20
	3.06, 2.86, 0.26	2.11, 2.24, 0.13
Moor Allerton	2.43, 2.53, 0.1	1.87, 2.01, 0.14
	2.35, 2.50, 0.31	1.82, 1.87, 0.09
	2.91, 3.02, 0.11	1.72, 1.81, 0.10
	2.80, 2.94, 0.1	1.97, 1.99, 0.20
	2.96, 3.10, 0.14	1.85, 1.86, 0.06
	2.54, 2.83, 0.29	1.89, 1.96, 0.07
	2.54, 2.63, 0.18	1.59, 1.69, 0.11
	2.70, 2.93, 0.2	1.64, 1.69, 0.09
	2.88, 2.89, 0.15	1.67, 1.75, 0.16
	2.79, 3.63, 0.29	1.51, 1.51, 0.12
Moor Hall	2.06, 2.11, 0.07	2.72, 3.06, 0.38
	2.08, 2.07, 0.04	2.63, 2.83, 0.20
	2.13, 2.20, 0.07	2.70, 2.85, 0.15

	2.08, 2.04, 0.28	2.57, 2.45, 0.15
	2.01, 1.97, 0.09	2.52, 2.52, 0.13
Moortown	2.28, 2.34, 0.07	1.89, 1.95, 0.10
	2.55, 2.69, 0.15	2.09, 2.05, 0.10
	2.75, 2.67, 0.23	1.99, 1.83, 0.16
	2.11, 2.18, 0.18	2.07, 1.85, 0.35
	2.90, 2.90, 0	2.23, 2.19, 0.11
Newcastle-u-Lyme	2.30, 2.39, 0.09	2.47, 2.42, 0.14
	2.15, 2.24, 0.09	2.12, 2.20, 0.01
	2.15, 2.15, 0	2.17, 2.13, 0.04
	1.84, 2.07, 0.24	2.12, 2.12, 0
	1.98, 1.84, 0.14	1.95, 2.15, 0.20
Sandmoor	2.05, 2.01, 0.13	2.39, 2.39, 0
	2.11, 2.13, 0.11	
	2.62, 2.75, 0.13	
	2.17, 2.17, 0.05	2.25, 0.15, 2.39
	2.01, 2.15, 0.17	2.02, 2.01, 0.08
STRI Green	2.00, 1.96, 0.20	2.06, 1.96, 0.18
	2.14, 2.15, 0.33	2.00, 1.87, 0.17
	2.54, 2.36, 0.36	1.98, 1.88, 0.10
	2.22, 2.31, 0.10	2.21, 2.21, 0.05
	2.25, 2.21, 0.32	1.88, 1.79, 0.20
Sutton Park	2.01, 2.00, 0.10	2.23, 2.13, 0.10
	1.95, 1.88, 0.11	2.22, 2.23, 0.08
	1.97, 2.08, 0.11	2.34, 2.31, 0.12
	1.99, 2.06, 0.07	2.18, 2.24, 0.14
	1.84, 1.98, 0.14	2.26, 2.35, 0.12

G.10 Friction

This section contains the results from the sliding friction apparatus, measured in Newtons.

Austerfield Park	75, 70, 80, 80, 75, 75, 75, 80, 55, 55
Belfry	80, 80, 85, 89, 79
Bingley	80, 80, 85, 80, 78
Birkdale	No readings
Crewe	95, 90, 95, 90, 95
Formby	100, 70, 90, 85, 90
Ganton	75, 72, 71, 70, 78
Hallowes	70, 60, 50, 50, 65, 70, 70, 55, 50, 60
Keighley	86, 73, 80, 78, 70, 75, 78, 84, 82, 85, 79, 80, 77, 79, 88, 90, 81, 76, 71, 85
Hill Valley	80, 82, 85, 75, 75
Lindrick (1)	85, 70, 75, 70, 75, 75, 70, 60, 70, 60
Lindrick (2)	82, 85, 81, 90, 85
Moor Allerton	90, 83, 75, 89, 78, 82, 85, 80, 74, 88, 85, 75, 70, 84, 82, 71, 68, 82, 68, 75
Moor Hall	86, 90, 88, 85, 85
Moortown	70, 65, 75, 75, 80, 80, 80, 75, 75, 85
Newcastle-u-Lyme	82, 85, 85, 85, 90
Sandmoor	70, 65, 60, 70, 70, 75, 75, 75, 75, 85
STRI Green	50, 55, 45, 50, 45,
Sutton Park	80, 80, 90, 90, 92

Appendix H - The regression coefficients for the relationships between velocity, angle and spin before and after impact for rolling impacts.

The following tables contain data complimentary to the information in Tables 3.6, 3.7 and 3.8. Using the graphs in Appendix H, impacts in which slip occurred throughout impact were found and removed from the sets of data in Appendix E. Stepwise regressions were then carried out on the resultant sets of data, the results of which are shown here.

Velocity after impact									
Course	Int	C_V	dC_V	C_Θ	dC_Θ	C_ω	dC_ω	r	p
Austerfield	2.92	0.18	0.03	FIXED ANGLE		.0029	.0005	.72	0.0001
Belfry	13.52	0.20	0.04	-0.27	0.04	.006	.001	.93	0.0001
Bingley	2.47	0.24	0.03	FIXED ANGLE		.003	.001	.86	0.0001
Crewe	12.38	0.10	0.02	-0.16	0.01	.0042	.0004	.96	0.0001
Formby	3.05	0.19	0.02	FIXED ANGLE		.003	.001	.92	0.0001
Ganton	3.88	0.17	0.02	FIXED ANGLE		**.0052**	**.0007**	.87	0.0001
Hallowes	2.45	0.25	0.04	FIXED ANGLE		.004	.001	.88	0.0001
Hill Valley	13.27	0.12	0.06	-0.20	0.04	.0058	.0014	.93	0.0001
Keighley	6.45			FIXED ANGLE		.006	.001	.88	0.0001
Lindrick	3.80	0.14	0.04	FIXED ANGLE		.0028	.0006	.72	0.0001
M. Allerton	5.29			FIXED ANGLE		.004	.001	.62	0.0001
Moor Hall	5.35	0.06	0.02	FIXED ANGLE		.0052	.0004	.84	0.0001
Moortown									
Newcastle	13.21	0.05	0.02	-0.16	0.02	.0043	.0004	.93	0.0001
Sandmoor	3.78	0.16	0.02	FIXED ANGLE		.0044	.0006	.87	0.0001
Sutton Park	12.32	0.13	0.03	-0.19	0.03	**.005**	**.001**	.86	0.0001

TABLE H.1. The coefficients for the regressions between the velocity of the rebounding ball and the incoming velocity, angle and spin for rolling impacts only. The coefficients in italics are significantly different from the corresponding coefficients in Table 3.6 where all impacts were included in the regression.

Angle after impact									
Course	Int	C_V	dC_V	C_Θ	dC_Θ	C_ω	dC_ω	r	p
Austerfield	25.80	1.1	0.2	FIXED ANGLE		-0.024	0.004	.77	0.0001
Belfry	-32.76	0.7	0.3	1.5	0.3	-0.048	0.009	.85	0.0001
Bingley	28.99	0.6	0.2	FIXED ANGLE		-0.032	0.006	.75	0.0001
Crewe	-23.69	1.0	0.2	1.1	0.1	-0.034	0.004	.94	0.0001
Formby	34.74	0.4	0.1	FIXED ANGLE		-0.029	0.007	.65	0.0001
Ganton	25.26	0.7	0.2	FIXED ANGLE		-0.030	0.005	.84	0.0001
Hallowes									
Hill Valley	-42.07	1.3	0.5	1.4	0.3	-0.029	0.012	.89	0.0001
Keighley	16.27	1.5	0.2	FIXED ANGLE		-0.062	0.009	.91	0.0001
Lindrick	42.66			FIXED ANGLE		-0.024	0.005	.68	0.0001
M. Allerton	-13.27	3.1	0.5	FIXED ANGLE		-0.04	0.01	.86	0.0001
Moor Hall	14.10	1.5	0.3	FIXED ANGLE		-0.043	0.005	.86	0.0001
Moortown	17.21	1.6	0.3	FIXED ANGLE				.62	0.0001
Newcastle	-53.67	1.2	0.2	1.5	0.2	-0.038	0.005	.90	0.0001

Angle after impact -continued									
Course	Int	C_V	dC_V	C_Θ	dC_Θ	C_ω	dC_ω	r	p
Sandmoor	35.66	6.6	0.2	FIXED ANGLE		-0.028	0.006	.73	0.0001
Sutton Park	-50.38	1.2	0.2	1.7	0.12	**--0.046**	**0.006**	.92	0.0001

TABLE H.2. The coefficients for the regressions between the angle of rebound and the incoming velocity, angle and spin for rolling impacts only. The coefficients in italics are significantly different from the corresponding coefficients in Table 3.7 where all impacts were included in the regression.

Spin after impact									
Course	Int	C_V	dC_V	C_Θ	dC_Θ	C_ω	dC_ω	r	p
Austerfield	165.2	5.0	1.0	FIXED ANGLE		0.12	0.02	.61	0.0001
Belfry	369.3					0.87	0.05	.92	0.0001
Bingley	100.3	11.0	1.0	FIXED ANGLE		0.21	0.04	.89	0.0001
Crewe	442.7	3.7	1.6	**-5.0**	**0.9**	**0.32**	**0.03**	.88	0.0001
Formby	112.2	8.4	0.6	FIXED ANGLE		**0.17**	**0.05**	.93	0.0001
Ganton	187.3	6.4	1.2	FIXED ANGLE		**0.26**	**0.04**	.84	0.0001
Hallowes	90.3	9.6	1.6	FIXED ANGLE				.80	0.0001
Hill Valley	9.56	16.6	3.6			0.70	0.06	.85	0.0001
Keighley	256.6			FIXED ANGLE		0.27	0.04	.78	0.0001
M. Allerton	217.5			FIXED ANGLE		0.18	0.03	.72	0.0001
Moor Hall	279.0			FIXED ANGLE		0.22	0.02	.85	0.0001
Moortown									
Newcastle	681.6			-8.3	1.0	0.21	0.02	.90	0.0001
Sandmoor	198.7	4.4	0.9	FIXED ANGLE		0.19	0.03	.79	0.0001
Sutton Park	482.5	5.6	2.7	**-6.3**	**2.2**	**0.61**	**0.05**	.85	0.0001

TABLE H.3. Tables containing the regession coefficients of the equations relating the spin after impact to the initial velocity and spin for rolling impacts only.

Appendix J - The equations of motion in a model of oblique impact in which the forces are proportion to the area of contact.

This model was first used by Rickerby and Macmillan to calculate the volume of the crater caused by the impact of a steel sphere on a rigid-plastic surface. Near the beginning of the impact the sphere is in contact with the whole of the surface of the crater formed by the impact and the equations of motion are,

$$m\frac{d^2x}{dt^2} = -\mu P \qquad \text{eqn. J.1}$$

$$m\frac{d^2y}{dt^2} = P \qquad \text{eqn. J.2}$$

where $P = \pi a^2 P_d$. P_d is the "dynamic hardness" and is related to the properties of the surface. At a later time in the impact the equations of motion become more complex and are,

$$m\frac{d^2x}{dt^2} = -P\sin(\Theta_i + \beta) - \mu P\cos(\Theta_i + \beta) \qquad \text{eqn. J.3}$$

$$m\frac{d^2y}{dt^2} = P\cos(\Theta_i + \beta) - \mu P\sin(\Theta_i + \beta) \qquad \text{eqn. J.4}$$

where $$P = P_d(A_1\sin(\gamma - \Theta_i) + A_2\cos\gamma \qquad \text{eqn. J.5}$$

The areas A_1 and A_2, β and γ are found in terms of the depth of the crater l, the radius of the ball r and the angle of incidence. These are,

$$\gamma = \sin^{-1}\left\{\frac{l - r(1 - \cos\Theta_i)}{2r\sin\beta}\right\}$$

$$\beta = \sin^{-1}\frac{1}{2r}\{(l - r(1-\cos\Theta_i))^2 + (a - r\sin\Theta_i)^2\}^{\text{™}} \qquad \text{eqn. J.6}$$

$$A_1 = \frac{r^2}{2}(\phi_1 - \sin\phi_1) \qquad \text{eqn. J.7}$$

$$\phi_1 = 2\cos^{-1}\left\{\frac{r - l}{\cos\Theta_i}\right\} \qquad \text{eqn. J.8}$$

$$A_2 = \frac{a^2}{2}(2\pi - \phi_2 + \sin\phi_2) \qquad \text{eqn. J.9}$$

$$\phi_2 = 2\cos^{-1}\{(l - r)\tan(\frac{\Theta_i}{a})\} \qquad \text{eqn. J.10}$$

$$a = \{l(2r - l)\}^{\text{™}} \qquad \text{eqn. J.11}$$

The equations above were calculated iteratively using a program written in BASIC for the Apple Macintosh. The program is shown below.

```
PRINT TAB(1);"This program uses the Hutchings equations (using m and r for"
PRINT TAB(1);"a golf ball to calculate the velocities and angles of a sphere"
PRINT TAB(1);"on a rigid- plastic surface after impact. There is also a"
PRINT TAB(1);"modification for the rebound of the ground which incorporates"
PRINT TAB(1);"a spring constant, k."
REM***::::::::::::::::::::::::::::::::::::::::::::::::::Read in the initial values::::::::::::::::::::::::::::::::::::::::::::
READ Vi,I,mu,L,TSUM,H
READ PD,K
READ FSUM,XSUM,ZSUM,YSUM,XDDO,YDDO,WSUM,WDDO,WDSUM
REM***::::::::::::::::::::::::::::::::::::::::::::::::::::::::::::::::::::::::::::::::::::::::::::::::::::::::::::::::::::::::::::
PRINT ":::::::::::::::::::::::::::  Vi= ";Vi;", K= ";K;", PD= ";PD;"  ::::::::::::::::::::::::::::::::::::::"
REM***The following equations calculate the accelerations in the X and Y direc-
REM***tions. The forces essentially arise from the a force normal to the area
REM***of contact. The areas of contact are approximated. The program jumps
REM*** to a subroutine when the impact is not detached.
```

```
REM**:::::::::::::::::::::::::::::::::::::::::::::The main program:::::::::::::::::::::::::::::::::::::::::::::::::::::::
XDSUM=Vi*COS(I)
YDSUM=Vi*SIN(I)
10 I=ATN(YDSUM/XDSUM)
A=SQR(L*(.0426-L))
K1=1-L*46.948
IF K1 =1 THEN 400
DELTA=-ATN(K1/SQR(-K1*K1+1))+1.5708
GOTO 405
400 DELTA =0
405 IF ABS(I)>DELTA THEN GOSUB 1050 ELSE 410
GOTO 660
410 N=N+1
IF A=0 THEN 470
C1=(L-.0213)*TAN(I)/A
IF C1>1 OR C1<-1 THEN 470
PHI=2*(-ATN(C1/SQR(-C1*C1+1))+1.5708)
GOTO 480
470 PHI=0
480 A2=(6.283195-PHI+SIN(PHI))*A*A*.5
C2=(1-46.948*L)/COS(I)
IF C2>1 OR C2<-1 THEN 530
THETA=2*(-ATN(C2/SQR(-C2*C2+1))+1.5708)
GOTO 540
530 THETA=0
540 A1=(SIN(THETA)-THETA)*.0002268
A1=ABS(A1)
C3=L-.0213*(1-COS(I))
C3=ABS(C3)
C4=SQR((A-.0213*SIN(I))^2+C3^2)*23.474
IF -C4*C4+1<0 THEN GOTO 620
B=ATN(C4/SQR(-C4*C4+1))
C5=C3*23.474/SIN(B)
IF -C5*C5+1<0 THEN GOTO 630
G=ATN(C5/SQR(-C5*C5+1))
GOTO 640
620 B=0
630 G=0
640 Q=K*L
P=PD*((A1*SIN(G-I))+(A2*COS(G)))
F=P+Q
m=(WDSUM-V/.0213)*H*1000
XDD=(-F*SIN(I+B+m)-mu*F*COS(I+B+m))*22.222
YDD=(F*COS(I+B+m)-mu*F*SIN(I+B+m))*22.222
WDD=mu*.0213*F/.0000082
PRINT "Calculations are being made"
660 REM***:::::::::::::::::::::::::::::::SIMPLE INTEGRATION ROUTINES:::::::::::::::::::::::::::
WD=(WDDO+WDD)*H*.5
W=(WDSUM+.5*WD)*H
WDDO=WDD
WDSUM=WDSUM+WD
WSUM=WSUM+W
XD=(XDDO+XDD)*H*.5
X=(XDSUM+.5*XD)*H
XDDO=XDD
XDSUM=XDSUM+XD
XSUM=XSUM+X
YD=(YDDO+YDD)*H*.5
Y=(YDSUM+.5*YD)*H
YDDO=YDD
```

```
YDSUM=YDSUM+YD
L=YSUM-Y
L=ABS(L)
YSUM=YSUM+Y
TSUM=TSUM+H
V=SQR(XDUM*XDSUM+YDSUM*YDSUM)
IF WDSUM-V/.0213<0 THEN m=(WDSUM-V/.0213)*H*100 ELSE m=0
IF I>0 AND ABS(I)>DELTA THEN 1000 ELSE 10
IF YSUM >0 THEN 1000 ELSE 10
REM***::::::::::::::::::::::::::::::::::::::OUTPUT OF DATA::::::::::::::::::::::::::::::::::::::::::::::::::::::::::::
1000 PRINT "ANGLE IN IS ",57.2957*-.7854;"DEGREES"
PRINT "VELOCITY IN IS",Vi;"M/S"
PRINT "ANGLE OUT IS  ",57.2957*ATN(YDSUM/XDSUM);"DEGREES"
PRINT "VEL OUT IS",SQR((XDSUM*XDSUM)+(YDSUM*YDSUM));"M/S"
PRINT "CONTACT TIME IS",TSUM/.001;"MILLISECS"
PRINT "FINAL SPIN IS",WDSUM
PRINT:PRINT
DATA 20,-.7854,0.5,0,0,1E-5
DATA 3E6,0
DATA 0,0,0,0,0,0,0,0,0,0
END
REM***::::::::::::::::::::This subroutine is used when the impact is not detached::::::::::::::::::
1050 G=0
P=3.141593*PD*A*A
B=0
Q=K*L
F=P+Q
XDD=-mu*282.0078*F
YDD=282.0078*F
WDD=mu*.0213*F/.0000082
PRINT "The impact is not detached"
RETURN
```

Appendix K - BASIC routines for calculating the rebound of a golf ball from a surface using visco-elastic models

K.1 A routine for solving differential equations using the Runga-Kutte fourth order set of equations

The folowing routine uses the Runga-Kutte fourth order set of equations to solve numerically a set of differential equations. The routine indicated by the command GOSUB 200 contains the equations to be solved.

```
FOR R=0 TO N
      LET y(R)=yo(R)
NEXT R
GOSUB 200
FOR R=0 TO N
      LET K1(R)=H*F(R)
      LET y(R)=yo(R)+K1(R)/2
NEXT R
GOSUB 200
FOR R=0 TO N
      LET K2(R)=H*F(R)
      LET y(R)=yo(R)+K2(R)/2
NEXT R
GOSUB 200
FOR R=0 TO N
      LET K3(R)=H*F(R)
      LET y(R)=yo(R)+K3(R)
NEXT R
GOSUB 200
FOR R=0 TO N
      LET yo(R)=yo(R)+(K1(R)+2*(K2(R)+K3(R))+H*F(R))/6
NEXT R
```

K.2 Kelvin-Voigt model of vertical impact

The equations of motion are shown in Chapter 5 (equation 5.15) and were translated into the format required in order to be solved using the routine above. These equations were located in a subroutine at the end of the program and were

F(0)=1 $\left(\frac{dt}{dt} = 1\right)$

F(1)=y(2) $\left(V = \frac{dy}{dt}\right)$

F(2)=-C1*y(1)-C2*y(2) $\left(\text{acceleration} = \frac{dV}{dt}\right)$

where C1 and C2 are the spring and damper constants, y(1) is the vertical displacement and y(2) is the vertical velocity. These equations were modified to incorporate an area of contact and required a separate set of equations for when the centre of the ball was below the level of the ground. These were,

area1=(.0426-y(1))*3.14159*y(1)
F(0)=1
F(1)=y(2)
F(2)=(-C1*y(1)-C2*y(2))*area1
for the centre of the ball above the level of the ground and,
area1=.0014253
F(0)=1
F(1)=y(2)
F(2)=(-C1*.0213-C2*y(2))*area1
for the centre of the ball below the level of the ground.

K.3 A two-layered viscoelastic model of vertical impact

The equations in the previous section were modified so that the surface was made up of two layers. The whole subroutine was written as follows,

```
200
REM**********************SUBROUTINE**************************
REM**************This section defines the equations used in the model**********
IF y(1)<0 THEN 1100
IF y(1)<L1 THEN 300
IF y(1)>L1 AND y(1)<L2 THEN 400
IF y(1)>L2 THEN 500

300 REM********THE BALL IS IN CONTACT WITH THE FIRST LAYER*********
IF y(1)<.0213 THEN 310 ELSE 320
310 REM***********The centre of the ball is above the level of the ground**********
area1=(.0426-y(1))*3.14159*y(1)
area2=0
area3=0
F(0)=1
F(1)=y(2)
F(2)=(-C1*y(1)-C2*y(2))*area1
GOTO 600

320 REM***********The centre of the ball is below the level of the ground***********
area1=.0014253
area2=0
area3=0
F(0)=1
F(1)=y(2)
F(2)=(-C1*.0213-C2*y(2))*area1
GOTO 600

400 REM***********THE BALL IS IN CONTACT WITH TWO LAYERS*********
IF y(1)<.0213 THEN 410
IF y(1)>.0213 AND y(1)-L1<.0213 THEN 420
IF y(1)>.0213 AND y(1)-L1>.0213 THEN 430
410 REM******The centre of the ball is above L1 and above the level of the ground*****
d=y(1)-L1
area3=0
area2=(.0426-d)*3.14159*d
area1=(.0426-y(1))*3.14159*y(1)-area2
F(0)=1
F(1)=y(2)
F(2)=(-C1*L1-C2*y(2))*area1- C3*y(2)*area2
GOTO 600

420 REM*****The centre of the ball is above L1 but below the level of the ground*****
d=y(1)-L1
area3=0
area2=(.0426-d)*3.14159*d
area1=.0014253
F(0)=1
F(1)=y(2)
F(2)=(-C1*(L1-y(1)-.0213)-C2*y(2))*area1- C3*y(2)*area2
GOTO 600
```

```
430 REM*****The centre of the ball is below L1 and below the level of the ground****
d=y(1)-L1
area3=0
area2=.0014253
area1=0
F(0)=1
F(1)=y(2)
F(2)=-C3*y(2)*area2
GOTO 600

600 REM**Next two lines set the vertical resistance to zero when it starts to become
negative.
IF F(2)<=0 THEN 700
700 RETURN
```

K.4 A two-layered visco-elastic model of oblique impact

The model of vertical impact above was modified to take into account horizontal forces and was used to simulate oblique impacts. F(3) and F(4) are the differential equuations for the horizontal velocity and acceleration while F(5) and F(6) represent the rotational velocity and acceleration. The whole program, including all printing and formatting statements is shown below.

```
REM************************IMPACT MODEL*****************************
REM*****************************S.J.Haake*******************************

N=6:                    REM**The number of dependent variables.
DIM y(N),yo(N),F(N)
C1=4E+08
C2=900000!
C3=0
C4=100000!
C5=0
C6=0
Vi=18
ANGi=1.308997
Wi=100
XF=.5:          REM**Maximum impact time of 500msecs
H=.0001:        REM**Step length of 0.1msecs
L1=.008:        REM**First discontinuity (mm)

PRINT "INITIAL CONDITIONS"
PRINT"Velocity = "Vi" m/sec;  Angle = "ANGi*57.29578" degrees"
PRINT"EQUATION PARAMETERS"
PRINT "spring constant = "C1";   dashpot constant = "C2
PRINT "Layer1 = "L1*1000" mm"
PRINT "        TIME        VEL        ANGLE        DEPTH        Spin"
PRINT"        (msecs)     (m/s)        deg          mm          rad/s"
PRINT"_____________________________________________________________"
10 Wi=-950
mu=.8:          REM** Coefficient of friction
I=0
yo(0)=0
yo(1)=0
yo(2)=Vi*SIN(ANGi)
yo(3)=0
yo(4)=Vi*COS(ANGi)
yo(5)=0
yo(6)=Wi
```

```
mm=0
m=0

REM**********************************STEP**************************
100 x=yo(3)
mm=m
IF yo(2)>0 THEN m=0 ELSE m=1
IF mm=0 AND m=1 THEN YMAX=yo(1)
V=SQR(yo(2)*yo(2)+yo(4)*yo(4))
ANG=ATN(yo(2)/yo(4))
PRINT USING "#######.###"; yo(0)*1000, V, ANG*57.2958, yo(1)*1000, yo(6),
F(6)/1E6
IF yo(0)>XF-.0000001 THEN 1000
FOR R=0 TO N
        LET y(R)=yo(R)
NEXT R
GOSUB 200
FOR R=0 TO N
        LET K1(R)=H*F(R)
        LET y(R)=yo(R)+K1(R)/2
NEXT R
GOSUB 200
FOR R=0 TO N
        LET K2(R)=H*F(R)
        LET y(R)=yo(R)+K2(R)/2
NEXT R
GOSUB 200
FOR R=0 TO N
        LET K3(R)=H*F(R)
        LET y(R)=yo(R)+K3(R)
NEXT R
GOSUB 200
FOR R=0 TO N
LET yo(R)=yo(R)+(K1(R)+2*(K2(R)+K3(R))+H*F(R))/6
NEXT R
GOTO 100
1000 PRINT "XF reached":PRINT "*****XF reached*****"
1100 PRINT:PRINT "The ball left the surface and the calculation stopped"
PRINT
"*****************************************************************"
PRINT USING "#######.###"; Wi, V, ANG*57.2958, yo(6), YMAX*1000,
Pitch*1000, yo(0)*1000
PRINT
"*****************************************************************"
IF Wi=-1000 THEN 1200
GOTO 10
1200 END

200 REM**********************SUBROUTINE**************************
REM *********This section defines the equations used in the model********
REM*************************************************************
IF y(1)<0 THEN 1100
IF y(1)<L1 THEN 300
IF y(1)>L1 THEN 400

300 REM********THE BALL IS IN CONTACT WITH THE FIRST LAYER*******
V=SQR(yo(2)*yo(2)+yo(4)*yo(4))
ANG=ATN(yo(2)/yo(4))
IF yo(6)>=V/.0213 THEN mu=0:yo(6)=V/.0213
IF yo(2)>0 THEN A=-1 ELSE A=1
```

```
IF y(1)<.0213 THEN 310 ELSE 320
310 REM*********The centre of the ball is above the level of the ground***********
state=1.1
area1=(.0426-y(1))*3.14159*y(1)
area2=0
area3=0
w1=1-y(1)/.0213
w2=SQR(1-w1*w1)
area4=.0004537*(ATN(w2/w1)-w1*w2)
area5=0
area6=0
dx=yo(3)-x
F(0)=1
F(1)=y(2)
F(2)=(-C1*y(1)-C2*y(2))*area1+A*.00852*ABS(F(6))*SIN(ABS(ANG))
F(3)=y(4)
F(4)=(-C1*dx-C2*y(4))*area4-.00852*ABS(F(6))*COS(ABS(ANG))
F(5)=y(6)
F(6)=117.37*mu*(ABS(F(2))*COS(ABS(ANG))+A*ABS(F(4))*SIN(ABS(ANG)))
GOTO 600
320 REM*********The centre of the ball is below the level of the ground**********
state=1.2
area1=.0014253
area2=0
area3=0
area4=.0007127
area5=0
area6=0
dx=yo(3)-x
F(0)=1
F(1)=y(2)
F(2)=(-C1*.0213-C2*y(2))*area1+A*.00852*ABS(F(6))*SIN(ABS(ANG))
F(3)=y(4)
F(4)=(-C1*dx-C2*y(4))*area4-.00852*ABS(F(6))*COS(ABS(ANG))
F(5)=y(6)
F(6)=117.37*mu*(ABS(F(2))*COS(ABS(ANG))+A*ABS(F(4))*SIN(ABS(ANG)))
GOTO 600

400 REM**********THE BALL IS IN CONTACT WITH TWO LAYERS*********
V=SQR(yo(2)*yo(2)+yo(4)*yo(4))
ANG=ATN(yo(2)/yo(4))
IF yo(2)>0 THEN A=-1 ELSE A=1
IF yo(6)>=V/.0213 THEN mu=0:yo(6)=V/.0213
IF y(1)<.0213 THEN 410
IF y(1)>.0213 AND y(1)-L1<.0213 THEN 420
IF y(1)>.0213 AND y(1)-L1>.0213 THEN 430
410 REM****The centre of the ball is above L1 and above the level of the ground****
state=2.1
d=y(1)-L1
area3=0
area2=(.0426-d)*3.14159*d
area1=(.0426-y(1))*3.14159*y(1)-area2
w1=1-y(1)/.0213
w2=SQR(1-w1*w1)
w3=1-d/.0213
w4=SQR(1-w3*w3)
area6=0
area5=.0004537*(ATN(w4/w3)-w3*w4)
area4=.0004537*(ATN(w2/w1)-w1*w2)-area5
dx=yo(3)-x
```

```
F(0)=1
F(1)=y(2)
F(2)=(-C1*L1-C2*y(2))*area1-C3*y(2)*area2 + A*.0085 *ABS(F(6))*
SIN(ABS(ANG))
F(3)=y(4)
F(4)=(-C1*dx-C2*y(4))*area4-C3*y(4)*area5-.00852*ABS(F(6))* COS(ABS(ANG))
F(5)=y(6)
F(6)=117.37*mu*(ABS(F(2))*COS(ABS(ANG))+A*ABS(F(4))*SIN(ABS(ANG))
GOTO 600

420 REM******The centre of the ball is above L1 but below the level of the ground****
state=2.2
d=y(1)-L1
area3=0
area2=(.0426-d)*3.14159*d
area1=.0014253
w3=1-d/.0213
w4=SQR(1-w3*w3)
area6=0
area5=.0004537*(ATN(w4/w3)-w3*w4)
area4=.0007127-area5
F(0)=1
F(1)=y(2)
F(2)=(-C1*(L1-y(1)-.0213)-C2*y(2))*area1-C4*y(2)*area2+A*.00852*ABS(F(6))*
SIN(ABS(ANG))
F(3)=y(4)
F(4)=(-C1*dx-C2*y(4))*area4-C3*y(4)*area5-.00852*ABS(F(6))*COS(ABS(ANG))
F(5)=y(6)
F(6)=117.37*mu*(ABS(F(2))*COS(ABS(ANG))+A*ABS(F(4))*SIN(ABS(ANG)))
GOTO 600

430 REM*****The centre of the ball is below L1 and below the level of the ground****
state=2.3
d=y(1)-L1
area3=0
area2=.0014253
area1=0
area6=0
area5=.0007127
area4=0
F(0)=1
F(1)=y(2)
F(2)=-C3*y(2)*area2+A*.00852*ABS(F(6))*SIN(ABS(ANG))
F(3)=y(4)
F(4)=-C4*y(4)*area5-.008528*ABS(F(6))*SIN(ABS(ANG))
F(5)=y(6)
F(6)=117.37*mu*(ABS(F(2))*COS(ABS(ANG))+A*ABS(F(4))*SIN(ABS(ANG)))

600 REM**Next two lines set the vertical resistance to zero when it starts to become
negative

IF F(2)<=0 THEN 700
F(2)=0
I=I+1
IF I=1 THEN Pitch=yo(1)
700 RETURN
```